

**ANN based Data Mining Technique to Achieve
Improved Accuracy to Predict ISMR from Ocean
–Atmosphere State Variables**

Thesis submitted to

Cochin University of Science and Technology

in partial fulfilment of the requirements for the degree of

Doctor of Philosophy

in

Applied Mathematics

Under the Faculty of Marine Sciences

By

Maya L Pai

Reg. No. 3796

**DEPARTMENT OF PHYSICAL OCEANOGRAPHY
SCHOOL OF MARINE SCIENCES
COCHIN UNIVERSITY OF SCIENCE AND TECHNOLOGY
COCHIN 682 016**

May 2016

ANN based Data Mining Technique to Achieve Improved Accuracy to
Predict ISMR from Ocean –Atmosphere State Variables

Ph.D. Thesis under the Faculty of Marine Sciences

By

Maya L Pai

Department of Mathematics
Amrita School of Arts and Sciences
Amrita Vishwa Vidyapeetham (University)
Brahmasthanam, Edappally North (P.O)
Cochin 682024
Email: mayalpai@gmail.com

Supervising Guide

Dr. A N Balchand

Dean, School of Marine Sciences &
Head, Department of Physical Oceanography
School of Marine Sciences
Cochin University of Science and Technology
Cochin 682016.
Email: balchand57@gmail.com

Co - guide

Dr. K V Pramod

Associate Professor
Department of Computer Applications
Cochin University of Science and Technology
Cochin 682022.
Email: pramodkv4@gmail.com

May 2016

**DEPARTMENT OF PHYSICAL OCEANOGRAPHY
SCHOOL OF MARINE SCIENCES
COCHIN UNIVERSITY OF SCIENCE AND TECHNOLOGY
COCHIN 682 016**

Dr. A N Balchand
Professor

Dr. K V Pramod
Associate Professor

 **Certificate**

This is to certify that the thesis entitled “**ANN based Data Mining Technique to Achieve Improved Accuracy to Predict ISMR from Ocean –Atmosphere State Variables**” is an authentic record of the research work carried out by **Smt. Maya L Pai** under our supervision and guidance at the Department of Physical Oceanography, Cochin University of Science and Technology, Cochin 682016, in partial fulfillment of the requirements for Ph.D degree of Cochin University of Science and Technology and no part of this has been presented before for any degree in any university. All the relevant corrections and modifications suggested by the audience during the pre-synopsis seminar and recommended by the Doctoral Committee have been incorporated in the thesis.

Kochi - 682016

May 2016

Dr. A N Balchand
(Supervising Guide)

Dr. K V Pramod
(Co-guide)

Certificate

This is to certify that all the relevant corrections and modifications suggested by the audience during the pre-synopsis Seminar and recommended by the Doctoral Committee of the candidate has been incorporated in the thesis.

Kochi - 682016

May 2016

Dr. A N Balchand
(Supervising Guide)

Dr. K V Pramod
(Co- Guide)

Declaration

I hereby declare that the thesis entitled “**ANN based Data Mining Technique to Achieve Improved Accuracy to Predict ISMR from Ocean –Atmosphere State Variables** ” is an authentic record of research work carried out by me under the supervision and guidance of Dr. A N Balchand, Dean, School of Marine Sciences and Head, Department of Physical Oceanography, Cochin University of Science and Technology and Dr. K V Pramod, Associate Professor, Department of Computer Applications towards the partial fulfillment of the requirements for the award of Ph.D. degree under the Faculty of Marine Sciences and no part thereof has been presented for the award of any other degree in any University/Institute.

Kochi-16
May 2016

Maya L Pai

Dedicated to my Parents...

Acknowledgement

I am deeply indebted to my supervising guide, Prof. (Dr). A N Balchand, Dean, School of Marine Sciences and Head, Department of Physical Oceanography and my co-guide Dr. K V Pramod, Associate Professor, Department of Computer Applications, Cochin University of Science and Technology, Kochi, for their guidance, encouragement and support without which this thesis would not have materialized.

I express my sincere thanks to Prof. (Dr.) P V Joseph, Emeritus Professor (Department of Atmospheric Sciences) for his invaluable suggestions when I embarked on this work. I extend my sincere thanks to Dr. M R Ramesh Kumar, Chief Scientist, NIO, Goa for his timely advice during the course of its execution.

I wish to express my gratitude to Dr. U Krishna Kumar, Director, Amrita School of Arts and Sciences, Kochi for providing the motivation and giving the required moral support to carry out this work. I express my sincere thanks to my colleagues Dr. M V Judy and Dr. Vijayalakshmi P P for the support given by them.

I acknowledge all the support and help rendered to me by Dr. Ch. V. Jayaram, Scientist, NRSC /ISRO. I wish to express my sincere thanks to Dr. R Sajeed, Associate Professor and Mr. P K Saji, Asst. Professor, Department of Physical Oceanography, for the suggestions and encouragement given during my research period. My heartfelt thanks go to

Dr. Venu G Nair, Mr. Mohammed Shafeeque, Mr. Phiroz Shah and Mr. Vasudevan S for their support. I also wish to thank the office staff of Department of Physical Oceanography for their co-operation.

I thank the data centers of IMD, ICOADS, Hadley and all the people who put in the effort to bring out the data that I made use of in this study.

I am deeply indebted to my husband and children for their unflagging love and support which has enabled me to achieve this goal. Also I thank each and every person who had directly or indirectly helped me to complete the thesis in time.

I bow in gratitude before Sat Guru Mata Amritanandamayi Devi without whose grace and blessings, this endeavor could not have materialized. Most of all, I thank God for showering His Blessings upon me.

Maya L Pai

Contents

| | |
|--|-------------|
| List of Figures | vi |
| List of Tables | xii |
| Chapter 1 Introduction | 1-18 |
| 1.1 Introduction to neural networks | 3 |
| 1.1.1 Artificial Neural Network [ANN] | 3 |
| 1.1.2 Similarities between Human and Artificial neuron | 5 |
| 1.1.3 Learning method | 6 |
| 1.1.4 Activation functions | 7 |
| 1.1.5 Back propagation | 7 |
| 1.1.6 Error calculation | 8 |
| 1.2 Mathematics and Earth System | 9 |
| 1.3 Atmosphere Ocean variability | 9 |
| 1.4 Indian Monsoons | 10 |
| 1.5 Earlier studies | 12 |
| 1.6 Objectives of the study | 17 |
| 1.7 Scheme of the Thesis | 18 |

| | |
|--|---------------|
| Chapter 2 Materials and Methods | 19-31 |
| 2.1 Introduction | 19 |
| 2.2 Data | 19 |
| 2.3 Area of study | 20 |
| 2.4 Principal Component Analysis (PCA) | 22 |
| 2.5 Hydrological Regions of India | 22 |
| 2.6 Preprocessing | 24 |
| 2.7 Auto Regressive Integrated Moving Average (ARIMA) | 24 |
| 2.8 Self Organizing Maps (SOM) | 25 |
| 2.9 Cluster validation | 25 |
| 2.9.1 Inter-Cluster Density (ID) | 26 |
| 2.9.2 Intra-cluster variance | 27 |
| 2.9.3 Silhoutte Coefficient | 27 |
| 2.10 Performance of the Model | 28 |
| 2.11 Trend analysis | 29 |
| 2.12 Methodology | 30 |
| 2.13 Software Tools | 31 |
| | |
| Chapter 3 Long term trends of SST, Sub Surface Temperature and its relationship with rainfall | 32-109 |
| 3.1 Introduction | 32 |
| 3.2 Spatial trend in SST | 36 |
| 3.3 Temporal trends of SST | 44 |
| 3.4 Spatial trend analysis of Sub Surface Temperature | 54 |
| 3.4.1 Annual Variability | 55 |

| | |
|--|----|
| a) At depth 25m | 55 |
| b) At depth 98 m | 56 |
| c) At depth 235 m | 57 |
| d) At depth 540 m | 57 |
| e) At depth 967 m | 58 |
| 3.4.2 Seasonal Variability | 59 |
| a) At depth 25m | 59 |
| b) At depth 98 m | 61 |
| c) At depth 235 m | 60 |
| d) At depth 540 m | 63 |
| e) At depth 967 m | 64 |
| 3.4.3 Monthly variability | 69 |
| a) At depth 25m | 69 |
| b) At depth 98 m | 69 |
| c) At depth 235 m | 70 |
| d) At depth 540m | 70 |
| e) At depth 967 m | 70 |
| 3.5 Spatial Trend Analysis of rainfall | 81 |
| 3.5.1 Epoch 1960 -2012 | 81 |
| 3.5.2 Epoch 1960- 1976 | 84 |
| 3.5.3 Epoch 1977-2012 | 88 |
| 3.6 Distribution plot of rainfall | 91 |
| 3.6 a) Meridional | 91 |
| 3.6.1 Epoch 1960- 2012 | 92 |

| | | |
|--|--------------------------------------|----------------|
| 3.6.2 | Epoch 1960-76 | 95 |
| 3.6.3 | Epoch 1977-2012 | 98 |
| 3.7 | Zonal trend analysis of rainfall | 101 |
| 3.7.1 | Epoch 1960- 2012 | 101 |
| 3.7.2 | Epoch 1960-76 | 103 |
| 3.7.3 | Epoch 1977-2012 | 104 |
| 3.8 | Conclusion | 106 |
| Chapter 4 Application of ANN in predicting rainfall for South West Coast of India | | 110-115 |
| 4.1 | Introduction | 110 |
| 4.2 | Factors influencing monsoon rainfall | 110 |
| 4.3 | Prediction models on monsoon | 111 |
| 4.4 | Methodology and Results | 113 |
| 4.4.1 | Methodology | 113 |
| 4.4.2 | Results | 114 |
| 4.5 | Conclusion | 115 |
| Chapter 5 ANN based prediction of ISMR for Indian hydrological region | | 118-147 |
| 5.1 | Introduction | 118 |
| 5.2 | Methodology and Results | 119 |
| 5.3 | Analysis - AS parameters | 130 |
| 5.4 | Analysis - BOB parameters | 130 |

| | | |
|--|------------------------------------|----------------|
| 5.5 | Analysis - SIO parameters | 130 |
| 5.6 | Comparison of results | 143 |
| 5.7 | Conclusion | 146 |
| Chapter 6 Prediction of extreme rainfall events using ANN | | 148-169 |
| 6.1 | Introduction | 148 |
| 6.2 | Standard Precipitation Index (SPI) | 148 |
| 6.3 | Methodology and Results | 150 |
| 6.4 | Forecast for 2013, 2014 and 2015 | 162 |
| 6.5 | Conclusion | 168 |
| Chapter 7 Summary and Conclusion | | 170-183 |
| Bibliography | | 184-201 |
| Publications | | 202 |

List of Figures

| | | |
|---------|---|----|
| 1.1 | Artificial neuron model | 5 |
| 1.2 | Biological Neuron model | 6 |
| 1.3(a) | Single layer artificial neural network | 7 |
| 1.3 (b) | Multilayer artificial neural network | 7 |
| 2.1 | Percentage of data density in ICOADS | 20 |
| 2.2 | Study region of Indian Ocean | 20 |
| 2.3 | 1° x 1° grids of India | 20 |
| 2.4 | Vertical boxes | 21 |
| 2.5 | Horizontal boxes | 21 |
| 2.6 | Indian Climatic Zone Map | 23 |
| 2.7 | Flow Chart on data processing | 31 |
| 3.2.1 | Spatial SST trends (°C/decade) of four seasons and annual for the period 1960-2012 | 37 |
| 3.2.2 | Spatial SST trends (°C/ decade) of the months January to June for the period 1960 to 2012 | 40 |
| 3.2.3 | Spatial SST trends (°C/decade) of the months July to December for the period 1960 to 2012 | 41 |
| 3.2.4 | Decadal trend of mean SST for the Tropical IO | 43 |
| 3.3.1 | Trend of SST for the period 1960- 2012 (a) annual (b) winter | |

| | |
|---|-------|
| (c) pre- monsoon (d) monsoon (e) post monsoon | 45-47 |
| 3.3.2 Trend of SST for the period 1960-1976 (a) annual (b) winter | |
| (c) pre -monsoon (d)monsoon (e)post monsoon | 48-50 |
| 3.3.3 Trend of SST for the period 1977-2012 (a) annual (b)winter | |
| (c) pre-monsoon (d)monsoon (e)post monsoon | 52-54 |
| 3.4.1 Annual variation of sub surface temperature for the period | |
| 1950-2011 at depths (a) 25m (b) 98m (c) 235m (d) | |
| 540m (e) 967m | 62 |
| 3.4.2 Seasonal variation of sub surface temperature for the period | |
| 1950-2011 at depth 25m for (a) winter (b) pre-monsoon | |
| (c) monsoon (d) post monsoon | 64 |
| 3.4.3: Seasonal variation of sub surface temperature for the period | |
| 1950-2011 at depth 98m for (a) winter (b) pre- monsoon | |
| (c) monsoon (d) post monsoon | 65 |
| 3.4.4 Seasonal variation of sub surface temperature for the period | |
| 1950-2011 at depth 235m for (a) winter (b) pre-monsoon | |
| (c) monsoon (d) post monsoon | 66 |
| 3.4.5 Seasonal variation of sub surface temperature for the period | |
| 1950-2011 at depth 540m for (a) winter (b) pre-monsoon | |
| (c) monsoon (d) post monsoon | 67 |
| 3.4.6 Seasonal variation of sub surface temperature for the period | |
| 1950-2011 at depth 967m for (a) winter (b) pre-monsoon | |
| (c) monsoon (d) post monsoon | 68 |

| | |
|--|-------|
| 3.4.7 Trend analysis of subsurface temperature for the months at depth 25m during the period 1960-2011 (a) January (b)February (c) March (d)April (e) May (f)June(g) July(h)August(i)September (j)October (k)November (l)December | 71-72 |
| 3.4.8 Trend analysis of subsurface temperature for the months at depth 98m during the period 1960-2011 (a) January (b) February (c) March (d) April (e) May (f) June (g) July (h) August (i) September (j) October (k) November (l) December | 73-74 |
| 3.4.9: Trend analysis of subsurface temperature for the months at depth 235m during the period 1960-2011 (a) January (b) February (c) March (d) April (e) May (f) June (g) July (h) August (i) September (j) October(k)November (l) December | 75-76 |
| 3.4.10 Trend analysis of subsurface temperature for the months at depth 540m during the period 1960-2011 (a) January (b) February (c) March (d) April (e) May (f) June (g) July (h) August (i) September (j) October (k)November (l) December | 77-78 |
| 3.4.11 Trend analysis of subsurface temperature for the months at depth 967m during the period 1960-2011 (a) January (b) February (c) March (d) April (e) May (f) June (g) July (h) August (i) September (j) October (k) November (l) December | 79-80 |
| 3.5.1 Slopes (mm/decade) of rainfall for the period1960-2012 (a) JJAS (b) June (c) July (d) August (e) September | 82-84 |

| | | |
|-------|--|---------|
| 3.5.2 | Slopes (mm/decade) of rainfall for the period 1960-1976 | |
| | (a) JJAS (b) June (c) July (d) August (e) September | 85-87 |
| 3.5.3 | Slopes (mm/decade) of rainfall for the period 1977-2012 | |
| | (a) JJAS (b) June (c) July (d) August (e) September | 89-91 |
| 3.6.1 | Distribution plot of ISMR for the period 1960-2012 for the longitude 78.5°E and for the latitudes (a) 9.5° to 10.5° N (b) 13.5° to 14.5°N (c) 18.5° to 19.5° N (d) 21.5° to 22.5°N (e) 25.5° to 26.5° N (f) 29.5° to 30.5°N (g) 33.5° to 34.5° N | 93-95 |
| 3.6.2 | Distribution plot of ISMR for the period 1960-1976 for the longitude 78.5°E and for the latitudes (a) 9.5° to 10.5° N (b) 13.5° to 14.5°N (c) 18.5° to 19.5° N (d) 21.5° to 22.5°N (e) 25.5° to 26.5°N (f) 29.5° to 30.5°N (g) 33.5° to 34.5° N | 96-98 |
| 3.6.3 | Distribution plot of ISMR for the period 1977-2012 for the longitude 78.5°E and for the latitudes (a) 9.5° to 10.5° N (b) 13.5° to 14.5°N (c) 18.5° to 19.5° N (d) 21.5° to 22.5°N (e) 25.5° to 26.5° N (f) 29.5° to 30.5° N (g) 33.5° to 34.5° N | 99-101 |
| 3.7.1 | Distribution plot of ISMR for the latitude 20.5° to 24.5°N , for the period 1960-2012 and for the longitudes (a) 74.5° to 77.5°E (b) 78.5° to 81.5°E (c) 82.5° to 85.5°E | 102 |
| 3.7.2 | Distribution plot of ISMR for the latitude 20.5° to 24.5°N , for the period 1960-1976 and for the longitudes (a) 74.5° to 77.5°E (b) 78.5° to 81.5°E (c) 82.5° to 85.5°E | 103-104 |

| | | |
|--------|---|---------|
| 3.7.3 | Distribution plot of ISMR for the latitude 20.5 ⁰ to 24.5 ⁰ N, for the period 1977-2012 and for the longitudes (a) 74.5 ⁰ to 77.5 ⁰ E (b) 78.5 ⁰ to 81.5 ⁰ E (c) 82.5 ⁰ to 85.5 ⁰ E | 105 |
| 4.1 | Actual rainfall versus Predicted rainfall (mm) | 114 |
| 4.2 | Probability Plot of Residual | 114 |
| 5.2.1 | Feed forward Neural Network | 125 |
| 5.2.2 | Observed and predicted clusters representing rainfall using the parameters of IO full for the years (a)1960 (b)1970 (c) 1985 (d) 1990 (e) 2000 (f) 2003 (g) 2009 (h)2012 | 126-129 |
| 5.3.1: | Observed and predicted clusters representing rainfall using the parameters of AS for the years (a)1960 (b)1970 (c) 1985 (d) 1990 (e) 2000 (f) 2003 (g) 2009 (h) 2012 | 131-134 |
| 5.4.1: | Observed and predicted clusters representing rainfall using the parameters of BOB for the years (a)1960 (b)1970 (c) 1985 (d) 1990 (e) 2000 (f) 2003 (g) 2009 (h) 2012 | 135-138 |
| 5.5.1 | Observed and predicted clusters representing rainfall using the parameters of SIO for the years (a)1960 (b)1970 (c) 1985 (d) 1990 (e) 2000 (f) 2003 (g) 2009 (h) 2012 | 139-142 |
| 6.2.1 | Standard Normal curve, drawn in MATLAB | 149 |
| 6.3.2 | Observed and predicted clusters representing rainfall for the drought years (a) 1965 (b) 1966(c) 1972 (d) 1974 (e) 1979 (f) 1982 (g) 1986 (h) 1987 (i) 2002 (j) 2004 | 154-158 |

| | |
|---|---------|
| 6.3.3: Observed and predicted clusters representing rainfall for the flood years (a) 1961 (b) 1970 (c) 1971 (d) 1975 (e) 1983 (f) 1988 (g) 1994 | 159-162 |
| 6.4.1: Predicted clusters representing rainfall for the years (a) 2013 (b) 2014 (c) 2015 | 166 |

List of Tables

| | | |
|-------|---|---------|
| 3.1 | Range of decadal trend in SST | 43 |
| 3.2 | Minimum and maximum slope ($^{\circ}\text{C}/\text{decade}$) for four seasons and annual for the depths | 56 |
| 4.1 | Prediction of rainfall in mm | 116-117 |
| 4.2 | Calculated Error Measures | 117 |
| 5.2.1 | Optimal partitioning found by S_Dbw index and Silhoutte coefficient | 121 |
| 5.2.2 | Range of values of the clusters and the centroids covering the full period 1960-2012 | 122 |
| 5.2.3 | Statistics of the results obtained for the training and the test data | 123 |
| 5.2.4 | CV of observed and predicted for the decades and for the epochs 1960-1976, 1977-2012, 1960-85 and 1986-2012 | 124 |
| 5.6.1 | Errors obtained for the 6 regions with respect to AS, BOB, SIO and IO parameters | 144 |
| 5.6.2 | Comparison of results using 1 parameter, 4 parameters and monsoon period parameters of IO | 144 |
| 5.6.3 | Centroids of the clusters of rainfall for the months June to September | 145 |

| | | |
|--------|--|------|
| 5.6.4 | Errors obtained for the two regimes with respect to IO Parameters for individual months | 145. |
| 5.6.5 | Comparison of experimental results of the proposed model and the model for training and test data after Singh and Bhogeswar (2013) | 146 |
| 6.2.1 | Standard Precipitation Index classification | 149 |
| 6.3.1 | Correlation coefficient between the observed and predicted clusters, at 99 % level of confidence | 151 |
| 6.3.2: | Percentage errors in drought and flood years | 152 |
| 6.4.1: | SPI classification for the period 2013-2015 | 167 |
| 6.4.2: | Mean and S.D for the six hydrological regions for the years 2013-2015 | 168 |

CHAPTER 1

INTRODUCTION

Introduction

Global Warming is contemporarily coined with climate change which refers to an average temperature increase globally. This has been a very critical issue concerning our planet. The variability in rainfall and cyclonic patterns are one of the main consequences of this changing phenomenon. Global warming could cause frequent and severe failures in the Indian summer monsoon during the next two centuries (Rajeevan , 2001; Kripalani et al., 2003; Zhou et al., 2008, Rao , 2013). Natural events, but dominating human activities are responsible for these impacts. According to the National Oceanic and Atmospheric Administration (NOAA), there are seven indicators that lead to increase in global temperature and the net effect is visible in increase in sea surface temperature, sea level, humidity, temperature over land, and within oceans. The Inter Governmental Panel on Climate Change (IPCC) 4th assessment model (2007) reports that there will be a significant increase in temperature towards the end of 21st century. Recently scientists have been working on the impact of these on Indian monsoon. A study based on the effect of climate change on seasonal monsoon in Asia and its impact on the variability of monsoon was carried out by Yen et al., 2015. Long range forecast of Indian Summer Monsoon Rainfall (ISMR) based on statistical methods have been used by India Meteorological Department (IMD). However these approaches have limitations and failed to predict the monsoon rainfall for the deficit years 2002 and 2004. Ashok Kumar et al., (2012) developed an eight parameter and later a ten parameter power regression model was used from 2003 to 2006. These authors have shown

that the Neural Network (NN) model performed better than the linear regression model and also showed that this model performed better than the model of Rajeevan et al., (2007). From 2007 onwards, the existing model was replaced by the ensemble method.

In this study, one of the Data Mining (DM) techniques namely Artificial Neural Network (ANN) is used to predict ISMR with improved accuracy surpassing that of the existing models. This will certainly benefit the agriculturists and farmers who are the backbone of the nation's economy thereby paving the way towards an enhanced economic status in the global scenario.

Data Mining is the process of gathering information or knowledge and discovering patterns from large amount of data. The common tasks involved in data mining are clustering, association, regression, anomaly detection and prediction. DM is widely used in Finance, Health Sciences and in Earth Sciences including climate change and meteorology. Commonly used techniques in DM are ANN, Decision Trees and Genetic Algorithm. Data mining is considered as a blend of Statistics, Artificial Intelligence and Database Research (Pregibon, 1997). The concept of DM has become more popular in every field due to its capability of identifying the patterns hidden in the data. These recognized patterns become very helpful in future predictions. Meghali et al., (2013) have discussed how to use data mining technique to analyze meteorological data. Chaudhari et al., (2013) discussed different data mining techniques to predict, associate, classify or to cluster the meteorological data. Ganguly et al., (2008) makes a case for the development of novel algorithms to address the issues in spatial, temporal and spatiotemporal data mining. Nagendra and Khare,

(2006) applied ANN to model large data with large dimension. Zahoor Jan et al., (2008) developed a model using K Nearest Neighbor (KNN) to classify historical weather data. They have used data mining techniques in forecasting monthly rainfall in Assam. Folorunsho et al., (2012) used predictive neural network model and decision tree algorithms to forecast maximum temperature, rainfall, evaporation and wind speed. These algorithms gave better results when compared to the standard performance metrics. Ganguly et al., (2014) proposed DM techniques to tackle the challenges in the interpretation, projection and prediction of extreme events such as heat waves, cold spells, floods, droughts, cyclones and tornadoes. Shanmuganathan et al., (2010) used DM techniques for modeling seasonal climate effects on grapevine yield and wine quality. The authors have found that DM techniques could be very useful in determining the weather variables that are significant to a better yield of wine. The aforementioned studies show that DM technique would be the most effective tool in weather forecasting and climate change studies.

1.1 Introduction to neural networks

1.1.1 Artificial Neural Network [ANN]

ANN's have wide applications in the fields like classifications; signal processing, pattern recognition and forecasting (Han et al., 2012). It has the capability of capturing the non linearity hidden in huge data. Conceptually, an Artificial Neuron (AN) mimics the characteristics of a biological neuron. Large number of interconnected elements seen in ANN is called artificial neurons. ANN's have been developed as generalization of mathematical models of human cognition based on the assumption:

1. Information processing occurs at many simple elements called neurons.
2. Signals are passed between neurons over connection links.
3. Each connection link has an associated weight which multiplies the signal transmitted.
4. Each neuron applies an activation function to its net input (sum of weighted input signals) to determine its output signal (Fausett, 2006).

The neurons are arranged in layers and the neurons in the same layer behave in a similar manner (Sivanandam and Paulraj, 2003). Same activation function is possessed by the neurons in each layer. The neurons are connected or not connected within each layer, but the neurons in each layer are connected to neurons in another layer. The arrangement of neurons into layers and the connection within and between the layers are called network architecture (Sivanandam and Paulraj, 2003). The main components of the network are a) Input layer- The neurons in this layer receive input signals from external and transfer them to the neurons in another layer, but does not perform any computation, b) Output layer- The neurons in this layer receive signals either from the input layer or from the hidden layer and c) Hidden layer- The layer of neurons that are connected between input layer and the output layer. NN's are classified into two: single layer network (figure 1.3(a)) and multilayer network (figure 1.3(b)). A single layer network consists of only one layer of connection weights between the input layer and the output layer, but a multilayer network consists of more than one or more hidden layers. The input layer neurons receive the input signals and the output layer neurons receive the output signals. The links carrying the weights connect every input neuron to the

output neuron but not vice-versa called feed forward. The input layer transmits the signals to the output layer. Hence the name single layer feed forward network. Multilayer feed forward network is made up of multiple layers. There will be one or more intermediate layers called hidden layers. The hidden neurons are the computational units. The input layer neurons are linked to the hidden layer neurons and the weights on these are called input- hidden layer weights. The hidden layer neurons are linked to the output layer neurons and the corresponding weights are called hidden-output layer weights. Figures 1.1 and 1.2 represent simple model of an artificial neuron and a biological neuron model respectively.

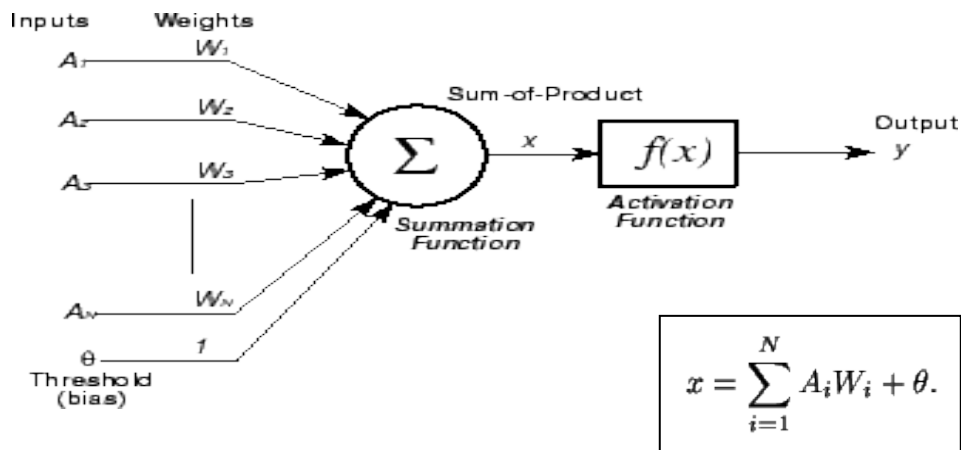


Figure 1.1: Artificial neuron model (Haykin and Simon, 1999).

1.1.2 Similarities between Human and Artificial neuron

A biological neuron has three types of components called *dendrites*, *soma* and *axon*. The many dendrites receive signals from other neurons. The soma or cell body sums the incoming signals. A neuron of the human brain collects signals from others through a swarm of fine

structures called *dendrites*. A long thin strand known as *axon* sends out spikes of electrical activity and splits into thousands of branches. There is a structure called *synapse* at the end of each branch converts the action from the axon into electrical effects that stimulate activity from the axon in the connected neurons. As soon as a neuron receives an input which is large compared to its input, it sends a piece of electrical activity down its axon. The influence of one neuron on another change thereby occurs learning, all the above concepts being well explained by Fausett, 2006.

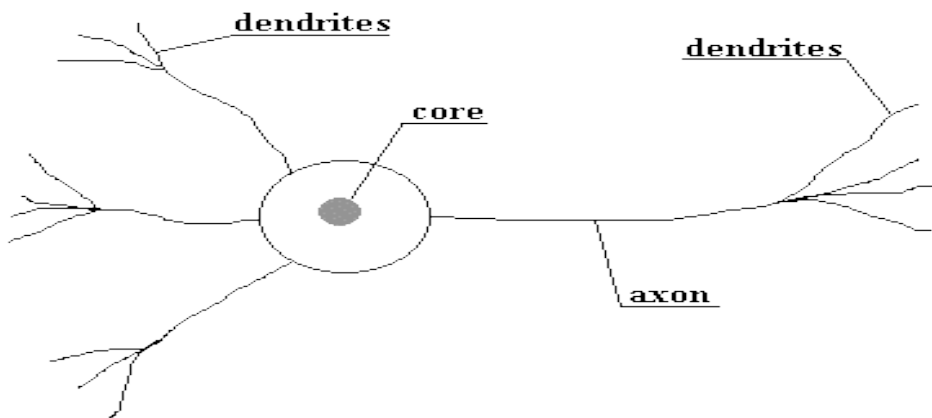


Figure 1.2: Biological Neuron model [Zurada and Jacek, 1992].

1.1.3 Learning method

There are 3 types of learning methods - supervised, unsupervised and reinforced. In supervised learning, the learning takes place with the help of a supervisor. In this, every input pattern is used to train the network which is associated with an output pattern, which is the known

target. In an unsupervised learning the target is not given to the network. Reinforced learning is similar to supervised learning.

1.1.4 Activation functions

Identity function $f(x) = x$ for all x .

Binary step function $f(x) = 1$ if $x \geq \theta$
 $= 0$ if $x < \theta$ where θ is the threshold value.

Sigmoid function $f(x) = \frac{1}{1 + e^{-x}}$

Bipolar sigmoid function $f(x) = \frac{2}{1 + e^{-x}} - 1$

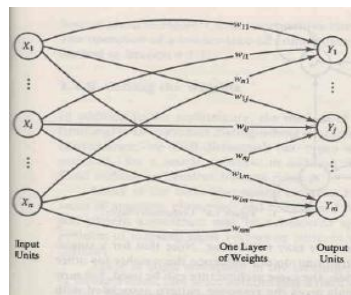


Figure 1.3(a): Single layer artificial neural network (Fausett, 2006).

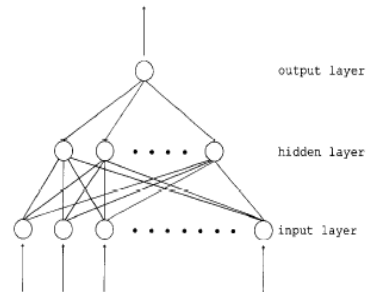


Figure 1.3(b): Multilayer artificial neural network (Svozil et al., 1997).

1.1.5 Back propagation

Back Propagation is a supervised learning method in which the net repeatedly adjusts its weights on the basis of the error, or the deviation from the target output, in response to the training patterns. Learning takes

place through a number of epochs. During each epoch, the training patterns are applied at the input layer and the signals flow from the input layer to the output layer through hidden layers (Han et al., 2012).

Back propagation training consists of three stages:

Feed forward of the training pattern, Back propagation of the error and weight adjustment. In this case, each input neurons receive an input signal and passes it to each hidden neuron, which in turn computes the activation function and passes it to each output neurons, which computes the activation function to get the net output. During the training phase, the net output is compared with the target and the error is calculated. The error factor obtained from the error is propagated back to the hidden layers to update the weights. This process is repeated until the error is minimized (Han et al., 2012).

1.1.6 Error calculation

For any k^{th} output neuron, the error norm in output for the k^{th} output neuron is

$$E_r^1 = \frac{1}{2} e_r^2 = \frac{1}{2} (T-O)^2$$

The Euclidean norm of error E^1 for the first training pattern is

$$E^1 = \frac{1}{2} \sum_{k=1}^n (T_{ok} - O_{ok})^2. \text{ Repeating the process for all training patterns,}$$

the error function is $E = \sum_{i=1}^{nset} E^i (V, W, I)$ where V and W are the weighted values and I the inputs.

1.2 Mathematics and Earth System

Mathematics could play an important and fundamental role in explaining the issues related to the complexity of Earth and more specifically, the environment. Mathematics can be used as a tool for understanding, solving, forecasting and decision making in environmental problems. Multi scale analysis is essential in climate studies. Statistics is important when data sets are considered to estimate the parameters, to make comparisons, validations and to compare models. Quantitative methods are used to simulate the interactions of atmosphere, oceans and land surface (Mujumdar and Nagesh Kumar, 2012). These models help to get a clear picture on the dynamics of the system and also to make useful predictions. After the development of Computers, we have been able to process large amounts of data through data mining process in both Oceanography and Meteorology.

1.3 Atmosphere Ocean variability

Local to regional climate primarily depends on the physical interactions between ocean and atmosphere. It is determined by the physical, biological and chemical interactions within the ocean and atmosphere and also by the solar radiations which brings about climate variability on spatial and temporal scale (Huffman et al., 1997; Daniel et al., 2002; Bothmer et al., 2006; <http://www.ucsus.org>; Mark Denny, 2011; Dubey, 2014). Wang et al., (2004) have made a global survey of Ocean –Atmosphere interaction and climate variability. According to working group II of 5th assessment IPCC report (2014), ocean plays a major role in Earth’s climate and has absorbed 93% of the extra energy

from the green house gases and 30% of anthropogenic CO₂ from the atmosphere. The authors have also remarked that global average Sea Surface Temperature (SST) has increased since the beginning of 20th century. The average SST of the Indian Ocean (IO) has increased by 0.65^oC over the period 1950-2009 (IPCC, 2013).

The Atmosphere and the Ocean exchange heat and water forming a coupled system, at the air-sea inter face. This heat transport on long term shapes and determines the climate of Earth. Understanding and analyzing the extent to which the Atmosphere and the Ocean actually influence each other is the subject of large scale air - sea interactions. India was the first country to introduce a systematic development of long range forecast techniques to estimate monsoon rainfall (Sharad et al., 2012).

1.4 Indian Monsoons

In a classical way, monsoons occur when the temperature on land is warmer or cooler than the temperature of the ocean. Asian monsoons may be classified as the South Asian Monsoon and East Asian monsoons. The south Asian monsoons affects India and the surrounding regions and the East Asian monsoon affects Southern China, Korea and parts of Japan. As known, the South West (SW) summer monsoons occur from June through September. The SW winds blowing from the Indian Ocean (IO) onto the Indian landmass during these months carry rain bearing clouds that bring rainfall to most parts of the subcontinent. Indian Ocean splits into two branches, namely, the Arabian Sea (AS) branch and the Bay of Bengal (BOB) branch near the southern part of India. The Kerala region receives rain from SW monsoon. Then this moves northwards towards

Konkan and Goa, west of Western Ghats. Since these winds do not cross the Western Ghats, the eastern areas of the Western Ghats do not receive much rain from SW monsoon. The BOB branch of SW monsoon flows over BOB towards North East India and Bengal picking more moisture from BOB. India receives about 70- 80 % of its total rainfall during the summer monsoon season June-September (Chang, 1967, Sahai et al., 2003). ISMR, the major component of Asian summer monsoon have impacts on Indian agriculture. India is an agricultural country and the major crops like rice, cotton, and oil seeds depend on monsoons. Forecasting of rainfall at an improved accuracy is of great application not only to the farmers of India but also to the socio-economic development of our Country.

According to IMD, the 4 seasons are categorized as follows:

- Winter season - January and February (JF).
- Pre monsoon - March, April and May (MAM).
- Monsoon - June, July, August and September (JJAS).
- Post monsoon - October, November and December (OND).

Normally, in India during pre monsoon and post monsoons severe rain storms are associated with meteorological systems such as active low pressure areas, depressions and cyclonic storms. Generally these systems originate from the neighboring seas of the BOB and the AS and after crossing the respective coastal areas these move in land (Sharad et al., 2012).

1.5 Earlier studies

During the past two decades, both short term and long term studies have been extensively carried out in the field of predicting monsoon rainfall. Most of the rainfall in India occurs during the summer season June, July, August and September (JJAS). There is a high spatial and temporal variability in ISMR pattern. A high variation is seen on intra seasonal to inter annual and inter decadal time scales. Performance of the parametric and power regression models showed reasonably accurate results (Gowariker et al., 1991). Krishna Kumar et al., (1995) made a review on the seasonal forecasting of ISMR. These models are used by IMD for long range forecasts in India. But these statistical models have some limitations. So attempts were made to develop better, alternate techniques for long range forecasts of summer monsoon rainfall of India. Empirical modeling approaches were used to forecast ISMR. Later, Krishna Kumar et al., (1995) and Sahai et al., (2000) presented reviews on such empirical models. Navone and Ceccatto (1994) have developed an ANN model to predict ISMR and showed that this approach gives better performance than the conventional methods. Many researchers have used SST of AS as an important input to predict ISMR [Joseph and Pillai (1984); Rao and Goswami (1988); Vinayachandran and Shetye (1991), Aralikatti (2005), Tripathi et al., (2008)]. Aralikatti (2005) used 67 grids of AS for the period 1951-80 to study the relationship of ISMR and SST with regression model and observed that SST can be used as one of the parameters for forecasting ISMR. Rajeevan et al., (2006) have developed new statistical models for long range forecast of south west monsoon rainfall over India. They have used 6 predictors for forecasting the

monsoon. Gadgil et al., (2005) made a general overview of forecasting models for ISMR. ANN has the capability of capturing complex non-linearity in the time series and also in prediction. Many researchers have discussed several NN architectures too (Muller and Reinhardt, 1991; Bose and Liang, 1998). Back propagation neural network is the one which is significant among them (Bryson and Ho, 1969; Rumelhart et al., 1986). IMD was using the parametric and power regression models for long range forecasts for India before the 1950's, but with limitations. Many researchers have made attempts to develop better models to improve the accuracy; these attempts have limited predictive values. NN technique studies the dynamics within the time series data (Elsner et al., 1992). In the early twentieth century ANN's were used to predict ISMR [Goswami and Srividya (1996), Venkateswan et al., 1997, Guhathakurta et al., 1999]. The 8 parameter hybrid principal component model was developed by using a 30 year (1958-87) data as training period and a 10 year period (1988-97) as verification period (Guhathakurta et al., 1999). An artificial intelligence approach for regional rainfall forecasting for Orissa state, India, on monthly and seasonal time scales was attempted by Nagesh Kumar et al., (2007). In his study, possible relation between regional rainfall over Orissa and the large scale climate indices like EL-Nino Southern oscillation (ENSO), Equatorial Indian Ocean Oscillation (EQUINOO) and a local climate index of ocean – land temperature contrast were studied first and then proceeded to forecast monsoon. The coefficient of correlation (CC) during training and testing for JJAS seasonal model were 0.9975 and 0.8951 respectively. A time series approach was used to predict the future values by Goswami and Srividya (1996). Venkateswan et al., (1997) have predicted ISMR with the help of some predictors and compared the result

with linear regression technique. Guhathakurta et al., (1999) have used hybrid principal component and NN approach to predict ISMR. Sahai et al., (2000) applied ANN technique to the monthly time series of June, July, August and September rainfall and observed that ANN technique gave better results than regression models. Iyengar and Raghu Kanth (2005) too used ANN for predicting ISMR. They have divided the whole time series into two series- linear part and non-linear part and applied ANN technique to the nonlinear part. However the above attempts have been limited to local / regional theatres and have limited predictive results.

Rajeevan et al., (2006) developed a new statistical method for long range forecast of ISMR with the help of six predictors. They used ensemble multiple linear regression and projection pursuit regression techniques and gave good forecasts for the two drought years (2002 and 2004). Suryajit Chattopadhyay (2007) developed an ANN model step by step to predict the average rainfall over India during summer monsoon. Goutami Chattopadhyay et al., (2010) have used Neuro computing and statistical approaches to forecast the winter monsoon rainfall of India using SST anomaly as a predictor. Singh and Bhogeshwar (2013) have developed an ANN model to predict ISMR of a given year using the observed time series data. Tripathi et al., (2008) have used SST of Southern Indian Ocean (SIO) as a predictor to predict ISMR. Four indices of quarterly mean SST values were extracted for SIO and ANN technique was used. They have found that the combination of indices would result in better performance. The Indian crops depend on monsoons for their high yield. The monsoon rainfall is random in nature both spatially and temporarily (Mooley and Parthasarathy (1984), Rupa Kumar et al., 1992).

Ramesh Kumar et al., (1998) studied the air-sea interaction over IO during the two contrasting monsoon years 1987 (deficit rainfall) and 1988 (excess rainfall) and found that evaporation rate over south IO and the low level cross equatorial moisture flux play an important role on the monsoon activity over India while the evaporation over AS is less important. There is no direct relationship between increasing rainfall and increasing maximum temperature when monthly or seasonal pattern is considered over meteorological subdivisions, but the relation between the trends of rainfall and temperature have large scale spatial and temporal dependence (Subash and Sikka, 2014). Extreme weather conditions such as floods, droughts, storms etc for the period 1991-2004 have been studied by De et al., (2005). The inter-decadal variability of the relationships between SST and the all India rainfall index have been studied by Clark et al., (2000) and showed that IO has undergone significant secular variation associated with a climate shift in 1976. This climate shift is characterized by significant changes in the structure and evolution of ENSO (Trenberth, 1990; Graham, 1994; Wang, 1995). Increase in SST was found in the tropics of the central and eastern Pacific and IO. Rajeevan et al., (2008) have examined the long term trends of extreme rainfall events over central India using 104 years (1901-2004) data. They have observed that inter-annual, inter-decadal and long term trends of extreme rainfall events are modulated by the SST variations over the tropical IO. Prasanna (2014) studied the impact of monsoon rainfall on the total food grain yield over India. The author has noticed that there is a strong relationship with all – India summer monsoon rainfall and all India crop yield. Kharif (summer) season is affected by day to day variations of summer monsoon. An increase (decrease) in food grains yield is associated with an increase

(decrease) in rainfall. Maharana and Dimri (2014) studied the seasonal climatology and inter annual variability over India and its sub-regions using a regional climate model. Rajeevan et al., (2008) suggested different criterion for active and break spells of ISMR using the daily gridded rainfall data for the period 1951-2007. These were compared with the low level wind and pressure fields. Winds were used as the criteria to monitor the active and break events of ISMR on a real time basis. Sahai et al., (2003) in their paper presents a methodology for making use of SST for long range of prediction of ISMR. Further Rajeevan et al., (2010) studied active and break cycles of ISM. Srivastava et al., (1992) observed that the mean seasonal rainfall has not changed in the past century. But, Goswami et al., (2006) had studied on the significant changes in the trends of heavy rainfall events.

Apart from the trends of rainfall, trends of SST and subsurface temperature also play an important role on Indian monsoons. Various researchers have studied the trend analysis of SST. Alory et al., (2007) studied the temperature trends in the IO over 1960-1999 and found that the warming is large in the subtropics and extends down to 800meters around 40-50° S. Rao et al., (2012) observed that the reason behind the warming of IO is the green house gas effect induced changes in air-sea flux. The net surface heat flux is also responsible for warming. Levitus et al., (2005) observed that the world ocean heat content increased 1.4×10^{22} J corresponding to a mean temperature increase of 0.037° C at a rate of 0.20 Wm^{-2} during 1955-1988. Nilesh et.al., (2014) identified the trends in maximum, minimum and mean temperatures over India during the 4 seasons by using daily gridded data from IMD for the period 1969-2005.

They have observed that the maximum temperature over the west coast of India show increasing trend in winter ,monsoon and post-monsoon seasons but do not show any significant trend over the other parts of the country. Minimum temperature regions show increasing trend over the North Indian states in all seasons and an increasing trend over the west coast of India in winter and SW monsoon seasons. Francis et al., (2013) have observed that there is a strong association of extremes of ISM with ENSO and EQINOO. Monsoons are very much essential for Indian agriculture, power, water, hygiene etc. Sudipta and Menas (2004) had made a study on the inter-annual variability of vegetation over India and its relation to the different meteorological parameters. They have used Empirical orthogonal function (EOF) and wavelet analysis to study the variability of vegetation for the period 1982-2000 and observed that monsoon precipitation and land surface temperature have significant impact on the distribution of vegetation. Bryan (1979) observed in his study that in summer a warmer AS or IO is weakly associated with decreased rainfall and increased sea level pressure over India using the data of sea temperature, rainfall, sea level pressure for the period 1949-72.

It is evident from the earlier studies that ocean state factors are highly linked to Indian monsoons.

1.6 Objectives of the study

This study aims to achieve the following objectives:

1. ANN based long range forecast of Indian summer monsoon rainfall for the hydrological regions of India using ocean and atmosphere state parameters with improved accuracy.

2. Trend analysis of SST, sub surface temperature of Indian Ocean and that of ISMR.
3. Prediction of extreme rainfall events using ANN.

1.7 Scheme of the Thesis

Chapter 1 introduces the study topic with a brief review along with objectives of this thesis and Chapter 2 deals with materials and methodology adopted. Chapter 3 gives emphasis on the trends of SST, subsurface temperature and the rainfall. Chapter 4 describes the ANN model to predict ISMR for the south west coast of India using parameters from IO. Chapter 5 is the generalization of this methodology to the six hydrological regions of India. Chapter 6 is about the role of ANN to predict the extreme events. Summary and conclusion is explained in Chapter 7. The thesis concludes with a section on references cited.

CHAPTER 2

MATERIALS AND METHODS

2.1 Introduction

The Indian monsoon rainfall is highly dependent on Indian Ocean state factors SST, Sea Level Pressure (SLP), Humidity, Zonal (U) wind and Meridional (V) wind, it is postulated. It depends on many pre-monsoon factors of IO as projected by Rao and Goswami,1988;Nagesh Kumar et al.,2007; Krishna Kumar et al.,2010; Agboola et al.,2012. In order to study the relation between rainfall and the above stated parameters, data from the following sources have been accessed / downloaded.

2.2 Data

The $1^{\circ}\times 1^{\circ}$ gridded monthly data for SST, SLP, Humidity, U and V winds in IO (30°S to 30°N , 40°E to 120°E) were obtained from ICOADS for the years 1960-2012 in American Standard Code for Information Interchange (ASCII) format. The data set has been prepared for $1^{\circ}\times 1^{\circ}$ boxes since 1960, after climatologically outlier trimming (Woodruff et al., 2011). The variables are summarized with a set of 10 statistics, namely mean, median and number of observations (Worley et al., 2005). The data so obtained contains missing values. The ICOADS data density in percentage is computed at each grid for all months [figure 2.1]. From the figure, it is clear that 100% data density is available only along ship tracks.

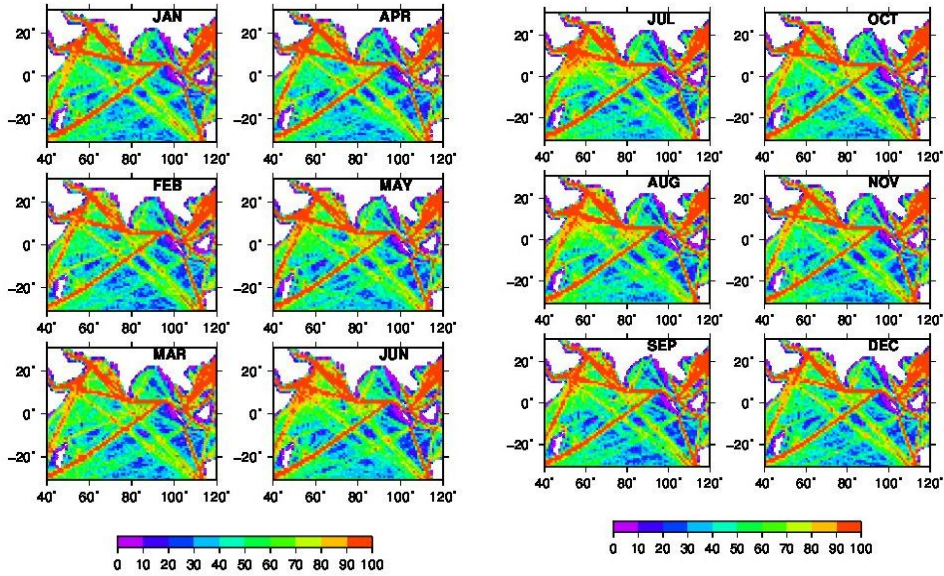


Figure 2.1: Percentage of data density in ICOADS.

2.3 Area of study

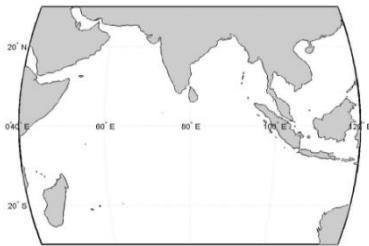


Figure 2.2: Study region of Indian Ocean (prepared in MATLAB).

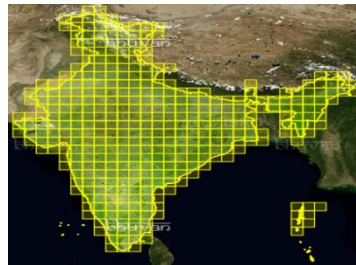


Figure 2.3: $1^{\circ} \times 1^{\circ}$ grids of India (Source: Bhuvan, ISRO, India).



Figure 2.4: Vertical boxes.



Figure 2.5: Horizontal boxes.

The parameters of study of the IO region (open ocean area of figure 2.2) constitute SST, SLP, Humidity, U wind and V wind of IO (30° S to 30° N, 40° E to 120° E) which act as inputs to ANN tool. There are in total 4,800 (60×80) grids. Each year contains 57,600 ($60 \times 80 \times 12$) values. In total, there are 30, 52, 800 data points ($60 \times 80 \times 12 \times 53$) from 53 years, out of which nearly 25% of the data was missing in each of the parameters. Missing data are filled by spline interpolation. Resulting input is a $[30, 52, 800 \times 5]$ matrix. After pre-processing, average value of SST for 3 months March-May (MAM) is calculated. Finally, the input matrix has been found to be of the order $[53 \times 5]$.

The $1^{\circ} \times 1^{\circ}$ subsurface temperature data from IO at 26 depths from 5m to 967m were accessed from the site [http:// apdrc. soest.hawaii. edu/ datadoc/hadley en4.php](http://apdrc.soest.hawaii.edu/datadoc/hadleyen4.php).

The daily rainfall data of India (8.5° N to 37.5° N; 68.5° E to 97.5° E) for the months June to September for each grid within the period 1960-2012 collected from the IMD site was subjected to numerous analysis. The area of study for the rainfall data is given in figure 2.3. The

ISMR for the four months June to September acts as the output for the network.

To get a clear picture of the rainfall pattern, seven boxes vertically along the line 78.5⁰E (9.5⁰ to 10.5⁰, 13.5⁰ to 14.5⁰, 18.5⁰ to 19.5⁰, 21.5⁰ to 22.5⁰, 25.5⁰ to 26.5⁰, 29.5⁰ to 30.5⁰, 33.5⁰ to 34.5⁰) and three boxes (20.5⁰ to 24.5⁰N, 74.5⁰ to 77.5⁰E; 20.5⁰ to 24.5⁰N, 78.5⁰ to 81.5⁰ E; 20.5⁰ to 24.5⁰N, 82.5⁰ to 85.5⁰E) horizontally are considered (figures 2.4 & 2.5). The study was carried out for three epochs 1960-2012, 1960-76 and 1977-2012.

2.4 Principal Component Analysis (PCA)

The PCA technique was used to establish the correlation of the above mentioned parameters with respect to rainfall. Eigen value is the measure of amount of total variance in the data explained by each factor. Looking at the Eigen value, one can determine if the factor explains sufficient amount of variance to be considered as a meaningful factor. An Eigen value less than 1 means that the factor explains less variance than a single variable, and therefore should not be considered to be a meaningful factor.

2.5 Hydrological Regions of India

On the basis of rainfall distribution and other meteorological parameters, India has been divided into different meteorologically homogeneous Sub-divisions. IMD (1981) has published a comprehensive rainfall Atlas of India, using rainfall data of stations for the period 1901-

1950. It contains 98 maps on different aspects of rainfall distribution (Sharad et al., 2012).

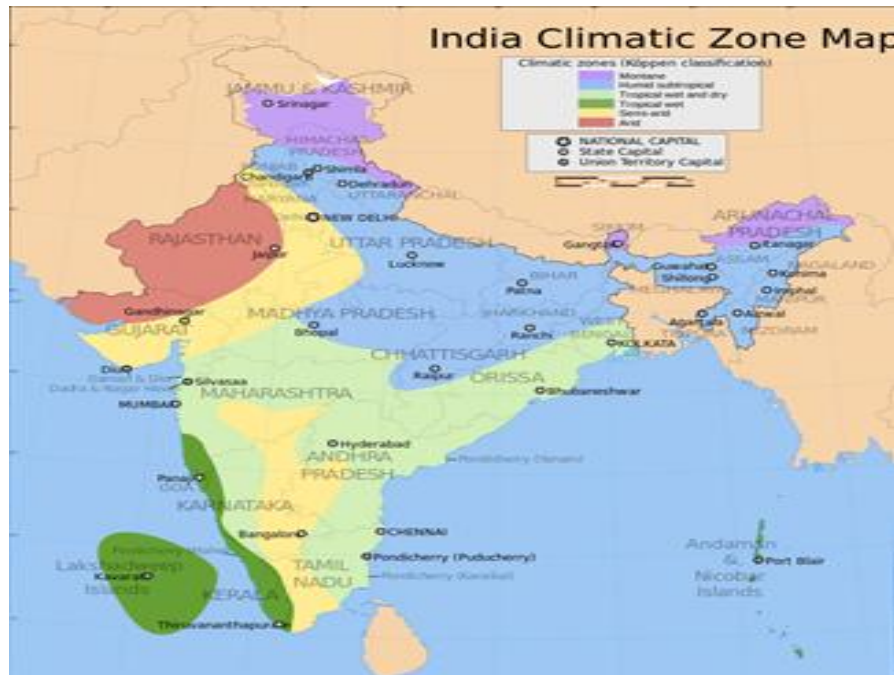


Figure 2.6: Indian Climatic Zone Map, after Koppen (Heitzman and Worden, 1996).

According to Koppen classification, India is divided into six hydrological climatic regions namely Desert, Semi Arid, Hill type, Humid Subtropical, Tropical wet and dry and Tropical wet (figure 2.6). The rainfall data for Indian subcontinent fall within a total of 347 grids of $1^{\circ} \times 1^{\circ}$. The Desert region (55 grids) consists mainly of Rajasthan and falls within 23.5° to 31.5° N and 69.5° to 75.5° E. Parts of Gujarat and Karnataka constitute the Semi Arid region of 94 grids (8.5° to 32.5° N; 70.5° to 79.5° E). The Hill type consists of 51 grids covering Himachal Pradesh and Arunachal Pradesh (26.5° to 36.5° N; 80.5° to 97.5° E). The Humid Sub

tropical consists of Uttar Pradesh having 108 grids (21.5⁰ to 31.5⁰ N; 77.5⁰ to 97.5⁰E). The Tropical wet and dry includes the states of Tamil Nadu and Andhra Pradesh having 104 grids (11.5⁰ to 23.5⁰ N; 76.5⁰ to 88.5⁰ E). Kerala and Goa constitute 67 grids of Tropical Wet (8.5⁰ to 21.5⁰ N & 69.5⁰ to 78.5⁰E).

2.6 Preprocessing

Pre processing of data is essential to preserve consistency in the data. The missing values of the parameters are filled by spline interpolation. It is the most efficient method because the interpolant is a piecewise polynomial called spline. Also the interpolation error can be made very small by using the lower degree polynomials for the spline.

2.7 Auto Regressive Integrated Moving Average (ARIMA)

A time series $\{Z_t\}$ is said to be an autoregressive process of order p , denoted as AR(p) if it is a weighted linear sum of the past p values plus a random shock so that $Z_t = \phi_1 Z_{t-1} + \phi_2 Z_{t-2} + \dots + \phi_p Z_{t-p} + \varepsilon_t$, where $\{\varepsilon_t\}$ denotes a purely random process with 0 mean and constant variance σ^2 . Using the backward shift operator B , such that $BZ_t = Z_{t-1}$ the AR (p) model can be written in the form $\phi(B)Z_t = \varepsilon_t$, where $\phi(B) = 1 - \phi_1 B - \phi_2 B^2 - \dots - \phi_p B^p$ is a polynomial in B of order p . A time series $\{Z_t\}$ is said to be a moving average process of order q , denoted as MA (q) if it is a weighted linear sum of the last q random shocks so that

$Z_t = \varepsilon_t + \theta_1 \varepsilon_{t-1} + \theta_2 \varepsilon_{t-2} + \dots + \theta_q \varepsilon_{t-q}$. Using the backward shift operator B the MA (q) model may be written in the form

$Z_t = \theta(B) \varepsilon_t$, where $\theta(B) = 1 + \theta_1 B + \theta_2 B^2 + \dots + \theta_q B^q$ is a polynomial in B of order q . A mixed autoregressive moving average model with p autoregressive terms and q moving average terms is denoted by ARMA (p, q) is $Z_t - \phi_1 Z_{t-1} - \phi_2 Z_{t-2} - \dots - \phi_p Z_{t-p} = \varepsilon_t + \theta_1 \varepsilon_{t-1} + \theta_2 \varepsilon_{t-2} + \dots + \theta_q \varepsilon_{t-q}$.

Using the backward shift operator B , this can be denoted in the form

$\phi(B)Z_t = \theta(B)\varepsilon_t$, where $\phi(B)$ and $\theta(B)$ are polynomials in B of finite order p and q , respectively. An ARIMA (p, d, q) model can be written as $\phi(B)(1-B)^d Z_t = \theta(B)\varepsilon_t$ (Box et al., 1976).

2.8 Self Organizing Maps (SOM)

SOM is a clustering and data visualization technique based on NN. The aim of an SOM is to find a set of centroids and to assign each object in the data set to the centroid that is closest to that object (Sivanandam and Paulraj, 2003). There is one neuron associated with each centroid. SOM is an unsupervised learning technique. By attempting so, each object in the dataset is assigned to the centroid which is the best approximation of that object (Dostal and Pokorny, 2008; Sarah et al., 2011).

2.9 Cluster validation

There are several cluster validity measurement techniques proposed by different authors (Kovács, 2005). The criteria widely

accepted among them for partitioning a data set into a number of clusters are: a) the separation of clusters and b) the compactness. Halkidi and Michalis, (2001) define the clustering validity index, S_Dbw, based on cluster's compactness (in terms of intra-cluster variance) and density between clusters (in terms of inter-cluster density).

2.9.1 Inter-Cluster Density (ID)

It evaluates the average density in the region among clusters in relation with the density of clusters.

$$Dens_bw(c) = \frac{1}{c(c-1)} \sum_{i=1}^c \sum_{j=1}^c \frac{density(u_{ij})}{\max\{density(v_i)density(v_j)\}}$$

where v_i and v_j are centers of clusters, c_i and c_j respectively and u_{ij} the middle point of the line segment defined by the cluster's centers v_i and v_j .

$$Density(u) = \sum_{i=1}^{n_{ij}} f(x_i, u)$$

where n_{ij} number of tuples that belong to the clusters, c_i and c_j , i.e. $x_i \in c_i \cup c_j \subseteq S$, (the data set) represents the number of points in the neighborhood of u . Also,

$$f(x, u) = \begin{cases} 0, & \text{if } d(x, u) > stdev \\ 1, & \text{otherwise} \end{cases}$$

where $stdev = \frac{1}{c} \sqrt{\sum_{i=1}^c \|\sigma(v_i)\|}$ is the average standard deviation of clusters.

2.9.2 Intra-cluster variance- Average scattering for clusters

$Scat(c) = \frac{1}{c} \sum_{i=1}^c \frac{\|\sigma(v_i)\|}{\|\sigma(S)\|}$ The p^{th} dimension of $\sigma(S)$ is defined by

$\sigma_x^p = \frac{1}{n} \sum_{k=1}^n (x_k^p - \bar{x}^p)^2$ and that of $\sigma(v_i)$ is given by

$$\sigma_{v_i}^p = \frac{1}{n_i} \sum_{k=1}^{n_i} (x_k^p - v_i^p)^2 .$$

Then the validity index is defined as $S_Dbw(c) = Scat(c) + Dens_bw(c)$

The number of clusters c that minimizes the above index is considered as an optimal value for the number of clusters present in the data set.

2.9.3 Silhoutte Coefficient

For a data set D , of n objects, let D be partitioned into k clusters c_1, \dots, c_k . For each object $o \in D$, $a(o)$ is the average distance between o and all other objects in the cluster to which o belongs. $b(o)$ is the minimum average distance from o to all clusters to which o does not belong. [Han, 2012]. For $o \in c_i, 1 \leq i \leq k$, $a(o) = \frac{\sum_{o' \in c_i, o' \neq o} dist(o, o')}{|c_i| - 1}$ and

$$b(o) = \min_{c_j: 1 \leq j \leq k, j \neq i} \left\{ \frac{\sum_{o' \in c_j, o' \neq o} dist(o, o')}{|c_j|} \right\} \text{ where } o' \text{ is the complement of } o .$$

The Silhoutte coefficient is given by $s(o) = \frac{b(o) - a(o)}{\max[a(o), b(o)]}$.

2.10 Performance of the Model

The performance of the model is evaluated using the following parameters:

- a) Correlation Coefficient

$$CC = \frac{n \sum O_i P_i - (\sum O_i)(\sum P_i)}{\sqrt{n(\sum O_i^2) - (\sum O_i)^2} \sqrt{n(\sum P_i^2) - (\sum P_i)^2}}$$

Where O_i, P_i are the observed and the predicted values of rainfall for the year i respectively and n is the total number of years to be predicted.

- b) Root Mean Square Error $RMSE = \sqrt{\frac{\sum (y_i - \hat{y}_i)^2}{N}}$ where y_i are the observed values, \hat{y}_i are the predicted values for rainfall and N is the number of observations.

- c) The normalized root-mean-square error (NRMSE) is the RMSE divided by the range of observed values of a variable being predicted and is expressed as a percentage. $NRMSE = \frac{RMSE}{x_{\max} - x_{\min}}$ where x_{\max} and x_{\min} are the maximum and minimum of the observed values.

- d) Coefficient of variation (CV) is defined as $CV = \frac{\sigma}{\bar{x}} \times 100$ where σ and \bar{x} are standard deviation and arithmetic mean respectively.

e) Mean Absolute Error (MAE)

$$\text{MAE} = \frac{|y_i - \hat{y}_i|}{N}$$

Where y_i the observed values and \hat{y}_i are the predicted values for rainfall and N is the number of observations.

f) Prediction error

$$E = 1 - \frac{\sum_{i=1}^N (O_i - P_i)^2}{\sum (O_i - \bar{O})^2}$$

Where o_i is the observed value, p_i . predicted value, \bar{O} - observed mean.

g) Accuracy = 100 - RMSE.

2.11 Trend analysis

Trend analysis is used to study the past events and also to predict the future events. It is a statistical technique to extract the pattern hidden in a time series data. Regression analysis is used to find the slopes, rate of change of the dependent variable with respect to the independent variable. The magnitude of trend of SST/ rainfall/ sub surface temperature was found using regression analysis. The linear trend value, from $y = mx + c$, representing the slope of the regression line indicates the rate of rise/fall in the variable, fitted to each grid. The slopes m_i of all data pairs are calculated by $m_i = \frac{x_j - x_k}{j - k}$ for $i = 1, 2, \dots$ where x_j and x_k are the values at j and k ($j > k$). Trend analysis was performed with a level of significance of 95%.

2.12 Methodology

The raw weather data are in the form of a time series. The data is pre processed. To preserve smoothness and consistency, the missing values are filled by spline interpolation which is an effective method in the case of a time series data where the missing value is related to its previous and next values. Then the outliers are filled by the extreme values. The data is divided into 3 subsets, one for training, second subset for validation and the third for testing. Since it is difficult to analyze large amount of data, clustering is done for the rainfall data because clustering improves the understanding of natural climate processes, to assess the quality of results and to identify prevailing system features and their typical scales for specific atmospheric regions (Nocke et al., 2004; Dostal and Pokorny, 2008; Sarah and El-Halees, 2011). The inputs are fed to the system and feed forward back propagation algorithm is applied to it. The flow chart on the procedure is given in figure 2.7.

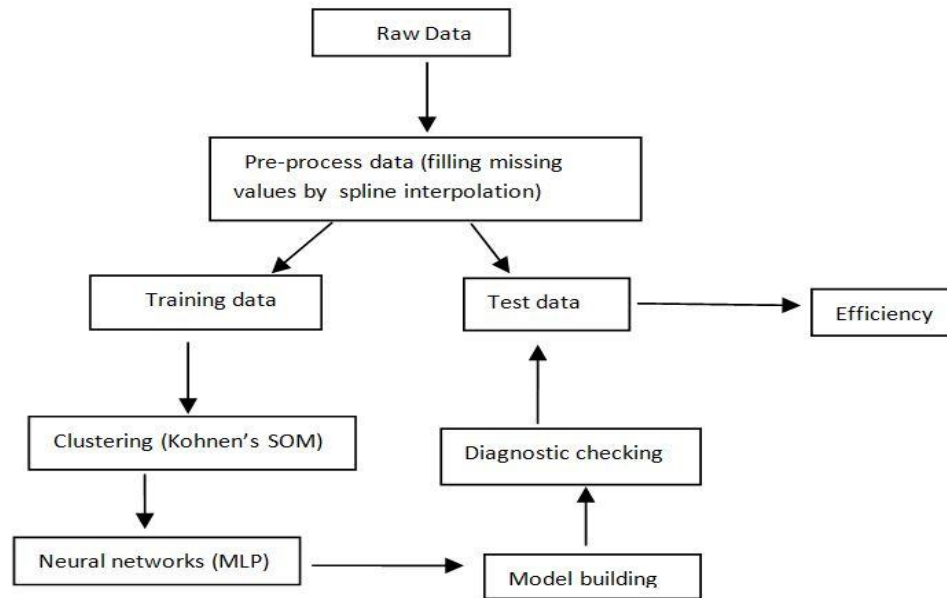


Figure 2.7: Flow chart on data processing.

2.13 Software Tools

To process and analyze the data, the following software packages were made use of:

- SPSS - For statistics analysis
- MINTAB - For drawing the temporal trends
- MATLAB - For the major data analysis
- GMT - For drawing the spatial trends and clusters

CHAPTER 3

LONG TERM TRENDS OF SST, SUB SURFACE TEMPERATURE AND ITS RELATIONSHIP WITH RAINFALL

3.1 Introduction

Oceanographers and Meteorologists have indicated great interest by continuing their investigations on the trends of SST in the context of Global Warming. It is obvious that oceans play an important role in the climate system as they absorb the excess solar heating from the green house gases due to their large heat capacity (Levitus et al., 2005). A warming trend in the oceans has been observed in recent decades (IPCC, 2001; Levitus et al., 2001, 2005). According to IPCC Fifth Assessment Report, (2013) the upper ocean (above 700m) has warmed from 1971 to 2010. Global average SST has increased from the beginning of 1950's and the average SST of IO has increased by 0.65°C within the period 1950-2009. They have observed that the strongest warming occurs (0.09°C to 0.13°C / decade) near the sea surface in the upper 75m between 1971 and 2010. However, based on 5 year averages, oceans had warmed between depths, 700m and 2000m from 1957 to 2009 (IPCC, 2013) and had warmed from 300m to the bottom from 1992 to 2005, but no significant trends in global average temperature could be observed between 2000m and 3000m depth during this period. Interestingly, warming below 3000m has been noticed as the largest in the Southern Ocean. They have also suggested that the regional changes observed in winds, stratification, ocean currents, oxygen depth, nutrient availability, surface salinity in many oceanic regions may be a result of anthropogenic greenhouse gas emissions. Oceans will continue to warm and acidify and the rates will differ from region to region (IPCC, 2013). Importantly, SST has a positive trend higher than $0.01\pm 0.005^{\circ}\text{C}$ /year for the past 24 years (1982-2005)

within 300-1000km band northward of the Antarctic coast. But for the Southern Ocean it has a negative trend of $-0.02 \pm 0.003^{\circ}\text{C}/\text{year}$. Trends in SST are more than $-0.065 \pm 0.007^{\circ}\text{C}/\text{year}$ in the area between the south west Pacific Basin and Pacific -Antarctic Ridge, and southward of the Argentine Basin and Mid-Atlantic Ridge (Lebedev, 2007). Aoki (1997) had observed significant warming trends 0.02 to $0.04^{\circ}\text{C}/\text{year}$ throughout the depths of 200-400m in the western region of IO (50° to 90°E , 58° to 61°S). Rajeevan et al., (2008) supports the hypothesis that the increasing trend of extreme rainfall events in the last five decades is associated with the increasing trend of SST and surface latent heat flux over the Tropical IO. Chowdary et al.,(2006) had studied the changing trends in the Tropical IO SST during La Nina years and found that the variability in the latent heat flux anomalies after 1976 to remain consistent with the SST anomalies. The variability in the long term temperature and sea level over north IO during the period 1958-2000 has been investigated by Bijoy et al., (2008). They have observed that both SST and sea level show an increasing trend. The SST anomalies over the western and eastern poles of the IO dipole show a clear warming trend during 1880-2004, particularly after 1950 (Ihara et al., 2008). During 1880-1919, more negative IO dipole events occurred in September – November months than positive events. Strong and positive events occur after the year 1960. According to Singh and Sarker (2003), an increasing trend in SST was seen in the coastal regions of north IO during all seasons. Haron and Afsal (2012) observed that warmer SST's over AS cause a weak precipitation and lower temperatures over Pakistan. Roxy et al., 2014 reveals that the western tropical IO has been warming for more than a century at a rate faster than

any region of the tropical oceans and in this process, has attained the warm pool SST values of 28°C . The western basin experienced an increase of 1.2°C in summer SST's. North IO SST's has witnessed an increasing trend of 0.4°C to 0.8°C during May from 1961-86 (Singh, 1999). Krishnan et al., (2006) noted that SW monsoon is largely affected by the SST of IO. Again, Roxy et al., (2014) have observed that the western IO (5°S to 10°N , 50° to 65°E) shows a continuous warming since the beginning of 20th century; but the rest of the IO including warm pool, the warming is prominent only after 1950. The mean summer SST over the Western IO was cooler in comparison to the rest of the IO. And during 1901-2012, the western IO experienced a warming of up to 1.28°C , and resultant warm pool warming was around 0.78°C . In this context, ocean warming features invite special attention, since such system changes bring about large scale alterations in associated phenomenon.

A wide range of variability is often noticeable in Indian Summer Monsoon Rainfall (ISMR), based on daily, seasonal, decadal and annual analyses. Many meteorologists have worked on the spatial and temporal trends of rainfall in India (Goswami et al., 2006, Guhathakurta and Rajeevan, 2008; Ghosh et al., 2009; Dugam., 2012). One of the latest studies by Subash and Sikka (2014) observed that there is a significant variation in the monthly mean rainfall within the meteorological subdivisions of India, in which the North East (NE) received the extensive quantum of rainfall in all months except January while all other regions received the highest rainfall during July; but the peninsular region recorded two rainfall peaks [bi-modal], one in July and another in October. Naidu et al., (1999) studied the trends and periodicities of annual rainfall

for 29 sub divisions of India for a long period of 124 years (1871-1994) using linear regression technique. They used 11 year moving averages and found that in some subdivisions the trend in one direction reversed its direction after a few years. Oza and Kishtawal, (2014) studied the linear trend analysis of daily gridded rainfall data ($1^0 \times 1^0$ spatial resolution) for the period 1951-2010 and they observed that there is a decreasing trend in ISMR and based on rainfall, a strong agreement between gridded and meteorological subdivisions. According to Goswami et al., (2006) even though the climatological mean of ISMR had remained constant for the past 100 years with mild variations in inter decadal cases; there is a significant increase in the extreme monsoon events in central India over the past 50 years. Nair et al., (2014) have studied spatio- temporal analysis of Indian rainfall over a period of 100 years spanning from 1901 to 2000. They have reported that rainfall trend is decreasing significantly in almost all regions. Again, Oza and Kishtawal, (2014) studied the spatial trends for the period 1951-2010 using the $1^0 \times 1^0$ gridded rainfall data and observed that there is a decreasing trend in ISMR especially in NE. These studies all indicate that rainfall pattern over India is changing and is a subject of great interest given its significant role for an agro-based country.

An attempt is made in this chapter to analyze the trend of ISMR during the period 1960-2012 along with the spatial and temporal trends in SST in IO and with the analysis of sub-surface temperatures (up to 967m) to evolve a clear idea on ocean heating progression and verify the results from earlier workers.

3.2 Spatial trend in SST

A detailed study was carried out on the spatial and temporal trend analysis of SST from IO for the period 1960-2012 for four seasons namely winter, pre monsoon, monsoon and post monsoon, and annual (January to December), and for all the individual 12 months, which is depicted in the following figures 3.2.1 and 3.2.2. The slope of annual SST ($^{\circ}$ C/decade) indicates very distinct features for the entire IO. The linear trend in the time series is determined using regression analysis for SST/Sub surface temperature/ rainfall (discussed in the last chapter).

The most evident result pertains to an increased warming rate for the region south of equator in the central IO having an area covering 60° E to 90° E and up to around 16° S. This result agrees with the findings of Roxy et al, 2014. Significant warming trend was also observed in Bay of Bengal (BOB) [0.2 to 0.3° C/decade] than in Arabian Sea (AS) which agrees with the observations of Dinesh Kumar, 2016. Significant warming (0.2 to 0.3° C/decade) is noticed in the subtropics for annual and for all seasons [figure 3.2.1] except for winter and pre monsoon. “Madagascar High” (a pocket of higher warming rate is observed near Madagascar) is noticed for annual and for all seasons. During winter, warming at central IO extends up to 25° S and is seen above the equator on the east of 100° E. A significant change is noticed for 5° S to 25° S, 55° E to 70° E when the season changes from monsoon to post monsoon. For the season, monsoon, a significant warming is noticed from 65° E to 100° E. Warming trend in BOB is more significant than that in AS for all seasons. There is a positive trend in temperature near the equator and south IO during all the four

seasons. A warming trend was noted during all seasons (figure 3.2.1) which is in tune with the results of Singh and Sarker, 2003.

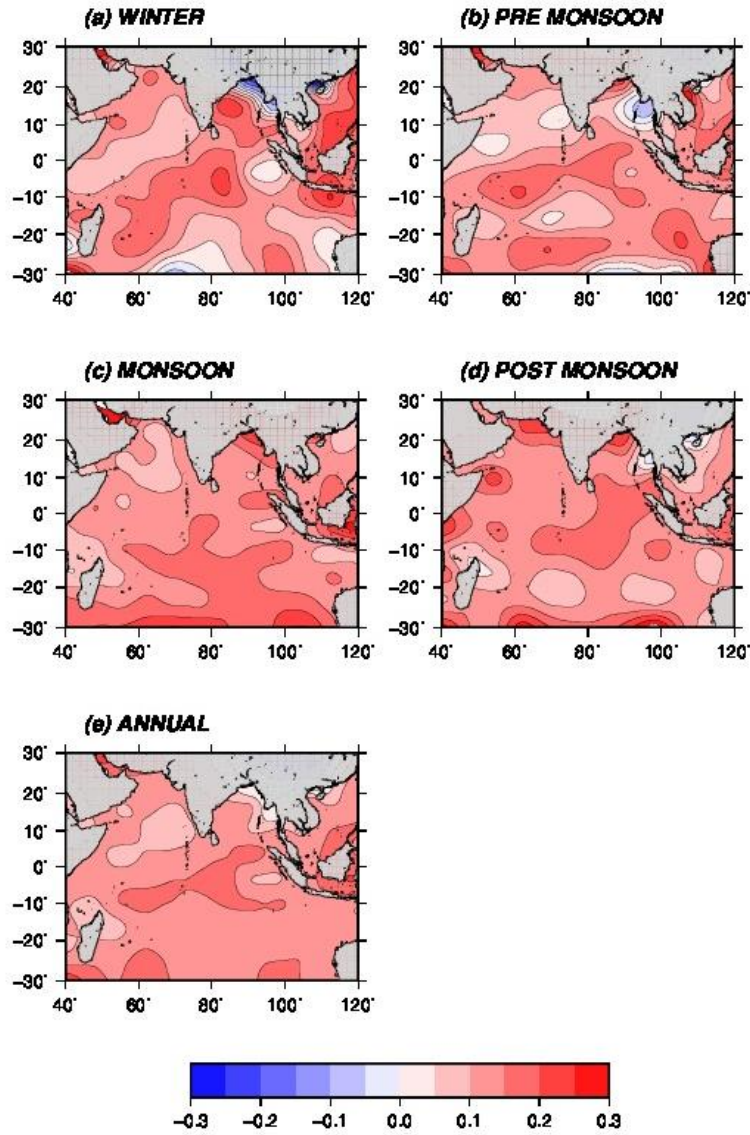


Figure 3.2.1: Spatial SST trends ($^{\circ}\text{C}/\text{decade}$) of four seasons and annual for the period 1960-2012.

In order to further delineate ocean surface features with respect to warming and cooling trend over the past 53 years (1960-2012), regression analysis was performed on monthly SST data (figures 3.2.2 & 3.2.3). This analysis helped in identifying those regions which are consistently indicating warming trends along with a few other locations which also reflect either cooling or no significant change. A particular point of interest is that none of these months indicate SST cooling except for some parts of North East (NE) and subtropics which might have occurred due to the artifact of ship track arising out of ICOADS data formulations. While many months support the warming trend with core values exceeds $0.25^{\circ}\text{C}/\text{decade}$ (figures 3.2.2 & 3.2.3). This result supports previous findings [Rao et al., 2012]. The earlier figure shows a net positive slope of around $0.25^{\circ}\text{C}/\text{decade}$, while on the lower side cooling is restricted to around $-0.15^{\circ}\text{C}/\text{decade}$ for some parts of NE oceanic region. In light of above, the monthly trends help to deduce the following features.

The waters south of 20°S reports an overall warming trend admixed with few locations of lower rate or no change. Interestingly, parts of Eastern AS & Eastern BOB indicate surface waters which neither warm nor cool and any such cooling trend is of a minor magnitude. To generalize the analysis based on annual SST values, from a perspective of climate change, rising SST's strongly indicate the established presence of warming processes in IO. Particular emphasis falls on central south waters which indicate an overall rise of 0.25° to 0.3°C for this part of the ocean which is in agreement to the finding of Roxy et al., 2014. These analysis have paved way towards identifying those regions which are consistently indicating warming trends along with a few other locations which also

reflect either cooling or no change. Such a statement would be an under estimation of events that occur at this location when considering slopes on a monthly basis which occurred due to the low density of data. For example, in the month of January, the central region in contrast to the eastern section indicate cooling tendency counteracting the warming trends around 85°E. Other areas show a mixed response. February, March and even during April, the cooling trend continue to dominate in the NE areas which could be again due to uneven data samplings. A marked change is observed for the month of May resulting in values close to 0.3°C/decade for these waters. The warming trend of June is followed by another warming phenomenon during August, September and November. During October and December, a small pocket of cooling is observed in the NE around 20°N. “Madagascar High” is observed during almost all months. It was noticed that for the region south of 20°S both warming and cooling processes had co-occurred.

Often quoted in literature, the vast waters of SIO exhibit highest warming trend among all other oceanic waters [Annamalai (2005), Rao et al., (2012)] which is confirmed in this study. January and February are the months of increased warming in the central regions (equator to 20°S). However during March, the foci of the warming shifts westward to around 60°E. The months January to April indicate basically a warming trend of lower dimension intertwined with regions of cooling in the NE which is an artifact of ship tracking of ICOADS data. The April SST based analysis has resolved an area just north of the equator around 54°E to 62°E to be a location to promote cooling. Often the cooling occurred around the subtropics and 85° NE which is an area of low data density. However

October promotes positive rate of increase in temperatures followed by more intense heating on the eastern parts of SIO. The cumulative impacts in the realm of climate change can be easily summarized as net gain in surface temperatures for this part of the ocean.

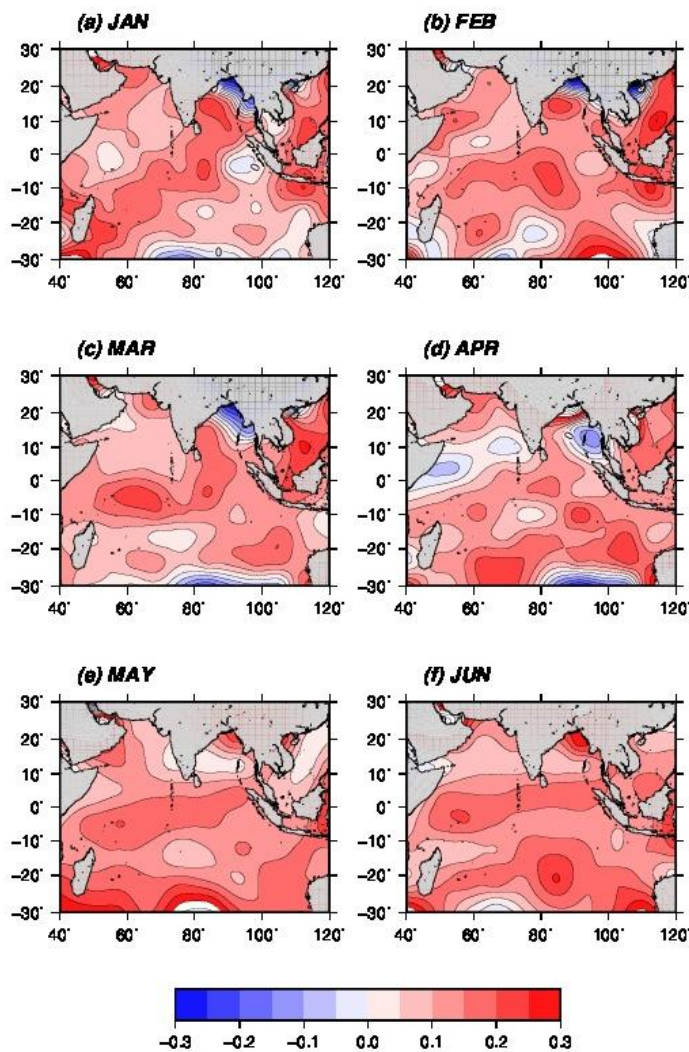


Figure 3.2.2: Spatial SST trends ($^{\circ}\text{C}/\text{decade}$) of the months January to June for the period 1960 to 2012.

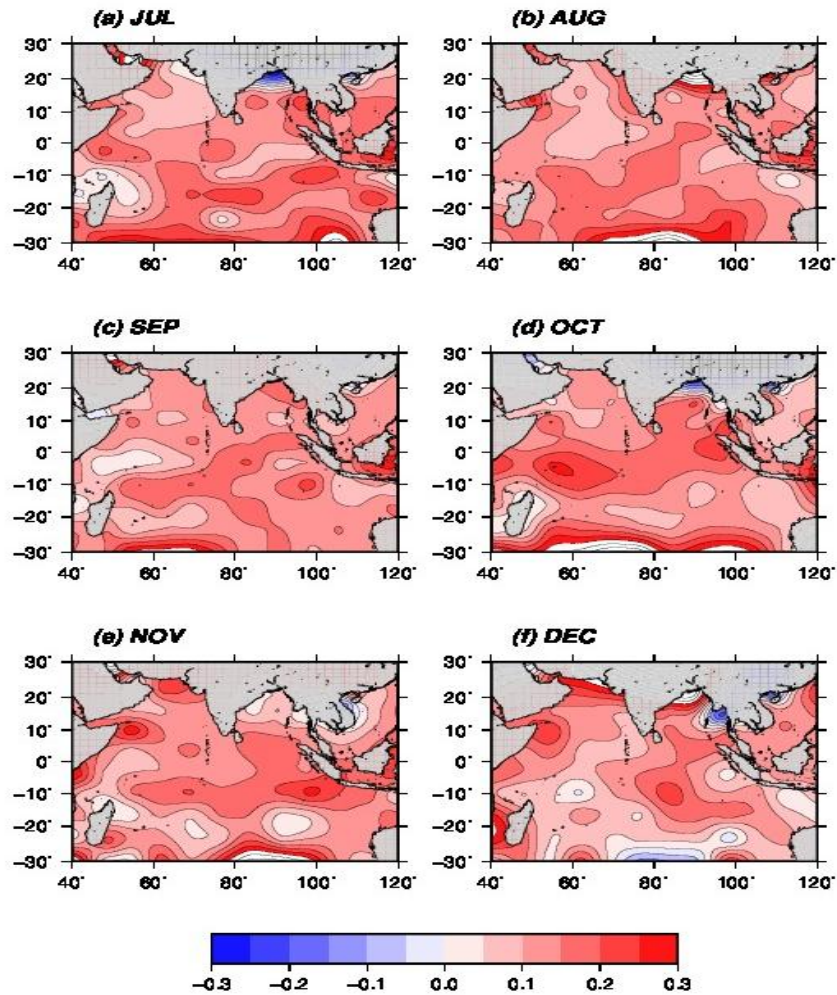


Figure 3.2.3: Spatial SST trends ($^{\circ}\text{C}/\text{decade}$) of the months July to December for the period 1960 to 2012.

Next, we consider the two sectors of the northern IO (NIO) namely AS on the west and BOB on the east. Both the sectors reveal interesting features. Eastern waters often indicate no appreciable changes or likely are to be cooled based on half a century of data while the western ocean show

positive trends in warming. This aspect was closely counterchecked through the monthly charts and conspicuously 7 out of 12 months exhibit the dual behavior of a cooler east compared to a warmer west in either of the NIO basins. The contrast occurs during April for AS. A number of reasons could be attributed to such variability during the above stated months and one such factor could be the monsoonal rains along with cloud cover bringing about changes in incoming solar radiations. Often the cooling occurs around 60°E or further westwards and finds support in the studies by Kenyon, 2014. However, October promotes positive rate of increase in temperatures followed by more intense heating on the eastern parts of SIO which culminates in more areas indicating a warming trend during December. The cumulative impacts in the realm of climate change can be easily summarized as net gain in surface temperatures for this part of the ocean. Further parts of these basins are inadequately probed, and with refinement, better resolution of features could be expected. Table 3.1 shows the decadal trend in SST and the figure 3.2.4 shows the decadal trend of mean SST for the tropical Indian Ocean.

In a global warming scenario, contradictions could be expected. The monthly SST based analyses have resolved an area just north of the equator around 54°E to 62°E to be a location to promote cooling, a feature which is also supported by the observations of Vivekanandan (2010). Reasons as to this stand alone phenomenon cannot be resolved by trend analysis studies. In the discussion to follow, better attempts are being made to understand the variability by comparing pre-fixed areas in separate sections of the ocean.

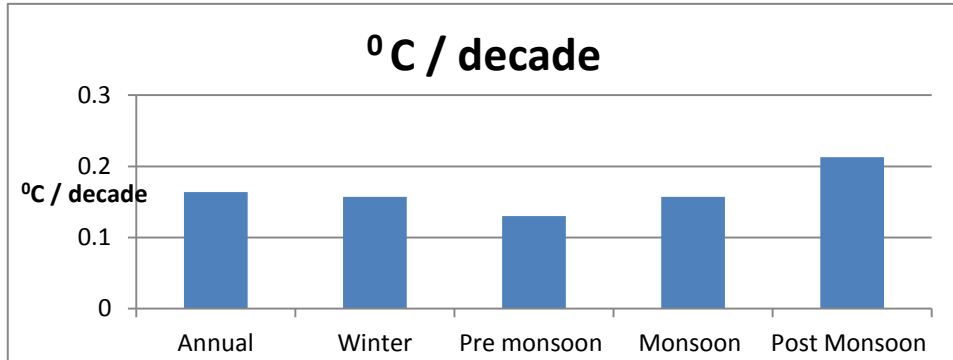


Figure 3.2.4: Decadal trend of mean SST for the Tropical IO.

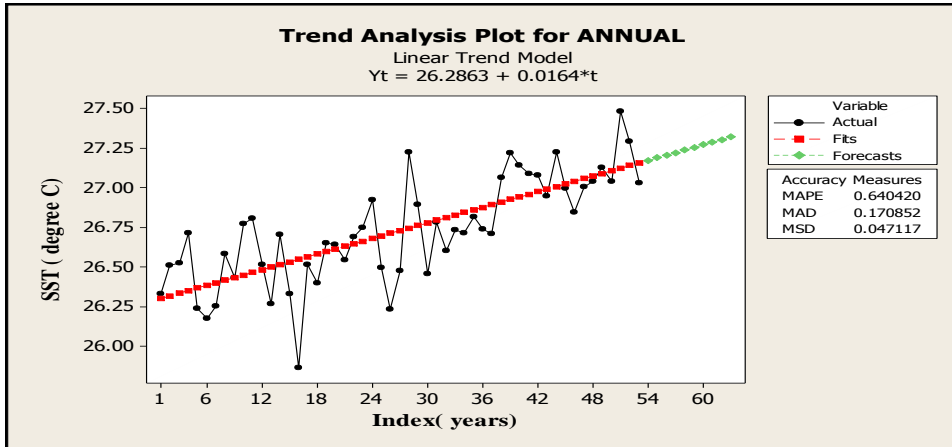
Table 3.1: Range of decadal trend in SST.

| | |
|--------------|-----------------------------|
| Annual | 0.05 to 0.25 ⁰ C |
| Winter | -0.1 to 0.3 ⁰ C |
| Pre monsoon | -0.1 to 0.3 ⁰ C |
| Monsoon | 0.05 to 0.3 ⁰ C |
| Post monsoon | 0.05 to 0.3 ⁰ C |
| January | -0.1 to 0.3 ⁰ C |
| February | -0.1 to 0.3 ⁰ C |
| March | -0.1 to 0.3 ⁰ C |
| April | -0.1 to 0.3 ⁰ C |
| May | 0.05 to 0.25 ⁰ C |
| June | 0.05 to 0.3 ⁰ C |
| July | -0.15 to 0.3 ⁰ C |
| August | 0.05 to 0.3 ⁰ C |
| September | 0.05 to 0.3 ⁰ C |
| October | -0.1 to 0.3 ⁰ C |
| November | 0.05 to 0.3 ⁰ C |
| December | -0.1 to 0.3 |

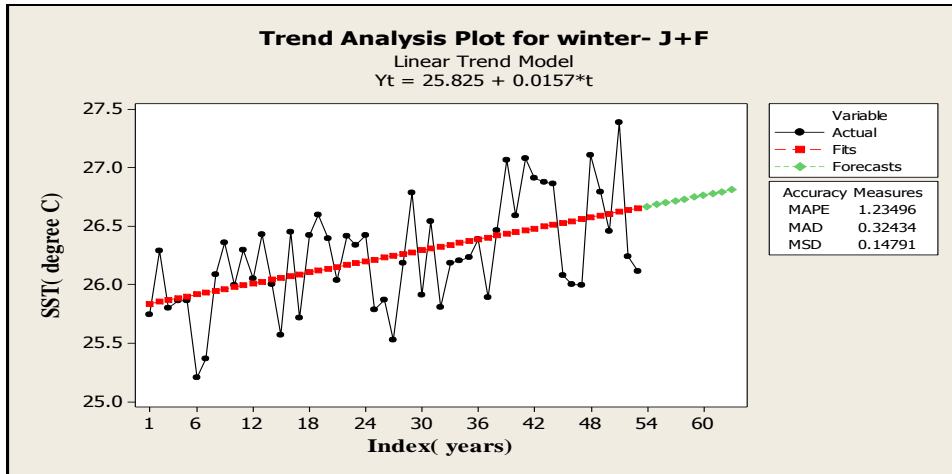
3.3 Temporal trends of SST

Temporal trend analysis of SST, averaged over the tropical IO for the period 1960-2012 for annual and for the four seasons is depicted in the figure 3.3.1. Slopes are calculated in $^{\circ}\text{C}/\text{year}$. In the annual, we have noticed a steady increase of warming of about 1°C in 50 years. Temperature is more scattered up to the year 1985 and becomes steady later. There were 3 cooling and 2 warming events prior to 1985. Decrease in average values are observed since 2010. During winter season the warming trends are milder compared to the annual. Yearly averages are equally distributed on either side of the best fit. Since 2000, winter variability either positive or negative is largely amplified than the past 40 years. For pre monsoon season, 3 extreme conditions post 1985 (for the years 1987, 1998, and 2010) with positive increase dominates the analysis. No average values indicate extensive cooling. All other values indicate uniform spread within the envelope with gradual increasing. During monsoon season, no large scale variations are observed on either side of the mean, but oceans are consistently warming. The trend of post monsoon is similar to that of annual, pre monsoon and monsoon. Monsoon and Post monsoon cooling events are two to four in number in the case of pre1985 events. Now it can be authentically stated that irrespective of seasons based on linear analysis, IO is in a warming state more significantly since 1985. It is evident that for the region under discussion namely south of 20°S , a location where both warming and cooling processes along with long span of months of mixed behavior will culminate in a net warming trend of around 0.15°C to $0.20^{\circ}\text{C}/\text{decade}$. Now it can be authentically

stated that irrespective of seasons based on linear analysis, Indian Ocean is warming definitely, post 1985.

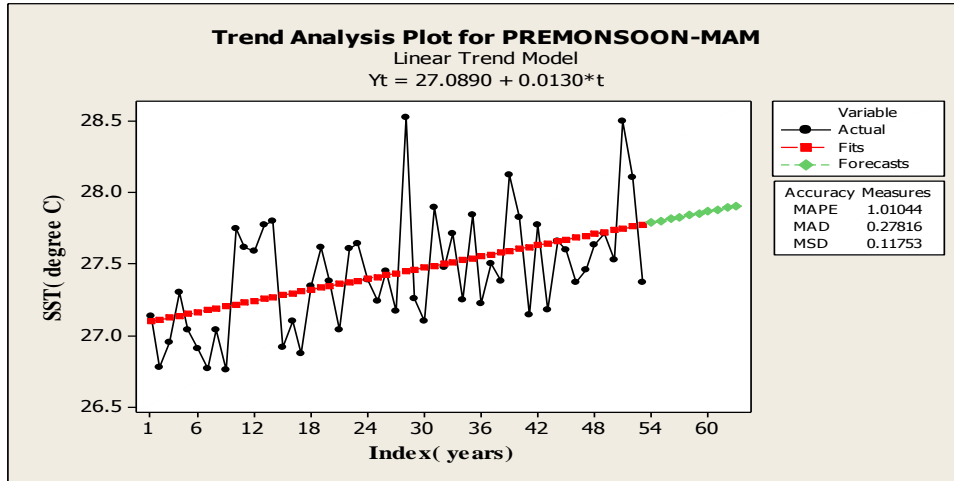


(a)

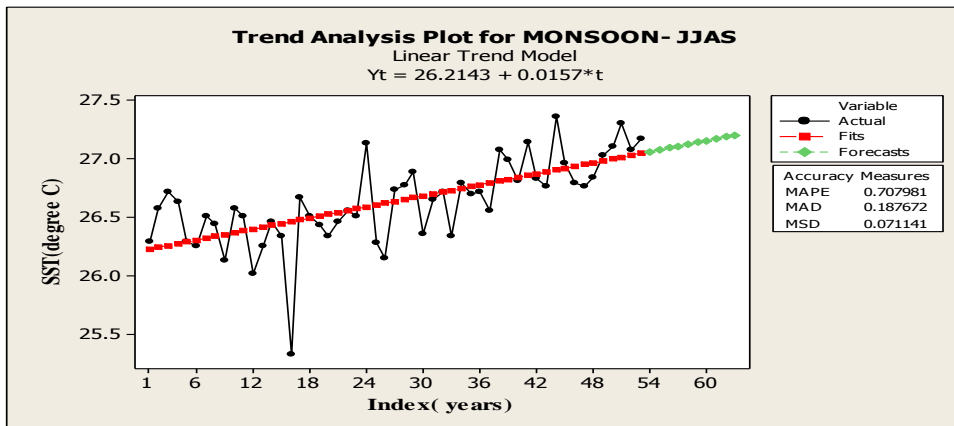


(b)

Figure 3.3.1: Trend of SST for the period 1960-2012 (a) annual (b) winter.

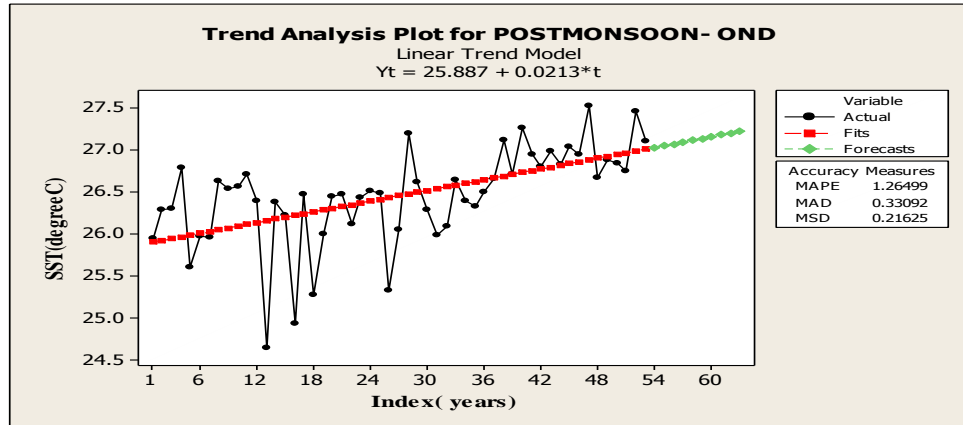


(c)



(d)

Figure 3.3.1: Trend of SST for the period 1960-2012 (c) pre monsoon. (d) monsoon.



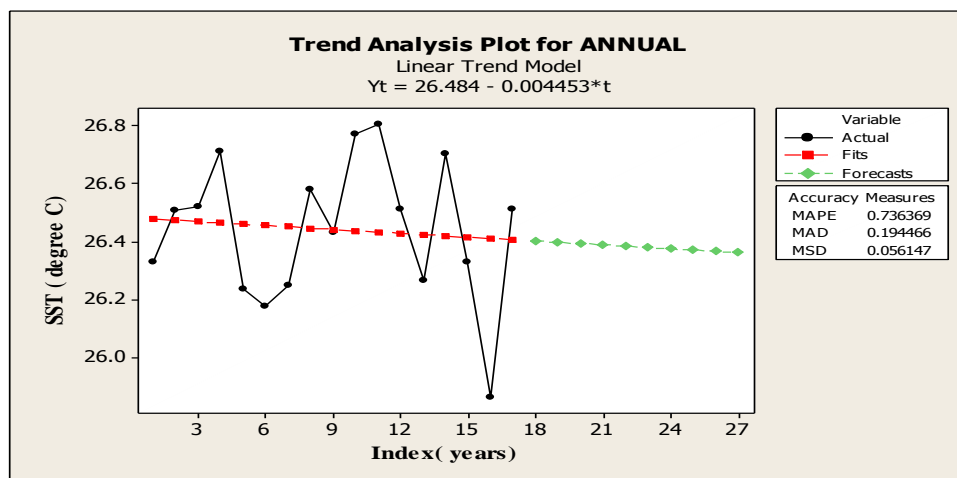
(e)

Figure 3.3.1: Trend of SST for the period 1960-2012 (e) post monsoon.

Meteorologically 1976-78 is a known episode on changes from one pattern to another. Many researchers have studied the reasons for the climate shift which occurred after 1976. The SST anomalies too support this fact (Kitoh, 1993 and Graham, 1994). To understand the behavior of SST trends in detail, the two epochs 1960-76 (figures 3.3.2) and 1977-2012 (figures 3.3.3) are also considered for this study.

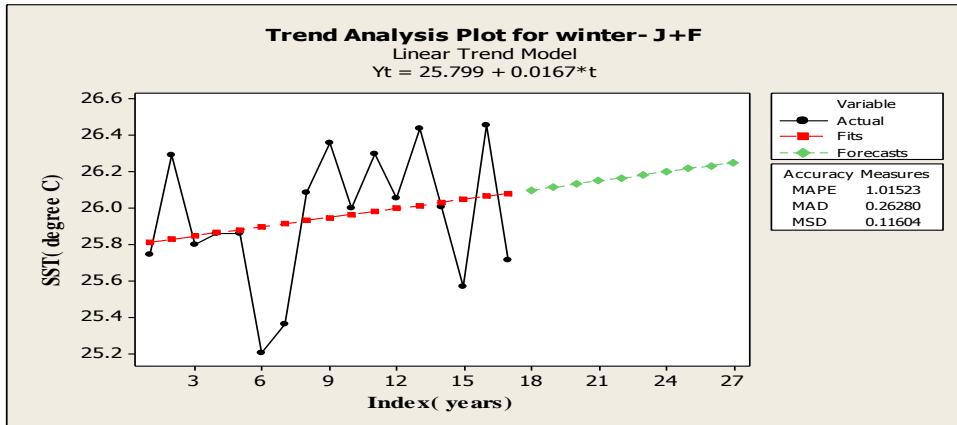
When the epoch of 1960-76 was considered, the following observations have been made. The annual analysis shows a decreasing trend. Three warming and three cooling trends are visibly noticed (figures 3.3.2).

- The trends of the winter season show an increase of around 0.30°C . There are four warming and three cooling points observed.
- During pre monsoon season, a high variation of the order of 0.80°C to 1.00°C is noticed prior to 1976. Four warming events and four cooling events are noted.
- During monsoon season, the trend show no large scale variations on either side of the trend line except for the years 1975 and 1976.
- For post monsoon season, Oceans were warming consistently but two cooling events occurred prior to 1976.

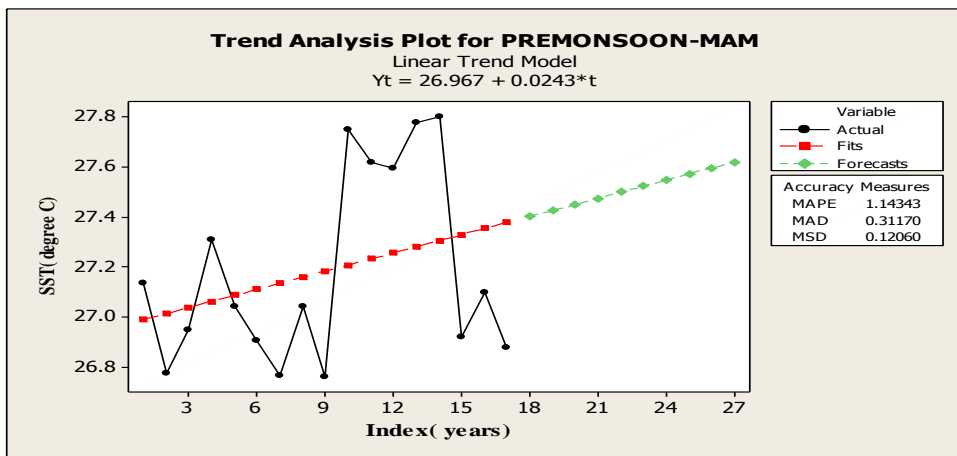


(a)

Figure 3.3.2: Trend of SST for the period 1960-1976 (a) annual.

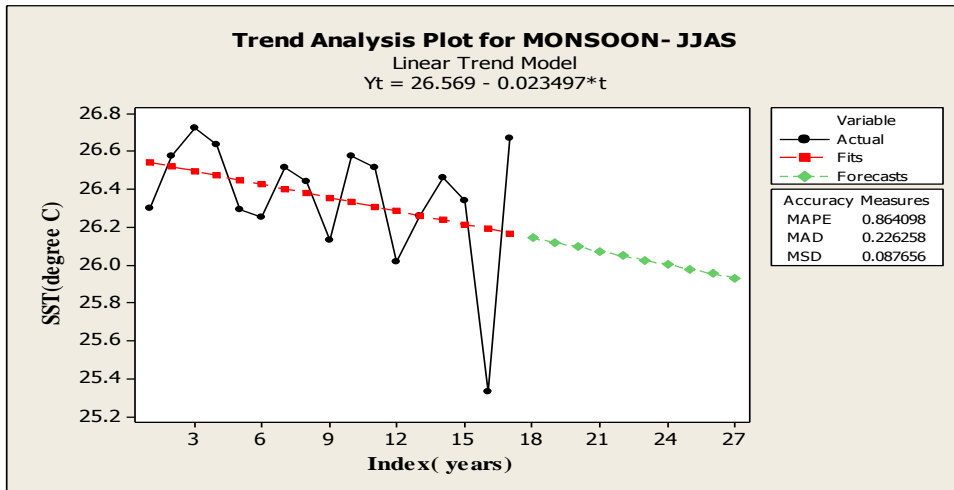


(b)

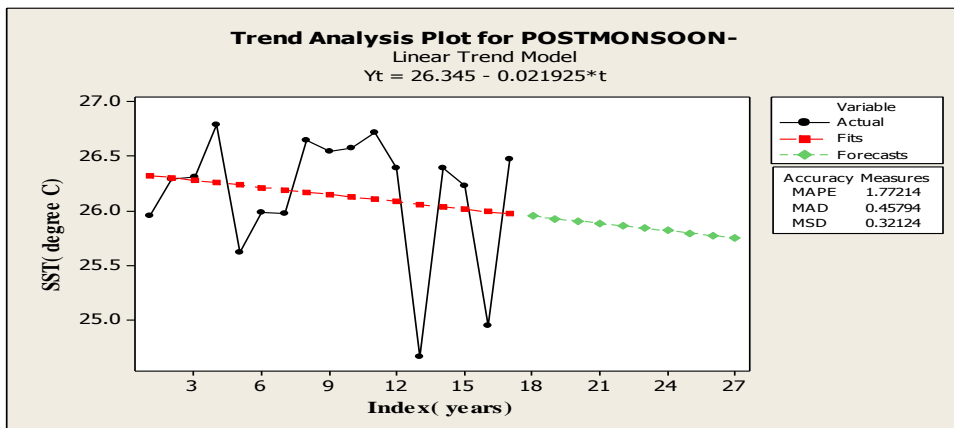


(c)

Figure 3.3.2: Trend of SST for the period 1960-1976 (b) winter (c) pre monsoon.



(d)



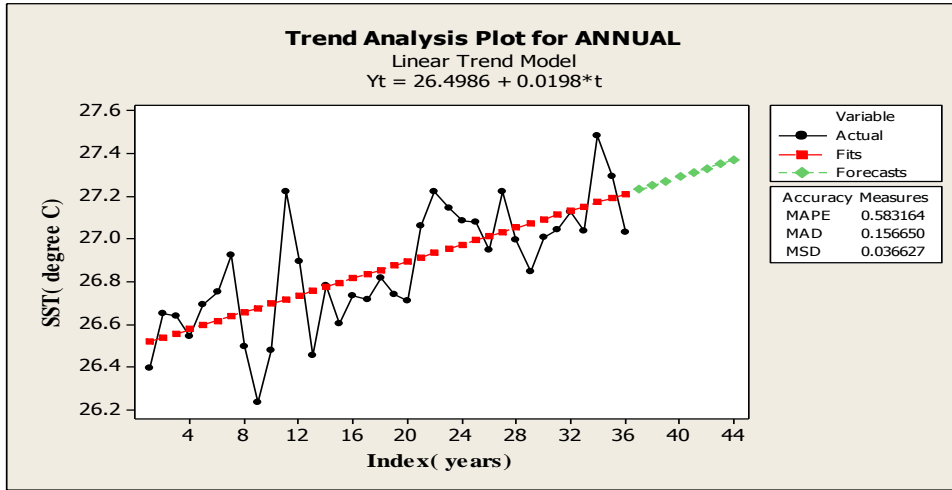
(e)

Figure 3.3.2: Trend of SST for the period 1960- 1976 (d) monsoon

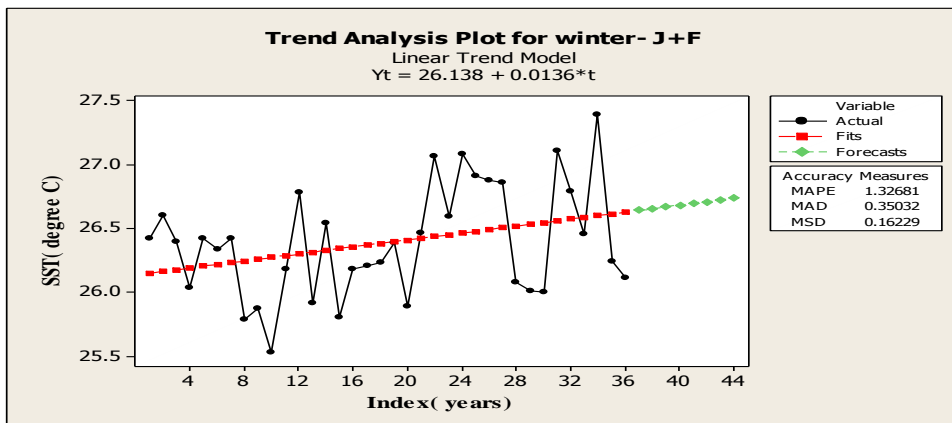
(e) post monsoon.

The trend analysis plots given below depict the trends during the epoch 1977-2012 (figures 3.3.3).

- A very high increase in temperature of about 1°C is noticed for Annual, which is evident in the year 2010.
- During winter, a variation of the order of 1°C is observed. Five warming events and five cooling events are noticed.
- The temperature showed an increase of up to 28.4°C for two years during Pre monsoon.
- During Monsoon season, no large scale variations on either side of the trend line are observed, but the oceans are consistently warming.
- An increase of around 1.50°C during post monsoon season.

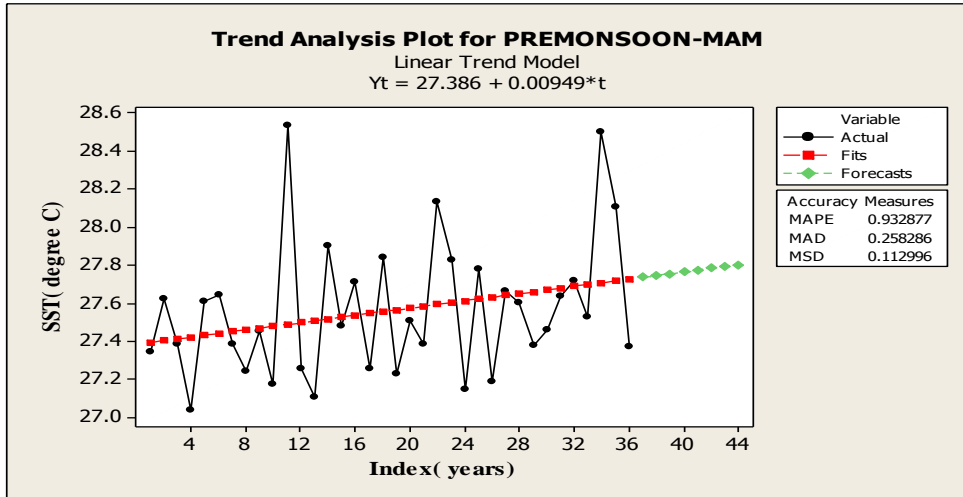


(a)

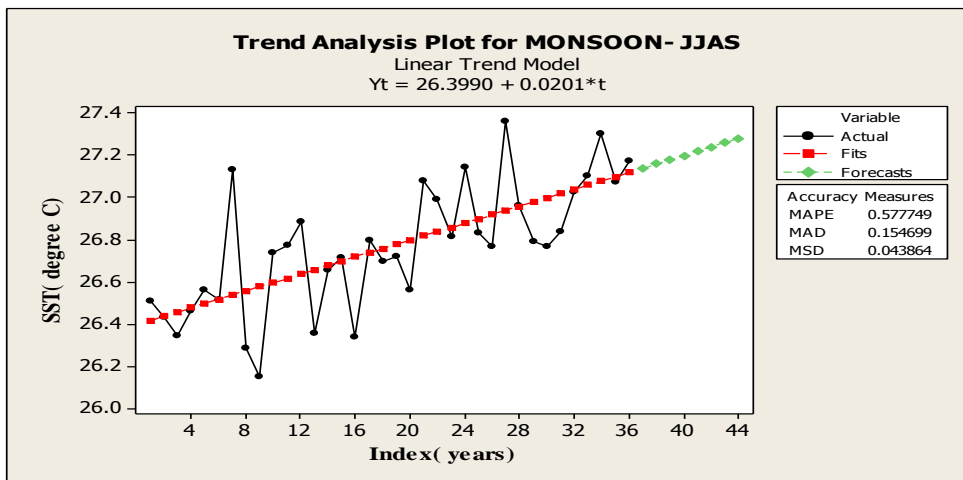


(b)

Figure 3.3.3: Trend of SST for the period 1977-2012 (a) annual
 (b) winter.



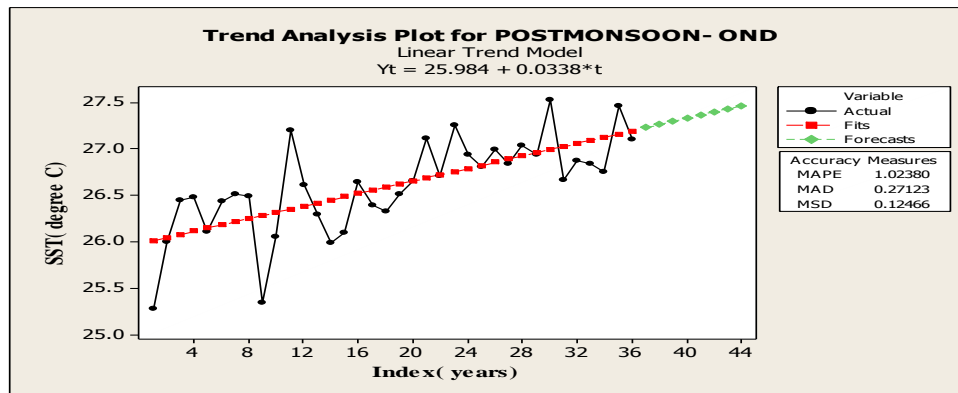
(c)



(d)

Figure 3.3.3: Trend of SST for the period 1977-2012 (c) pre-monsoon

(d) monsoon.



(e)

Figure 3.3.3: Trend of SST for the period 1977-2012 (e) post monsoon.

3.4 Spatial trend analysis of Sub Surface Temperature

According to IPCC, 2013 the global ocean will continue to warm during the 21st century. As a result of this, heat will penetrate from the surface to the deep ocean and will affect ocean circulation. The behavior of the oceans at different depths from the surface for the period 1950-2011 is also considered in this study to ascertain whether the warming trend occurs at the sub surface layers also. Long term trends in the subsurface ocean temperature are important to climatic change and require special attention. Limited and uneven data coverage from the ocean can result biased estimates of trends especially in data sparse areas such as southern ocean. To overcome the data limitation, the use of modeled or analyzed data is inevitable. In this study, we focus on the subsurface temperature trends in Indian Ocean utilizing an evenly distributed analyzed global ocean temperature data set. Thence, trends of subsurface temperature for

annual, apart from four seasons and even, individual months are considered.

3.4.1 Annual Variability

The minimum and maximum slope ($^{\circ}\text{C}/\text{decade}$) for four seasons and annual for the depths is given in table 3.2 and the annual variability for each depth is depicted in figures 3.4.1.

a) At depth 25m

This immediate subsurface depth that mostly falls within the mixed layer identifies four distinct regions where mild warming of 0.17 to $0.21^{\circ}\text{C}/\text{decade}$ stands distinguishable. However more areas of IO are decorated by cooling trends or rather remain neutral. Attention is invited to the vast expansion of SIO on the central and eastern regions as well as the western section of Equatorial waters; three pockets of warming are located close to the coastal regions of Somalia, east coast of India and Indonesia and within the open ocean, parts of west southern regions. From previous studies on the long term trend of Sea Surface Temperature (SST), it is observed that the tropical IO is warming consistently at a rate of 0.25°C to 0.30°C per decade (Rao et al., 2012, Roxy et al., 2014, Pai et al., 2015). The highest warming rate noticed at the central equatorial region in our study agrees with the previous studies but with a lower magnitude.

Table 3.2: Minimum and maximum slope ($^{\circ}\text{C}/\text{decade}$) for four seasons and annual for the depths.

| Depth | Winter | | Pre monsoon | | Monsoon | | Post monsoon | | Annual | |
|-------|--------|------|-------------|-------|---------|------|--------------|------|--------|------|
| | Min: | Max: | Min: | Max: | Min: | Max: | Min: | Max: | Min: | Max: |
| 25 m | -0.07 | 0.21 | -0.07 | 0.20 | -0.07 | 0.19 | -0.08 | 0.21 | -0.05 | 0.17 |
| 98 m | -0.25 | 0.21 | -0.22 | 0.22 | -0.21 | 0.23 | -0.23 | 0.25 | -0.15 | 0.17 |
| 235 m | -0.11 | 0.12 | -0.11 | 0.099 | -0.10 | 0.09 | -0.12 | 0.13 | -0.10 | 0.10 |
| 540 m | -0.67 | 0.08 | -0.05 | 0.06 | -0.03 | 0.05 | -0.06 | 0.09 | -0.04 | 0.06 |
| 967m | -0.08 | 0.06 | -0.06 | 0.06 | -0.05 | 0.05 | -0.05 | 0.05 | -0.06 | 0.05 |

b) At depth 98 m

The horizontal section at this depth further indicates vast regions of warming at the entire SIO and a high cooling trend at the western and equatorial IO. This cooling trend does not have coherence with the trend at the above depth and produce alternating sign of trends in the vertical. Another feature is a cooling trend observed in the central equatorial region where equivalent cooling is registered. The northern IO (NIO) shows both cooling and warming positions juxtaposition. To specifically record, the northern waters of Madagascar are occupied by warming waters which has been observed in the long term trend of SST by Pai et al., 2015. There is an overall agreement of our estimate with that of Harrison and Carson (2007) that used hydrographic profiles only to estimate long term trend. Since the data used by them had limited spatial and temporal coverage, the trend estimate was not conclusive in southern oceanic areas and also at higher depths. To have a better coverage, use of analyzed and model

assimilated data is inevitable. The annual trend at this depth compares reasonably well with that of Harrison and Carson (2007). A cooling trend was found south of equator in both the studies. The significant warming trend found at southern latitudes in our analysis is but different from their results.

c) At depth 235 m

At this depth, which mostly falls within the thermo cline region, there is a well-established mild warming trend within the SIO across all along east west including the “Madagascar High”. A cursory analysis along all other regions of IO, including equatorial water do not indicate any strong trends of warming or cooling except for post monsoonal cooling trend along Somalia and eastern Indian Coastal waters. The equatorial waters do not exhibit any significant warming or cooling trend at this depth. Two isolated pockets, one along the eastern coast of Indian sub-continent and another at the farthest regions of western IO do reveal mild amounts of cooling which is in agreement with the observations of Alory et al., 2007.

d) At depth 540 m

Interesting results emerge from the trend analysis of the temperature at 540m depth. The magnitude of warming trend was decreased substantially to 0.06(table1).The “Madagascar High” warming trend is no longer visible now. At this depth the warming is weak and do not indicate any significant warming/cooling. Hence it can be said that the warming trend do not penetrate deeper than 500m in IO and is therefore

confined to the upper waters only. However it can be noted that the NIO indicates relatively a warming trend compared to SIO except for two isolated pockets. Most areas of IO are either mildly cooling or remain more or less at constant temperatures.

e) At depth 967 m

The deep waters of IO are well discerned by established features at SIO south of 20°S having cooling trends up to a magnitude of -0.02 °C/decade (blue shades in figures 3.4.1). This feature was however not seen in the upper waters. In contrast, most regions north of 20°S including the equatorial and northern most parts of AS comes under positive warming trend up to 0.06 °C. The only exception is the waters close to Somalia coast and at the head of BOB which are neutral or mildly show negative changes in temperature. Hence it can be concluded that the deep waters of NIO undergo a milder warming trend over the entire domain except for a cooling trend at southern IO.

To summarize the annual trends, it is stated that the water column within the thermo cline roughly 100m to 250m of SIO indicates a warming trend in the region of 0.10 °C to 0.17 °C/decade, whereas deeper waters in the 500m to 1000m range is dominated with the presence of cooling waters (-0.04 to -0.06 °C/decade). On the contrary, the NIO and parts of Equatorial waters from 25m to 250m indicate a cooling trend while the vertical section around 500m to 1000m has waters which warm over a period of time, though the range of cooling and warming fall within a narrow range of ± 0.1 °C/decade.

3.4.2 Seasonal Variability

a) At depth 25m

The immediate subsurface waters at 25m have a pattern of evolution through the four seasons. As regards the NIO, comprising of AS and BOB, this region is well known for features associated with winter cooling (Chauhan et al., 2001; Vinayachandran, 2009). The northern most waters are conspicuous for cooler waters, especially in the AS compared to BOB (figures 3.4.2). The observations are:

- A warming trend all over the tropical IO for all seasons except for a smaller area at 20°S of central IO.
- Maximum warming trend at the southwest IO and at northern AS and BOB.
- Higher warming trends appear as pockets rather than broad area.
- Among the seasons, warming trend was strongest during winter.

Exceptionally, the past 60 years indicates a trend of cooling of -0.1°C for the southern waters east of 80°E . Conversely, the waters on the west indicate a positive trend. The above findings are valid for all the seasons which are seen in the annual trend also.

b) At depth 98m

The seasonal analysis of warming and cooling trends at 98m depth indicates two consistent phenomena (figures 3.4.3). The SIO south of 15°S most often across all seasons show a warming trend up to $0.2^{\circ}\text{C}/\text{decade}$ consistent with the Southern Hemisphere, the central south waters indicate higher trends of warming. The second phenomenon refers to Equatorial

cooling around 80⁰E sandwiched between mild to extensive warming on either sides. Incidentally, the cooling trend at these depths is not in agreement with long term SST variations at the same locations (figures 3.2.1). Only during the post monsoon season, waters around 80⁰E appear to be diffused with admixture of warming and cooling waters.

The horizontal section at this depth further indicates vast regions of warming at the entire SIO and a high cooling trend at the western and equatorial IO. This cooling trend does not have coherence with the trend at the above depth and produce alternating sign of trends in the vertical. Another feature is a cooling trend observed in the central equatorial region where equivalent cooling is registered. The northern IO (NIO) shows both cooling and warming positions juxtaposition. To specifically record, the northern waters of Madagascar are occupied by warming waters which has been observed in the long term trend of SST by Pai et al., 2015. There is an overall agreement of our estimate with that of Harrison and Carson (2007) that used hydrographic profiles only to estimate long term trend. Since the data used by them had limited spatial and temporal coverage, the trend estimate was not conclusive in southern oceanic areas and also at higher depths. To have a better coverage, use of analyzed and model assimilated data is inevitable.

In our previous analysis at 25m horizontal, the NIO had indicated winter cooling which is not so at 98m depths. However, waters around Somalia region do experience a cooling trend in the range less than – 0.10⁰C/decade. Another but localized phenomenon is the presence of warming waters north of Madagascar Island which indicates warming

trends irrespective of seasonal variations. The sum total of the four seasonal variations is well imbibed in the annual chart as discussed earlier.

c) At depth 235m

At these intermediate depths mostly within the thermo cline regions, a well established warming trend is well depicted within SIO across all East West sectors including the “Madagascar High”. A cursory analysis along all other regions of IO including Equatorial waters do not indicate any strong trends of warming or cooling except for post monsoonal cooling along Somalia and Eastern Indian Coastal waters (figures 3.4.4).

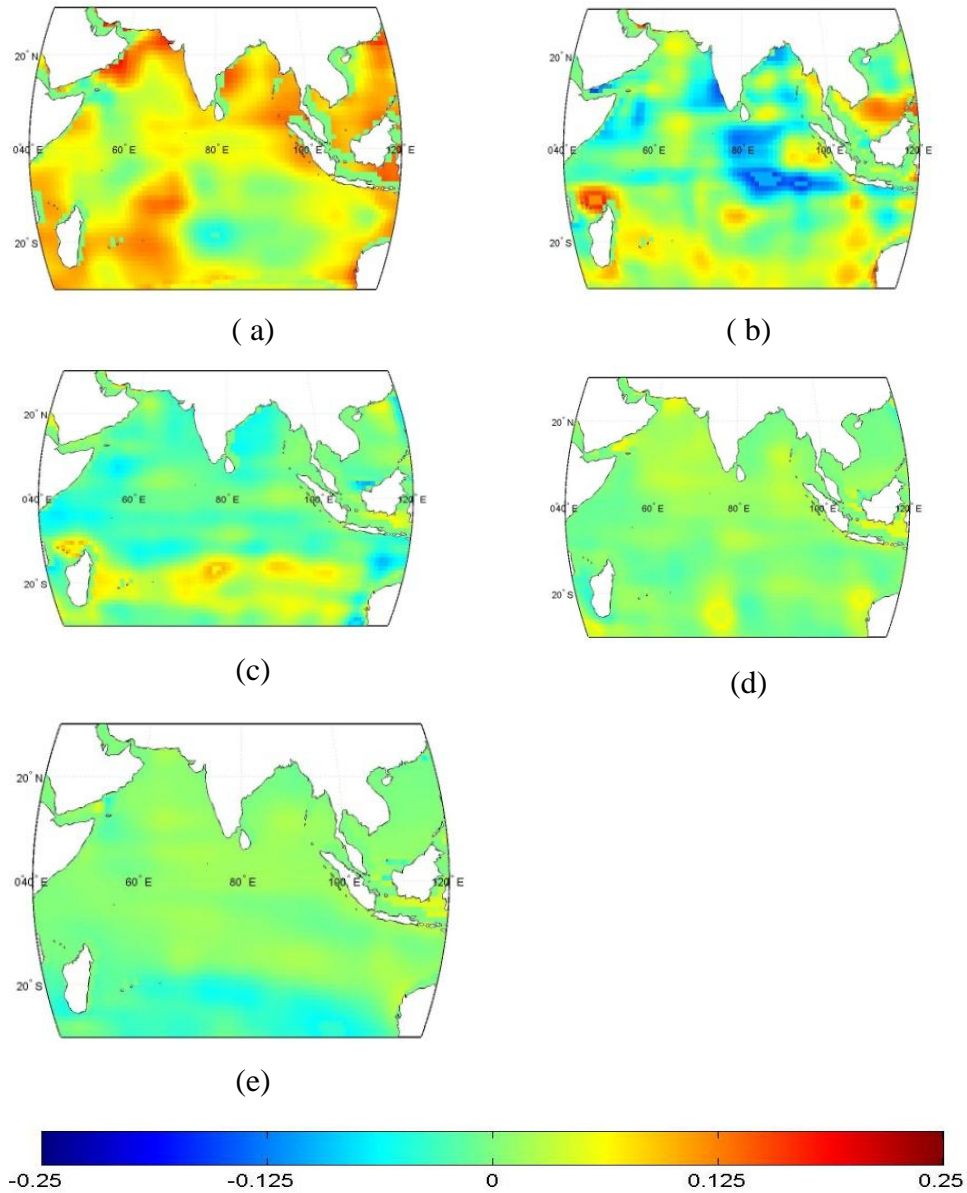


Figure 3.4.1: Annual variation of sub surface temperature for the period 1950-2011 at depths (a) 25m (b) 98m (c) 235m (d) 540m (e) 967m.

d) At depth 540 m

Interesting results are emerging from the trend analysis of the temperature at 540m depth. Converse to the earlier findings at these intermediate depths the SIO is indicating a mixed result of numerous pockets of alternate warming/cooling (figures 3.4.5). The “Madagascar High” warming trend is no longer visible. Rather this area is neutral to either warming/cooling.

We wish to suggest that in the vertical, the intermediate waters may be acting as a barrier to change from warming to cooling with increase of depths. Interestingly another phenomenon is developing in the NIO. Consistent warming is indicated across all seasons along the coastal waters of Saudi Arabia, Iran and parts of West coast of India. A similar warming trend is again noted for central BOB ranging from 0.02⁰C to 0.10⁰C commencing from post monsoons intensify during winter. All other regions of IO have only mild warming/cooling of varied seasonal scales.

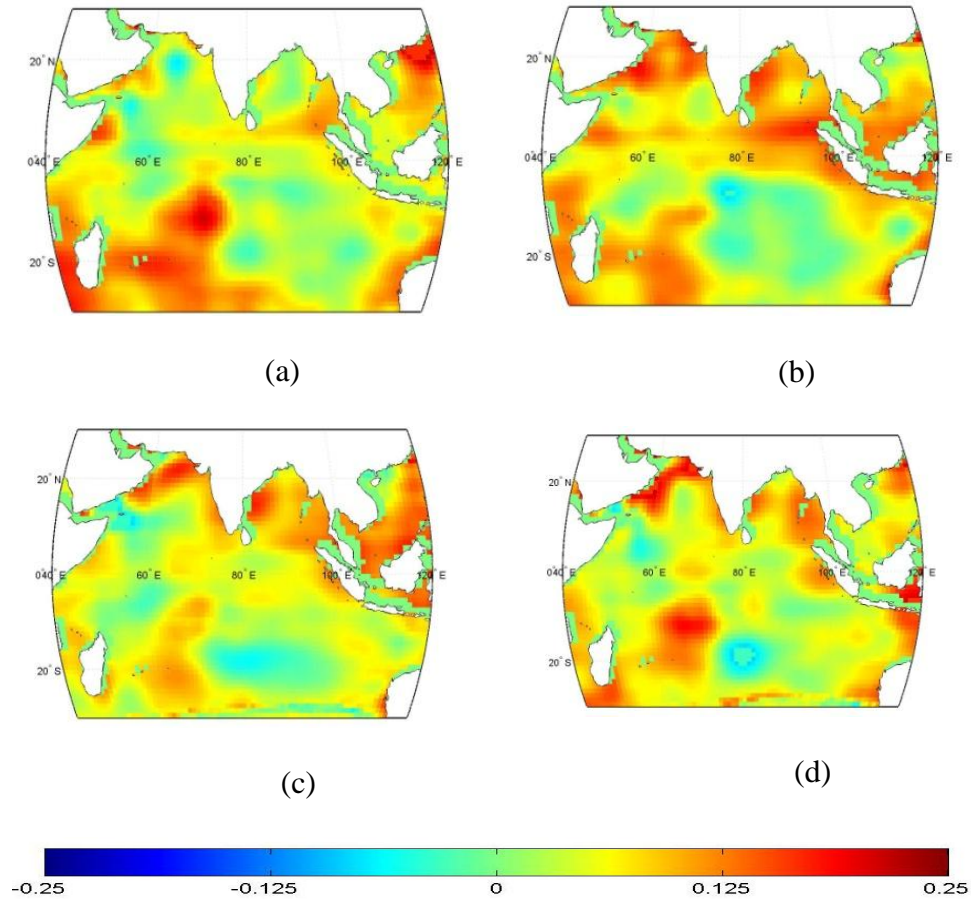


Figure 3.4.2: Seasonal variation of sub surface temperature for the period 1950-2011 at depth 25m for (a) winter (b) pre monsoon (c) monsoon (d) post monsoon.

e) At depth 967 m

a) The deep waters of IO are well discerned by established features which are SIO around 20° S and further south consistently indicate cooling trends in the range of -0.02°C to $-0.08^{\circ}\text{C}/\text{decade}$ (blue colors in figures 3.4.6).

b) In contrast, most regions north of 20°S including the Equatorial and northern most parts of AS come under different rates of increase in temperature showing a positive warming trend up to 0.06°C. The only exception is waters close to Somalia coast and the head of BOB which are neutral or mildly show negative changes in temperature.

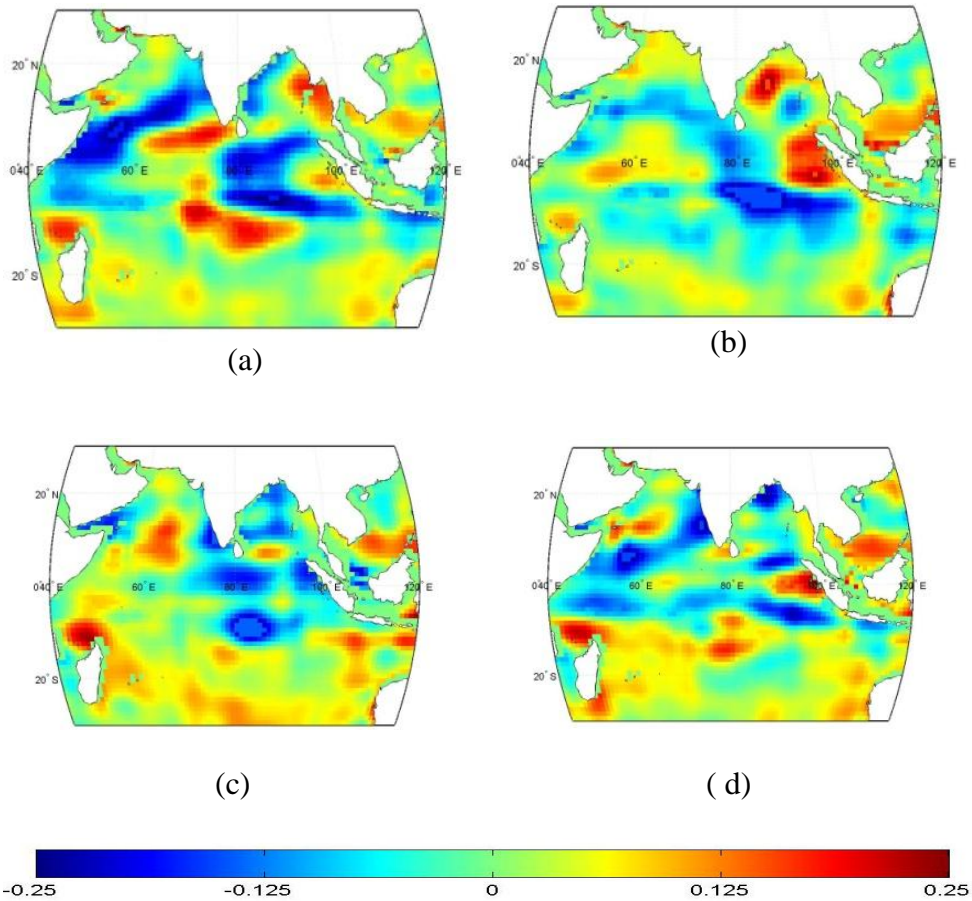


Figure 3.4.3: Seasonal variation of sub surface temperature for the period 1950-2011 at depth 98m for (a) winter (b) pre monsoon (c) monsoon (d) post monsoon.

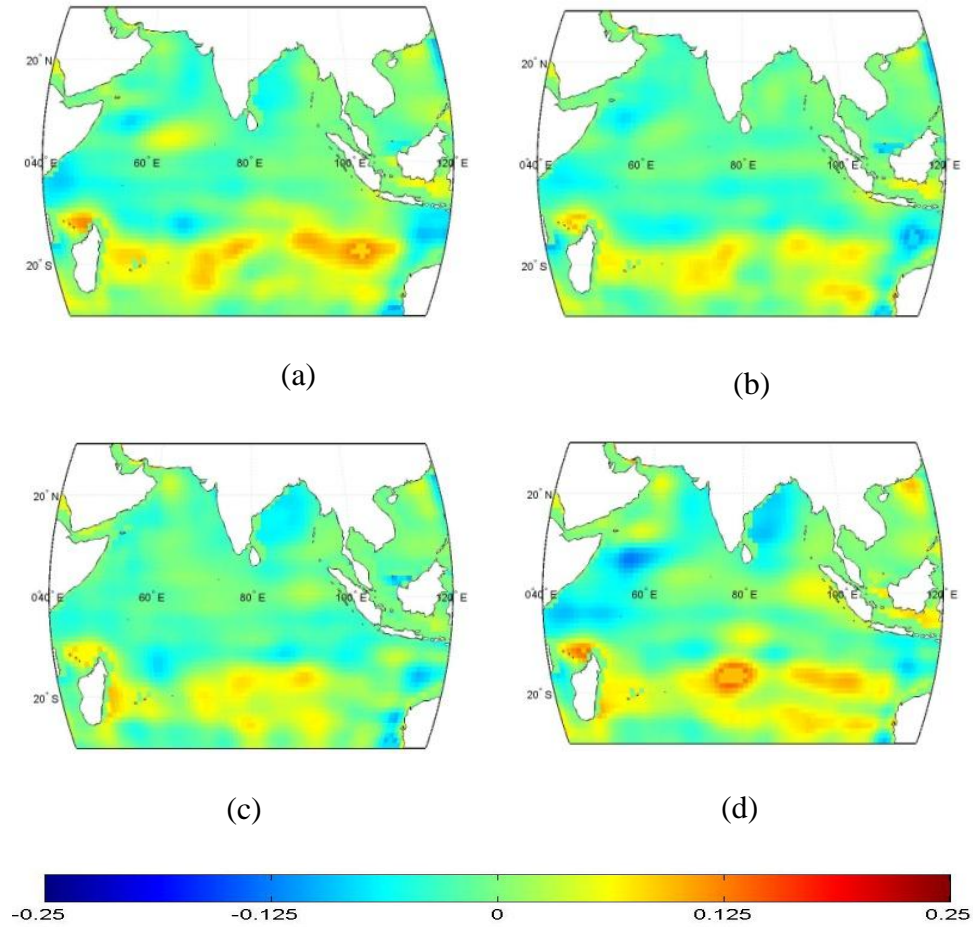


Figure 3.4.4: Seasonal variation of sub surface temperature for the period 1950-2011 at depth 235m for (a) winter (b) pre monsoon (c) monsoon (d) post monsoon.

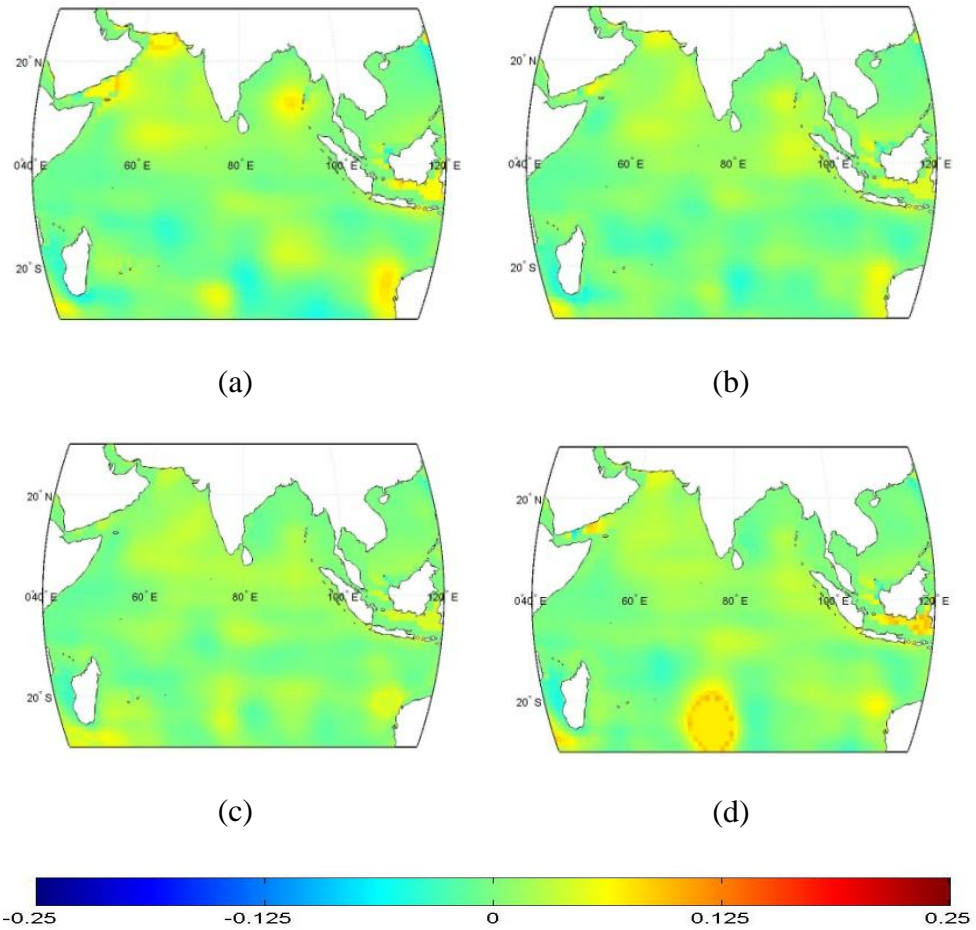


Figure 3.4.5: Seasonal variation of sub surface temperature for the period 1950-2011 at depth 540m for (a) winter (b) pre monsoon (c) monsoon (d) post monsoon.

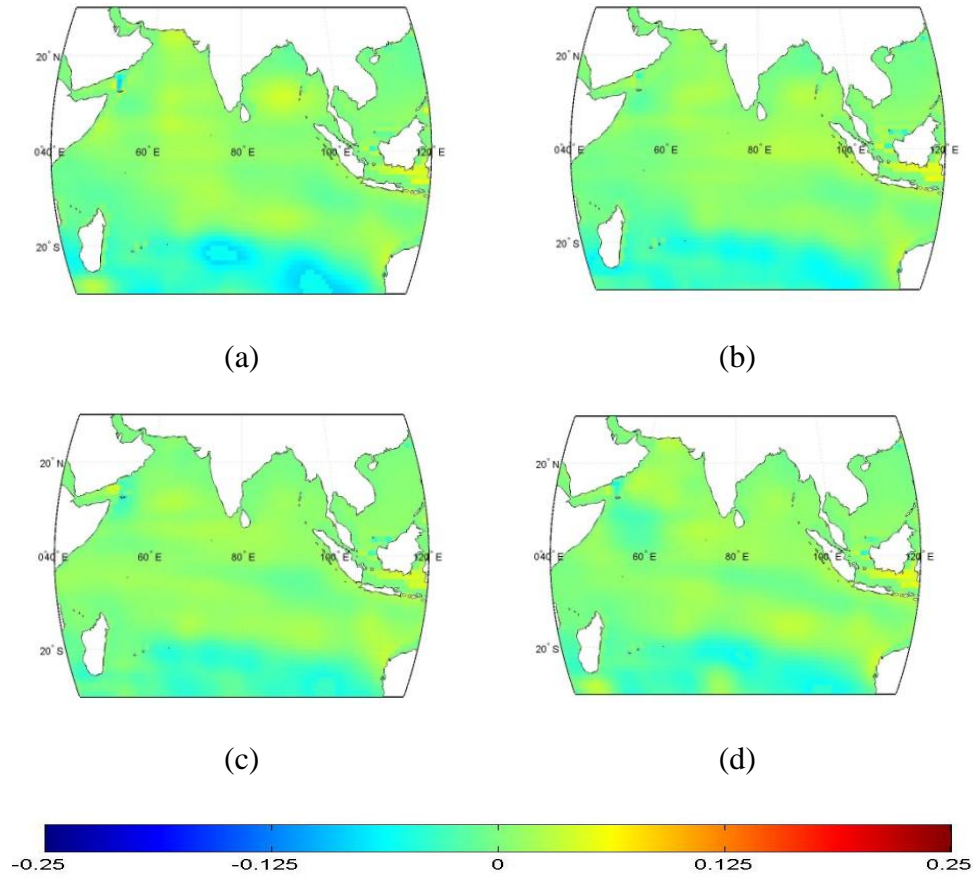


Figure 3.4.6: Seasonal variation of sub surface temperature for the period 1950-2011 at depth 967m for (a) winter (b) pre monsoon (c) monsoon (d) post monsoon.

3.4.3 Monthly variability

a) At depth 25m

Figures 3.4.7 show the monthly charts of sub surface temperature at depth 25m during the period 1960-2011. In the monthly charts of January and February both AS and BOB show cooling trend. But when March commences, a mild warming is noticed in this region. Ocean waters are warming near 20⁰S, 60⁰ to 70⁰E which decreases during the next few months. AS and BOB waters started warming during April, May and June but mild warming for August, November and December. The East Equatorial IO shows cooling from January to August. “Madagascar High” is observed for the months January to August. Northern parts of BOB show significant warming trend during April to July and thereafter shows mild warming trend. Near the Somalia Coast, north of equator, a significant warming trend is observed during the months January to June and thereafter the warming trend becomes less significant.

b) At depth 98m

The monthly variability at depth 98m is shown in the figures 3.4.8. A significant warming is generally noticed at depth 98m during the months March to May. The same is experienced for the months January to March above the Equator between 60⁰E to 80⁰E. “Madagascar High” is again seen for almost all months whereas it is less significant for April. February and September months experienced a cooling trend near the Equator between 80⁰E to 100⁰E, while a mixed behavior is observed for

rest of the months at this region. Warming trend is more predominant for all months below 20°S.

c) At depth 235 m

The monthly charts at depth 235m are depicted in the figures 3.4.9. BOB waters show a cooling trend for all the months except for March and April. Warming trend is significant for January to March above the Equator near 60°E to 70°E, but it is less significant for the next few months up to August. A significant warming trend starts in the AS from the month September and it continues till December. The subtropical region below 20°S shows a warming trend throughout the months. “Madagascar High” is also visible throughout the months.

d) At depth 540 m

Figures 3.4.10 show the monthly charts at depth 540m. Both AS and BOB show a warming trend for all months. The warming trend noticed at the subtropics for depth 235m was relatively decreasing at depths of 540m. And again it reappears since September. The northwest equatorial region, near Somalia coast show cooling throughout the months.

e) At depth 967 m

Figures 3.4.11 show the monthly charts at depth 967m. The warming trend is decreased compared to the above depths. The sub tropics below 20°S near 60°E to 100°E, maintain cooling features from January to September and from October onwards a small pocket of warming is also noticeable.

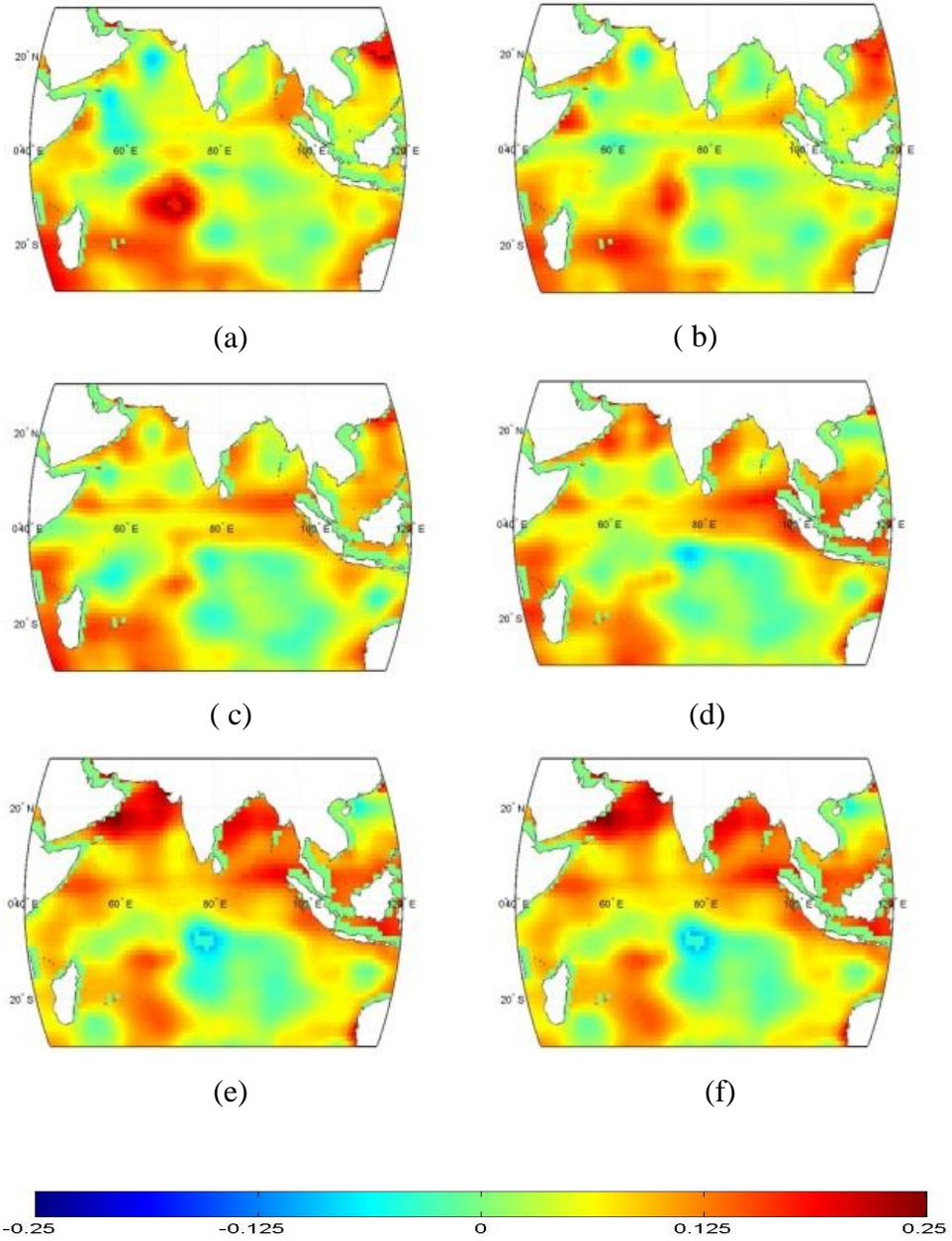


Figure 3.4.7: Trend analysis of subsurface temperature for the months at depth 25mduring the period 1950-2011 (a) January (b) February (c) March (d) April (e) May (f) June.

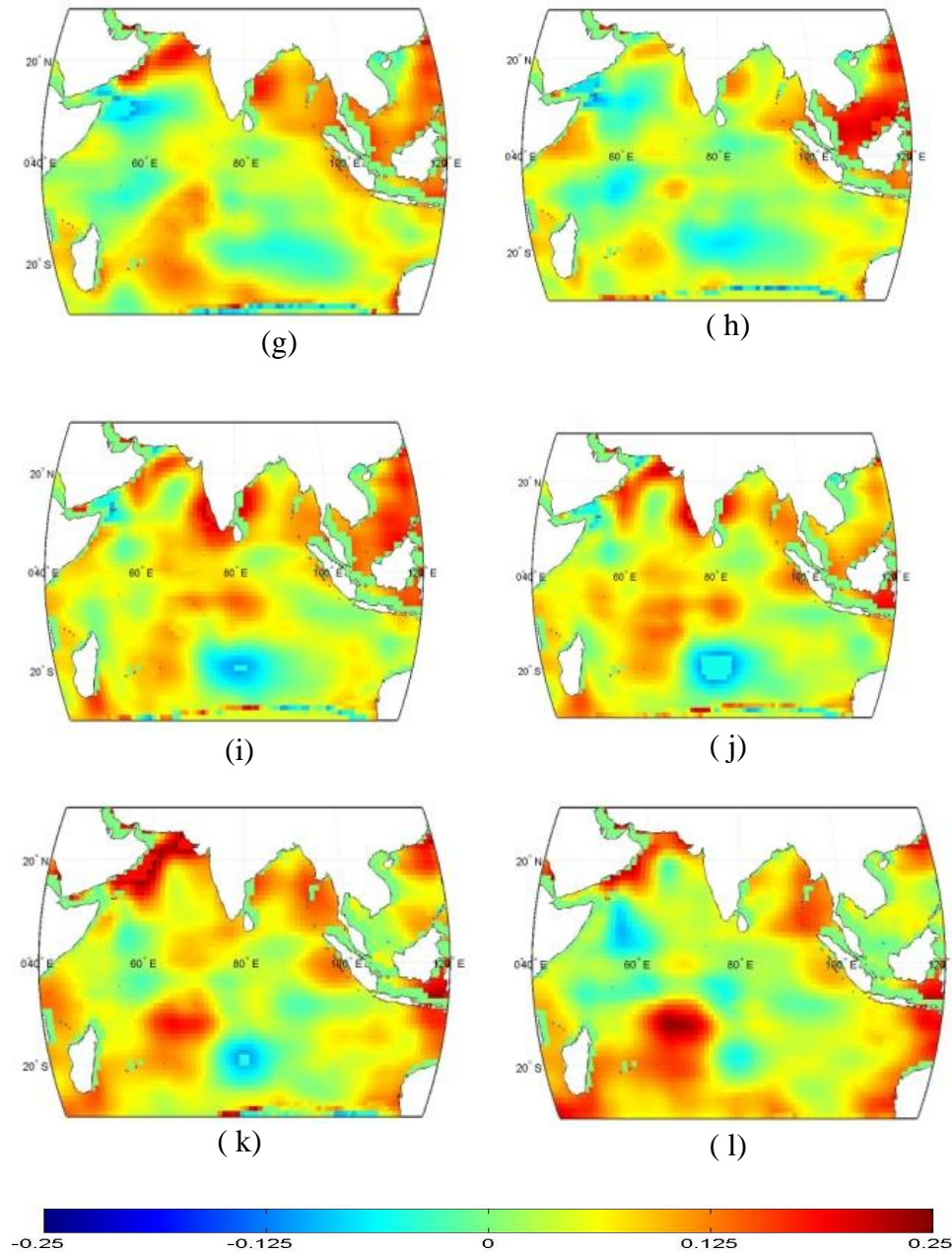


Figure 3.4.7: Trend analysis of subsurface temperature for the months at depth 25m during the period 1950-2011 (g) July (h) August (i) September (j) October (k) November (l) December.

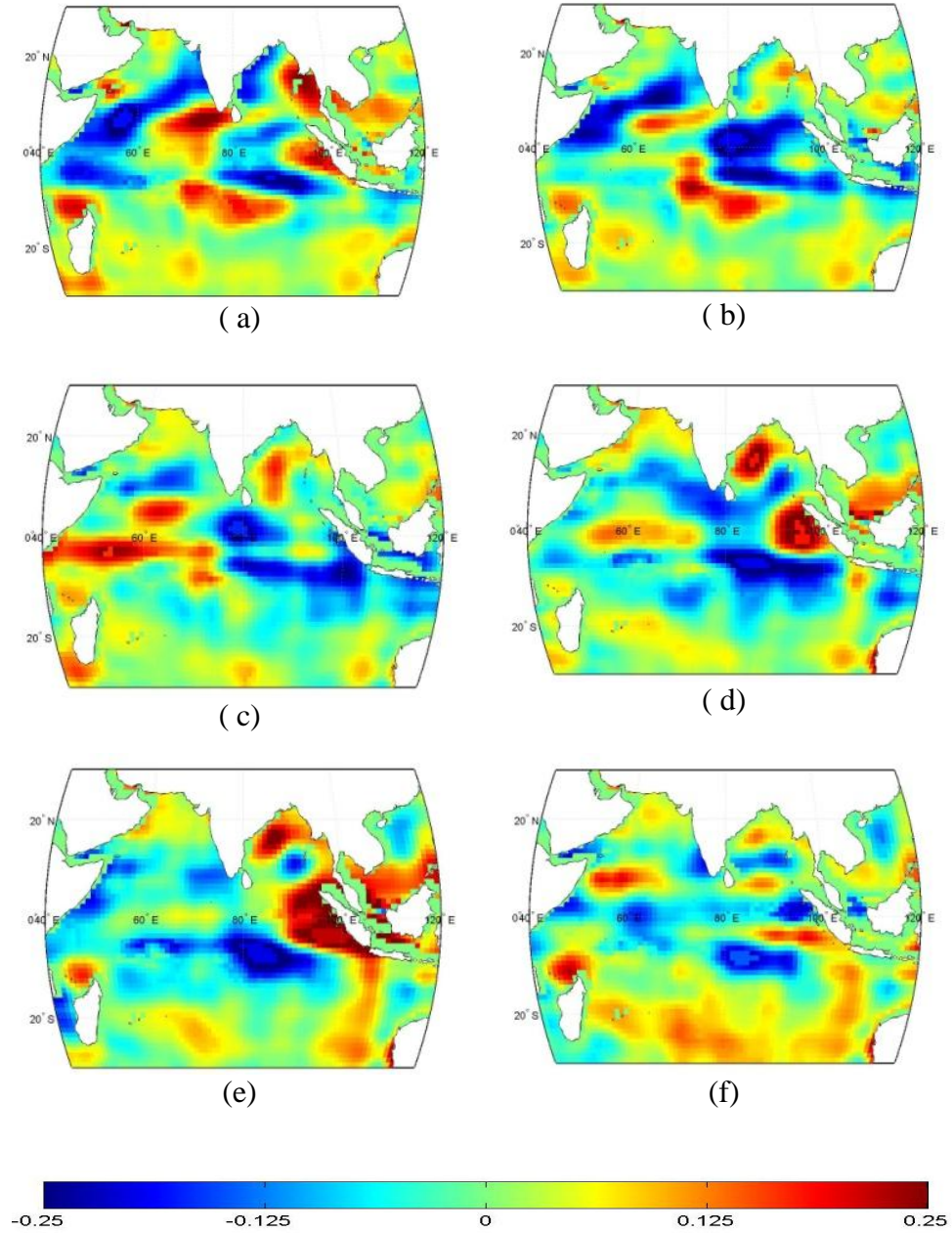


Figure 3.4.8: Trend analysis of subsurface temperature for the months at depth 98m during the period 1950-2011 (a) January (b) February (c) March (d) April (e) May (f) June.

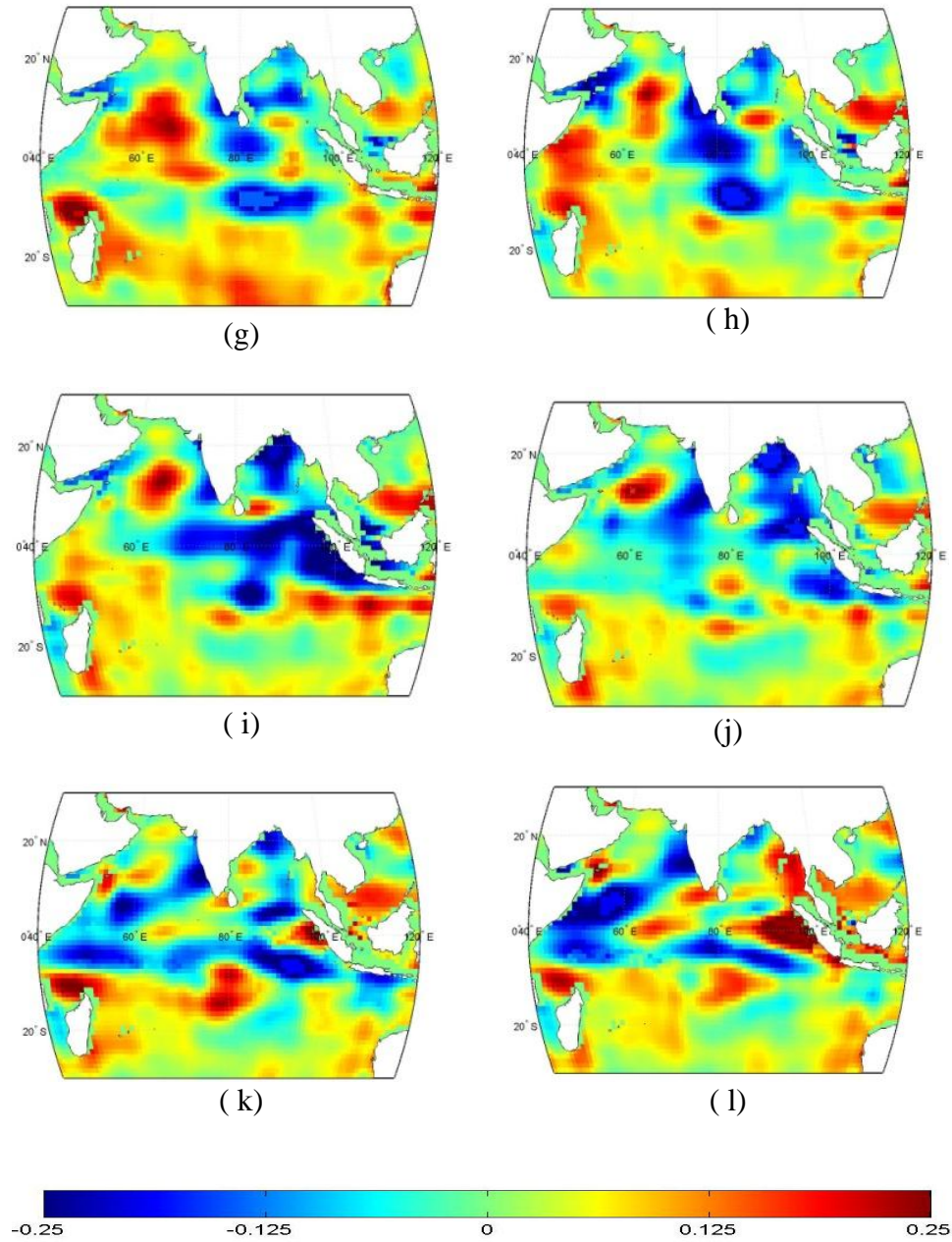


Figure 3.4.8: Trend analysis of subsurface temperature for the months at depth 98m during the period 1950-2011 (g) July (h) August (i) September (j) October (k) November (l) December.

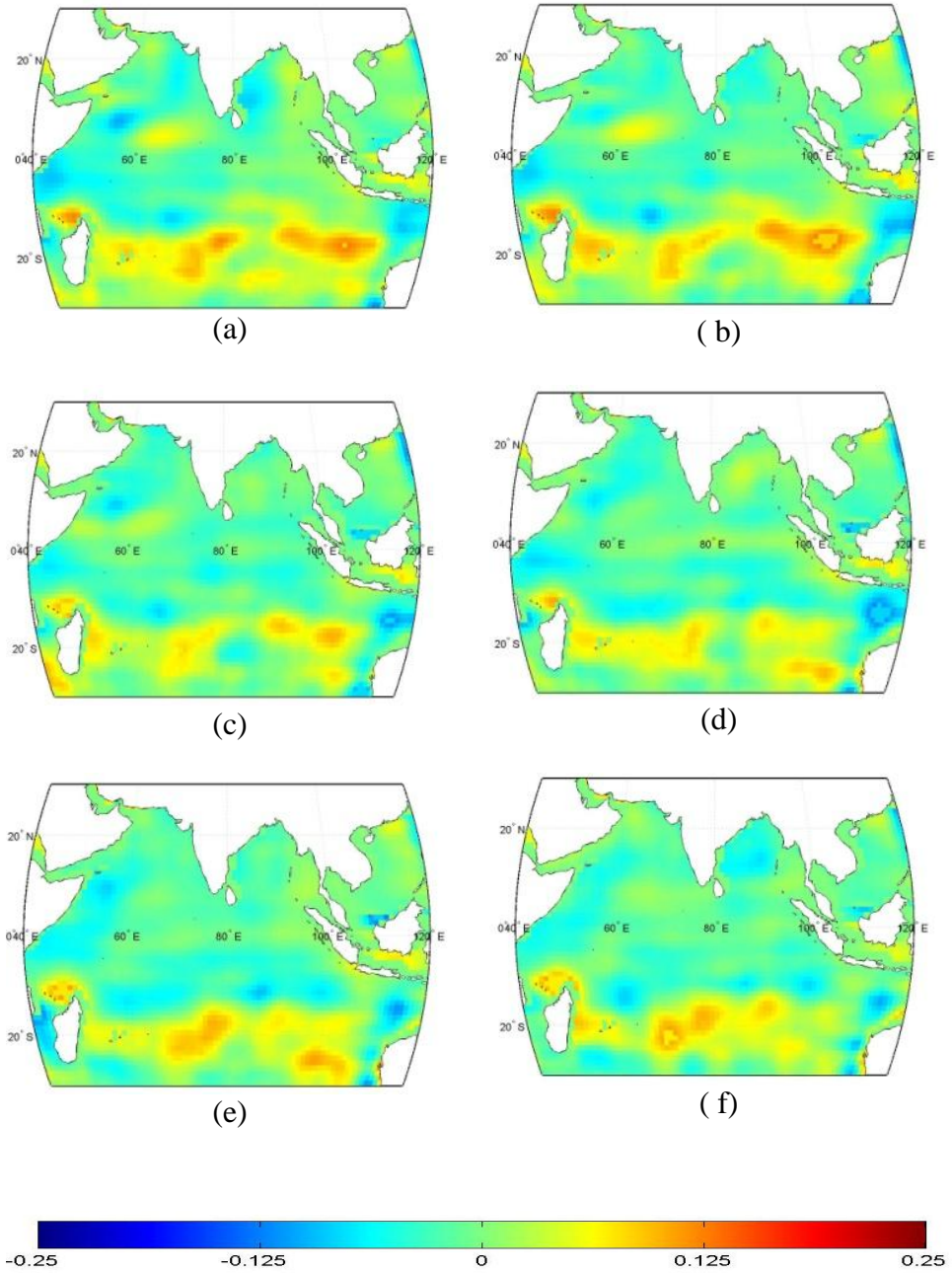


Figure 3.4.9: Trend analysis of subsurface temperature for the months at depth 235m during the period 1950-2011 (a) January (b) February (c) March (d) April (e) May (f) June.

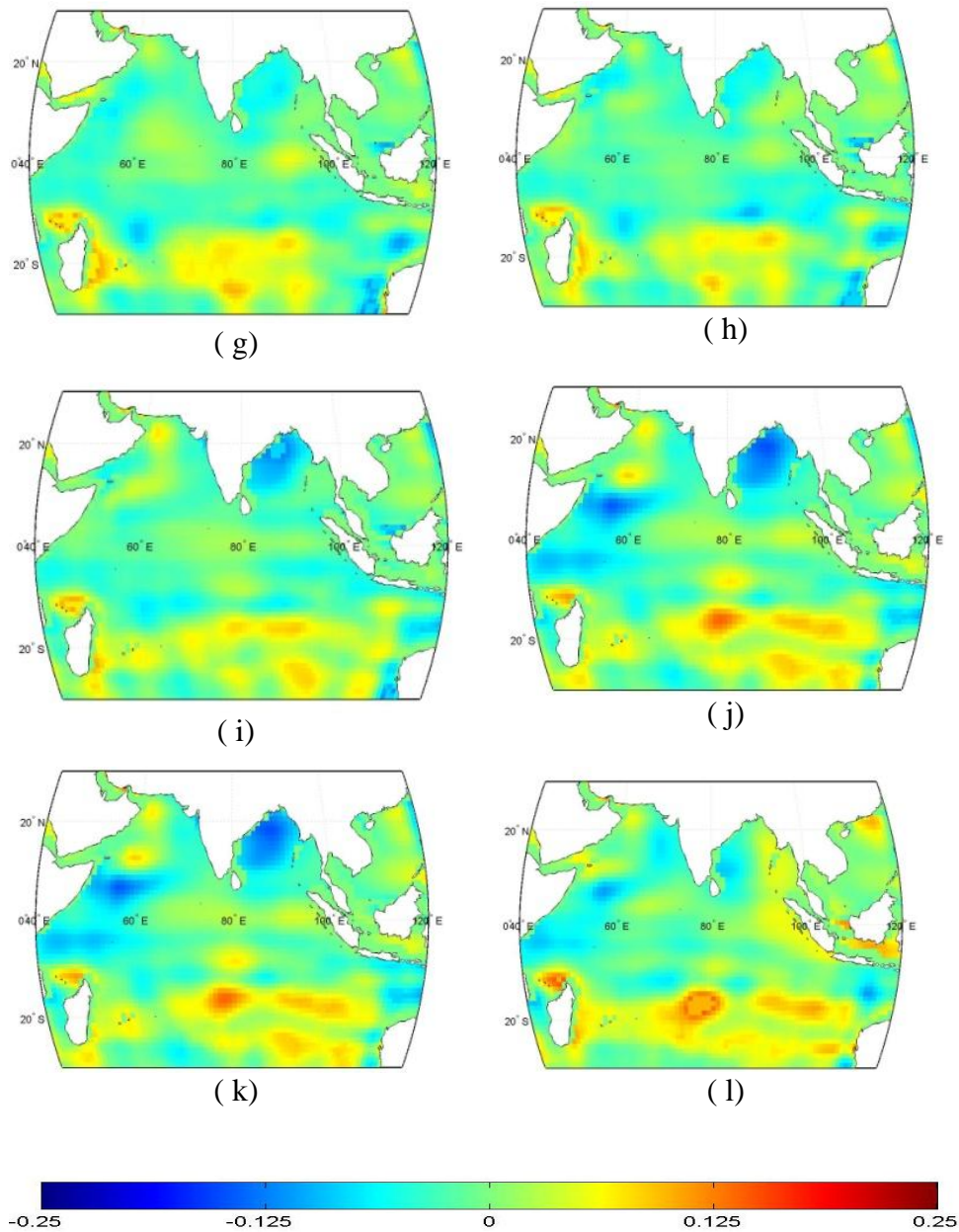


Figure 3.4.9: Trend analysis of subsurface temperature for the months at depth 235m during the period 1950-2011 (g) July (h) August (i) September (j) October (k) November (l) December.

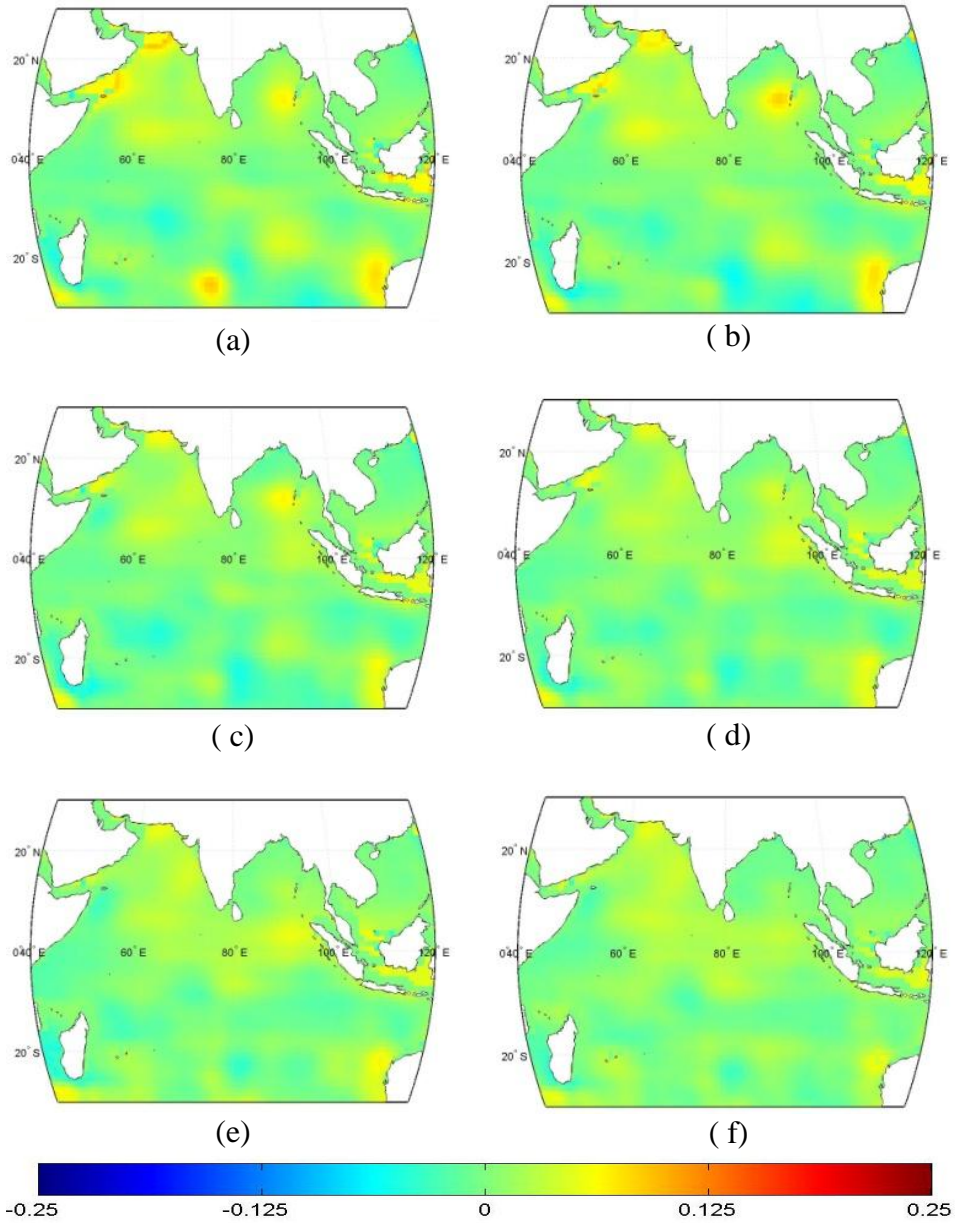


Figure 3.4.10: Trend analysis of subsurface temperature for the months at depth 540m during the period 1950-2011 (a) January (b) February (c) March (d) April (e) May (f) June.

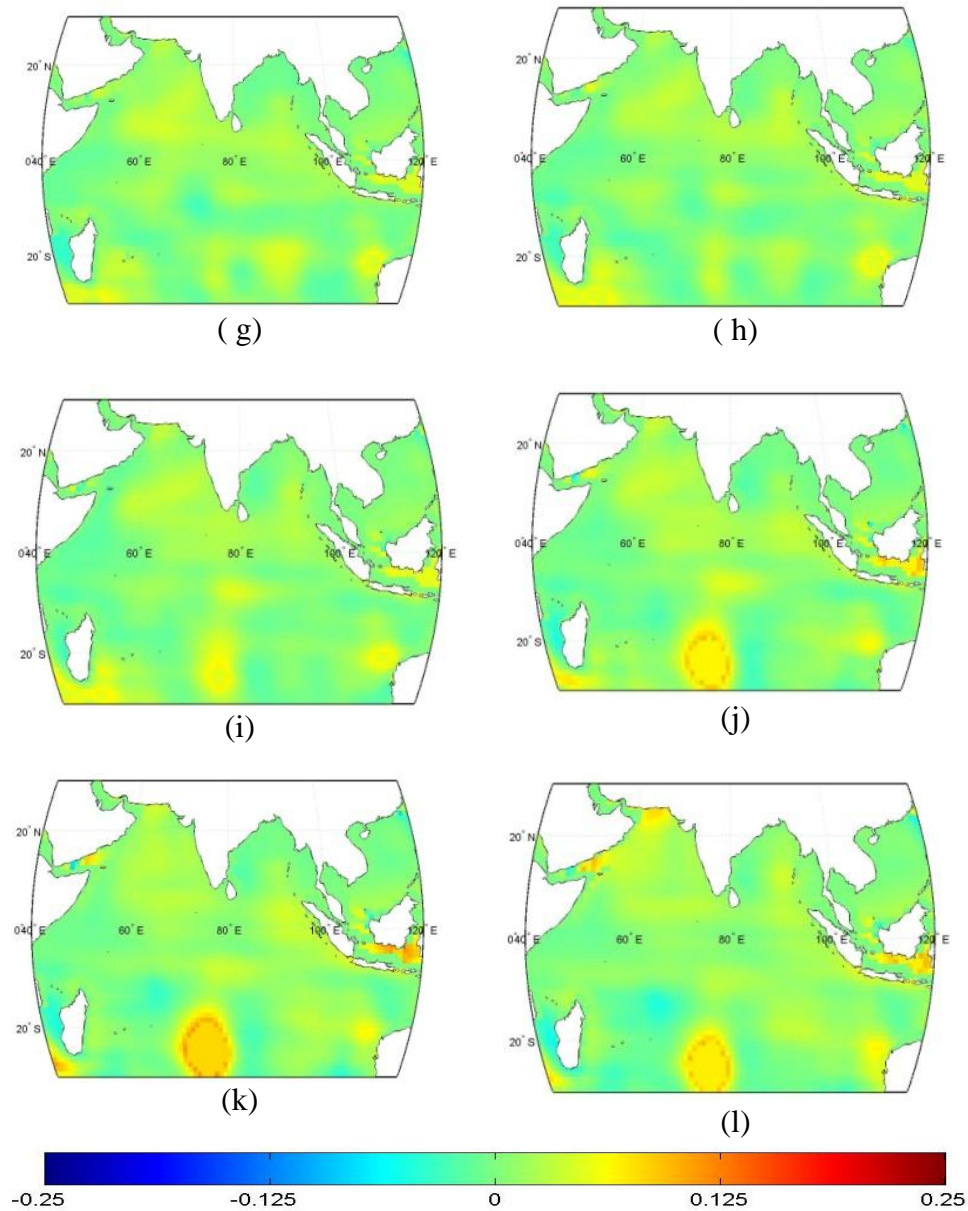


Figure 3.4.10: Trend analysis of subsurface temperature for the months at depth 540m during the period 1950-2011 (g) July (h) August (i) September (j) October (k) November (l) December.

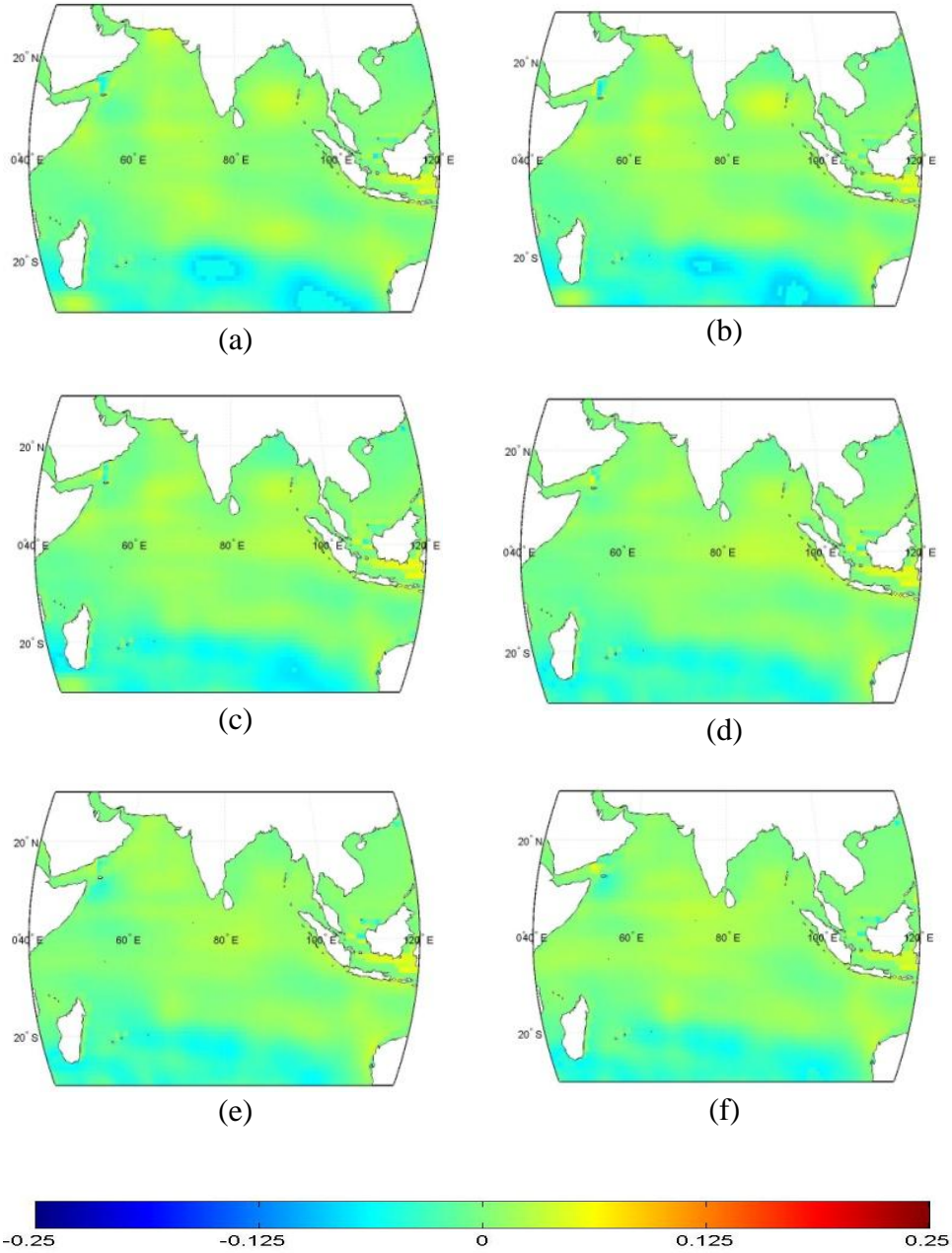


Figure 3.4.11: Trend analysis of subsurface temperature for the months at depth 967m during the period 1950-2011 (a) January (b) February (c) March (d) April (e) May (f) June.

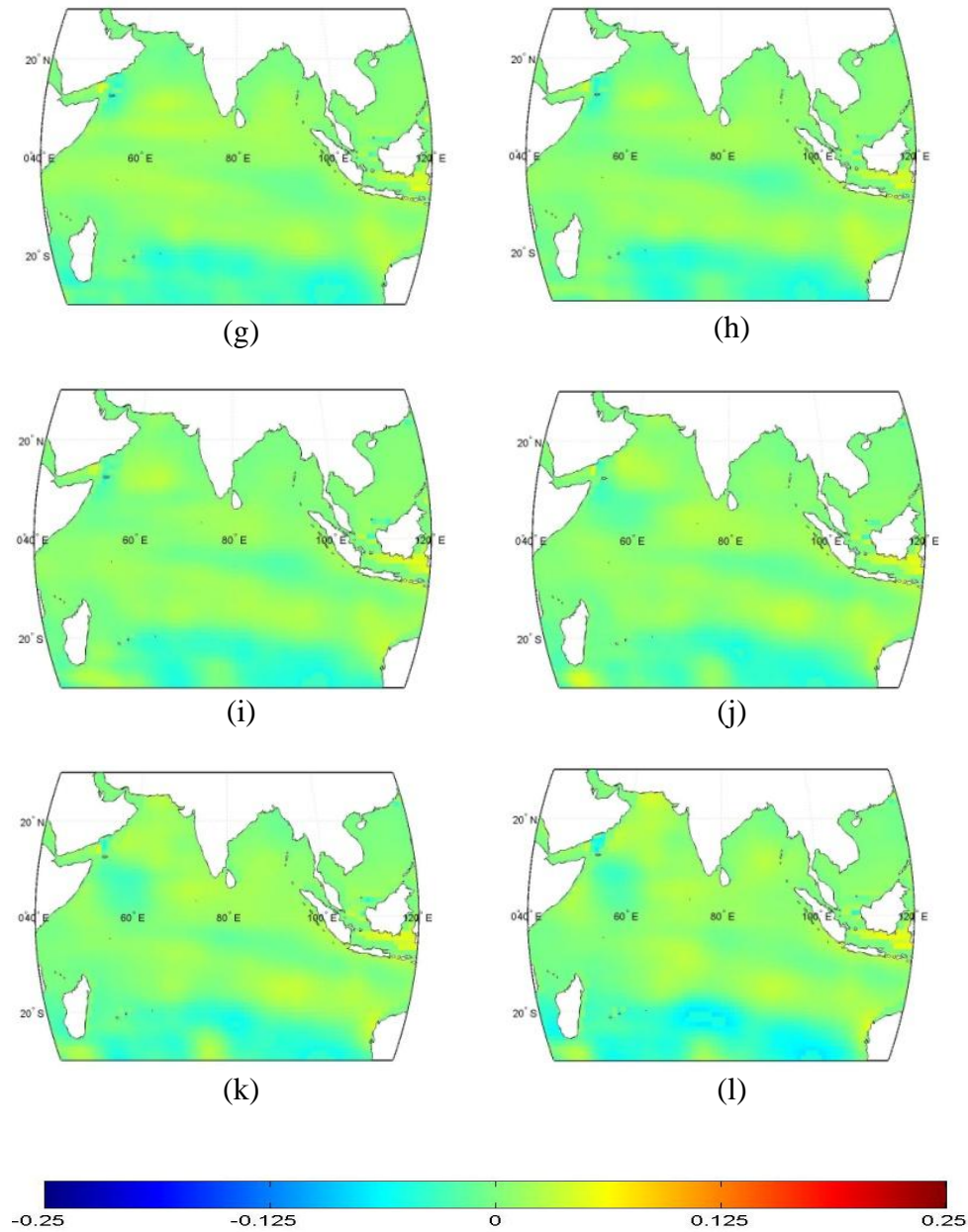


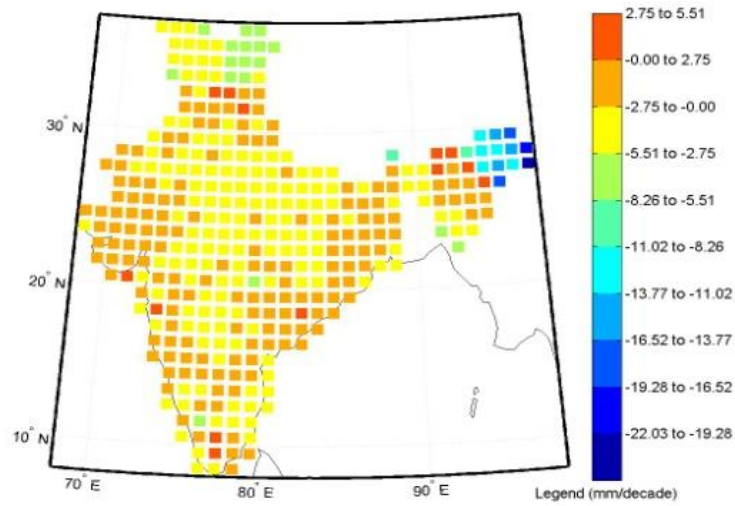
Figure 3.4.11: Trend analysis of subsurface temperature for the months at depth 967m during the period 1950-2011 (g) July (h) August (i) September (j) October (k) November (l) December.

3.5 Spatial Trend Analysis of rainfall

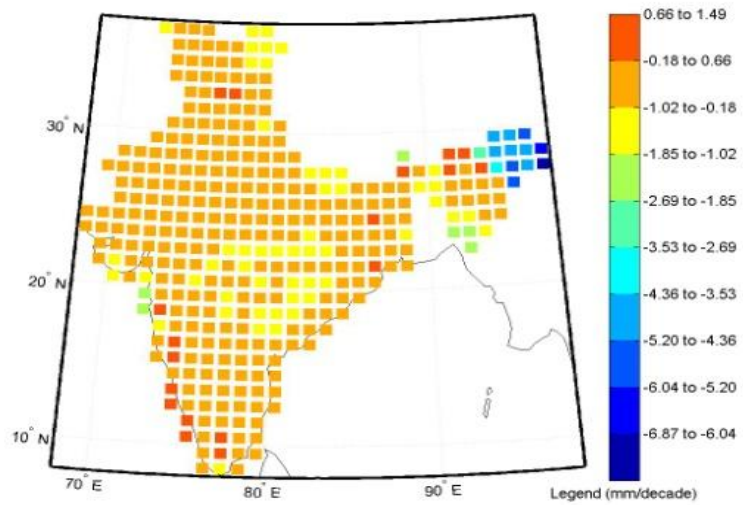
3.5.1 Epoch 1960 -2012

The figures 3.5.1 depict slopes of ISMR [cumulative of JJAS], followed by trends for individual months, namely June, July, August and September in mm/decade. The following results were observed.

- There is a decreasing trend in ISMR in all the six regions and exceptional decrease for some parts of hill type and humid subtropical region.
- An increasing trend (0 to 0.66 mm per decade) is observed for all regions in June except for some grids including hill type. But for July, a significant decreasing trend is noticed for tropical wet, hill type and humid subtropical regions. An increasing trend is noticed in most of the other grids of India for these months but it is less significant.
- A significant decreasing trend is observed in most grids of humid subtropical [Central India] and hill type regions [parts of NE] for August. Semi arid and tropical wet and dry experiences a significant increase. All other grids of the remaining regions show negligible increasing trends.
- In September, a significant decreasing trend is observed except for some grids of India, especially those falling within tropical wet.

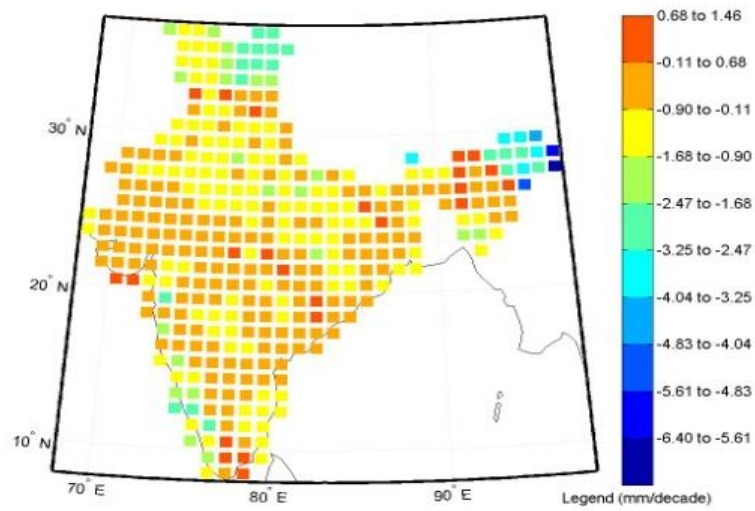


(a)

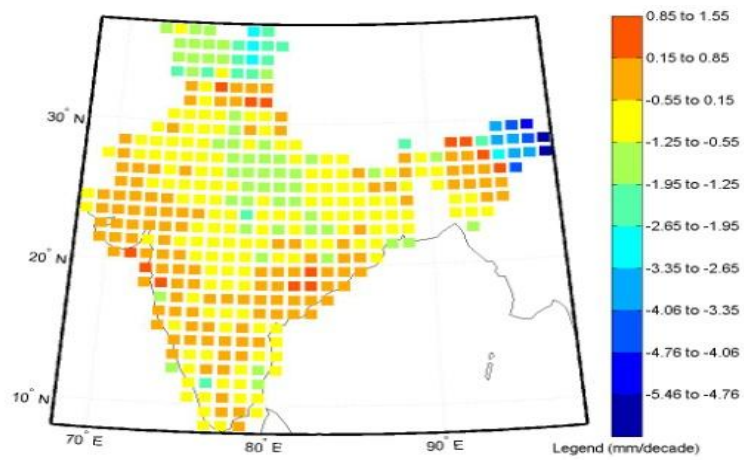


(b)

Figure 3.5.1: Slopes (mm/decade) of rainfall for the period 1960-2012 (a) JJAS (b) June.

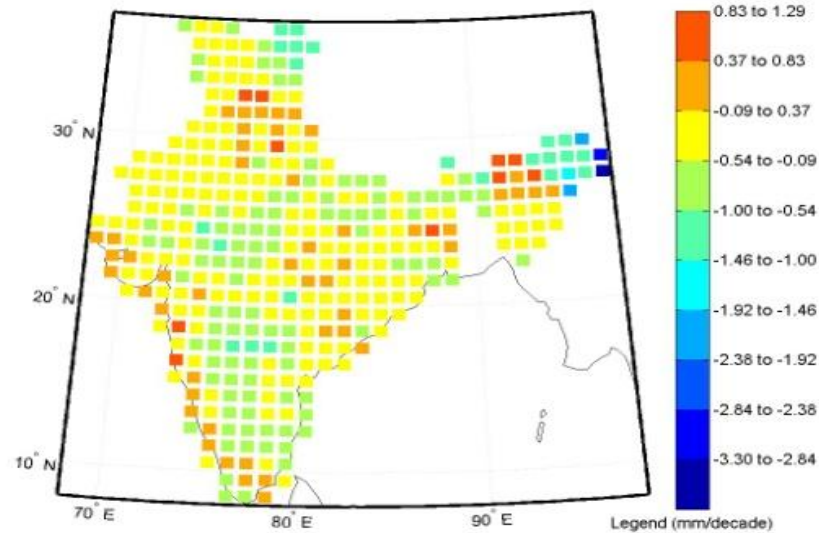


(c)



(d)

Figure 3.5.1: Slopes (mm/decade) of rainfall for the period 1960-2012
(c) July (d) August.



(e)

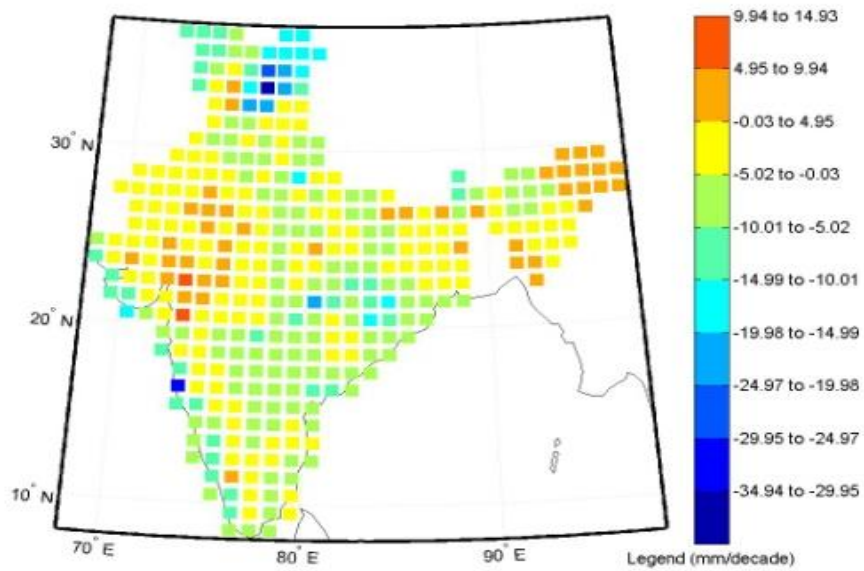
Figure 3.5.1: Slopes (mm/decade) of rainfall for the period 1960-2012 (e) September.

3.5.2 Epoch 1960- 1976

- A very significant increasing trend in seasonal rainfall (about 4.95 mm to 9.94 mm/decade) is realized in the hill type region as well as semi-arid for the period 1960-76. Most of the other regions show decreasing trends (figures 3.5.2). Parts of coastal regions [tropical wet] also show a decreasing trend.
- Some grids of central part of India and hill type show an increasing trend for June and July. An increasing trend also seen in the humid subtropical and semi arid region except for some grids during July. Other regions mostly show a decreasing trend. The case during

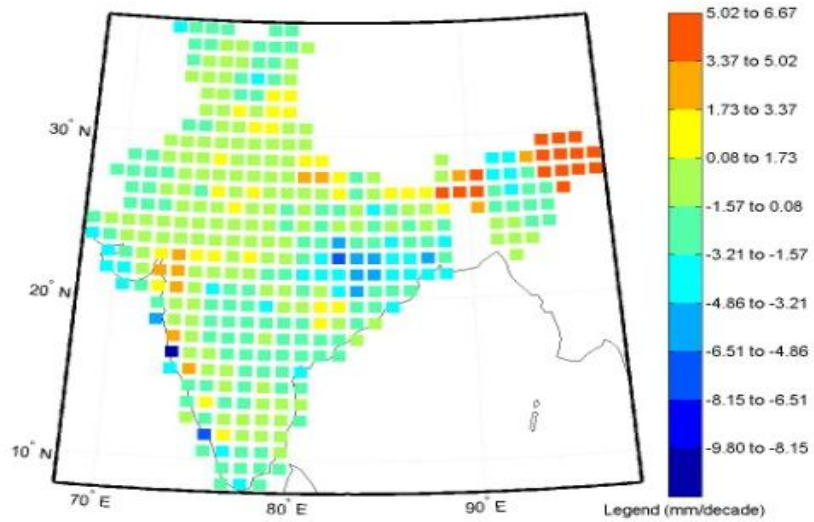
August for central part of India shows a significant increasing trend during this month. Most of the grids of India show a trend of increase.

- In September, lots of grids from central India down to east coast show a decreasing trend while west coast and parts of hill type indicate positive increasing trends.

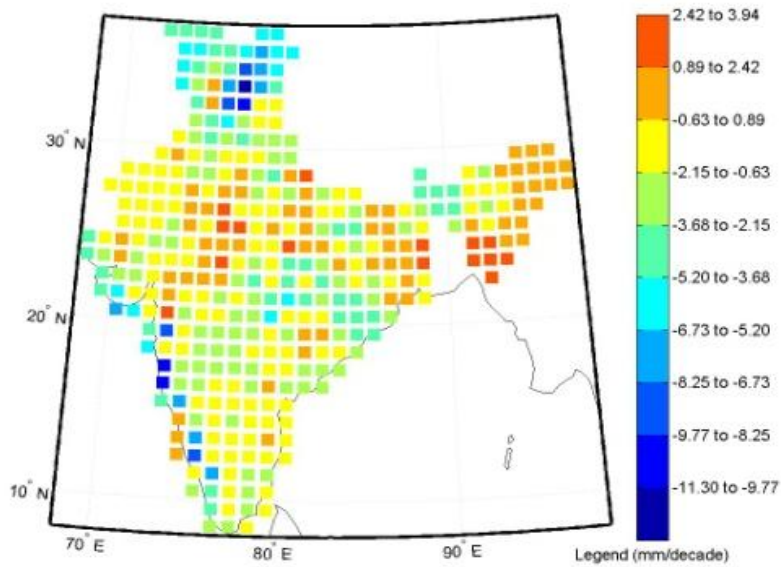


(a)

Figure 3.5.2: Slopes (mm/decade) of rainfall for the period 1960-1976 (a) JJAS.

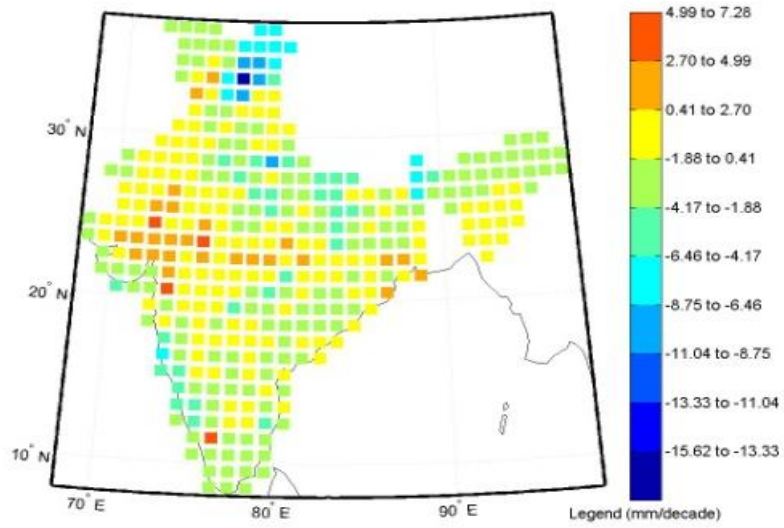


(b)

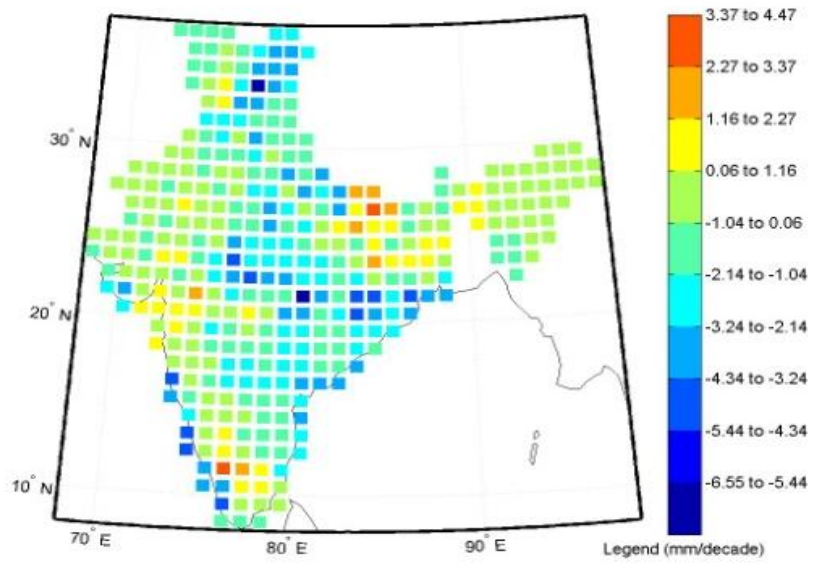


(c)

Figure 3.5.2: Slopes (mm/decade) of rainfall for the period 1960-1976 (b) June (c) July.



(d)

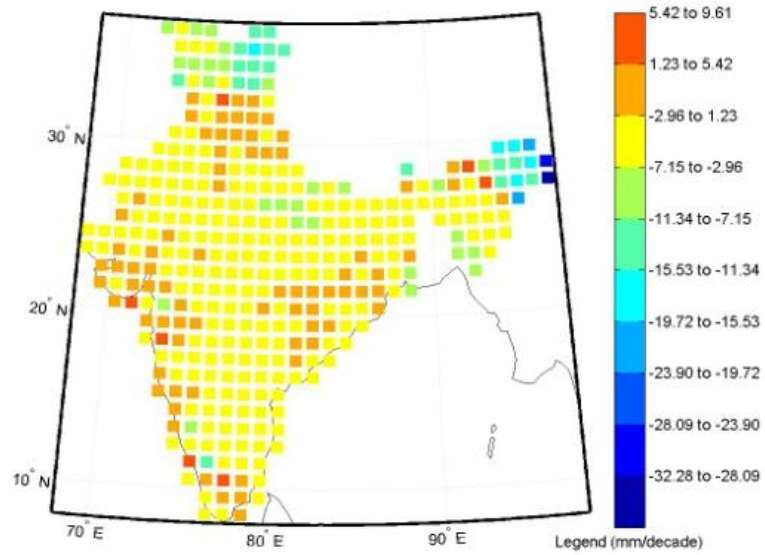


(e)

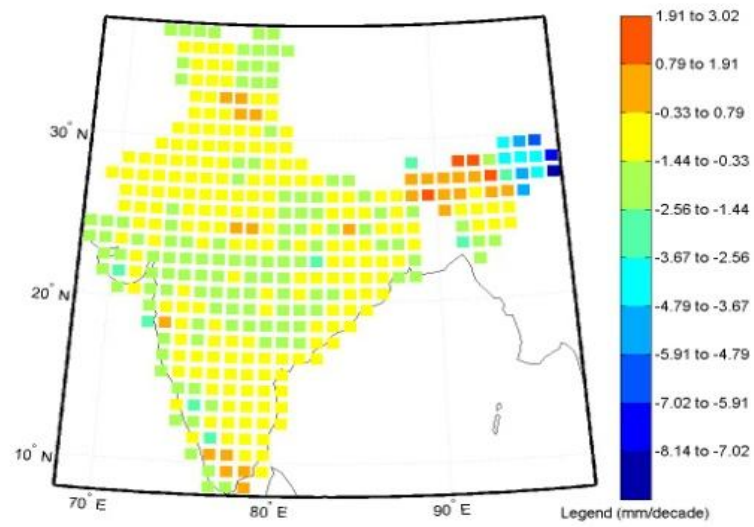
Figure 3.5.2: Slopes (mm/decade) of rainfall for the period 1960-1976 (d) August (e) September.

3.5.3 Epoch 1977-2012

- For the period 1977-2012, summer monsoon rainfall, as cumulative of 4 months, shows mild increasing trends [at a few locations, there is a likely hood of negative trends too] in all regions except for hill type (figures 3.5.3).
- In June, there is a significant decreasing trend in the hill type region. Central parts of India and tropical wet region experience a mixed trend in rainfall. In July, there is an increasing trend in all the regions except for hill type.
- But in August, central parts of India and grids of hill type show a decreasing trend while periphery locations indicate an increasing trend.
- The case is reversed in September. A significant increasing trend is seen in tropical wet, semi-arid and parts of central India while the southern periphery regions indicate decreasing trends.

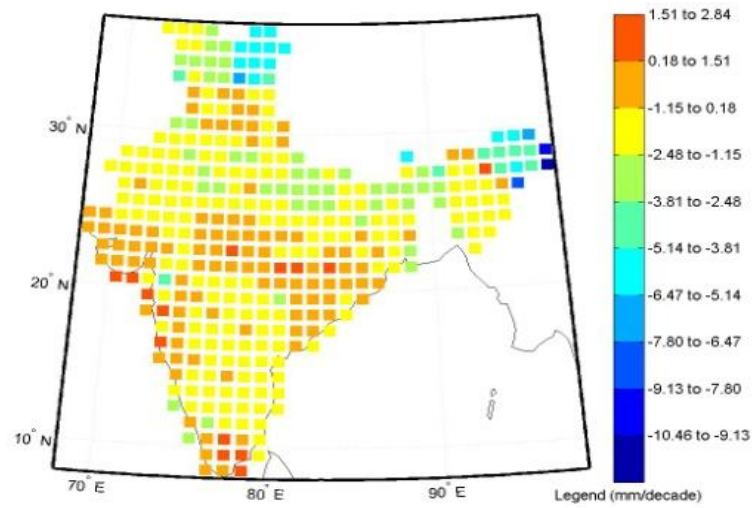


(a)

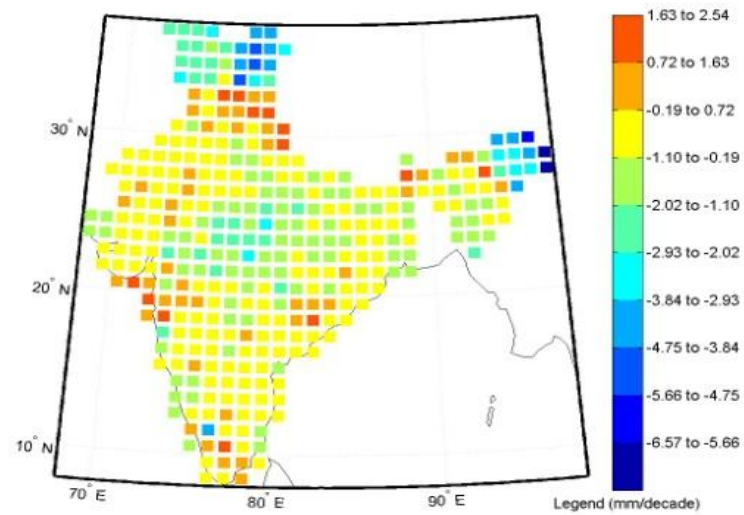


(b)

Figure 3.5.3: Slopes (mm/decade) of rainfall for the period 1977-2012 (a) JJAS (b) June.

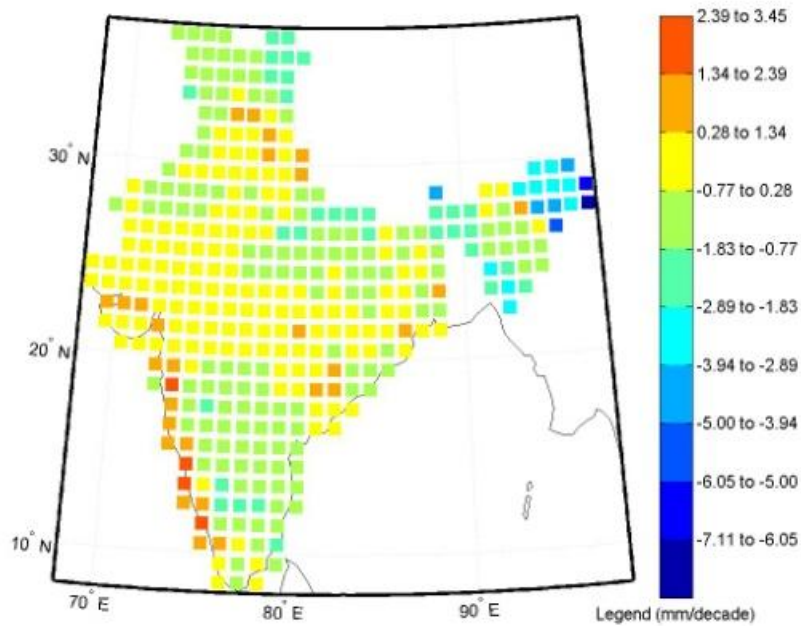


(c)



(d)

Figure 3.5.3: Slopes (mm/decade) of rainfall for the period 1977-2012 (c) July (d) August.



(e)

Figure 3.5.3: Slopes (mm/decade) of rainfall for the period 1977-2012 (e) September.

3.6 Distribution plot of rainfall

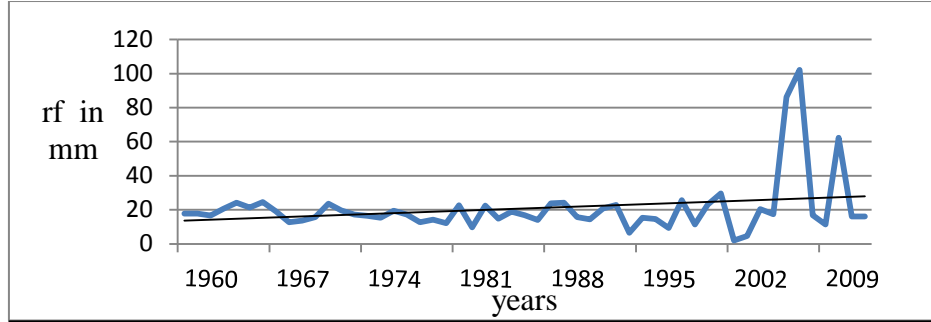
3.6 a) Meridional

To understand more about the rainfall pattern along the longitudinal and horizontal section, seven boxes along the longitudinal 78.5° E (9.5° to 10.5° , 13.5° to 14.5° , 18.5° to 19.5° , 21.5° to 22.5° , 25.5° to 26.5° , 29.5° to 30.5° , 33.5° to 34.5°) and three box grids [4 x 3 degrees] within 20.5° to 24.5° N and 74.5° to 77.5° E, 78.5° to 81.5° E and 82.5° to

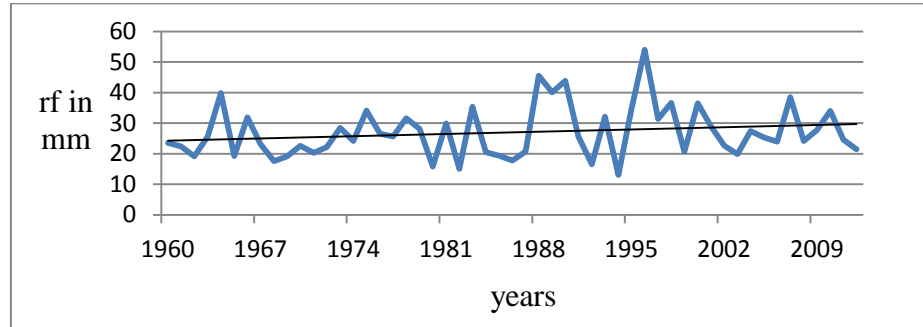
85.5⁰E (figures 2.4 and 2.5) were also considered for study and were analyzed for the years 1960-2012, 1960-76 and 1977-2012. The x-axis denotes the years and the y-axis, the cumulative rainfall (rf) for the years selected in mm. Figures 3.6.1, 3.6.2 and 3.6.3 show the yearly distribution plots of ISMR for the boxes and for the epochs 1960-2012, 1960-76 and 1977-2012 respectively.

3.6.1 Epoch 1960- 2012

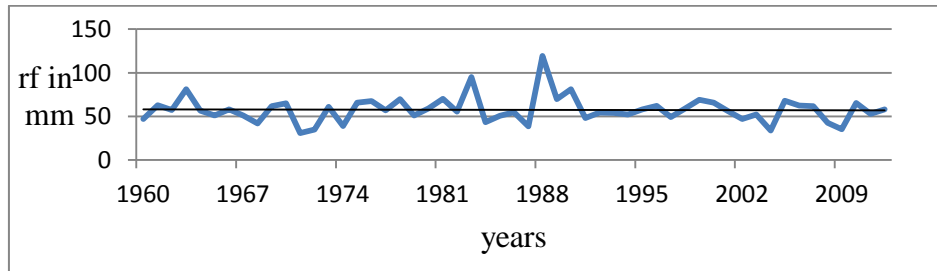
There was a significant increase in rainfall (about 102mm) during the year 2007 in the box 9.5⁰ to 10.5⁰ where as in the year 2002, only 1.9mm of rain was obtained (figures 3.6.1). But 22mm of rain was obtained in the box 13.5⁰ to 14.5⁰ in 2002. An increasing trend is seen in both the boxes 9.5⁰ to 10.5⁰ and 13.5⁰ to 14.5⁰. Five high peaks were noticed in this box during this period. During 1988, 120mm of rain was obtained in the grid 18.5⁰ to 19.5⁰. Four high peaks were observed in the grid 21.5⁰ to 22.5⁰ during the 1960-201. A decreasing trend was noticed in the grid 25.5⁰ to 26.5⁰ and in the box 33.5⁰ to 34.5⁰. A decreasing trend in rainfall was observed for the box 29.5⁰ to 30.5⁰ for most of the years. Two very high peaks of rainfall (above 100mm) during 1961 and 1988 were noticed in the box 33.5⁰ to 34.5⁰.



(a)

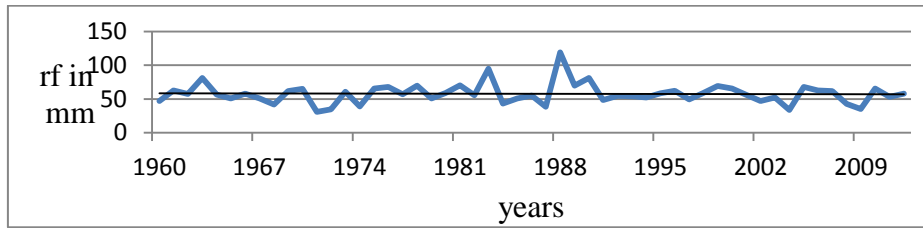


(b)

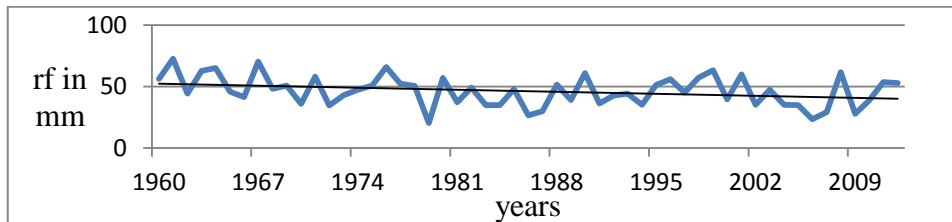


(c)

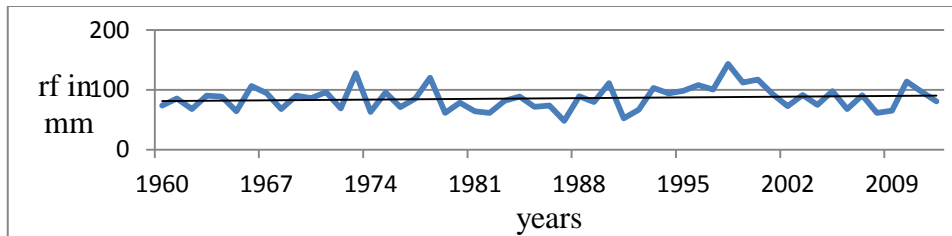
Figure 3.6.1: Distribution plot of ISMR (rf in mm) for the period 1960- 2012 for the longitude 78.5°E and for the latitudes (a) 9.5° to 10.5° N (b) 13.5° to 14.5°N (c) 18.5° to 19.5° N.



(d)

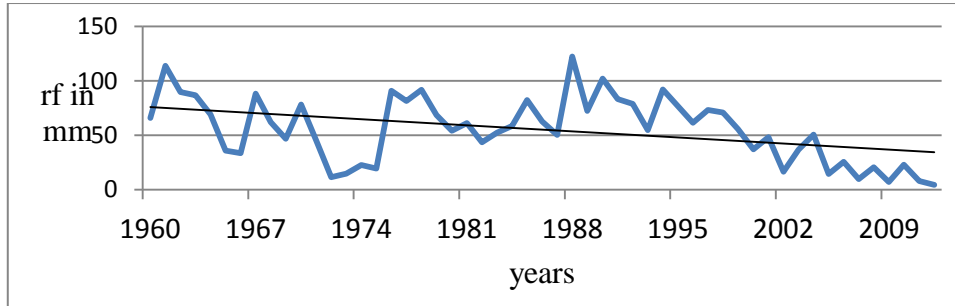


(e)



(f)

Figure 3.6.1: Distribution plot of ISMR (rf in mm) for the period 1960-2012 for the longitude 78.5°E and for the latitudes (d) 21.5° to 22.5° N (e) 25.5° to 26.5° N (f) 29.5° to 30.5° N.

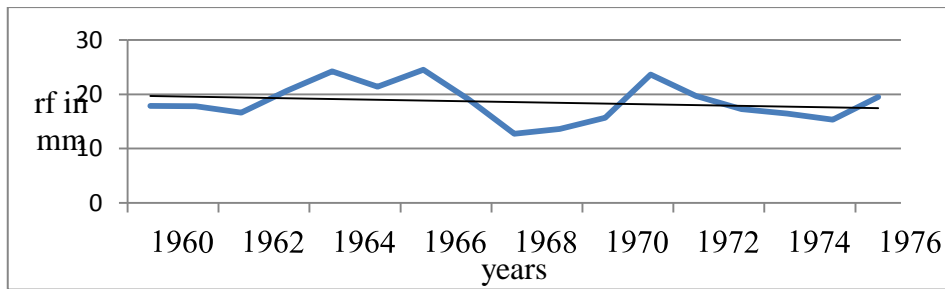


(g)

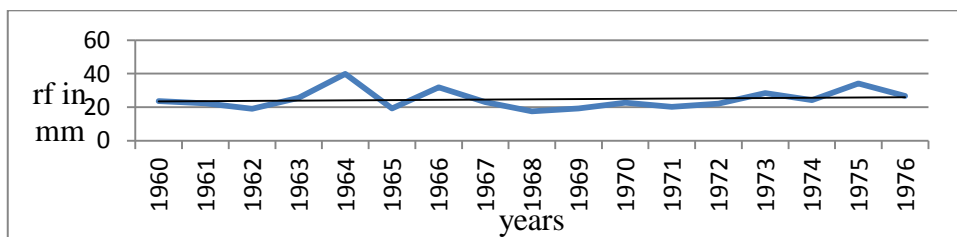
Figure 3.6.1: Distribution plot of ISMR (rf in mm) for the period 1960-2012 for the longitude 78.5°E and for the latitude (g) 33.5° to 34.5°N .

3.6.2 Epoch 1960-76

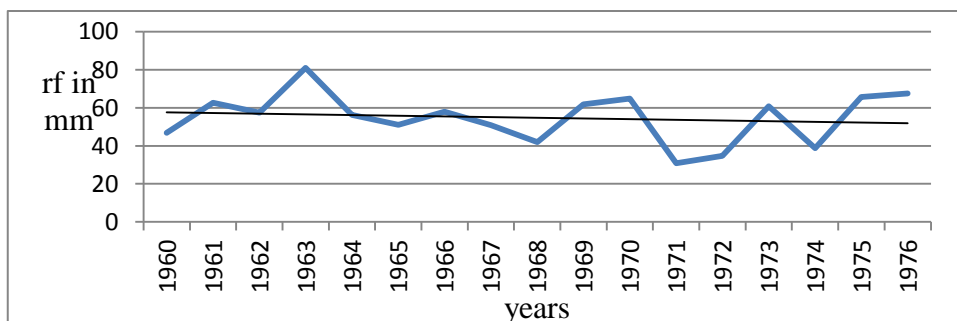
A consecutive increase and decrease was observed in the box 9.5° to 10.5° for the period 1960-76 (figures 3.6.2). Similar pattern was observed for the box 13.5° to 14.5° . A very high peak in the year 1963 and a decrease in the year 1971 noticed in the box 18.5° to 19.5° respectively. During 1961, an increase of around 100 mm was observed in the grid 21.5° to 22.5° . The year 1961 itself (around 72mm) experienced the highest rainfall for the grid 25.5° to 26.5° . For the box 29.5° to 30.5° a highest peak (around 128 mm) was noticed for the year 1973. The box 33.5° to 34.5° experienced a low rainfall of about 11mm in the year 1972 and a high of around 114 mm in the year 1961.



(a)

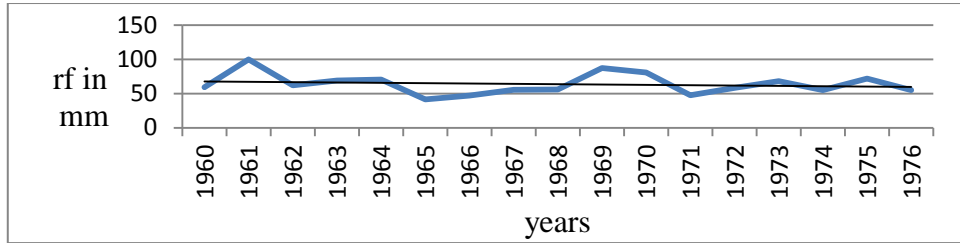


(b)

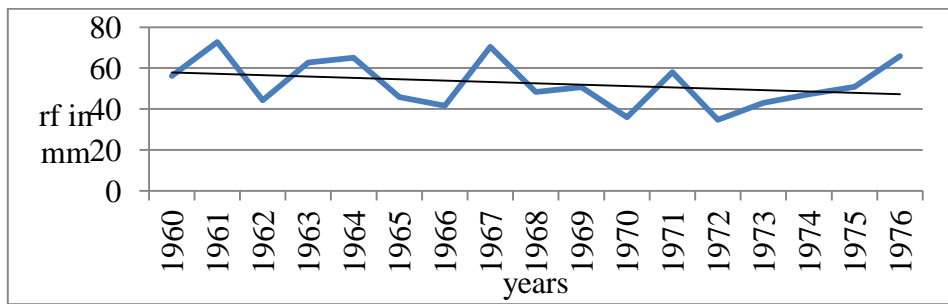


(c)

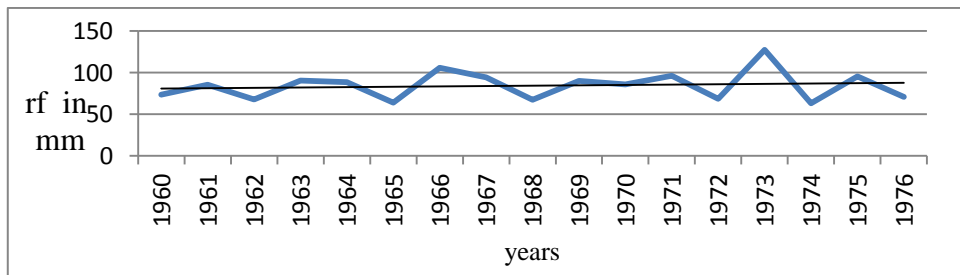
Figure 3.6.2: Distribution plot of ISMR (rf in mm) for the period 1960-1976 for the longitude 78.5°E and for the latitudes (a) 9.5° to 10.5° N (b) 13.5° to 14.5°N. (c) 18.5° to 19.5° N.



(d)

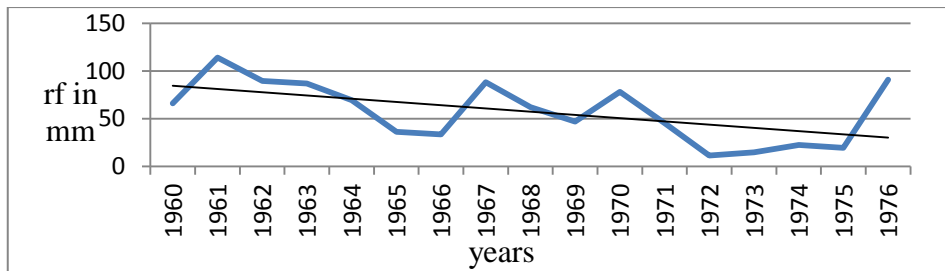


(e)



(f)

Figure 3.6.2: Distribution plot of ISMR (rf in mm) for the period 1960-1976 for the longitude 78.5°E and for the latitudes (d) 21.5° to 22.5°N (e) 25.5° to 26.5°N . (f) 29.5° to 30.5°N .

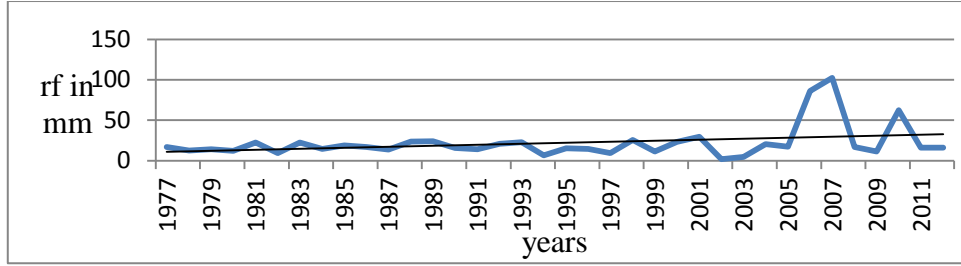


(g)

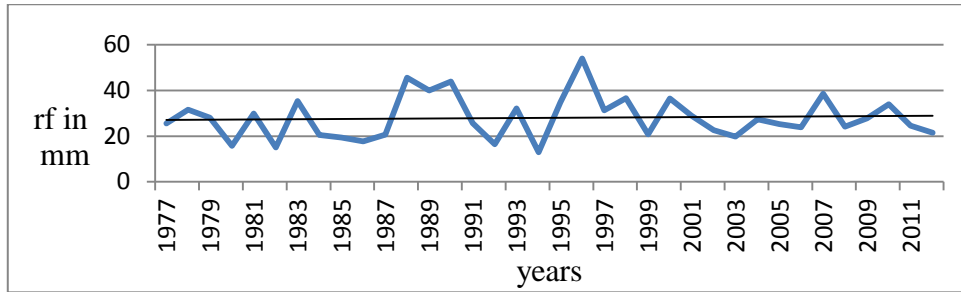
Figure 3.6.2: Distribution plot of ISMR (rf in mm) for the period 1960-1976 for the longitude 78.5°E and for the latitude (g) 33.5° to 34.5°N .

3.6.3 Epoch 1977-2012

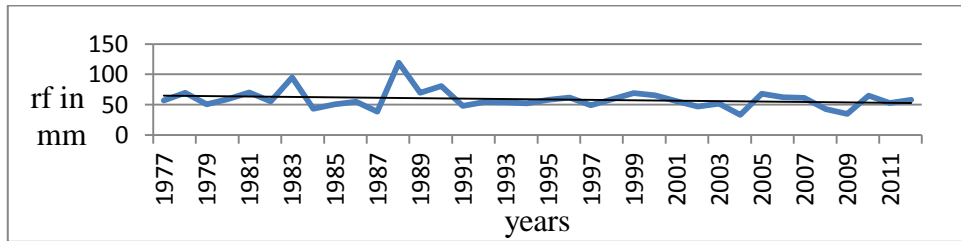
During 1977-2012, in the box 9.5° to 10.5° , the rainfall pattern showed a consistency up to the year 2005 and then increased to about 86mm in the year 2006 and further increased to 103mm in the year 2007. After 2007, a decreasing pattern is observed except for the year 2010 (figures 3.6.3). For the box 13.5° to 14.5° , an increase in rainfall pattern was noticed for 1996 and a decrease pattern for 1994. An increase and decrease pattern was noticed for the box 18.5° to 19.5° except for the year 1988. Similar pattern was observed in the grid 21.5° to 22.5° except for the year 1999. A consistent increase and decrease pattern was noticed in the grids 25.5° to 26.5° and 29.5° to 30.5° . A very significant decreasing trend in rainfall is seen for the box 33.5° to 34.5° .



(a)

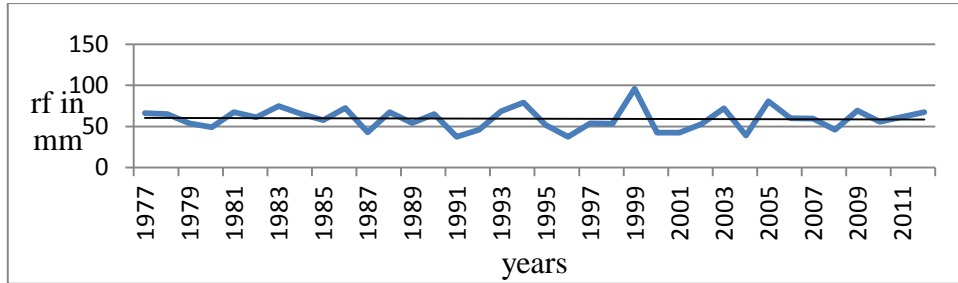


(b)

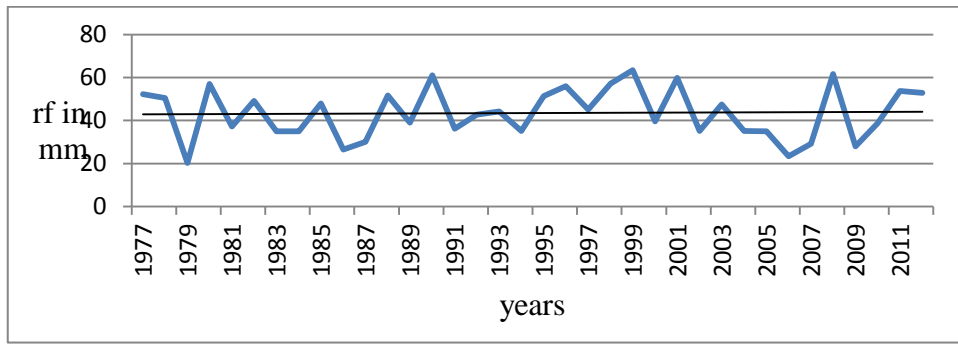


(c)

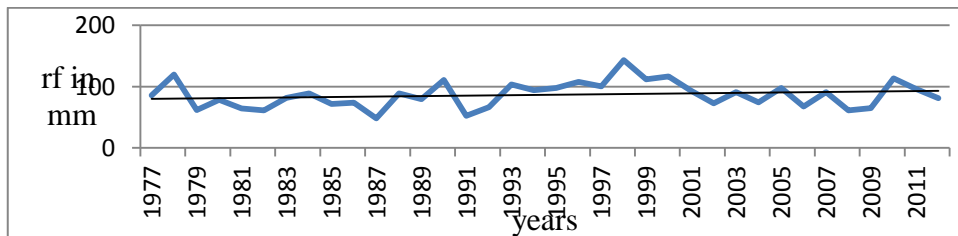
Figure 3.6.3: Distribution plot of ISMR (rf in mm) for the period 1977-2012 for the longitude 78.5°E and for the latitudes (a) 9.5° to 10.5° N (b) 13.5° to 14.5° N (c) 18.5° to 19.5° N.



(d)

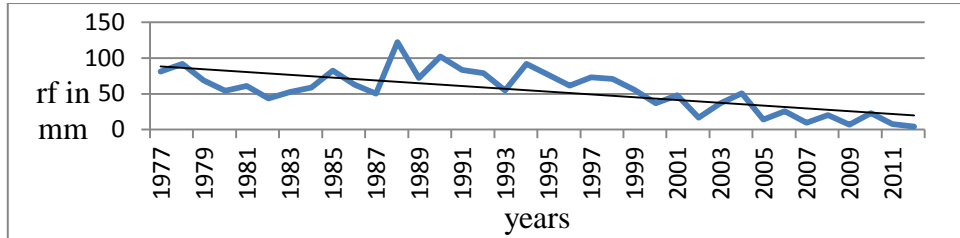


(e)



(f)

Figure 3.6.3: Distribution plot of ISMR (rf in mm) for the period 1977-2012 for the longitude 78.5°E and for the latitudes (d) 21.5° to 22.5° N (e) 25.5° to 26.5° N (f) 29.5° to 30.5° N.



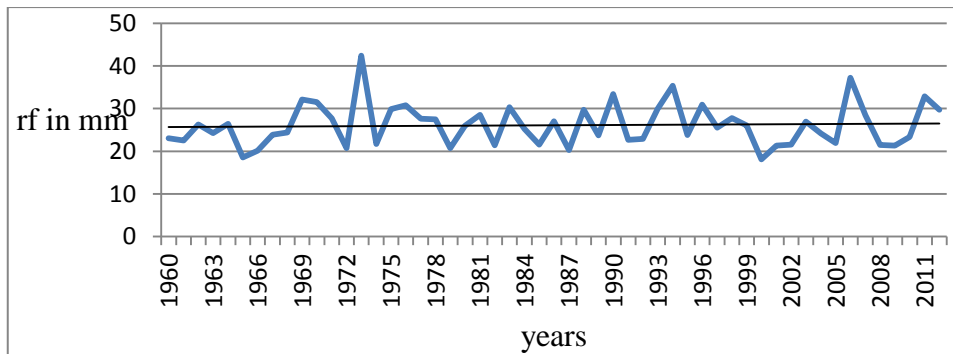
(g)

Figure 3.6.3: Distribution plot of ISMR (rf in mm) for the period 1977-2012 for the longitude 78.5°E and for the latitude (g) 33.5° to 34.5°N .

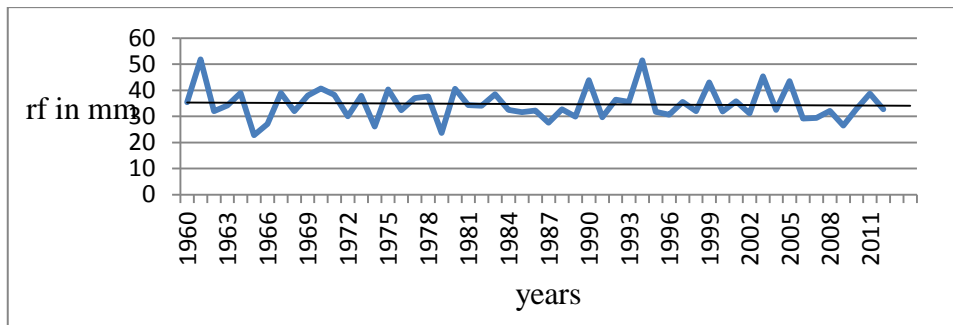
3.7 Zonal trend analysis of rainfall

3.7.1 Epoch 1960- 2012

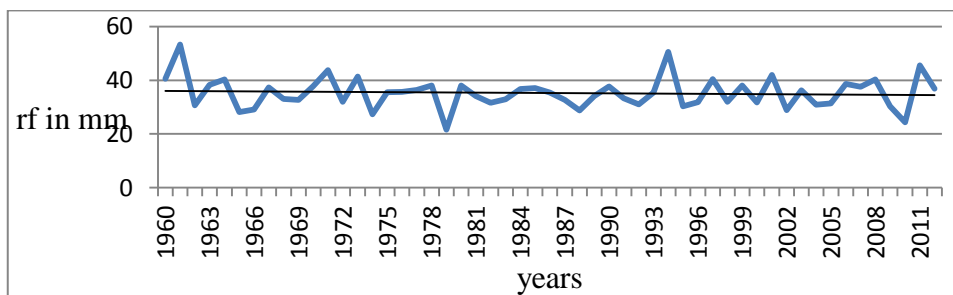
This study gives emphasis to the rainfall pattern over the Indian zonal transects. To accomplish this, the years 1960-2012, 1960-76 and 1977-2012 were analyzed. Figures 3.7.1 show the yearly distribution plots of ISMR for the respective boxes. The x-axis denotes the years and the y-axis, the cumulative rainfall (rf) for the years selected in mm. In the box 74.5° to 77.5°E , a highest rainfall of 42 mm was observed in the year 1973 and minimum was in the year 2000. In the second box, 78.5° to 81.5°E , a maximum of 52mm was observed for the years 1961 and 1994. Again for 1961, maximum rainfall of 53mm was noticed in the box 82.5° to 85.5°E .



(a)



(b)

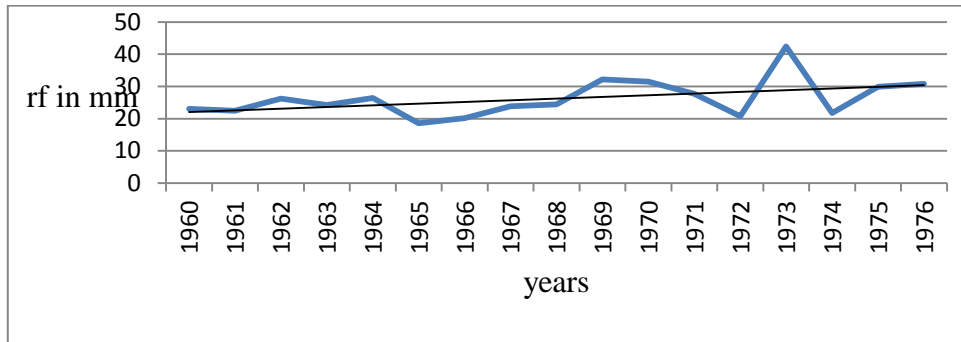


(c)

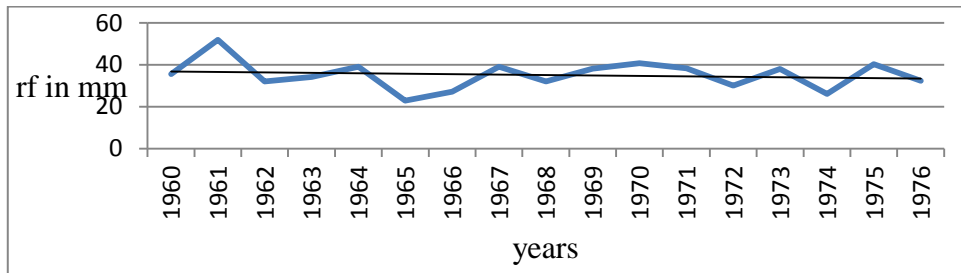
Figure 3.7.1: Distribution plot of ISMR (rf in mm) for the latitude 20.5° to 24.5° N, for the period 1960-2012 and for the longitudes (a) 74.5° to 77.5° E (b) 78.5° to 81.5° E (c) 82.5° to 85.5° E.

3.7.2 Epoch 1960-76

When the epoch 1960-76 is considered, a maximum rainfall of 42mm was observed for the year 1973 in the box 74.5° to 77.5° E. There is a steady increase and decrease in the box 78.5° to 81.5° E. About 53mm of rainfall is obtained in the box 82.5° to 85.5° E in the year 1961 which was a flood year (figures 3.7.2).

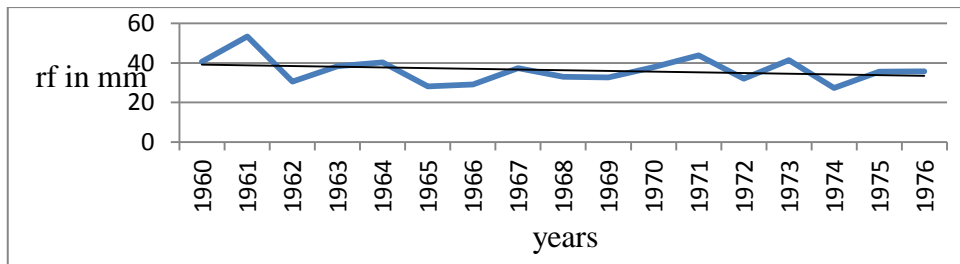


(a)



(b)

Figure 3.7.2: Distribution plot of ISMR (rf in mm) for the latitude 20.5° to 24.5° N, for the period 1960-1976 and for the longitudes (a) 74.5° to 77.5° E (b) 78.5° to 81.5° E.

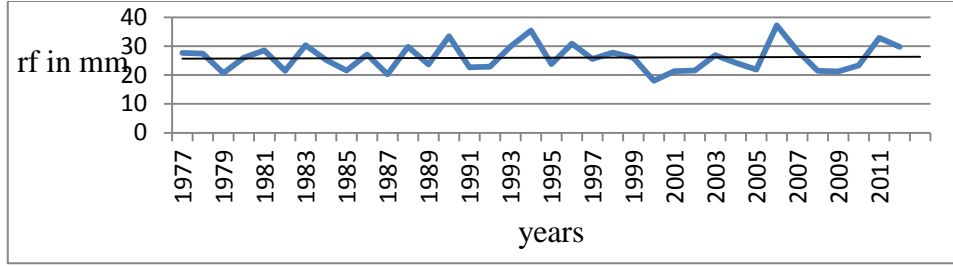


(c)

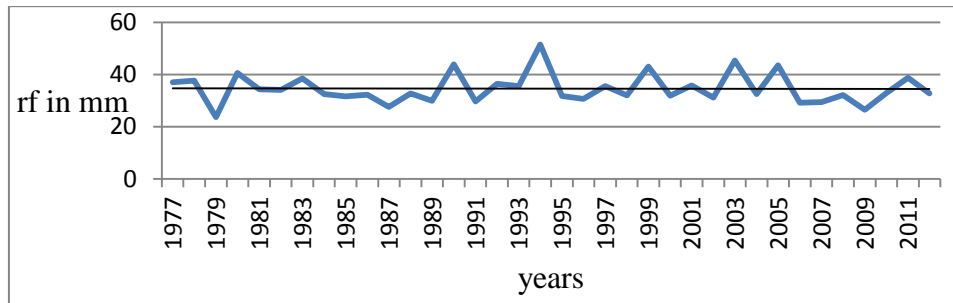
Figure 3.7.2: Distribution plot of ISMR (rf in mm) for the latitude 20.5° to 24.5° N, for the period 1960-1976 and for the longitude (c) 82.5° to 85.5° E.

3.7.3 Epoch 1977-2012

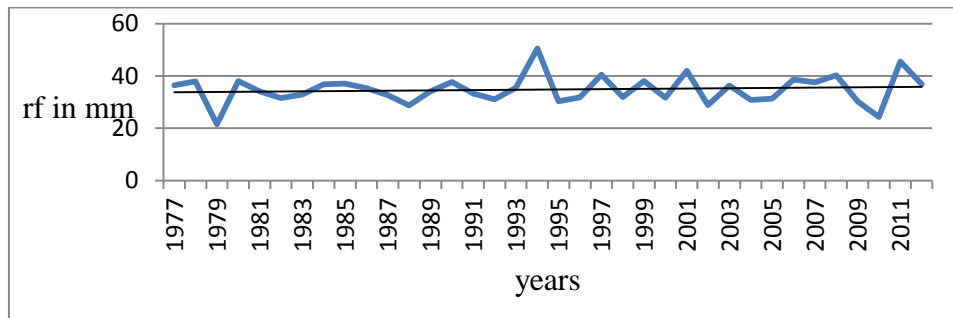
There is generally a significant decrease in the rainfall pattern when the epoch 1977-2012 is considered. In the box 74.5° to 77.5° E, highest rainfall of 37mm occurred in the year 2006 whereas 51mm of rain is obtained in 1994 for 78.5° to 81.5° E. In the box 82.5° to 85.5° E, rainfall of 50mm is obtained for the year 1994(figures 3.7.3).



(a)



(b)



(c)

Figure 3.7.3: Distribution plot of ISMR (rf in mm) for the latitude 20.5° to 24.5° N, for the period 1977-2012 and for the longitudes (a) 74.5° to 77.5° E (b) 78.5° to 81.5° E (c) 82.5° to 85.5° E.

3.8 Conclusion

This study helps to conclude that western IO has been warming steadily, based on annual trends and irrespective of the seasons, which is in good agreement with the study of Singh and Sarker (2003) and Roxy et al., (2014). Rate of SST warming was uniform for both AS and BOB during all months which supports the observations of Dinesh Kumar et al., (2016). From the long term trend analysis of SST, it is observed that tropical Indian Ocean was warming consistently at a rate of 0.25°C to 0.30°C per decade. The highest warming rate noticed at the central equatorial region was consistent throughout the annual period and is in agreement with previous studies of Rao et al., 2012 and Roxy et al., 2014. For winter and post monsoon seasons, BOB warms at a higher rate compared to AS which is in agreement with the observations of Dinesh Kumar et al., 2016. This is reflected in the annual case also. The negative (cooling) trend especially at the northern IO regions are believed to be an artifact of interpolation due to large spatial in homogeneity of the data set used. Even then, the data had produced comparable results in majority of areas. This study also shows that the IO warming is not seasonally biased.

Sub surface warming trend in IO was estimated for the period 1950 to 2011 making use of Hadley centre data. A warming trend was observed near Madagascar at 25m, 98m and 235m depths, whereas a mixture of warming and cooling trend can be seen at 540m and such warming trends completely disappear at the depth 967m; BOB experiences a warming trend at 25m which decreases at 98m and later, cooling was noticed at 235m. Both AS and BOB show cooling trend during winter at 25m, but, a warming trend is well noticeable for the other three seasons. A mixed

behavior of warming and cooling is indicated near south east equatorial region during post monsoon at a depth 98m. At 25m depth, a pocket of warming is observed near Indonesia during pre monsoon, monsoon and post monsoon and no such behavior was observed for winter and pre monsoon at depths 235m. When we go further deeper, at 967m, cooling was observed at the sub tropics for all seasons except for post monsoon which is in agreement with the observations of Alory et al., 2007, that the south equatorial waters of subsurface are prominently exhibiting cooling trends.

To conclude, the waters of IO synthesized for its vertical trends in either warming or cooling, the following prominent features are easily resolved for the NIO. Seasonality plays an important role for waters up to 235m, where mostly cooling trends have been noticed. However for waters beyond 500m to depths of 1000m, a warming trend is confirmed, even being established beyond 700m, which constitutes a continuation of the results from studies of IPCC, 2013 that the oceans have warmed to the depths of 700m. The results show a penetration of warming trend to higher subsurface levels but with a weakening in magnitude. Consistent with the warming trend in SST, temperature at sub surface also show warming trends in majority of areas. The magnitude of warming trend showed a decrease with increase in depth. However, the cooling trend at depths did not show any consistency with depth. Highest cooling trend was observed at 98 m depth. The area of warming trend below 25 m remains nearly constant with depth except for a low value at 235 m. In contrast to the NIO, the SIO indicates just the opposite phenomena (beyond 20⁰S). Waters up to 250m indicate warming trends across most seasons whereas

waters around 500m is sandwiched between the deep waters around 1000m wherein an established cooling trend is noticed. This study also noticed a warming trend around 20°S which extends to 235m depth in agreement with the observations of Alory et al., 2007. When we go beyond 540m, warming is pronounced in the Southern Ocean which agrees with the observations of IPCC, 2013.

When the temporal trends are considered, the winter and pre monsoon seasons of the epoch 1960-76 show an increasing trend in warming whereas a decreasing trend is noticed for monsoon and post monsoon seasons and annual too. But for the epoch 1977 - 2012, a warming trend was observed irrespective of the seasons. This supports the theory of a climate shift after 1976 (Clark et al., 2000; Hartmann and Gerd., 2005). A warming trend was observed in the annual dataset also. The marked change in the trend, post 1976, indicates that the IO was warming consistently, irrespective of the seasons, for the last 53 years.

Besides the trends of SST and subsurface temperature, study of rainfall trends of ISMR for the individual months June, July, August, September as well as combining the above four months. The spatial study on a 1°x1° grid reports the trends in ISMR for the six hydrological regions (as detailed in chapter 2) of India for the epochs 1960-2012, 1960-1976 and 1977-2012 at 5% significance level. In addition to above, the temporal trend analysis attempts study of ISMR for the entire country for the three epochs stated above.

It is well known that there was a climatic shift after the year 1976 (Clark et al., 2000; Hartmann and Gerd., 2005). Hence the rainfall trends

for the epochs 1960-76 and 1977-2012 are given special attention. The ISMR slope during 1960-2012 is in the range 2.75 mm to 5.1mm/decade. J, J, A, and S months individually have the slope in the range 0.66 to 1.55 mm /decade. There is a significant increasing trend in ISMR (9.94mm to 14.93 mm/decade) for the epoch 1960-76 and the maximum increase was observed in the month of August (4.99 mm to 7.26 mm/ decade). But the case is reversed for the next epoch 1977-2012. The ISMR trend is in the range 5.42 to 9.61 mm/decade but the rainfall trend of individual months fall in the range 1.5 mm to 3.45 mm/ decade. From the analysis of 53 years of $1^0 \times 1^0$ data, it is evident that, there is a significant decreasing trend in ISMR at 5% significance level. This supports the observations of Sharad et al., 2012 and Oza and Kishtawal, (2014). Moreover, the rainfall pattern of the humid subtropical regime, NE part of India is showing a significant decreasing trend for both the individual months as well as ISMR for the period 1960-2012 which agrees with the study of Oza and Kishtawal, 2014. For the epoch 1960-76, there is a significant increasing trend for ISMR and for the months June and July, but August and September show decreasing trend (-1.88 to 1.16mm/ decade). Also a significant decreasing trend is seen for ISMR and for the individual months for the epoch 1977-2012. The tropical wet regime also experiences a significant decreasing rainfall pattern which is evident from the data given. The results obtained through this study confirm the views expressed by Oceanographers and Meteorologists, that along with global Warming, there has been a decrease in rainfall after 1976.

CHAPTER 4

APPLICATION OF ANN IN PREDICTING RAINFALL FOR SOUTH WEST COAST OF INDIA

4.1 Introduction

Monsoon is a tropical phenomenon of Indian sub-continent. Forecast of Indian summer monsoon rainfall (June-September) has been very crucial and advantageous for farmers of India. The summer monsoon involves wind blowing from south-west direction (often known as southwest monsoon) from the Indian Ocean onto the Indian landmass during the months of June through September. These are generally rain-bearing winds, blowing from sea to land, and bring rains to most parts of the subcontinent. As noted earlier, they split into two branches, the Arabian Sea Branch and the Bay of Bengal Branch near the southernmost end of the Indian Peninsula. The monsoon of India depends on many pre-monsoon factors of the Indian Ocean (Nagesh Kumar et al., 2007; Krishna Kumar et al., 2010; Agboola et al., 2012). Neural networks are used to model complex relationships between inputs and outputs or to find patterns in data.

4.2 Factors influencing monsoon rainfall

Oceanographically, the Indian Ocean is the least explored of the major oceans. Empirical forecasting of Indian monsoon rainfall has been performed using combinations of climatic parameters, including atmospheric pressure, wind, SST, snow cover and the phase of El Niño–Southern Oscillation ENSO (Shukla and Mooley, 1987; Parthasarathy, 1988). Regression models based on these and other empirical correlations have been able to predict 60%–80% of the total seasonal Indian rainfall by the month of May preceding the summer monsoon (Hastenrath, 1988).

SST is an important oceanic parameter because it influences directly the air-sea exchange of heat.

4.3 Prediction models on monsoon

The initial work on Asian monsoon prediction is from Walker (1910). Bryan (1979) showed that in summer, warmer AS or IO is weakly associated with decreased rainfall and increased sea level pressure over India. Several attempts were carried out by Thapliyal, 1982, Gowariker et al., 1989 and Gowariker et al., 1991 leading to the development of better models for long range forecast of summer monsoon rainfall of India. Performance of the parametric and power regression models (Gowariker et al., 1991) showed reasonably accurate results. These models are used by IMD for long range forecasts in India. But these statistical models have some limitations. So attempts were made to develop better, alternate techniques for long range forecasts of summer monsoon rainfall of India. The 8 parameter hybrid principal component model was developed by using 30 year (1958-87) data as training period and 10 year period (1988-97) as verification period (Guhathakurta et al., 1999). An artificial intelligence approach for regional rainfall forecasting for Orissa state, India, on monthly and seasonal time scales was attempted by Nagesh Kumar et al., 2007. In his study, possible relation between regional rainfall over Orissa and the large scale climate indices like ENSO, EQUINOO and a local climate index of ocean – land temperature contrast were studied first and then used to forecast monsoon rainfall. The time series of all India summer monsoon rainfall was generated by area weighting the rainfall at 306 rain gauges across the country (Mooley and Parthasarathy, 1984). Empirical modeling approaches were used to forecast Indian

summer monsoon rainfall (ISMR). Gadgil et al., (2002) made a general overview of forecasting models for ISMR. Later, Krishna Kumar et al., (1995) and Sahai et al.,(2000) presented reviews on such empirical models.

Artificial neural networks (ANN) have the capability of capturing complex non-linearity in the time series, complex patterns hidden in the data, and also in prediction. Neural network technique learns the dynamics within the time series data (Elsner and Tsonis, 1992). In the early twentieth century ANN's were used to predict ISMR (Goswami and Srividya, 1996; Venkateswan et al., 1997; Guhathakurta et al., 1999). The time series approach was used to predict the future values by Goswami and Srividya (1996). Venkateswan et al., (1997) have predicted Indian monsoon rainfall with the help of some predictors and compared the result with linear regression technique. Guhathakurta et al., (1999) have used hybrid principal component and neural network approach to predict ISMR. Sahai et al., (2000) applied ANN technique to the monthly time series of June, July, August and September rainfall and observed that ANN technique gave better results than regression models. Iyengar and Raghu Kanth (2005) too used ANN for predicting ISMR. They have divided the whole time series into two series- linear part and non-linear part and applied ANN technique to the nonlinear part. However the above attempts have been limited to local/regional theatres and have limited predictive results.

4.4 Methodology and Results

4.4.1 Methodology

A seasonal ARIMA model was fitted to the rainfall of South West India for the period 1951 -2002 and rainfall for 2003 was predicted using Box-Jenkins methodology. But the forecast accuracy was not satisfactory, because ARIMA model has its own limitations.

As a preliminary exercise, ANN is applied to predict ISMR for a portion of Indian Subcontinent namely the west coast from Kerala region extending up to Bombay. The $1^{\circ} \times 1^{\circ}$ grids of the IO (0.5° - 24.5° N and 50.5° - 77.5° E) for the parameters SST, SLP, Humidity, U-wind and V-wind (25x 28 grids) is considered for the study. The monsoon months June to September (JJAS) over South West (SW) India (8.5° - 22.5° N and 74.5° - 78.5° E) depends on the above said pre-monsoon factors of the IO, as postulated. Hence data of these parameters during the pre-monsoon months March, April and May (MAM) is considered. Pre-processing of data was performed to obtain accurate results, because each of the parameters has about 25% of the data missing. The rainfall data is clustered using self organizing maps (SOM). Thirty six years (1960-1995) of data was used for training and nine years for validation (1996-2003) and one year (2004) for testing. The network had 30 hidden layers and each neuron in the network used a Levenberg- Marquardt activation function. Seventy nets were generated using feed- forward back propagation algorithm and the net converged for 300 iterations. Rainfall of the $1^{\circ} \times 1^{\circ}$ grids of SW India is predicted for one year (figure 4.1). The probability plot of residuals is plotted (figure 4.2).

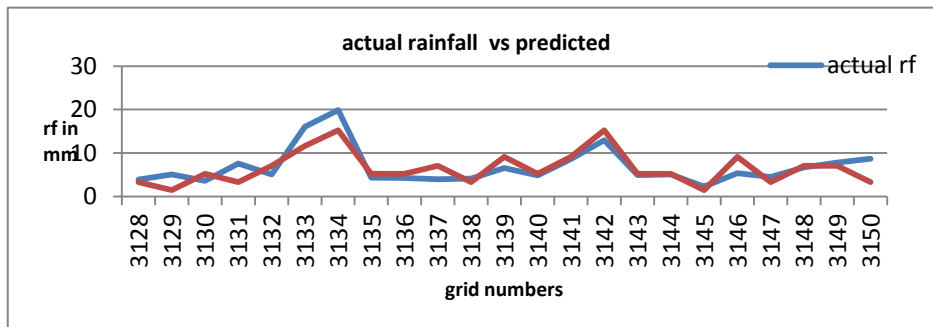


Figure 4.1: Actual rainfall versus Predicted rainfall (mm).

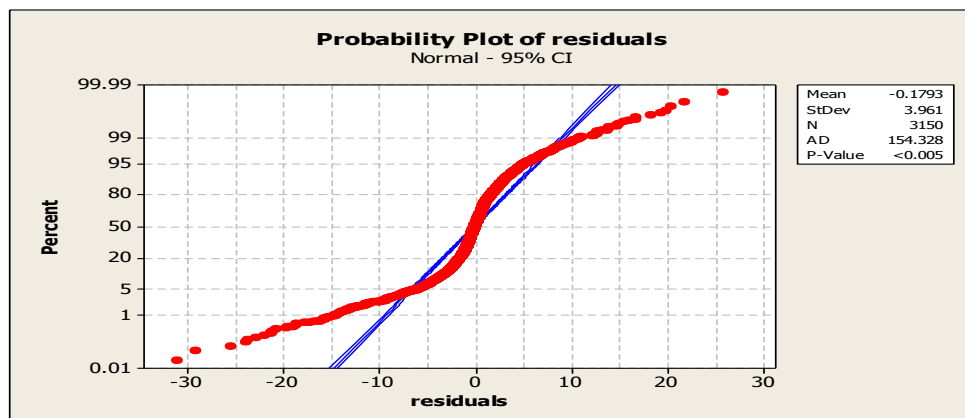


Figure 4. 2: Probability Plot of Residual.

4.4.2 Results

By applying clustering based Artificial Neural Networks methodology, rainfall of SW India has been hind cast. Table 4.1 shows the comparison of ANN forecasted rainfall with observed rainfall for the months JJAS. It can be observed that except for some grids, the model

results are fairly accurate and this model well predicts the trials of testing period. Figure 4.1 shows the plot of actual and predicted rainfall. It is directly evident from the performance of this model that at RMSE at 3%, excellent results are predictable. Error and accuracy is depicted in table 4.2. The present ANN model has performed comparatively better than such other models (Thapliyal, 1992; Guhathakuta et al., 1999; Nagesh Kumar et al., 2007; Krishna Kumar et al., 2010).

4.5 Conclusion

In this study, we have considered the tropical wet region extending up to Bombay and with the help of the highly influencing five parameters which have been selected to predict the SW monsoon rainfall by clustering based ANN technique. The rainfall data is clustered into 10 clusters and the clusters matches well for most of the grids. The model trained for thirty six years, followed by validation of eight years was tested for one year. The overall results are promising and can be applied as a meaning tool for work involving rainfall prediction.

Table4.1: Prediction of rainfall in mm.

| Year | Longitude | Latitude | Actual Rainfall (mm) | Actual Clusters | Predicted Clusters | Predicted Rainfall(mm) |
|------|-----------|----------|----------------------|-----------------|--------------------|------------------------|
| 2004 | 76.5 | 8.5 | 33.71 | 6 | 6 | 36.60 |
| 2004 | 77.5 | 8.5 | 12.26 | 9 | 9 | 13.47 |
| 2004 | 78.5 | 8.5 | 4.42 | 10 | 10 | 5.94 |
| 2004 | 76.5 | 9.5 | 45.24 | 5 | 6 | 36.60 |
| 2004 | 77.5 | 9.5 | 22.77 | 8 | 10 | 5.94 |
| 2004 | 78.5 | 9.5 | 5.52 | 10 | 10 | 5.94 |
| 2004 | 75.5 | 10.5 | 53.12 | 5 | 4 | 61.02 |
| 2004 | 76.5 | 10.5 | 50.61 | 5 | 9 | 13.47 |
| 2004 | 77.5 | 10.5 | 31.25 | 7 | 10 | 5.94 |
| 2004 | 78.5 | 10.5 | 14.88 | 9 | 10 | 5.94 |
| 2004 | 75.5 | 11.5 | 70.67 | 3 | 2 | 100.29 |
| 2004 | 76.5 | 11.5 | 32.2 | 7 | 7 | 28.46 |
| 2004 | 77.5 | 11.5 | 7.71 | 10 | 9 | 13.47 |
| 2004 | 78.5 | 11.5 | 8.36 | 10 | 10 | 5.94 |
| 2004 | 74.5 | 12.5 | 68.40 | 4 | 2 | 100.29 |
| 2004 | 75.5 | 12.5 | 50.12 | 5 | 1 | 127.50 |
| 2004 | 76.5 | 12.5 | 16.40 | 9 | 10 | 5.94 |
| 2004 | 77.5 | 12.5 | 7.54 | 10 | 10 | 5.94 |
| 2004 | 74.5 | 13.5 | 55.81 | 4 | 3 | 78.17 |
| 2004 | 75.5 | 13.5 | 14.67 | 9 | 1 | 127.50 |
| 2004 | 76.5 | 13.5 | 10.69 | 9 | 10 | 5.94 |

| | | | | | | |
|------|------|------|-------|----|----|--------|
| 2004 | 77.5 | 13.5 | 9.59 | 10 | 10 | 5.94 |
| 2004 | 74.5 | 14.5 | 76.64 | 3 | 1 | 127.50 |
| 2004 | 75.5 | 14.5 | 10.42 | 9 | 9 | 13.47 |
| 2004 | 76.5 | 14.5 | 10.43 | 9 | 9 | 13.47 |
| 2004 | 77.5 | 14.5 | 9.59 | 10 | 9 | 13.47 |
| 2004 | 73.5 | 15.5 | 69.90 | 3 | 3 | 78.17 |
| 2004 | 74.5 | 15.5 | 84.44 | 3 | 6 | 36.60 |
| 2004 | 75.5 | 15.5 | 64.30 | 4 | 9 | 13.47 |
| 2004 | 76.5 | 15.5 | 10.43 | 9 | 10 | 5.94 |
| 2004 | 77.5 | 15.5 | 9.79 | 9 | 8 | 20.92 |
| 2004 | 73.5 | 16.5 | 93.96 | 2 | 1 | 127.50 |
| 2004 | 74.5 | 16.5 | 24.90 | 7 | 7 | 28.46 |

Table 4.2: Calculated Error Measures

| NRMSE | RMSE | MAE | Accuracy |
|-------|------|-----|----------|
| 0.088 | 8.8% | 8.3 | 91.2% |

CHAPTER 5

**ANN BASED PREDICTION OF ISMR
FOR INDIAN HYDROLOGICAL
REGIONS**

5.1 Introduction

Monsoon has been a complex climate phenomenon. The Indian monsoon is of historical importance to both people of the Indian subcontinent and to the ecosystem of Indian Ocean (Walker, 1910). Krishna Kumar et al., (1995) have made a detailed review on seasonal forecasting of ISMR. Many attempts were thenceforth carried out towards improved understanding of this phenomenon in totality with the aid of advanced regression and parametric models aimed at long range prediction. Once the limitations of these statistical methods were recognized, attempts were made to develop better models using tools like ANN, which have the capability to capture the patterns hidden in data sets and therefore are applied for classification and prediction. A few studies were carried out to predict rainfall using ANN technique (Sahai et al., 2000; Iyengar and Raghu Kanth., 2005; Nagesh Kumar et al., 2007). If the Meteorologists are able to predict rainfall with good accuracy, it would help the farmers and agriculturists and which in turn will improve the economic and social status of our country.

The study deals with the prediction of ISMR with the help of five ocean state parameters using ANN approach. Prediction of ISMR is also carried out using AS, BOB and SIO parameters to understand the behavior of the ocean on Indian monsoon. Moreover, prediction of ISMR is done using the four Parameters (SST SLP, u wind and v wind) of IO. Most of the earlier studies show that SST plays an important role in Indian monsoons [Joseph and Pillai (1984); Rao and Goswami (1988); Vinayachandran and Shetye (1991)]. This study also uses SST, for the prediction of ISMR. Apart from this, the heavy rainfall regions of India

namely Tropical Wet and Humid Subtropical are also given special attention to know which month contributes more rainfall to ISMR, the prediction of rainfall for the months June, July, August and September individually using the five ocean-state parameters of IO is also considered for prediction.

5.2 Methodology and Results

To preserve consistency, the inputs are preprocessed and the missing values are filled via spline interpolation. The parameters, viz. SST, SLP, humidity, u wind and v wind of the whole IO act as inputs for ANN. The target data, rainfall is clustered using an unsupervised visualization technique called SOM. By attempting so, each object in the data set is assigned to the centroid which is the best approximation of that object [Dostál and Pokorný (2008); Kohail and El-Halees (2011)]. The whole data is divided into 6 hydrological climatic regions of $1^0 \times 1^0$ grids. The 5 inputs are fed to the network to predict rainfall in each grid for all 6 regions. Forty years (1960-1999) of data are used for training, eight years for validation (1999-2007) and five years (2008-2012) for testing. The numerical simulations were carried out for different cluster numbers ranging from 2 to 20 via two different cluster validation techniques and the error was found to be minimum for 10 clusters (shown in bold in table 5.2.1). The training of the network was carried out using 40 hidden neurons and each neuron in the network used a Levenberg - Marquardt activation function. The respective nets were generated using the feed-forward back propagation algorithm and the net converged after 500 iterations. In this case, we use a sigmoid function for the hidden layer. Figure 5.2.1 shows the network architecture of the model developed. The

correlation between the observed and predicted clusters used in training was found to be 0.785 at 99 % level of confidence. Once the network was trained, it was used to predict the rainfall for the years, 2008-2012. The actual and predicted clusters for this period have a correlation coefficient of 0.427 at 99% level of confidence.

Table 5.2.1 shows the optimal partitioning by the two methods S Dbw and Silhouette coefficient. The values obtained show that the error was found to be minimum for 10 clusters (shown bold). Table 5.2.2 shows the range of values of the clusters and the centroids covering the full period 1960-2012. Table 5.3 shows the statistics of the results obtained for the training and the test data of the 6 hydrological regions.

Table 5.2.2 has relevance to figures 5.2.2 which show the observed and predicted clusters of the ISMR using the parameters of IO full for the years 1960, 1970,1985,1990,2000 and 2003- all normal years respectively (figures 5.2.2(a) to (f)). From the figures, it is observed that for the normal years, the observed and predicted match extremely well for 4 hydrological regions namely, Tropical Wet, Desert, Hill Type and Humid subtropical. Figures 5.2.2(g) and (h) show the observed and predicted clusters for the year 2009 and 2012, which are the years used for testing the model. This analysis again is a clear indicator of the predictive exercises that an ANN can support. Also, four hydrological regions indicate proven comparison with good cluster matching. As a precursor to the rainfall instances, the oceanic state analyzed through measurable known variables, will be of immense value to an agro based nation like India. The mean, standard deviation, CV of the observed and the predicted for the decades and for the epochs 1960-1976, 1977-2012, 1960-85 and 1986-2012 are shown in table

5.2.4. It is observed from the table that there is a good match between the observed and the predicted. For example, tables 5.2.3 indicate the statistics of the results obtained for the training and the test data pertaining to this study and it is very obvious that the outcome from this study utilizing ocean based predictors for each of the hydrological zones will serve the intended purpose to a better extent.

Table 5.2.1: Optimal partitioning found by S_Dbw index and Silhouette coefficient.

| Number of clusters | S_Dbw | Silhouette coefficient |
|---------------------------|---------------|-------------------------------|
| 2 | 1.8319 | -0.4999 |
| 3 | 1.7252 | 0.2309 |
| 4 | 1.6237 | 0.4872 |
| 5 | 1.4794 | 0.7337 |
| 6 | 1.49 | 0.8016 |
| 7 | 1.5795 | 0.8453 |
| 8 | 1.4264 | 0.8915 |
| 9 | 1.3997 | 0.9245 |
| 10 | 1.3851 | 0.9444 |
| 11 | 1.7801 | 0.9463 |
| 12 | 2.4703 | 0.9121 |
| 13 | NAN | 0.9126 |
| 14 | 2.1425 | 0.9299 |
| 15 | 2.0444 | 0.9571 |
| 16 | 1.8905 | 0.9384 |
| 17 | 1.7894 | 0.9067 |
| 18 | 1.7315 | 0.9764 |
| 19 | 1.6489 | 0.9587 |
| 20 | 1.5692 | 0.9837 |

Table 5.2.2: Range of values of the clusters and the centroids covering the full period 1960-2012.

| Clusters | Range of values in which clusters lie | Centroid |
|-----------------|--|-----------------|
| C1 | [116.55, 188.90] | 129.74 |
| C2 | [89.80, 114.69] | 101.06 |
| C3 | [69.90, 88.85] | 78.40 |
| C4 | [53.52, 69.68] | 60.90 |
| C5 | [41.76, 53.89] | 46.80 |
| C6 | [32.59, 41.74] | 36.70 |
| C7 | [24.62, 32.59] | 28.47 |
| C8 | 16.97, 24.62] | 20.70 |
| C9 | [9.30, 16.97] | 13.17 |
| C10 | [0.02, 9.30] | 5.40 |

Table 5.2.3: Statistics of the results obtained for the training and the test data.

| Statistics- seasonal rainfall (JJAS) | Desert | Hill Type | Semi Arid | Humid sub Tropical | Tropical Wet | Tropical Wet and Dry |
|--|--------|-----------|-----------|--------------------|--------------|----------------------|
| Training data | | | | | | |
| Mean observed (mm) | 12.84 | 44.1 | 21.05 | 40.86 | 33.56 | 24.8 |
| Mean predicted(mm) | 13.63 | 46.2 | 22.65 | 41.08 | 33.92 | 25.3 |
| SD observed (mm) | 8.36 | 32.2 | 11.65 | 24.01 | 31.26 | 14.4 |
| SD predicted(mm) | 9.61 | 33.2 | 15.42 | 25.75 | 32.02 | 16.64 |
| CC between the actual and predicted rainfall | 0.56 | 0.75 | 0.56 | 0.69 | 0.88 | 0.62 |
| CC between the actual and predicted clusters | 0.59 | 0.77 | 0.61 | 0.69 | 0.88 | 0.67 |
| RMSE(mm) | 8.57 | 23.2 | 13.2 | 19.6 | 15.47 | 12.3 |
| NRMSE | 0.14 | 0.12 | 0.09 | 0.1 | 0.09 | 0.11 |
| Test data | | | | | | |
| Mean observed (mm) | 14.68 | 38.4 | 22.1 | 38.06 | 35.7 | 27.27 |
| Mean predicted(mm) | 13.45 | 44.9 | 23.09 | 41.77 | 34.03 | 28.43 |
| SD observed (mm) | 8.44 | 33.1 | 12.73 | 19.98 | 34.34 | 12.32 |
| SD predicted(mm) | 12.16 | 35.7 | 20.92 | 31.32 | 32.77 | 21.73 |
| CC between the actual and predicted rainfall | 0.28 | 0.42 | 0.26 | 0.42 | 0.74 | 0.33 |
| CC between the actual and predicted clusters | 0.25 | 0.46 | 0.24 | 0.33 | 0.74 | 0.36 |
| RMSE(mm) | 11.27 | 36.3 | 21.45 | 29.39 | 24.08 | 21.12 |
| NRMSE | 0.25 | 0.23 | 0.23 | 0.19 | 0.15 | 0.36 |

Table 5.2.4: CV of observed and predicted for the decades and for the epochs 1960-1976, 1977-2012, 1960-85 and 1986-2012.

| year | | actual rainfall | Predicted rainfall | CV actual | CV predicted |
|-----------|-----------------------|--------------------|-----------------------|--------------|-----------------|
| 1960-1969 | \bar{x} σ | 30.58 24.08 | 30.78 24.4 | 78.7 | 79.3 |
| 1970-1979 | \bar{x} σ | 30.64 24.13 | 31.51 25.23 | 78.8 | 80.1 |
| 1980-1989 | \bar{x} σ | 30.16 23.93 | 30.35 23.95 | 79.3 | 78.9 |
| 1990-1999 | \bar{x} σ | 30.42 22.43 | 30.55 23.42 | 73.7 | 76.7 |
| 2000-2007 | \bar{x} σ | 27.86 21.55 | 32.53 28.27 | 77.4 | 86.9 |
| 1960-1976 | \bar{x} σ | 30.82 24.73 | 31.15 24.83 | 80.2 | 79.7 |
| 1977-2012 | \bar{x} σ | 29.58 22.6 | 31.21 25.53 | 76.4 | 81.8 |
| 1960-1985 | \bar{x} σ | 30.63 24.28 | 31.01 24.69 | 79.2 | 79.6 |
| 1986-2012 | \bar{x} σ | 29.35 22.31 | 31.37 25.9 | 76 | 82.5 |

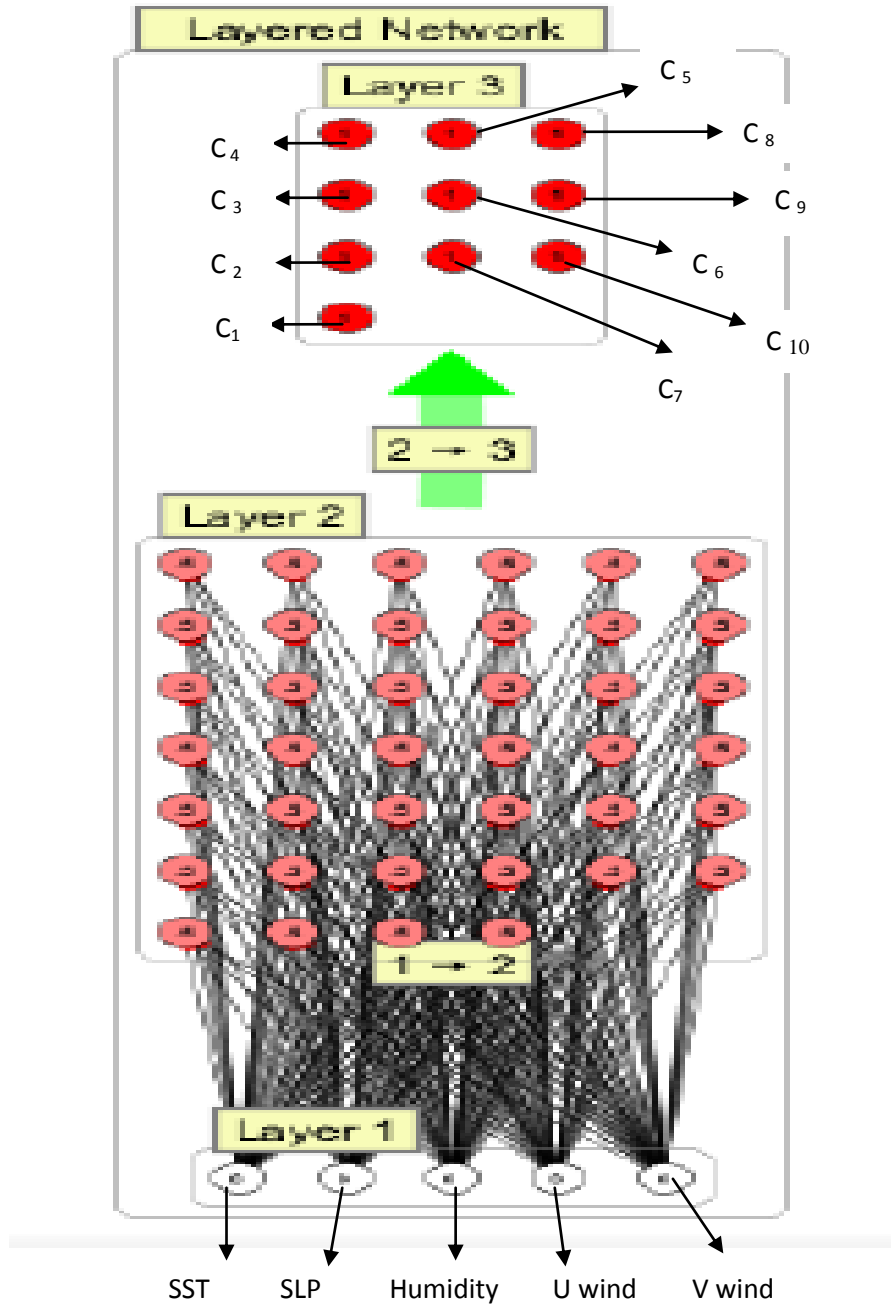


Figure 5.2.1: Feed forward Neural Network.

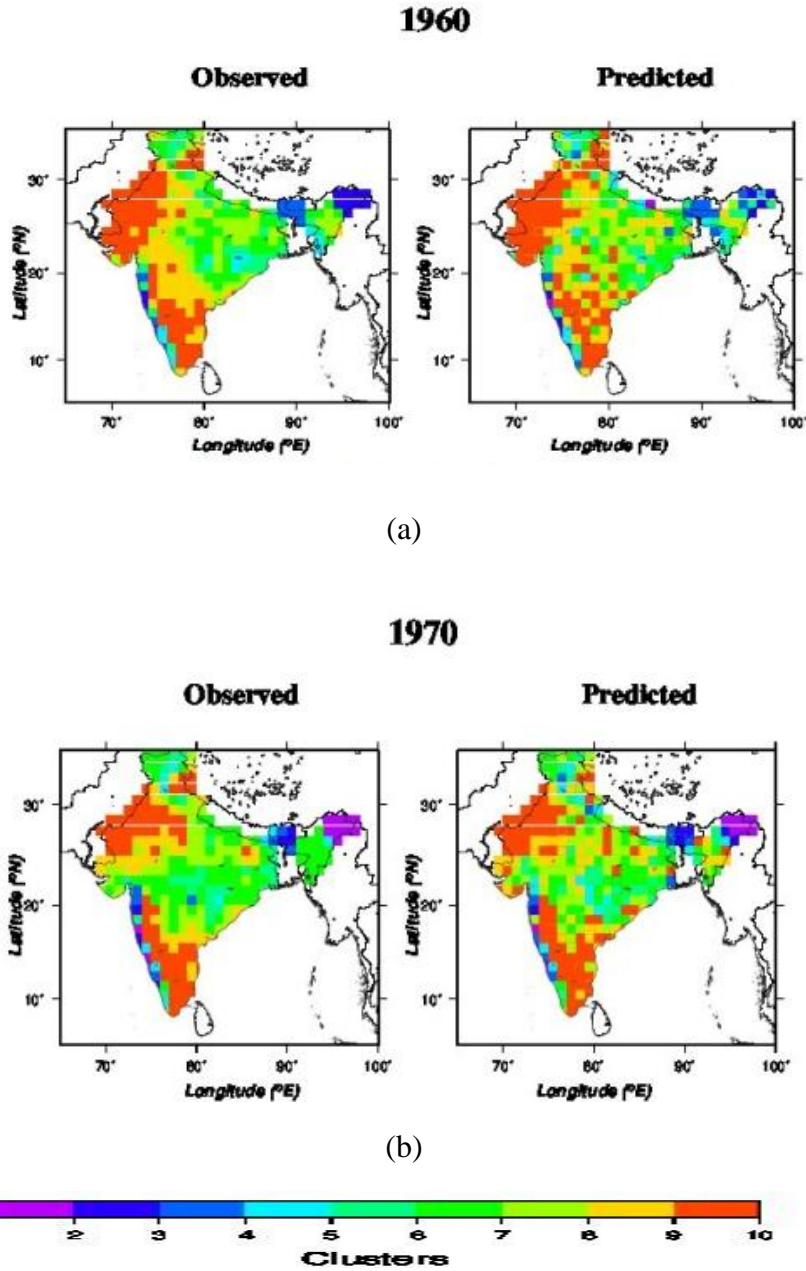


Figure 5.2.2: Observed and predicted clusters representing rainfall using the parameters of IO full for the years (a) 1960 (b) 1970.

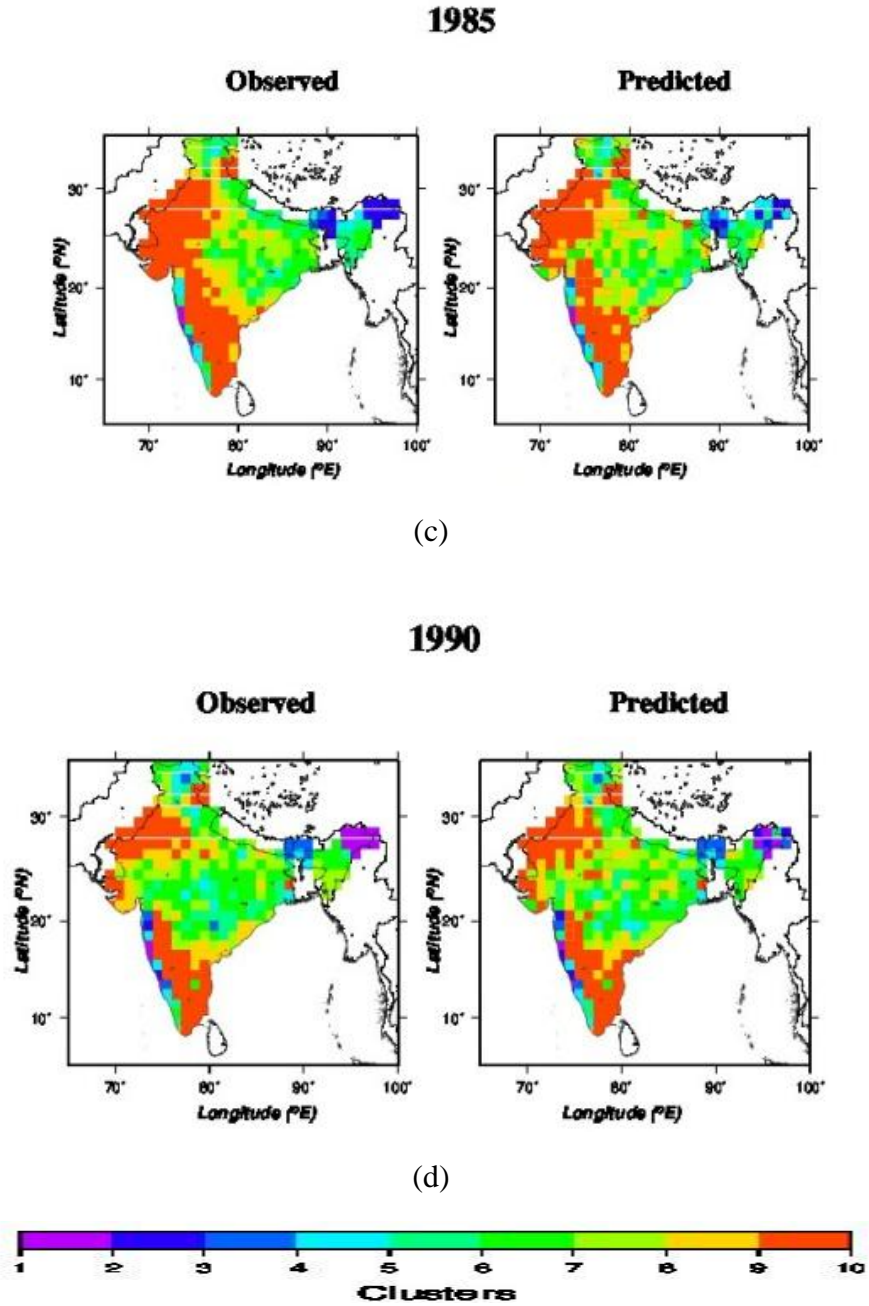


Figure 5.2.2: Observed and predicted clusters representing rainfall using the parameters of IO full for the years (c) 1985 (d) 1990.

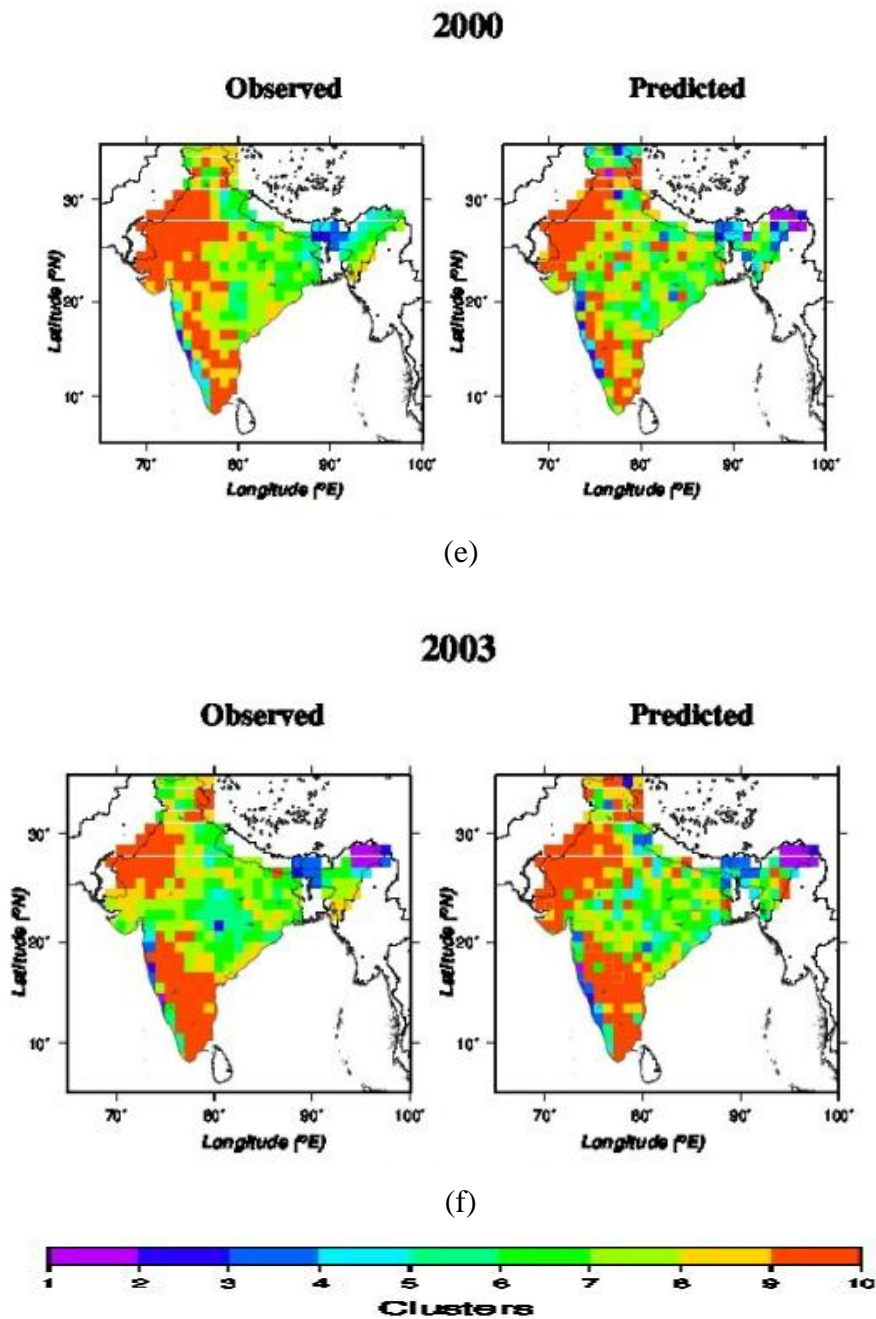


Figure 5.2.2: Observed and predicted clusters representing rainfall using the parameters of IO full for the years (e) 2000 (f) 2003.

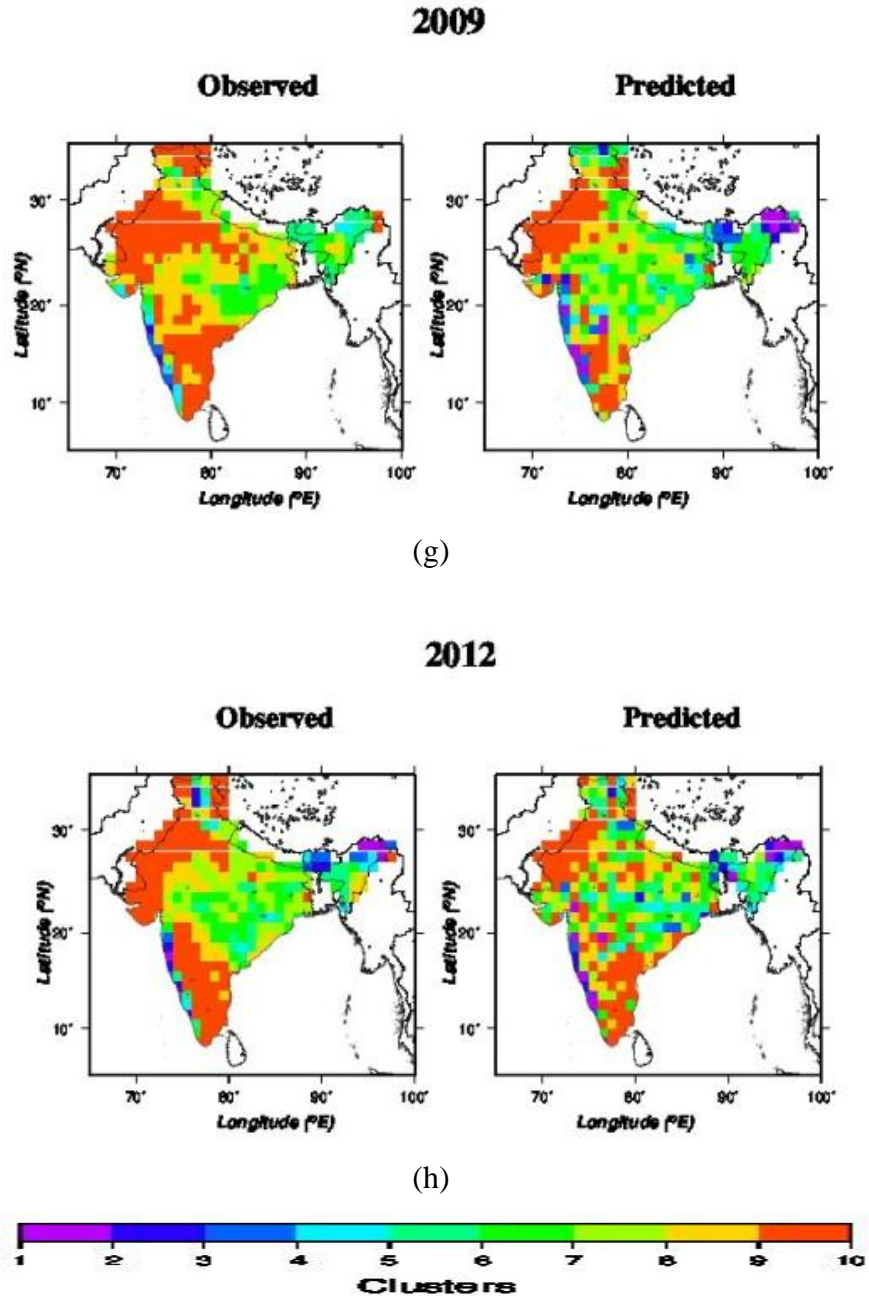


Figure 5.2.2: Observed and predicted clusters representing rainfall using the parameters of IO full for the years (g) 2009 (h) 2012.

Similar analysis is performed with the parameters of

- Arabian Sea (AS) - 0° to 25° N, 45° E to 80° E.
- Bay of Bengal (BOB) - 0° to 25° N, 80° E to 100° E.
- South Indian Ocean (SIO) - 0° to 30° S, 30° E to 120° E.

5.3 Analysis - AS parameters

Figure 5.3.1(a) to (f) show the observed and predicted clusters of ISMR obtained from AS parameters for the years 1960,1970,1985,1990,2000 and 2003-all normal years respectively. Figures 5.3.1(g) and (h) show the observed and predicted clusters for the year 2009 and 2012, which are the years used for testing the model.

5.4 Analysis- BOB parameters

Figure 5.4.1(a) to (f) shows the observed and predicted clusters of the ISMR obtained from BOB parameters for the years 1960, 1970,1985,1990, 2000 and 2003-all normal years respectively. Figures 5.4.1 (g) and (h) show the observed and predicted clusters for the year 2009 and 2012, which are the years used for testing the model.

5.5 Analysis - SIO parameters

Figures 5.5.1(a) to (f) show the observed and predicted clusters of ISMR obtained from SIO parameters for the years 1960,1970,1985,1990,2000 and 2003-all normal years respectively. Figures (g) and (h) show the observed and predicted clusters for the year 2009 and 2012, which are the years used for testing the model.

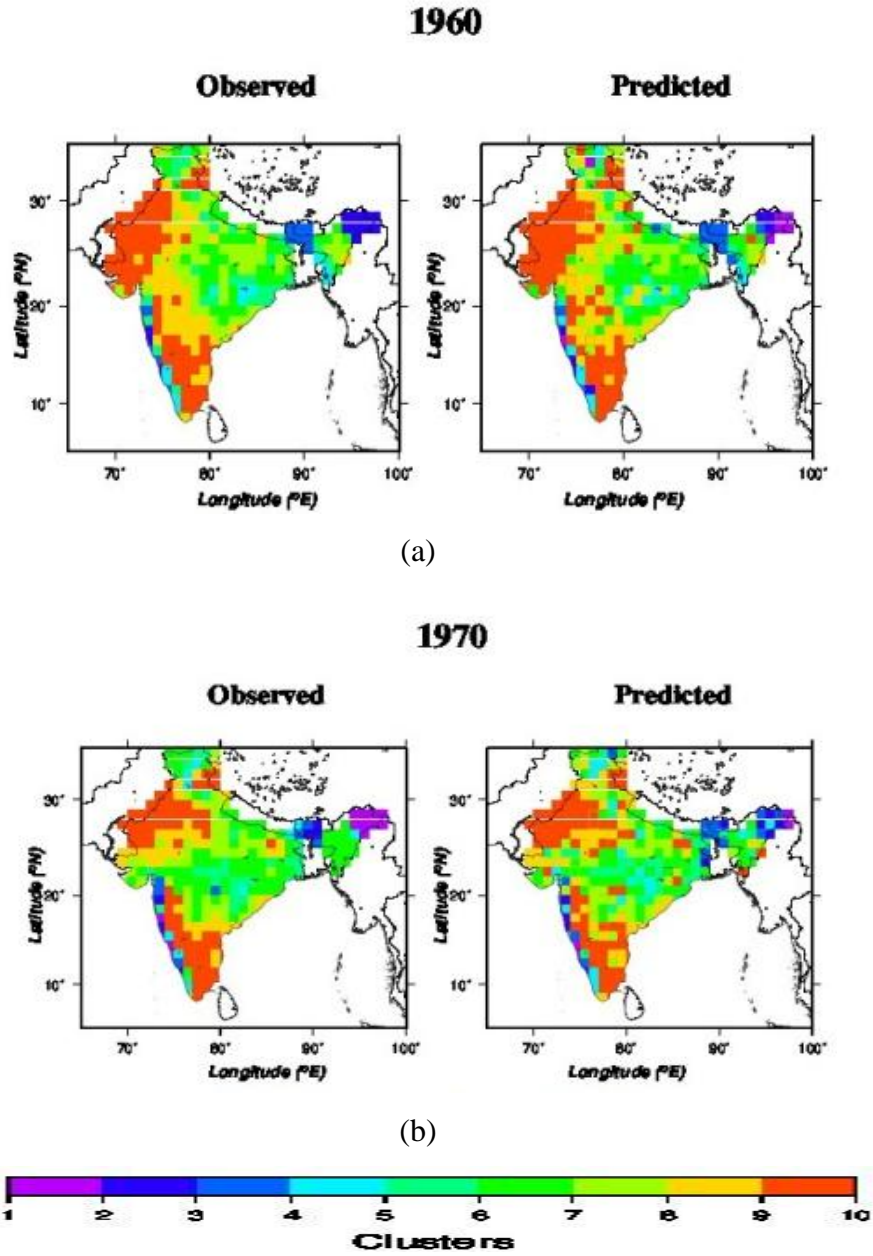


Figure 5.3.1: Observed and predicted clusters representing rainfall using the parameters of AS for the years (a) 1960 (b) 1970.

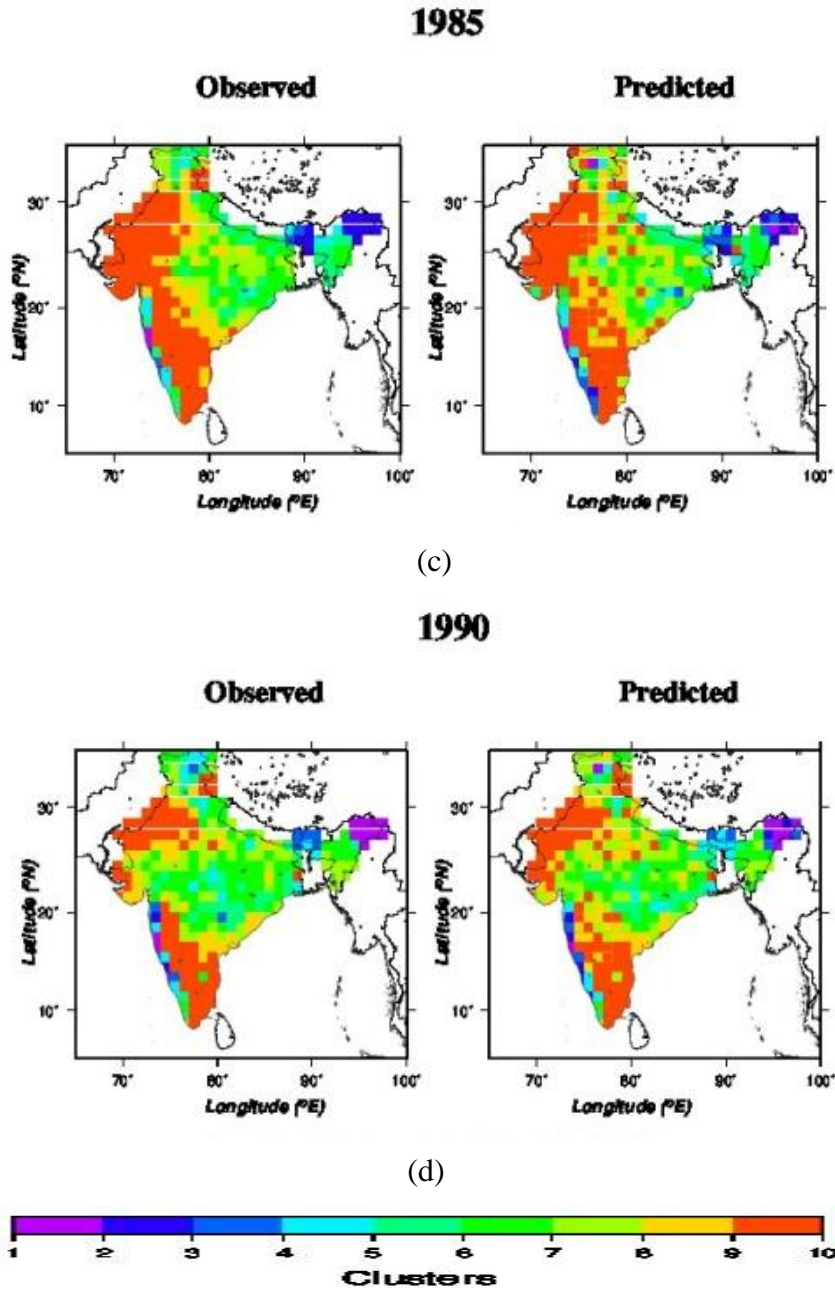


Figure 5.3.1: Observed and predicted clusters representing rainfall using the parameters of AS for the years (c) 1985 (d) 1990.

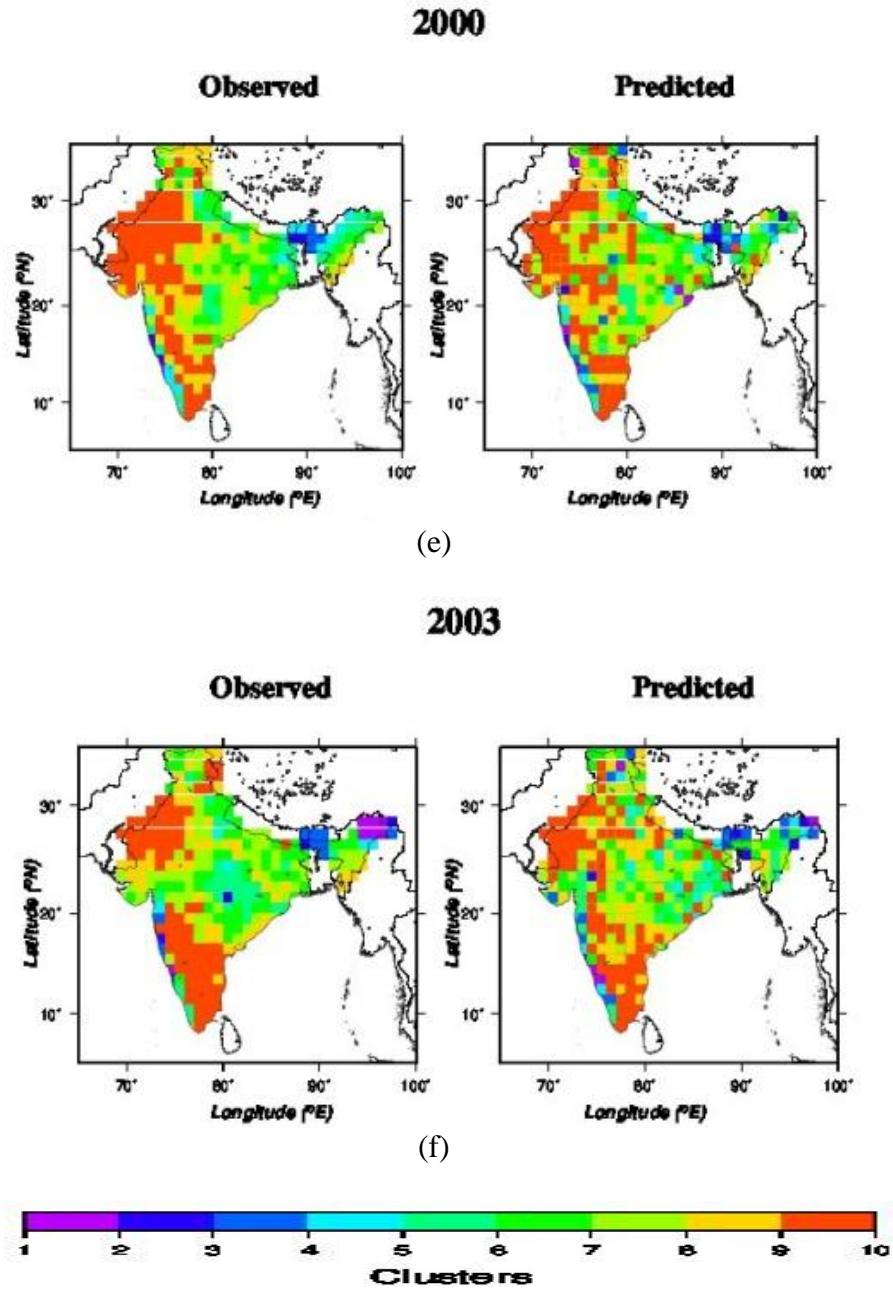


Figure 5.3.1: Observed and predicted clusters representing rainfall using the parameters of AS for the years (e) 2000 (f) 2003.

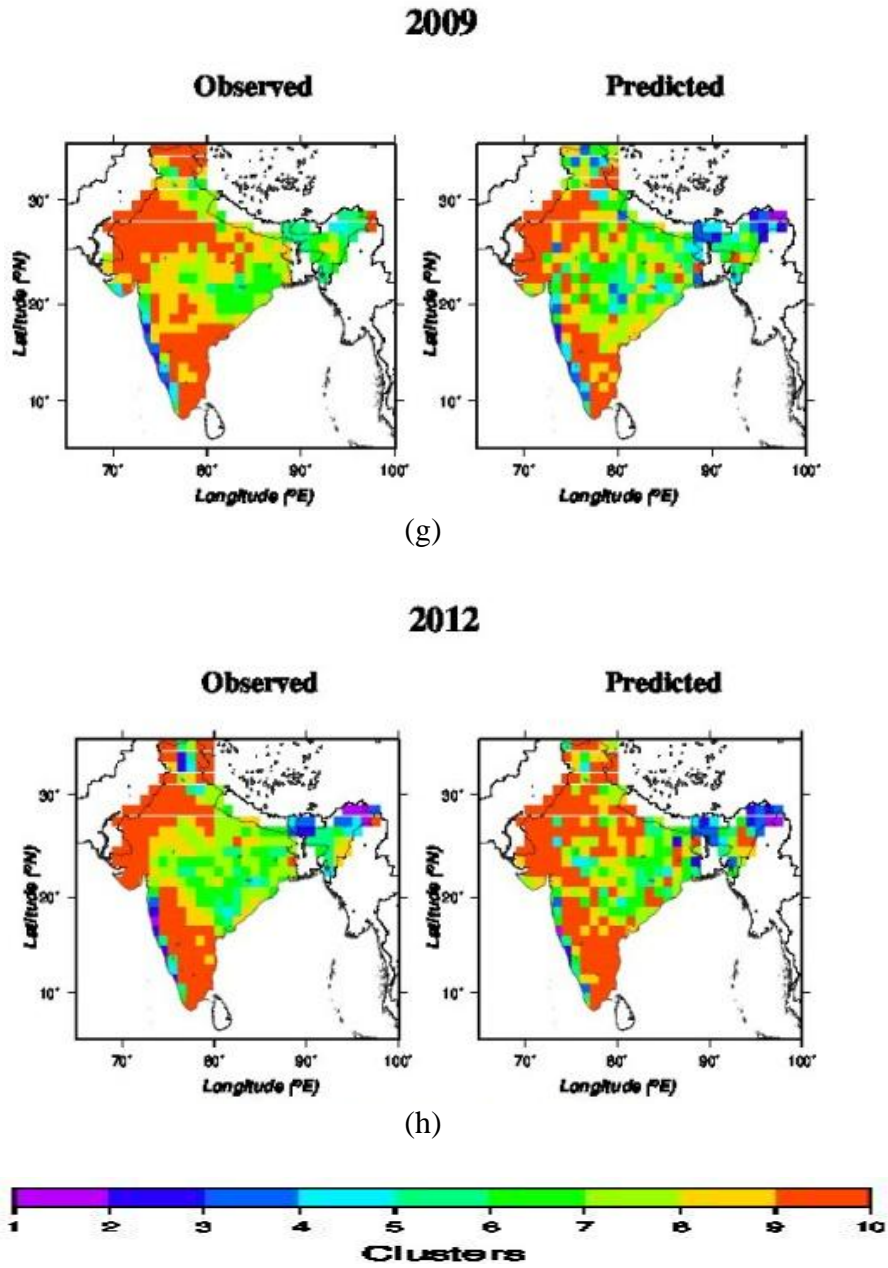


Figure 5.3.1: Observed and predicted clusters representing rainfall using the parameters of AS for the years (g) 2009 (h) 2012.

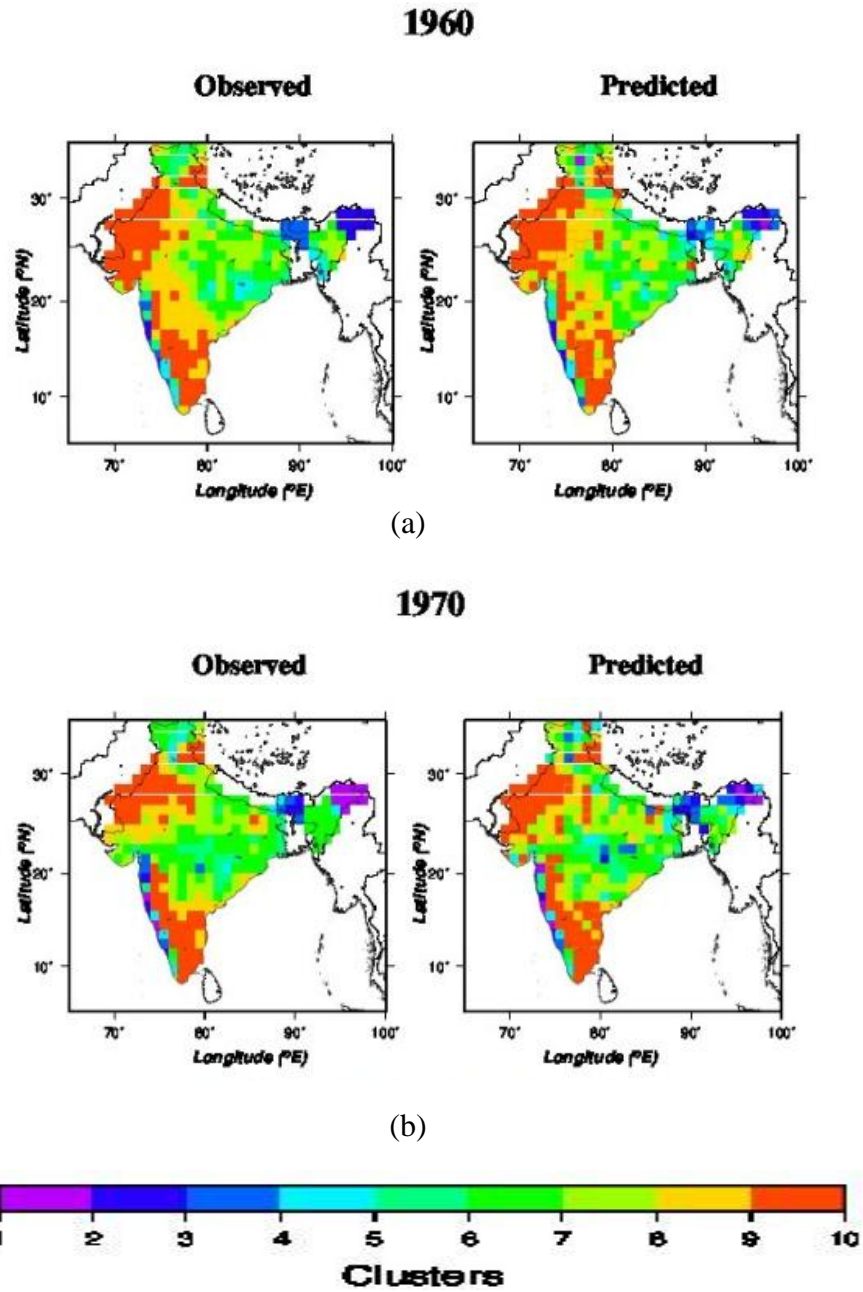


Figure 5.4.1: Observed and predicted clusters representing rainfall using the parameters of BOB for the years (a) 1960 (b) 1970.

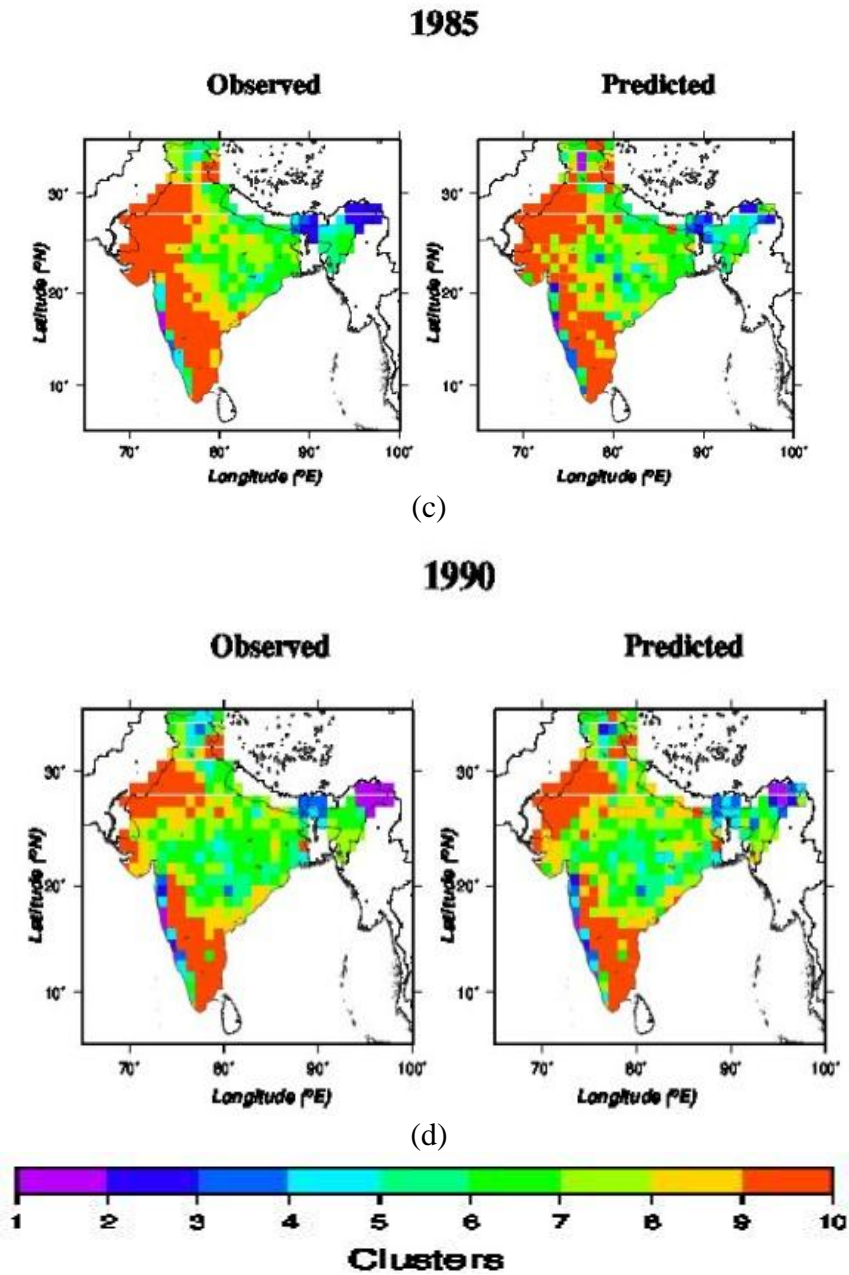


Figure 5.4.1: Observed and predicted clusters representing rainfall using the parameters of BOB for the years (c) 1985 (d) 1990.

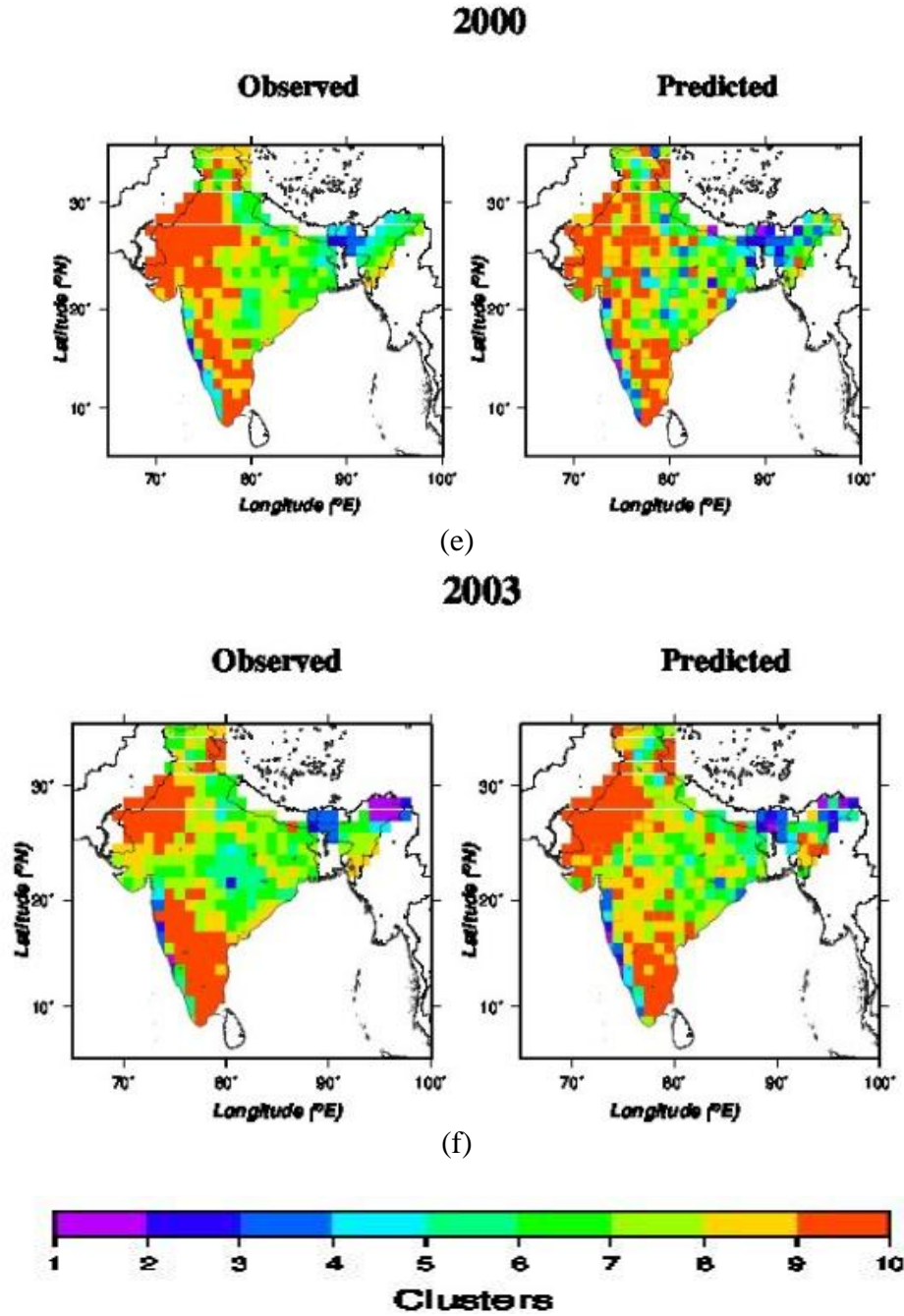


Figure 5.4.1: Observed and predicted clusters representing rainfall using the parameters of BOB for the years (e) 2000 (f) 2003.

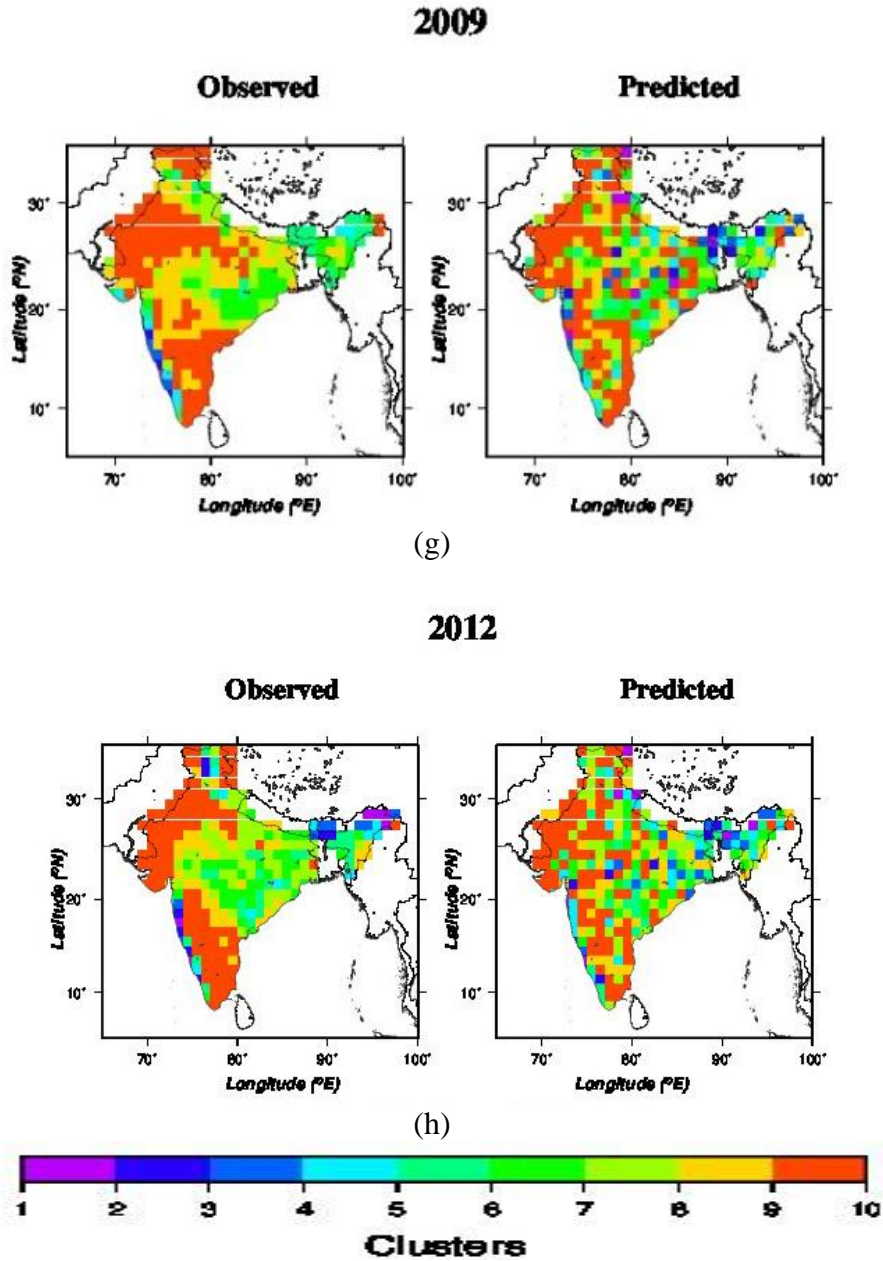


Figure 5.4.1: Observed and predicted clusters representing rainfall using the parameters of BOB for the years (g) 2009 (h) 2012.

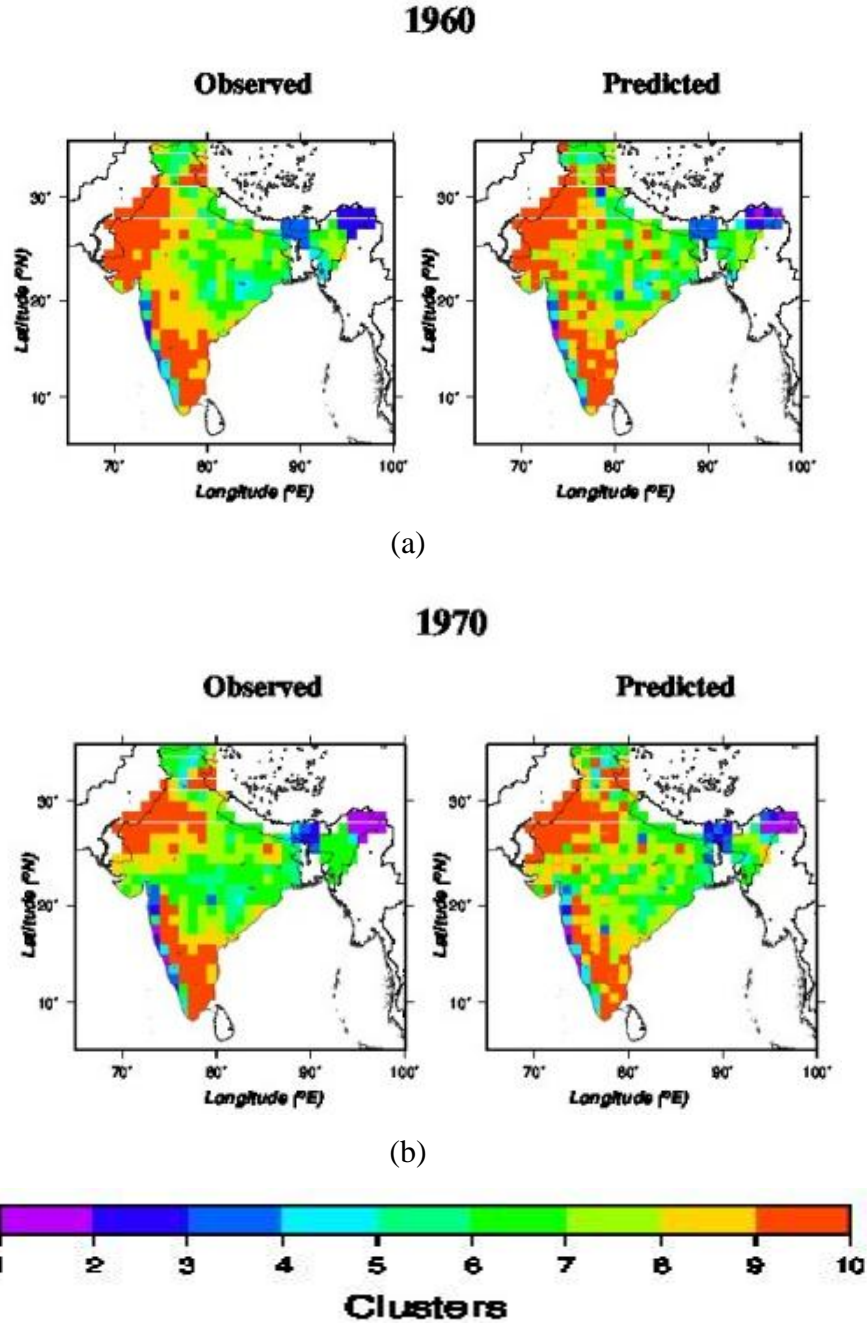


Figure 5.5.1: Observed and predicted clusters representing rainfall using the parameters of SIO for the years (a) 1960 (b) 1970.

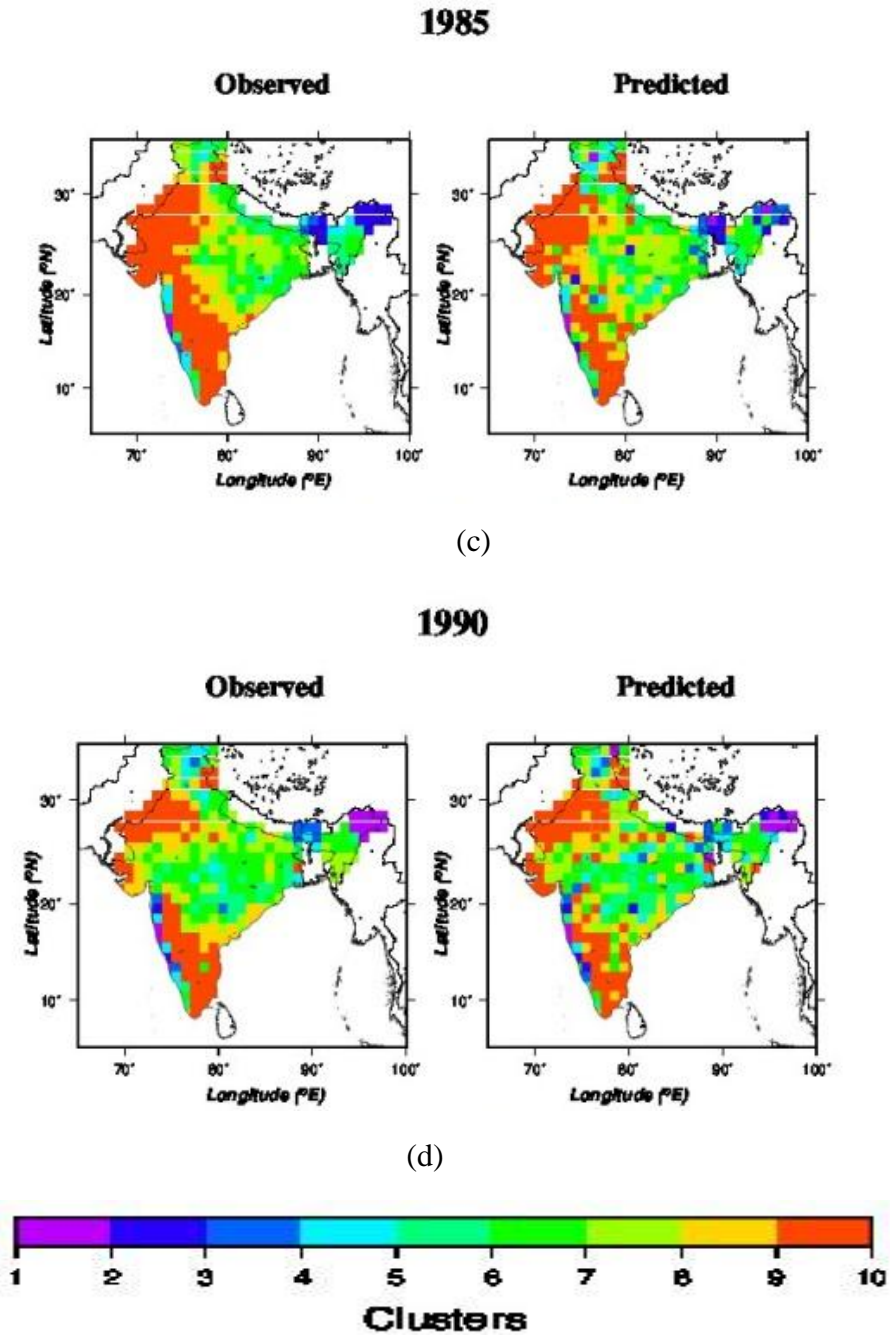


Figure 5.5.1: Observed and predicted clusters representing rainfall using the parameters of SIO for the years (c) 1985 (d) 1990.

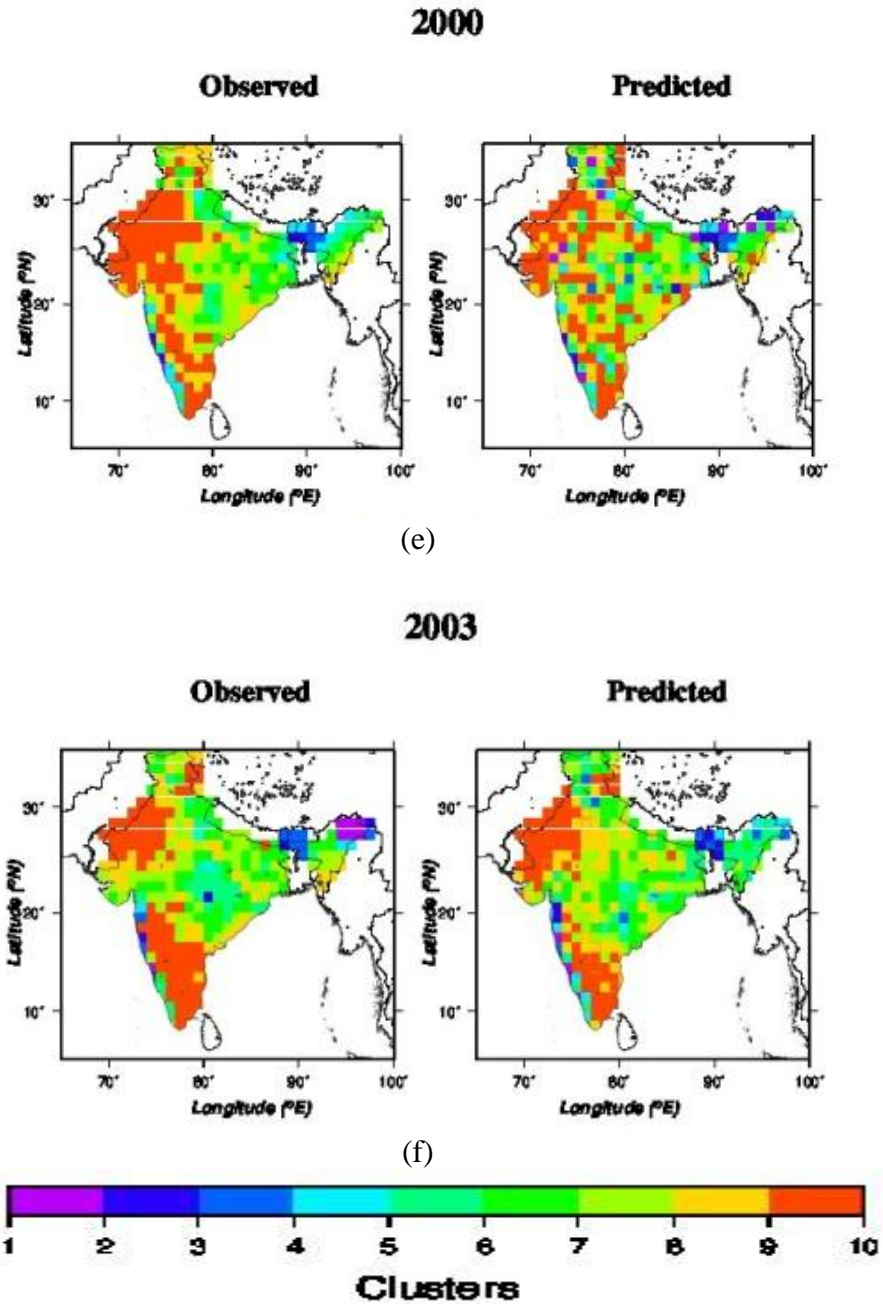


Figure 5.5.1: Observed and predicted clusters representing rainfall using the parameters of SIO for the years (e) 2000 (f) 2003.

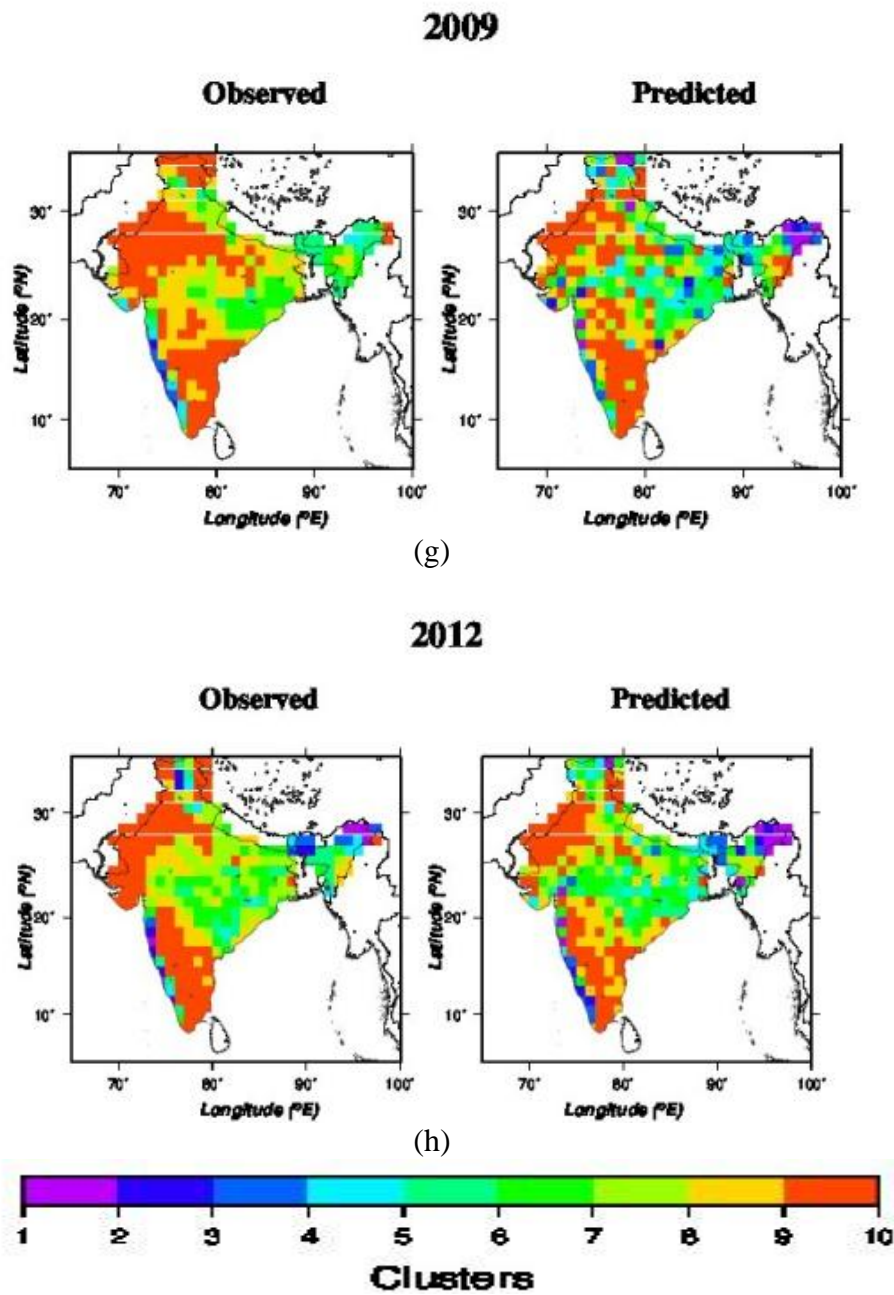


Figure 5.5.1: Observed and predicted clusters representing rainfall using the parameters of SIO for the years (g) 2009 (h) 2012.

5.6 Comparison of results

Table 5.6.1 shows the training and testing error for the six hydrological regions obtained in the prediction of ISMR using the parameters of AS, BOB, SIO and IO respectively. It is evident from the table that the testing error is minimum when rainfall is predicted using IO parameters.

Table 5.6.2 shows the comparison of results using one parameter (SST) only, four parameters SST, SLP, U wind, V wind and monsoon period (JJAS) parameters of IO respectively. From the table, it is clear that SST plays an important role on Indian monsoons. Tables 5.6.1 and 5.6.2, show that pre monsoon factors (MAM) depend highly on monsoons than monsoon period (JJAS) parameters. To know the rainfall pattern of the individual monsoon months, similar analysis is also carried out only for the regions tropical wet and humid sub tropical regions using IO parameters. Table 5.6.3 shows the centroids of the clusters of the rainfall for the months June to September respectively. Table 5.6.4 shows the training and testing error obtained for the two regions for the months predicted using IO parameters. Table 5.6.5 shows the comparison of experimental results of the proposed model and the model for training and test data after Singh and Bhogeswar (2013). Table 5.6.5 indicate recent and past publications and it is very obvious that the outcome from this study utilizing ocean based predictors for each of the hydrological zones will serve the intended purpose to a better extent.

Table 5.6.1: Errors obtained for the 6 regions with respect to AS, BOB, SIO and IO parameters.

| Regions | | AS | BOB | SIO | IO |
|--------------------|--------------|------|------|------|------|
| Desert | Train. error | 26.7 | 25.4 | 28.4 | 23.7 |
| | Test. error | 8.5 | 9.6 | 8.6 | 8.0 |
| Hill type | Train. error | 44.1 | 41.3 | 41.5 | 38.0 |
| | Test. error | 17.2 | 17.6 | 17.6 | 12.0 |
| Semi arid | Train. error | 35.7 | 34.6 | 37.7 | 31.0 |
| | Test. error | 15.9 | 15.8 | 15.6 | 11.0 |
| Humid sub tropical | Train. error | 40.4 | 41.0 | 38.6 | 36.9 |
| | Test. error | 17.0 | 17.0 | 17.0 | 11.8 |
| Tropical wet & dry | Train. error | 33.9 | 33.5 | 39.5 | 33.4 |
| | Test. error | 16.2 | 16.4 | 11.5 | 11.0 |
| Tropical wet | Train. error | 33.9 | 33.0 | 36.7 | 28.0 |
| | Test. error | 14.9 | 15.7 | 15.0 | 10.0 |

Table 5.6.2: Comparison of results using 1 parameter, 4 parameters and monsoon period parameters of IO.

| Regions | errors | SST of pre monsoon period | SST,SLP,U and V wind of pre-monsoon period | Five parameters of monsoon period |
|--------------------|--------------|---------------------------|--|-----------------------------------|
| Desert | Train. error | 28.4 | 25.14 | 25.5 |
| | Test. error | 7.9 | 8.61 | 10.1 |
| Hill type | Train. error | 38.2 | 38.54 | 33.5 |
| | Test. error | 11.9 | 13.02 | 12.8 |
| Semi arid | Train. error | 34.8 | 31.43 | 32.7 |
| | Test. error | 10.7 | 11.44 | 11.3 |
| Humid sub tropical | Train. error | 38.6 | 36.00 | 36.8 |
| | Test. error | 11.5 | 11.10 | 12.0 |
| Tropical wet & dry | Train. error | 33.4 | 35.34 | 32.9 |
| | Test. error | 10.3 | 11.46 | 10.8 |
| Tropical wet | Train. error | 31.6 | 33.59 | 29.2 |
| | Test. error | 9.6 | 11.09 | 10.7 |

Table 5.6.3: Centroids of the clusters of rainfall for the months June to September.

| Cluster numbers | Centroids | Centroids | Centroids | Centroids |
|-----------------|-------------|-------------|---------------|------------------|
| | June | July | August | September |
| 1 | 47.52 | 53.82 | 42.09 | 35.55 |
| 2 | 33.43 | 40.67 | 30.36 | 25.43 |
| 3 | 25.91 | 31.25 | 22.81 | 19.16 |
| 4 | 19.45 | 24.32 | 17.58 | 14.43 |
| 5 | 14.26 | 18.25 | 8.38 | 10.94 |
| 6 | 10.45 | 13.72 | 11.11 | 8.3 |
| 7 | 7.41 | 10.04 | 8.43 | 6.18 |
| 8 | 4.82 | 7.22 | 5.93 | 4.27 |
| 9 | 2.67 | 4.31 | 3.54 | 2.5 |
| 10 | 0.76 | 1.43 | 1.08 | 0.67 |

Table 5.6.4: Errors obtained for the two regions with respect to IO parameters for individual months.

| Regions | error | June | July | August | September |
|--------------------|--------------|-------------|-------------|---------------|------------------|
| Humid sub tropical | Train. error | 37.33 | 40.86 | 43.27 | 43.46 |
| | Test. error | 12.10 | 12.56 | 12.89 | 13.01 |
| Tropical wet | Train. error | 32.44 | 28.10 | 35.59 | 44.38 |
| | Test. error | 11.01 | 10.27 | 11.74 | 12.64 |

Table 5.6.5: Comparison of experimental results of the proposed model and the model for training and test data after Singh and Bhogeswar (2013).

| Seasonal rainfall (mm) | | | | | |
|---------------------------|---------------|----------------|-----------------------------------|---------------|----------------|
| Proposed model | | | Singh and Bhogeswar (2013) model | | |
| | Mean observed | Mean predicted | | Mean observed | Mean predicted |
| Training data (1960-2007) | 1074.42 | 1113.72 | Training data (1876-1960) | 855.30 | 852.40 |
| Test data (2008-2012) | 1017.54 | 1106.82 | Test data (1961-2010) | 833.03 | 825.95 |

5.7 Conclusion

PCA analysis revealed that the pre monsoon SST is the highly influencing parameter on Indian monsoon, which can be used reliably to forecast ISMR. But when the number of pre monsoon parameters is increased to five, an improved accuracy is obtained than using four parameters or monsoon period parameters. It is evident from table 5.6.2, that the analysis gives better results for all the six hydrological regions when the entire IO parameters are considered. It also shows that ANN analysis gives good results even if we use only one pre monsoon parameter namely SST than four pre monsoon parameters (SST, SLP, U wind and V wind) of IO. Also, it is evident from the table that pre monsoon parameters are more important than the monsoon period parameters, because the error percentage is less when the pre monsoon parameters are considered.

Further, ANN is performed on the individual rain bearing months June to September for tropical wet and humid subtropical regions. It also gives better results where testing error is below 13 % for all the individual months.

To conclude, ANN is being effectively used to predict ISMR with an improved predictive accuracy than the earlier studies. Also the pre monsoon factors are more important than the monsoon period factors. SST is an important parameter in the prediction of ISMR. The IO parameters from the whole area play an important role in ISMR than AS, BOB or SIO parameters considered separately. The prediction accuracy stands improved when we increase the input parameters of IO.

CHAPTER 6

**PREDICTION OF EXTREME
RAINFALL EVENTS USING ANN**

6.1 Introduction

The years 1965 and 1966 saw major parts of India under prolonged and severe drought conditions due to deficient monsoon rainfall. The Drought Research Unit (DRU) of India started conducting studies on different aspects of the Drought Standard Precipitation Index (SPI) developed by Mckee et al., (1993). The SPI is a tool developed for monitoring drought and is based on the precipitation data. Drought Research Unit (DRU) of IMD defines Meteorological drought based on rainfall deficiency (SW monsoon, JJAS) on a sub-division basis. The meteorological Droughts are classified into (a) moderate and (b) severe based on rainfall deficiency, i.e. 26 to 50% and more than 50% respectively.

According to the DRU and the IMD, the years 1965, 1966, 1972, 1974, 1979, 1982, 1986, 1987, 2002 and 2004 were identified as dry/drought/deficit years and 1961, 1970, 1975, 1983, 1988 and 1994 as wet/flood/excess years (Atri and Ajit, 2010).

6.2 Standard Precipitation Index (SPI)

As SPI values fit a typical normal distribution (figure 6.2.1), we expect these values to be within one standard deviation approximately 68% of time, with two standard deviations, 95% of time and with three standard deviations, 99% of time (Met Monograph No. Environment Meteorology-01/2010). Table 6.2.1 shows the Standard Precipitation Index classification.

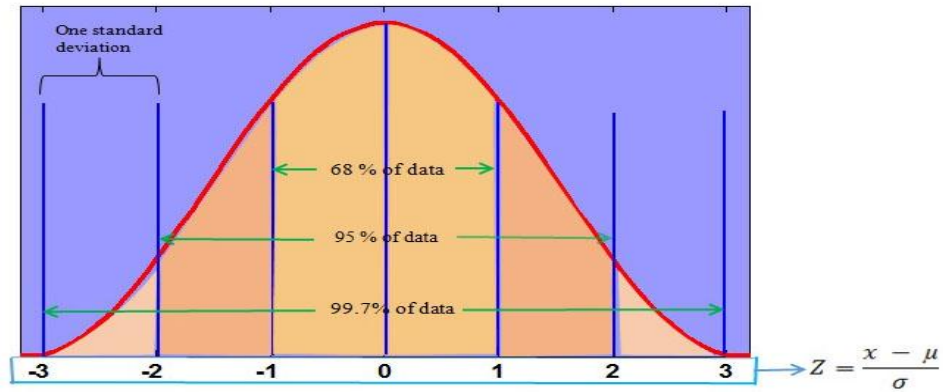


Figure 6.2.1: Standard Normal curve, drawn in MATLAB.

Table 6.2.1: Standard Precipitation Index classification.

| INDEX | INTERPRETATION |
|---------------|----------------------|
| >2.0 | Extremely Wet(EW) |
| 1.5 to 1.99 | Very Wet(VW) |
| 1 to 1.49 | Moderately Wet (MW) |
| -0.99 to 0.99 | Near Normal(NN) |
| -1.0 to -1.49 | Moderately dry(MD) |
| -1.5 to -1.99 | Severely dry(SD) |
| < -2 | Extremely dry(ED) |

6.3 Methodology and Results

The output predicted from ANN is subdivided into 7 classifications according to table 6.2.1 (Varikoden and Preethi, 2013). Further processing of rainfall data yielded significant results pertaining to drought and flood years, which are considered as extreme events in hydrology. Applying our model, the outcome during these years is very well predicted. Observed and predicted clusters representing rainfall for the drought years are given in figure 6.3.2 and for the flood years is depicted in the figures 6.3.3. Table 6.3.2 shows the error percentage in the prediction of rainfall for the drought and flood years obtained from the proposed model. The error percentage for 8 out of 10 years is within 10%. However, in the case of flood years, the model holds considerably better results with errors less than 12% (5 out of 7). Further, the offshoot of 27% in 2002 is a result of an isolated severe drought year, beyond the expected range of occurrence. As with regard to flood years, the off-set is limited to 15% or less among the two instances in 1961 and 1994.

Table 6.3.1 shows the correlation between the observed and predicted clusters for the drought years and flood years at 99 % level of confidence. The values indicate good correlation in most instances [> 0.70], except for the years 2002 and 2004 (figures 6.3.2 (i) and (j)). This shows that the cluster approach is an acceptable tool for forecasting. The year 1970 which was categorized under flood year exhibits highly acceptable results when comparing predicted values to those of observed on clusters except for a few (say, 4 - 5) grids of Central Eastern India. Most of the locations indicate compatibility. With intent, the extreme drought year of 2002 has been studied for predictive purpose and the same

is compared with observed; whereas the desert and humid sub tropical regions do indicate promise, parts of southern India and hill type regions in the northernmost sector fail to create matching responses. Nevertheless the approach does not fail to satisfy events in the rest of the three hydrological regions. This analysis again is a clear indicator of the predictive exercises that an ANN can support. Also, four hydrological regions indicate proven comparison with good cluster matching. We propose that the tool, the said mathematical tool apart from analyzing normal or near normal events, could also be applied to predict extreme events and in cases of drought, better applicability is achieved compared to reasonable accuracies in the case of flood events. As a precursor to the rainfall instances, the oceanic atmospheric state analyzed through measurable known variables, will be of immense value to an agro based nation like India.

Table 6.3.1: Correlation coefficient between the observed and predicted clusters, at 99 % level of confidence.

| Drought years | Correlation coefficient | Flood years | Correlation coefficient |
|----------------------|--------------------------------|--------------------|--------------------------------|
| 1965 | 0.872 | 1961 | 0.771 |
| 1966 | 0.852 | 1970 | 0.857 |
| 1972 | 0.815 | 1971 | 0.792 |
| 1974 | 0.861 | 1975 | 0.745 |
| 1979 | 0.843 | 1983 | 0.816 |
| 1982 | 0.721 | 1988 | 0.772 |
| 1986 | 0.893 | 1994 | 0.861 |
| 1987 | 0.763 | | |
| 2002 | 0.686 | | |
| 2004 | 0.524 | | |

Table 6.3.2: Percentage errors in drought and flood years.

| <u>Drought</u> <u>years</u> | Error% | Observed seasonal rainfall (mm) | Predicted seasonal rainfall (mm) | <u>Flood</u> <u>years</u> | Error% | Observed seasonal rainfall (mm) | Predicted seasonal rainfall (mm) |
|--|--------|--|---|--|--------|--|---|
| 1965 | 5.60 | 12542.8 | 13738.48 | 1961 | 15.00 | 17012.04 | 15814.83 |
| 1966 | 6.20 | 13852.43 | 14240.03 | 1970 | 8.00 | 16515.03 | 16046.44 |
| 1972 | 9.10 | 10937.51 | 13333.99 | 1971 | 10.00 | 15545.61 | 16315.69 |
| 1974 | 5.60 | 14439.39 | 14298.04 | 1975 | 11.80 | 16592.09 | 17013.60 |
| 1979 | 9.10 | 12258.17 | 13520.29 | 1983 | 8.50 | 16274.90 | 15035.23 |
| 1982 | 9.80 | 12781.56 | 14214.79 | 1988 | 11.00 | 16816.30 | 15552.18 |
| 1986 | 6.60 | 13444.91 | 14590.73 | 1994 | 13.80 | 15517.00 | 15485.11 |
| 1987 | 10.00 | 12583.22 | 13485.87 | | | | |
| 2002 | 27.00 | 11535.85 | 15406.84 | | | | |
| 2004 | 16.9 | 13299.29 | 15582.12 | | | | |

The Indian ocean state variables have a high influence on the Indian monsoon rainfall which can be beneficially used for studies in prediction [of rainfall] within the different hydrological climatic divisions using artificial neural networks; the 7 classifications, based on the SPI obtained from IMD were more helpful in this respect. The model predicts well for almost all grids of the hydrological regions of India (table 6.3.2), providing direct results on the actual and the predicted. The drought years have a better correlation coefficient of more than 0.70 at 99% level of confidence. The minimum rainfall year, 1972 and the maximum rainfall year, 1961 during the period 1960-2012 have correlation coefficient 0.815 and 0.771 and could be predicted well with an error of only 9% and 15% respectively (table 6.3.2). Past and recent studies in this context indicate an overall improvement in prediction in terms of application of newer tools as well as in data mining, apart from computing rainfall values closer to

actual: the works by Guhathakurta et al., 1999; Sahai et al., 2000; Iyengar and Raghu Kanth, 2005 and Singh and Bhogeswar,2013) have made significant contributions. This study focused on extreme events, are thus more relevant in the context of rainfall analyzes to mitigate hazardous conditions which may prevail on either case of drought or flood, within a homogenous division. We wish to point out that the RMSE, one among many indicators is helpful to reach a decisive conclusion. Therefore the model can be used to forecast Indian monsoon using the pre-monsoon Indian Ocean Atmosphere parameters, even for cases of drought and flood. To conclude, the model also shows good results for almost all grids, especially for the drought years and for the case tested in normal years too.

a) Drought years

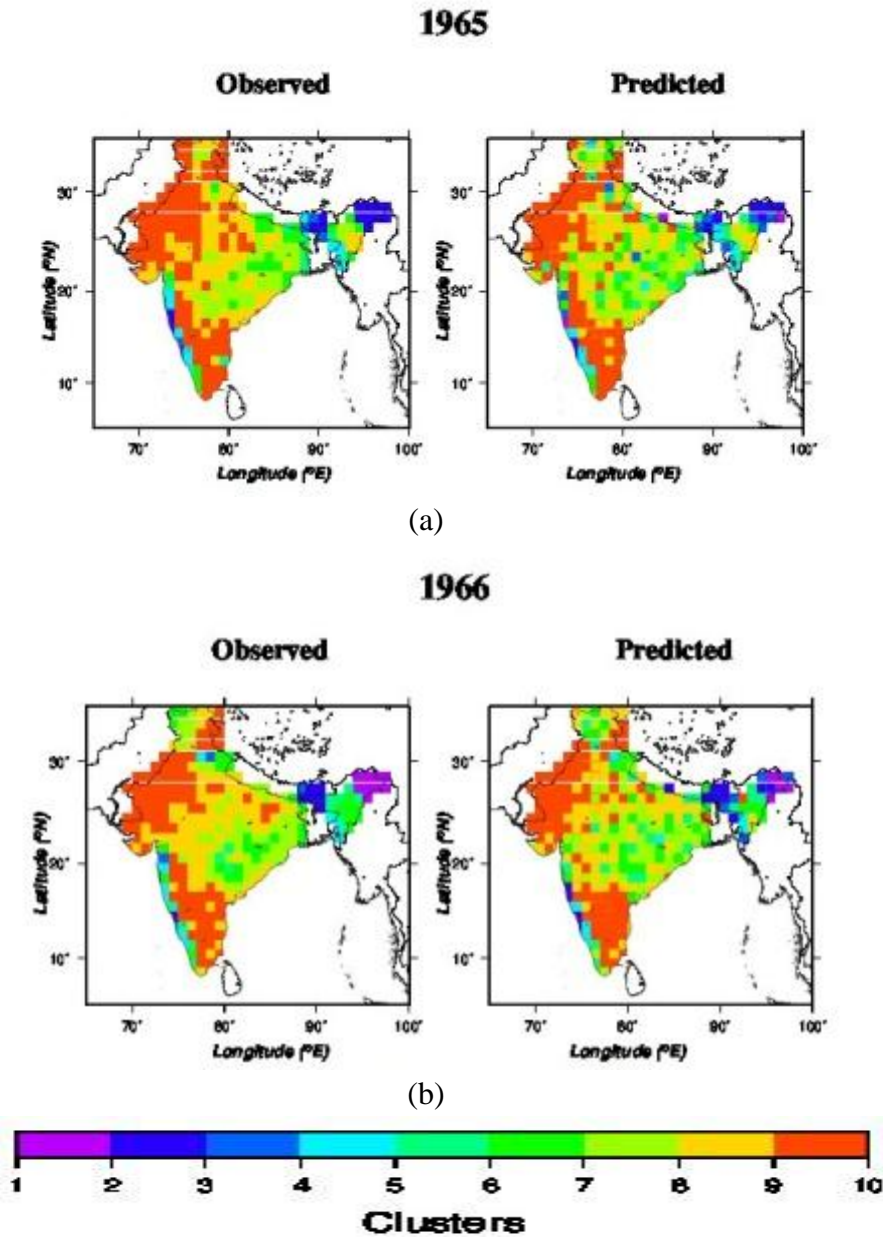
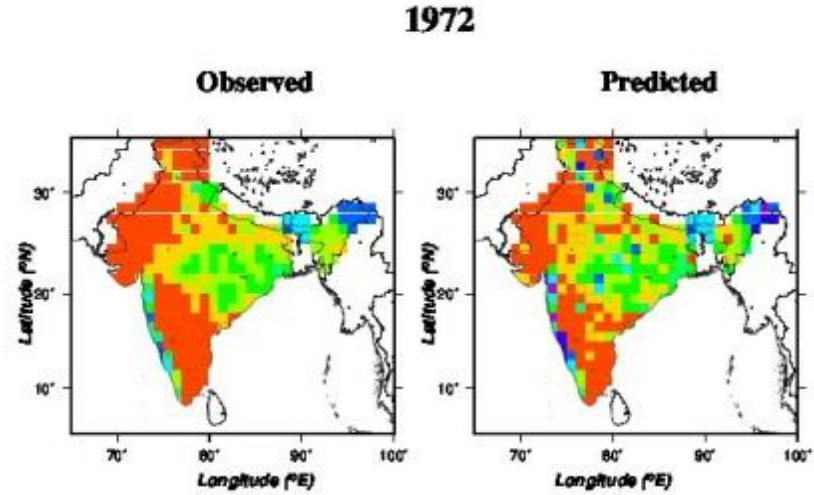
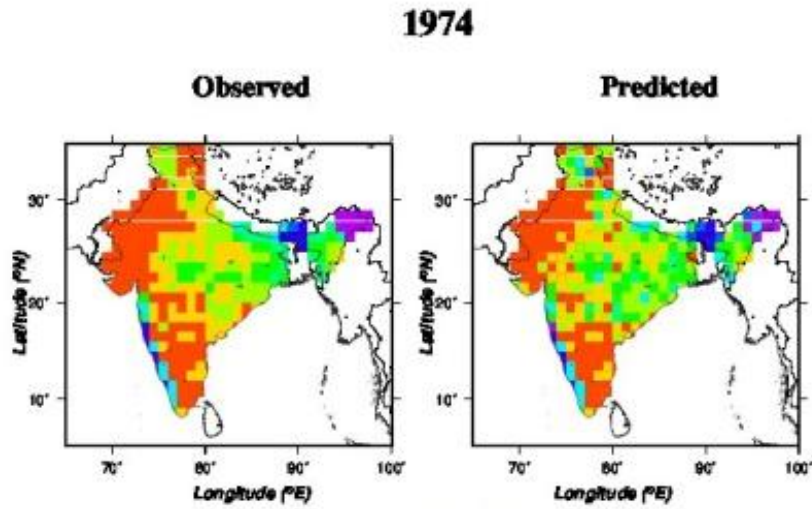


Figure 6.3.2: Observed and predicted clusters representing rainfall for the drought years (a) 1965 (b) 1966.



(c).



(d)



Figure 6.3.2: Observed and predicted clusters representing rainfall for the drought years (c) 1972 (d) 1974.

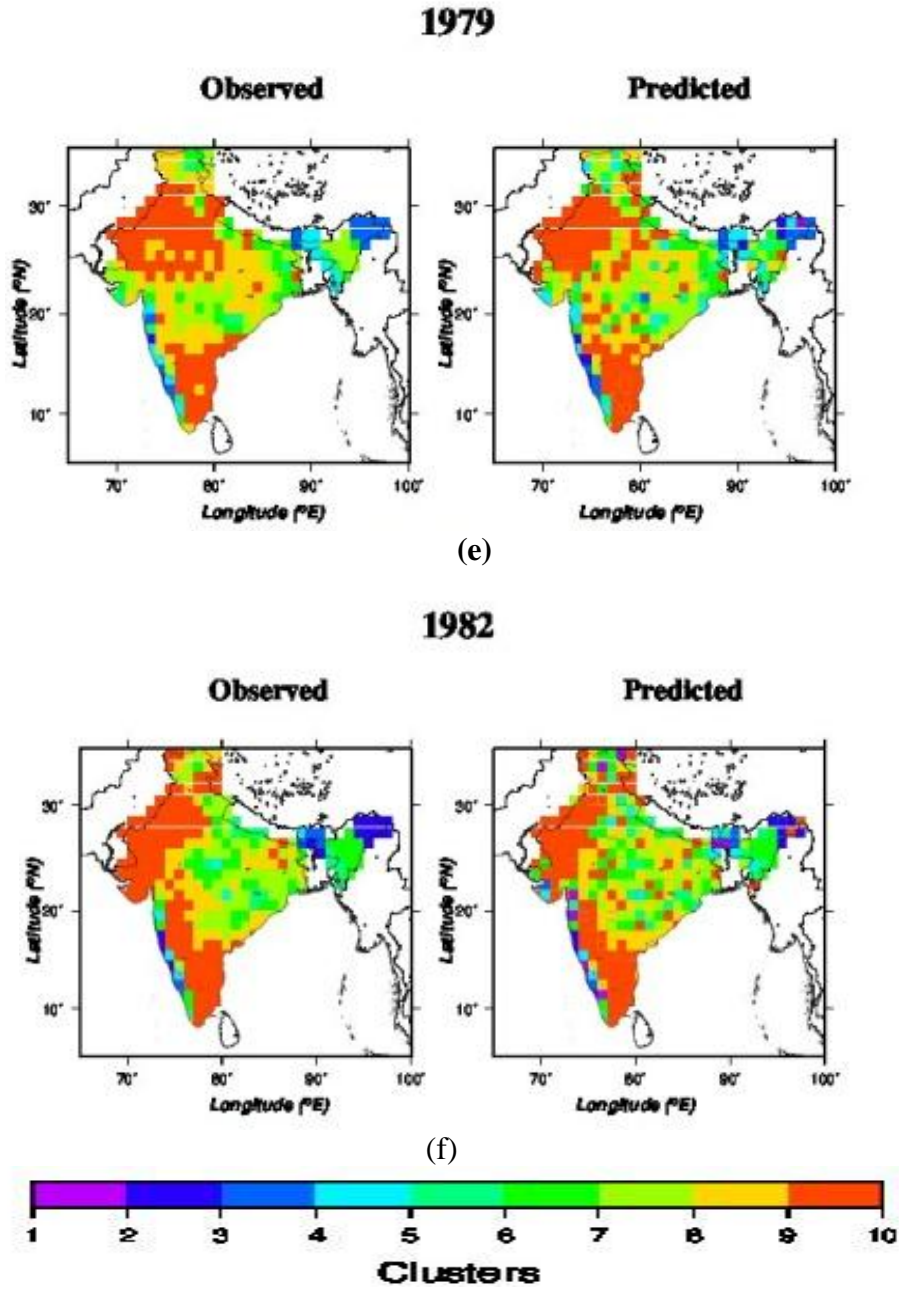


Figure 6.3.2: Observed and predicted clusters representing rainfall for the drought years (e) 1979 (f) 1982.

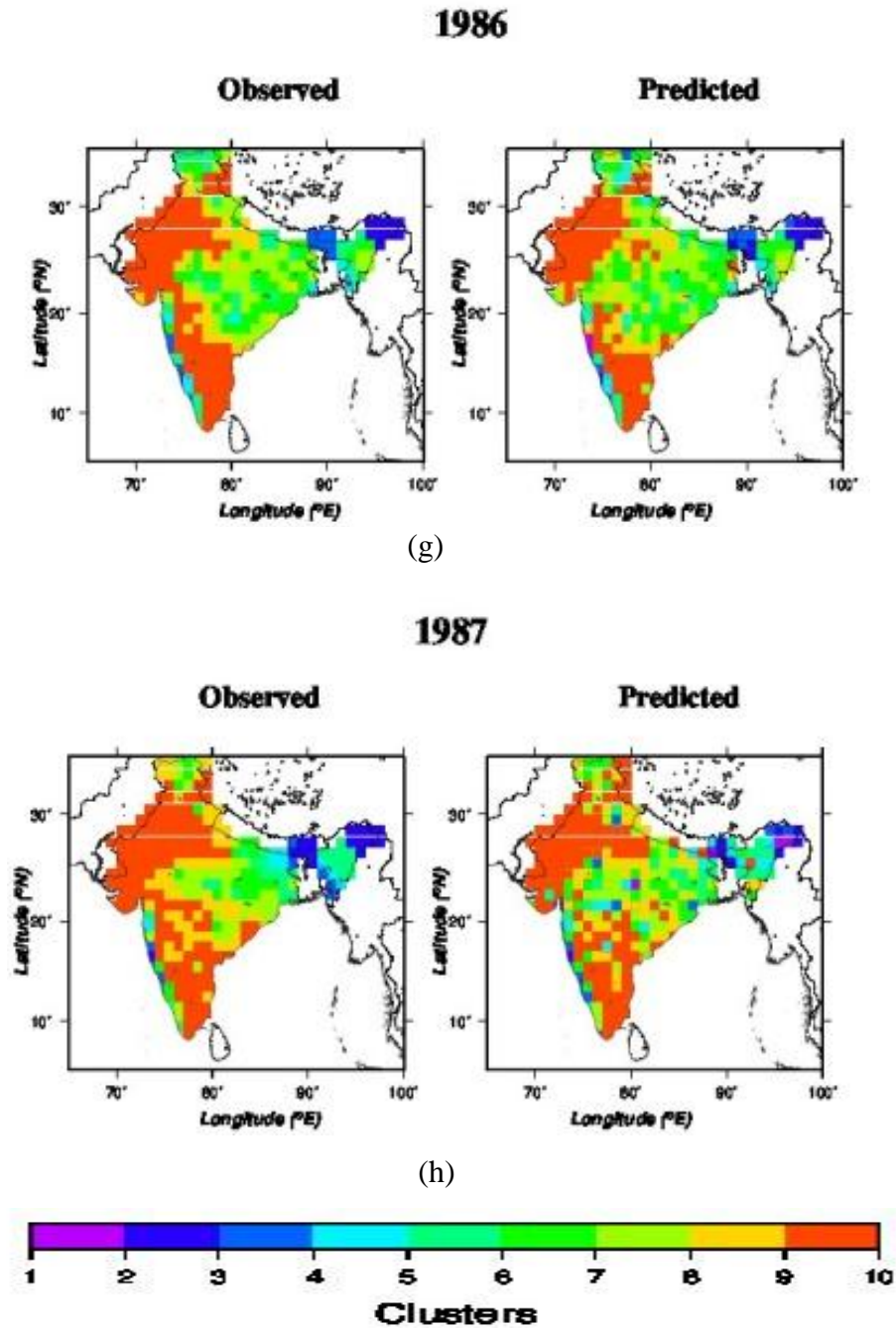


Figure 6.3.2: Observed and predicted clusters representing rainfall for the drought years (g) 1986 (h) 1987.

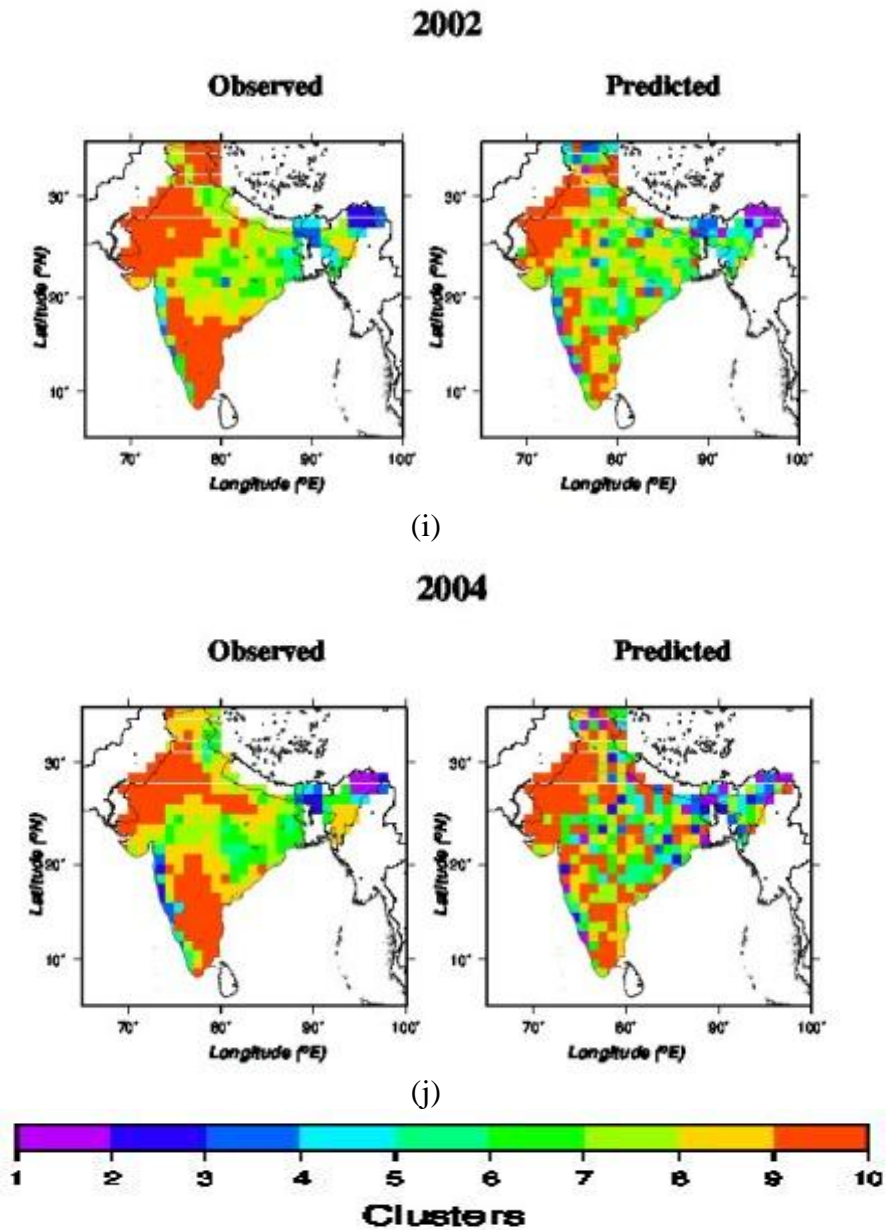


Figure 6.3.2: Observed and predicted clusters representing rainfall for the drought years (i) 2002 (j) 2004.

b) Flood years

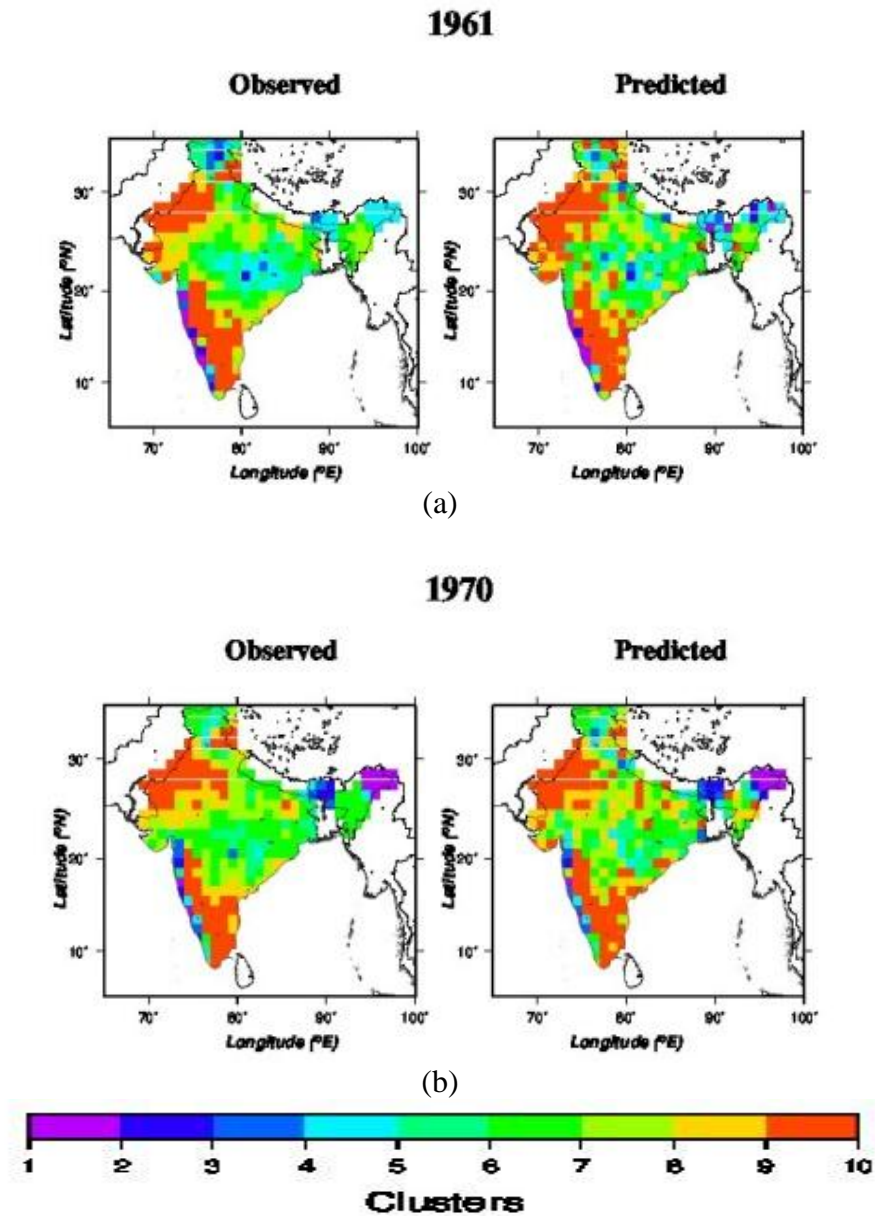


Figure 6.3.3: Observed and predicted clusters representing rainfall for the flood years (a) 1961 (b) 1970.

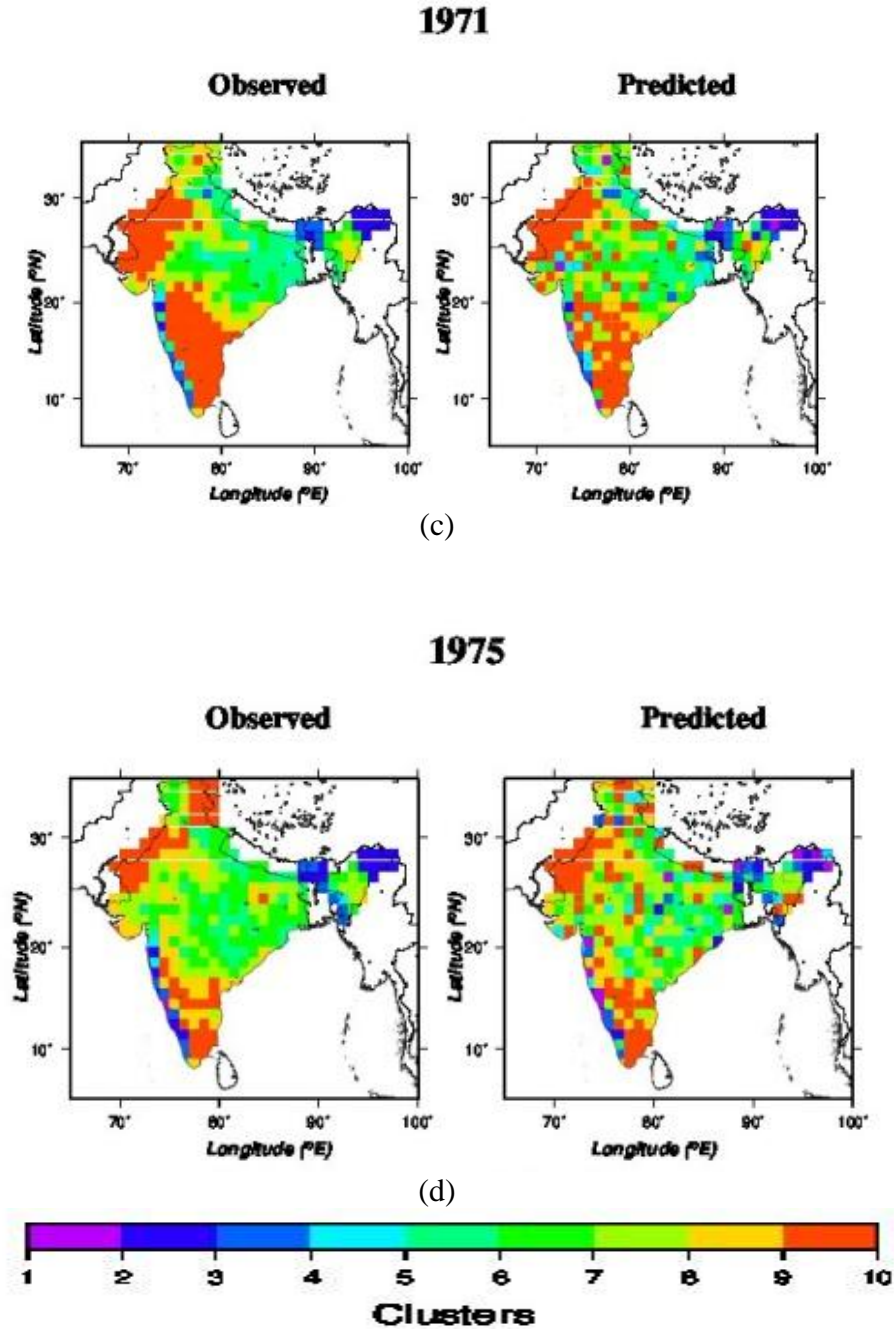


Figure 6.3.3: Observed and predicted clusters representing rainfall for the flood years (c) 1971 (d) 1975.

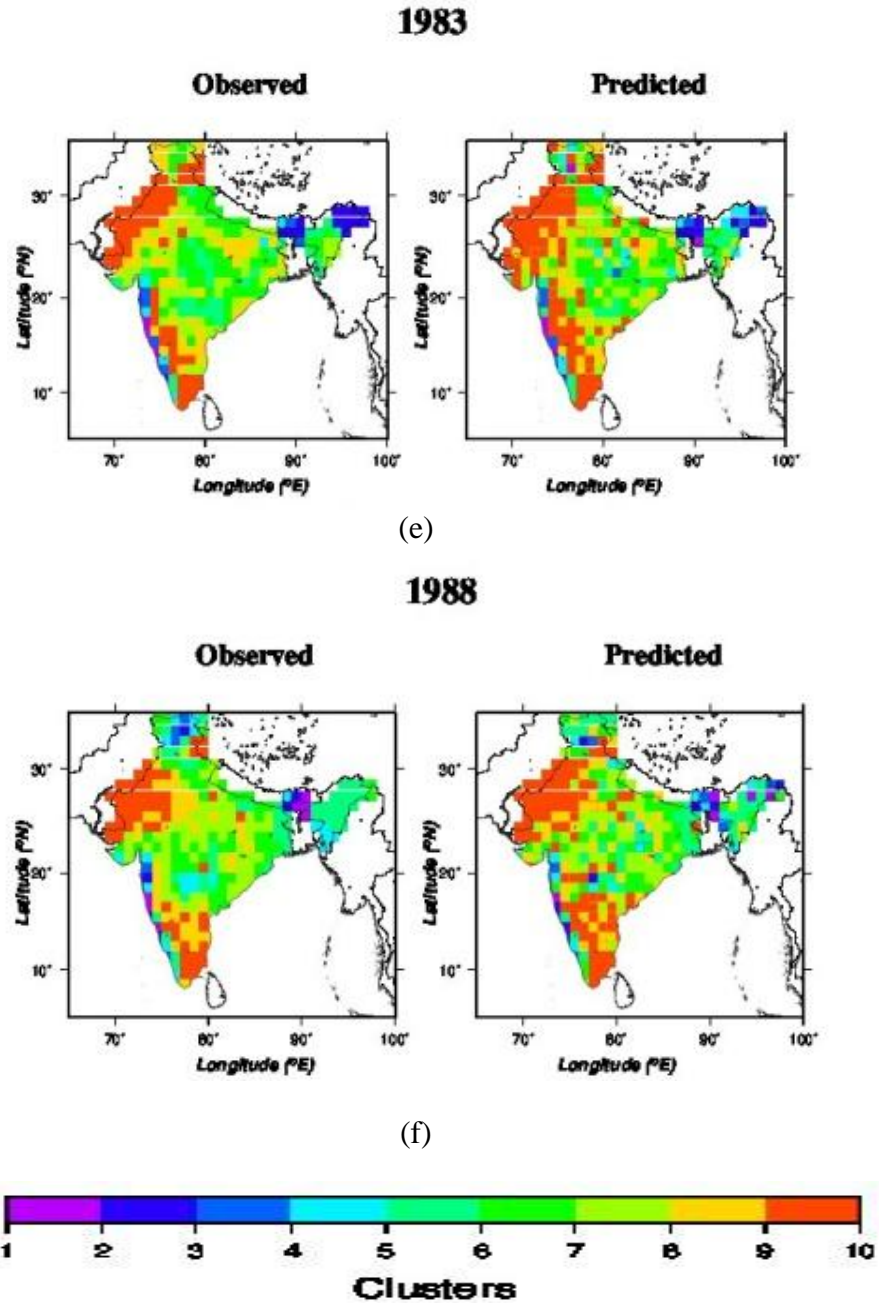


Figure 6.3.3: Observed and predicted clusters representing rainfall for the flood years (e) 1983 (f) 1988.

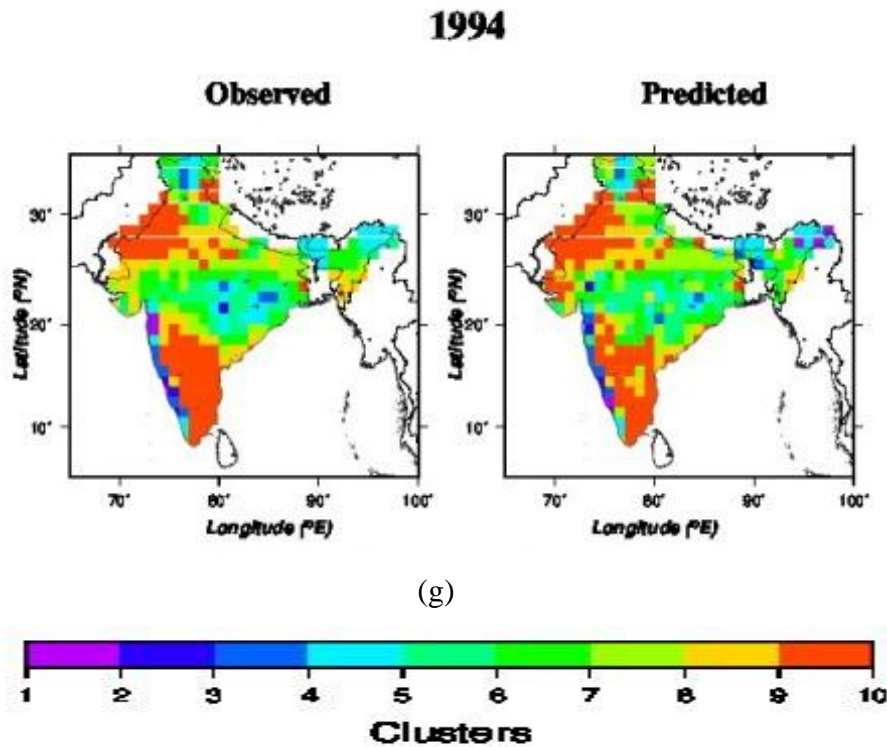


Figure 6.3.3: Observed and predicted clusters representing rainfall for the flood year (g) 1994.

6.4 Forecast 2013, 2014 and 2015

The ISMR for the period 2013-2015 is predicted using the model developed and with the help of the five pre monsoon parameters of IO and is depicted in figure 6.4.1. The SPI values of ISMR obtained from the forecast are given in table 6.4.1, and the mean and standard deviation of ISMR for the six regions are given in table 6.4.2.

Based on the SPI classification of this study, five grids of desert region are extremely wet and seven grids are moderately wet for 2013. For 2014, there are three extreme wet and four moderate wet grids and all

other grids are normal. But for 2015, only one grid is extremely wet, four grids very wet, sixteen grids are moderately wet, and all other grids are normal. When the semiarid region is considered, eight grids are extremely wet for 2014 and the moderately dry grids are 18, 17 and 9 for the years 2013, 2014 and 2015 respectively. Three grids are extremely wet for 2013 and 2015 and the moderately dry grids are four, eight and two in numbers for the years 2013, 2014 and 2015 respectively for the hill type region. Two severe dry grids are observed for humid sub tropical region for 2013 and 2015. For tropical wet and dry region, severe dry grids are four and six in numbers for the years 2013 and 2015 respectively. There are no severe dry grids for tropical wet region, but extremely wet grids are six each for 2013 and 2014 and three for 2015.

According to the annual rainfall report of IMD for the year 2013, Central and peninsular parts of the country received excess rainfall, northwestern parts of the country received normal rainfall, while eastern / northeastern parts of the country received deficient rainfall. Some subdivisions of the central region viz. West Madhya Pradesh, Vidarbha and Gujarat state as a whole received about 40 % of its respective normal rainfall in excess. However, large rainfall deficiency (about 30 to 35%) prevailed. Central and peninsular parts of the country received excess rainfall, northwestern parts of the country received normal rainfall, while eastern / northeastern parts of the country received deficient rainfall. Some sub-divisions of the central region viz. West Madhya Pradesh, Vidarbha and Gujarat state as a whole received about 40 % of its respective normal rainfall in excess. However, large rainfall deficiency (about 30 to 35%) prevailed over the subdivisions of northeastern region viz. Arunachal

Pradesh, Assam & Meghalaya and Nagaland, Manipur, Mizoram & Tripura and Bihar. Cumulative SPI values of ISMR from this study for the year 2013 indicate extreme wet or moderate wet conditions over parts of West Bengal, Assam, Arunachal Pradesh, parts of Karnataka, Goa and Maharashtra, Jammu and Kashmir, Madhya Pradesh, parts of Orissa and Bihar. Extreme dry conditions were observed over parts of Punjab, Gujarat, Haryana, Himachal Pradesh, coastal parts of Tamil Nadu and some grids of Andhra Pradesh. Almost all regions received normal or more than normal rainfall except for a few grids of the regions mentioned above.

Cumulative SPI values of the monsoon season of IMD report during 2014 indicate, extremely/severely wet conditions over small parts of Arunachal Pradesh, Odisha, Bihar, Jammu & Kashmir, West Madhya Pradesh, North & South Interior Karnataka, while extremely/ severely dry conditions were observed over most parts country *viz.* Arunachal Pradesh, Nagaland, Manipur, Mizoram & Tripura, Bihar, Jharkhand, East & West Uttar Pradesh, Uttaranchal, Haryana, Chandigarh & Delhi, Punjab, Himachal Pradesh, Jammu & Kashmir, East Madhya Pradesh, Coastal Andhra Pradesh and Telangana. Cumulative SPI values of ISMR from this study indicate extreme wet or moderate /very wet conditions over parts of West Bengal, parts of Assam, Arunachal Pradesh, and Karnataka. Parts of Maharashtra, Madhya Pradesh, some grids of Uttar Pradesh, and Gujarat, Manipur, Mizoram, Meghalaya, some grids of Madhya Pradesh, Orissa and Bihar, parts of Rajasthan, some grids of Gujarat, Maharashtra and Andhra Pradesh. Extreme dry conditions were observed for major grids of Tamil Nadu, North West Rajasthan, Gujarat and some grids of Karnataka.

The year 2014 witnessed lesser rainfall in comparison to 2013 for the tropical wet and dry region.

The report of IMD on cumulative SPI values of the monsoon season during 2015 indicate, extremely wet /severely wet conditions over parts of Assam & Meghalaya, Gangetic West Bengal, Odisha, Jammu & Kashmir, West Madhya Pradesh, Coastal Andhra Pradesh and Tamil Nadu, while extremely dry/severely dry conditions were observed over parts of Arunachal Pradesh, Assam & Meghalaya, Sub-Himalayan West Bengal & Sikkim, Odisha, Jharkhand, Bihar, East Uttar Pradesh, West Uttar Pradesh, Haryana, Chandigarh & Delhi, Punjab, East Madhya Pradesh, Gujarat Region, Konkan & Goa, Madhya Maharashtra, Marathwada, Chhattisgarh, Telangana, Coastal Karnataka, North Interior Karnataka and Kerala. This study indicate extreme wet/ severe wet conditions over some grids of north east parts of West Bengal, Assam, Arunachal Pradesh, some grids of Kerala, Karnataka and Maharashtra, Goa and Gujarat. Very wet or moderate wet conditions were observed in Jammu and Kashmir, some grids of Kerala, Orissa, Bihar, Jharkand, Chattisgargh and major grids of Madhya Pradesh. Extreme dry conditions were observed for Rajasthan, Gujarat, Haryana, some grids of Punjab and Madhya Pradesh, major grids of Tamil Nadu, Andhra, Karnataka, Maharashtra and Uttar Pradesh. Some grids of Karnataka received high rainfall in 2015.

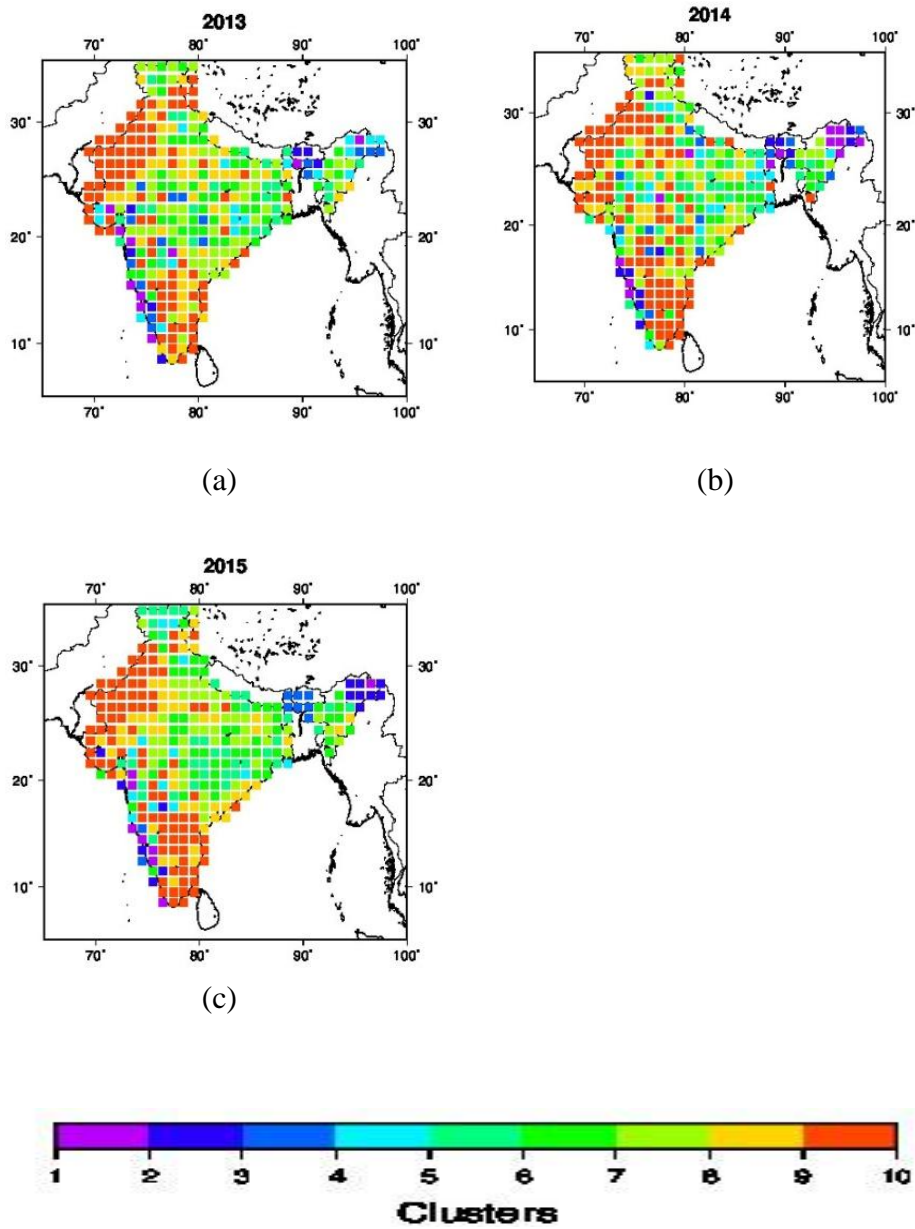


Figure 6.4.1: Predicted clusters representing rainfall for the years (a) 2013 (b) 2014 (c) 2015.

Table 6.4.1: SPI classification for the period 2013-2015.

| Hydrological regions | 2013 | 2014 | 2015 |
|----------------------|---|--|--|
| Desert | EW- 5 grids MD- 0 grids VW -0 grids MW- 7 grids NN - 43 grids SD - 0 grids | EW- 3 grids MD- 0 grids VW -0 grids MW- 4grids NN - 48 grids SD - 0 grids | EW- 1grid MD- 0 grids VW- 4 grids MW- 16 grids NN - 34 grids SD - 0 grids |
| Semi arid | EW- 5 grids MD- 18 grids VW - 2 grids MW-8 grids NN- 61 grids SD - 0 grids | EW- 8 grids MD- 17 grids VW -0 grids MW-0 grids NN- 69 grids SD - 0 grids | EW- 4 grids MD- 9 grids VW - 4grids MW-0 grids NN- 77 grids SD - 0 grids |
| Hill type | EW- 3 grids MD- 0 grids VW - 3 grids MW-7 grids NN- 38 grids SD - 0 grids | EW- 0 grids MD- 4 grids VW - 8 grids MW-4 grids NN- 35grids SD - 0 grids | EW- 3grids MD- 7 grids VW - 0 grids MW-6 grids NN- 35grids SD - 0 grids |
| Humid subtropical | EW- 5grids MD- 4grids VW - 6 grids MW-0 grids NN- 91grids SD- 2 grids | EW- 8grids MD- 8grids VW - 5 grids MW-0 grids NN- 87grids SD- 0 grids | EW- 9grids MD- 2grids VW - 8 grids MW-0 grids NN- 87grids SD- 2grids |
| Tropical wet and dry | EW- 3grids MD- 17grids VW - 4 grids MW-9 grids NN- 71grids SD- 4grids | EW- 3grids MD- 14grids VW - 9 grids MW-0 grids NN- 82grids SD- 0 grids | EW- 4grids MD- 19 grids VW - 0 grids MW-15 grids NN- 64grids SD- 6 grids |
| Tropical wet | EW- 6grids MD- 0grids VW - 0grids MW-4 grids NN- 57 grids SD- 0grids | EW- 6grids MD- 0grids VW - 1grids MW-3 grids NN- 57 grids SD- 0grids | EW- 3grids MD- 0grids VW - 7grids MW-3 grids NN- 54 grids SD- 0grids |

Table 6.4.2: Mean and S.D for the six hydrological regions for the years 2013- 2015.

| Hydrological regions | | 2013 | 2014 | 2015 |
|-----------------------------|------|-------------|-------------|-------------|
| Desert | Mean | 12.01 | 17.21 | 14.12 |
| | S.D | 7.73 | 13.35 | 7.70 |
| Semi Arid | Mean | 22.25 | 28.57 | 23.97 |
| | S.D | 14.50 | 22.83 | 13.85 |
| Hill Type | Mean | 41.85 | 50.92 | 51.24 |
| | S.D | 32.65 | 41.70 | 33.46 |
| Humid Sub Tropical | Mean | 40.30 | 49.22 | 42.47 |
| | S.D | 23.12 | 32.5 | 24.10 |
| Tropical wet and Dry | Mean | 29.94 | 29.81 | 28.80 |
| | S.D | 15.71 | 20.14 | 13.68 |
| Tropical Wet | Mean | 34.43 | 36.85 | 38.49 |
| | S.D | 31.22 | 36.39 | 35.81 |

6.5 Conclusion

The numerical results indicate that the prediction of ISMR based on the proposed model has been reasonably accurate. The rainfall for the normal years were predicted with an accuracy of over 90% and that for eight out of the ten drought years with an accuracy of about 95% at 99% level of confidence (Refer table 6.3.2 for the years 1965, 1966, 1974 and 1986). Even the predictions for the so-called extreme event years, viz. 2002 and 2004 have been more than 88% accurate at 99 % level of confidence.

In this study, using the pre monsoon parameters of Indian Ocean, ISMR for three years 2013-2015 was predicted and compared with the annual rainfall reports of IMD. According to their reports, for 2013, out of 36 meteorological divisions, 15 received excess rainfall, 12 received normal rainfall and 2 received scanty rainfall. In this study, for 2013, 27

grids are extremely wet and 6 grids are severe dry. Some grids of tropical wet and Humid subtropical are extreme wet which agrees with the IMD report stating that the Central and Peninsular regions received excess rainfall. The desert region received normal rainfall which agrees with the report that northwest region received normal rainfall.

For 2014, tropical wet and dry and the humid subtropical regions received normal rainfall which agrees with the IMD reports, that the Central and Peninsula region received normal rainfall. The hill type region received normal rainfall which is again in agreement with the report that the east and northeast part received normal rainfall.

For 2015, according to IMD report, West Rajasthan received excess rainfall which is reflected here also in that 16 grids of desert region are moderately wet, one grid is extremely wet and 4 grids are very wet. Some grids of tropical wet received more than 100 mm of rain which is in agreement with the report of IMD. Generally, model predictions have proven right; in the absence of grid data from IMD, one to one comparison could not be drawn out; as for any other ANN based study, longer and larger data sets help refine accuracy and predictability.

CHAPTER 7

SUMMARY AND CONCLUSION

Data Mining (DM), a major field in Computer Applications has been widely used in finding hidden patterns and to capture the complexities in large amounts of data. In this context, Artificial Neural Networks (ANN), a technique used in DM plays an important role in the classification, association and prediction in numerous fields and recently in climate studies too. Prediction accuracy is high in the case of ANN than the conventional methods, provided the data sets are large. In this study, ANN is used to predict the rainfall during Indian summer monsoon making use of ocean parameters; even the extreme events were reasonably predicted with good accuracy.

This thesis also attempts to study the long term trend analysis of sea surface temperature, sub surface temperature and rainfall. Often stated, the oceans have been warming during the past few decades and its implications within the realm of global warming are indicated in increase of the number of cyclones, increase of extreme rain events, changing pattern of rainfall etc. And any variation in the rainfall pattern over India will affect the farmers and agriculturists which in turn impact the socio – economic development of our country.

The spatial trends of SST of Indian Ocean (IO) exhibit the following features:

Annual

- An increasing warming rate within the region south of equator in central IO (60⁰ to 90⁰E and around 16⁰ S), a finding similar to Roxy et al., 2014.

- Warming is significant (0.25°C to 0.3°C per decade) in the subtropics and in Bay of Bengal (BOB) than Arabian Sea (AS) - in agreement with Dinesh Kumar et al., 2016.
- “Madagascar High” is a term suggested in this thesis to denote a warming feature around the said island at surface and subsurface layers.

Seasonal

- Warming at Central IO extends up to 25°S , around the equator on the eastern side of 100°E during winter season.
- A significant change is noticed for 5°S to 25°S , 55°E to 70°E when the season changes from monsoon to post monsoon.
- Significant warming during monsoon within $65^{\circ} - 100^{\circ}\text{E}$.
- Warming is significant in BOB than AS for all seasons.
- Positive trend in temperature is noted near equator and south Indian Ocean during all seasons.

Monthly

- None of the months indicate cooling except for some parts of north east and subtropics which might have occurred due to the artifact of absence of ship track arising out of ICOADS data.
- Most months support warming trend greater than $0.25^{\circ}\text{C} / \text{decade}$.
- A cooling trend in the eastern part near 85°E and continuing to dominate in February, March and April months has been noted in the NE area.

- A small pocket of cooling is also noted in the NE around 20⁰ N during October and December months.

Temporal trends in SST

Annual

- Increase of warming of about 1⁰C has occurred during the past 50 years.
- A particular feature noted during the warming phase was the zig zag pattern prior to 1985 which later appears to be absent, as temperature steadily increases.
- Prior to 1985, the zig zag feature is evidenced by 3 cooling and 2 warming events.
- Interestingly, the average temperature values have shown a mild decrease since 2010.
- It is also reported that the warming trends during winter are milder compared to the annual feature.
- We also report three extreme conditions post 1985 during pre monsoon season (1987, 1998 and 2010).
- Particular attention is drawn to the fact that there are no large scale variations during monsoon.

Epoch based reporting 1960-76

- Trends during winter season indicate an increase of nearly 0.3⁰ C.
- A high variation of 0.8⁰C to 1⁰C in SST has been observed prior to 1976 during pre monsoon months.
- As stated above, no large scale variations during monsoon with the exception during 1975 and 1976.

- Analyzing the post monsoon scenario, the oceans warm consistently but two cooling events embedded prior to 1976.

Epoch based reporting 1977-2012

- Since the report of “climate shift” in 1976-77, a rise in temperature of about 1°C , a standalone feature during the year 2010, while during winter again a similar variation is observed.
- Again no variations are reported during the monsoon months while an increase of about 1.5°C is often noticed during the post monsoon months.

Trends in Sub surface Temperature

This study attempts to look into the trend in the subsurface temperature of the large IO during the period 1950-2011. Data sets were extracted at five depths namely 25m, 98m, 235m, 540m, and 967m (Hadley dataset).

The salient features are:

- At a depth of 25m, a mild warming of 0.17°C to $0.21^{\circ}\text{C}/\text{decade}$ stands distinguishable. However there are a few areas of IO which are decorated by cooling trends or which remain neutral.
- As reported, (Rao et al., 2012, Roxy et al., 2014, Pai et al., 2015) the tropical IO SST's are warming consistently at a rate of 0.25°C to 0.30°C per decade.
- Results of our study is in agreement with previous studies which points out to the highest warming rate noticed in the central

equatorial Indian ocean , but we wish to report that this feature occurs at a lower magnitude.

- Considering the waters at the depth of 98m, both warming as well as cooling is reported within IO with a warming feature for the entire south IO, while a cooling trend has set in on the western and equatorial IO.
- To specifically state, the northern waters of Madagascar stand apart and mimic the observed long term warming trends in SST as reported by Pai et al., 2015.
- We differ and point out to a significant warming trend at the southern most latitude from earlier studies.
- A well established warming trend is noted at the depth of 235m including the “Madagascar High” region for the southern IO.
- Further into deeper waters the magnitude of warming trends stand substantially reduced as noted at depths of 540m, the “Madagascar High” is no longer true and the IO does not indicate any significant warming or cooling features; an exception is that comparing north and south IO, a relatively mild warming trend has been reported for the northern waters.
- Our investigations into waters around 1000m, by considering the data at 967m, indicate that waters south of 20⁰S show a cooling trend of magnitude - 0.02⁰C to -0.08⁰C /decade.

- However north of 20⁰S, a mild warming trend of 0.06⁰C / decade has been computed.
- On the whole , southern IO indicate a general warming trend in the subsurface waters while deeper waters beyond 500m, a reverse trend of different magnitude can be observed.
- The picture is different for the northern IO and the parts of equatorial waters where a mild cooling trend is vertically observed from 25m to 250m while deeper waters beyond 500m are warming over a period of time.
- This thesis also resolves the seasonal variability at the selected five depths as well as monthly variability which justify the above conclusions subject to mild variations in the seasonal and monthly patterns.
- To briefly explain the variations in temperature with depth, our studies indicate a warming trend on the western section of southern IO, but both AS and BOB exhibit dual characteristics. Apart, the seasonal variations are also prominent in AS and BOB. Noteworthy, a mixed behavior of warming and cooling was observed near south east equatorial regions particularly during post monsoon season. This study indicates a warming trend in SIO beyond 540m to depths of 1000m which is consistent with the remarks in IPCC, 2013. A few exceptions can be also noted in the SIO in deep waters around 1000m which show a cooling trend.

Spatial trends in rainfall

This study focus on the spatial trend of rainfall during June to September months termed as ISMR (Indian Summer Monsoon Rainfall). The study considers the year 1960-2012 as well as the two epochs 1960-76 and 1977-2012 over the Indian subcontinent – divided as six hydrological regions. Important information derived from this analysis show a decreasing trend in ISMR in all the six regions while for parts of hill type territory there has been an exceptional decrease. Though between the four months the trends do indicate reversals, with a significant decrease which is noted for tropical wet, hill type and humid subtropical regions. In the next attempt by considering two epochs, not many differences have come about except in month to month variations. Instances are reported of increasing trends in certain regions during certain months which does not impact the overall trend bringing about a decrease in rainfall. Between the two epochs, the monthly trend analysis has helped to bring about the increasing or decreasing trend for given types of regions; their cumulative impacts indicate the gradual decrease in the total quantity of rainfall during ISM.

Distribution plot of rainfall**Meridional- South -North variation**

A meridional study was initiated in seven boxes ($1^{\circ} \times 1^{\circ}$) along 78.5° E for the ISMR period and the results basically present a mixed picture on a year to year basis. In a nutshell, the distribution plot extending from 1960 to 2012 speaks off a mild increase in rainfall in the peninsular region of India while no changes are indicated within central India. A

significant deviation from the other regions of India was observed in the boxes selected over northern India which suggests larger variability with a visibly decreasing trend. However the penultimate box retains lesser variability with higher quantities of rain with no significant change during ISMR. Between the epoch 1960-76 and 1977-2012, individual boxes do not indicate variations in their general characteristics which point out to increase/ decrease in rainfall for south/ north regions with some of the locations showing no change. This implies that a climatic shift is prevalent between north and south of Indian peninsular regions with likely chances for enhance wet days while prevalence of dry weather may occur in the northern regions.

Zonal- East - West variation

In the next phase of study, zonal variation (east- west) for a $4^{\circ} \times 3^{\circ}$ box depicts interesting results. Long term distribution plots covering the years 1960-2012 basically indicate near steady conditions in all the 3 boxes in respect of average value with year to year variations. Compared to the central and eastern boxes, the western box receives lesser rainfall and also variability is higher from the mean values. We have again considered the two epochs 1960-76 and 1977-2012. In the western box, an initial surge has been noted which is not reflected in the second epoch. However, the central Indian box retains nearly a steady condition deduced through trend line. Interestingly, the third box in the eastern sector initially has indicated a reducing trend which later appears to be attaining near steady condition during the second epoch. East West variation is thus of little significance in comparison to North South variation.

With regard to ocean warming effects and its impact on the rainfall pattern, a direct one to one relation is yet to emerge. However past three decades exhibit changes in rainfall pattern to the extent that the north east part of India received lesser quantities as well as the tropical wet region [since 1976]. This fact is a significant observation which is supported by earlier workers. It is pointed out that the warming phenomenon observed in the IO has taken prominence since last two decades.

The following illustrate the findings of the specific study on the shift in rainfall pattern during ISMR for the six hydrological regions:

| Regions | 1960 -2012 | 1960-1976 | 1977-2012 |
|----------------|---|--|---|
| Desert | A very high decreasing trend during ISMR and for July, August and September. A positive trend for June. | An increasing trend of low magnitude during August and September but decreasing trend for ISMR and for June. | Positive trend for some grids during ISMR, June and July. Decreasing trend during August and September. |
| Tropical wet | Some grids show positive trend for ISMR, June, August and September. | Decreasing trend for all months and for ISMR. | Positive trend for ISMR, July, August and September. |
| Hill type | Decreasing trend for ISMR, and for July, | Significant increase for | Decreasing trend for Arunachal |

| | | | |
|--------------------|---|---|---|
| | August and September. Slight increase for June. Decreasing trend for Arunachal Pradesh seasonal and for all months. | seasonal and for months June and July for Arunachal Pradesh and it is less significant during August and September. | Pradesh seasonally and for all four months. |
| Semi Arid | Most of the grids show increasing trend seasonally and for July, and August. Significant increase for June for all grids. Less significant during September for Gujarat and decreasing trend for Karnataka. | Increasing trend for all months and seasonal. | Increasing trend but less significant. |
| Humid sub tropical | Increasing trend only for July. | Increasing trend is less significant for September. | Increasing trend seasonally but it is less significant for the four individual months |

| | | | |
|----------------------|---|--|--|
| Tropical wet and dry | Increasing trend for some grids of Tamil Nadu and Andhra Pradesh seasonally but is less significant for the four individual months. | Increasing trend seasonally and less significant for the four individual months. | Increasing trend seasonally and less significant for June, August and September. |
|----------------------|---|--|--|

Application of ANN

The ANN technique was applied to study the ISMR pattern and further extended the same for predictive purposes. In this exercise, five ocean and atmosphere related components namely SST, SLP, humidity, U wind and V wind was associated with rainfall over the Indian sub continent utilizing 1°x1° square grids. The cluster matching technique was found to be the best in this regard. The model was initially trained for 36 years followed by a validation of 8 years and next by testing which extended for 5 years. It is reported that the overall results are promising and ANN can be a meaningful tool in the field of rainfall prediction. Primarily as a first step, the model was applied to the south west coast of India to build confidence and the same methodology was extended to all six hydrological regions of India with a training period of 40 years. The correlation between observed and predicted works out to 0.75 at 99% level of confidence. During the normal rainfall years, the observed and predicted clusters match extremely well for six hydrological regions in the order of desert, tropical wet and dry, semi arid, tropical wet, humid sub tropical and hill type based on RMSE values for both training and test

data. The ANN analysis was further extended by considering ocean atmospheric parameters from 3 parts of the IO namely Arabian Sea, Bay of Bengal and South Indian Ocean. The overall analysis gives better results (testing error is minimum) when we use the parameters from the whole of the IO than by segregating the IO. In this context, it is pointed out that the strength of network is an important factor as and when the data points are increased in number which leads to improved results. Interestingly both observed and predicted grids of the desert region match very well irrespective of subdividing the ocean and atmosphere.

An internal checking was performed on the cohesiveness of the model by omitting the humidity factor and slightly better results emerge for the desert and humid subtropical region. On conduct of PCA analysis, the highly influential parameter namely SST alone was found to serve the purpose of predicting ISMR as results from the test data divulged minimum errors in all the six hydrological regions. A cross analysis indicates that whenever the testing error was below 15%, the ANN analysis provides good results- when total rainfall accounting was attempted under JJAS (June – September). It is emphasized that this study projects the rightful consideration of pre monsoon (March, April and May) ocean atmosphere parameters to analyze the ISMR pattern and prediction as compared to concurrent data sets pertaining to the monsoon period June, July, August and September months. This conclusion is drawn based on higher testing error percentages. Selectively two hydrological regions of greater importance, tropical wet and humid subtropical regions were checked for ANN performance based on individual rain bearing months and again the results were promising.

In order to gauge the extendibility of the ANN model in tackling the complex behavior within ISMR, 10 and 7 cases pertaining to drought and flood years respectively as identified by IMD, brought out interesting results. In the case of extreme drought years, the error percentage was around 5 to 10% while for two individual years, it off- shot to around 17 to 27 % (the years 2004 and 2002 respectively). The larger errors in the drought regions may probably be owing to some external factors that have not been considered in the present study. For instance, Ramesh Kumar et al., 2005 have shown that the evaporation rates were lower (higher) over the AS, during active (weak) monsoon months over the Indian sub continent, indicating its significant role on the ensuing monsoon activity over the Indian subcontinent for the 2002 monsoon. According to Bhat, 2006 several reasons for the drought of 2002 may be convection over the Indian region, surface conditions over the AS, upper air, Inversion characteristics and convective instability. Likewise, application of ANN to flood years was also promising as the error percentage was less than 15%.

Forecast 2013 , 2014 and 2015

Data sets were available for oceanic as well as ocean atmosphere during pre monsoon of the above 3 years. These inputs paved the way towards forecasting ISMR and in the absence of gridded rainfall data, cumulative seasonal SPI (Standard Precipitation Index) values as reported by IMD (Annual rainfall report , 2013) were compared. It is reported that for the year 2013, good matching results were obtained when extremely wet/ severe wet conditions prevailed over many parts of the country namely in Jammu and Kashmir, Madhya Pradesh , coastal Karnataka and Kerala and parts of Tamil Nadu. The dry conditions over Haryana,

Rajasthan, parts of Gujarat as well as parts of Tamil Nadu coastal Andhra could be captured by the model. However the Gangetic plains could not be captured, in a partial sense, prevailing drought conditions. The north east states did not match the predictive scenario.

For the year 2014, IMD has reported wet conditions over Andhra Pradesh, Odisha, Jammu and Kashmir, parts of Madhya Pradesh and Karnataka. Dry conditions prevailed over in Rajasthan, parts of Delhi, Uttaranchal, Punjab, coastal Andhra and Telengana (Attri et al., 2014). The model well predicts this behavioral pattern except that parts of Tamil Nadu too was deficient in rainfall. Good match of deficiency in rainfall is in agreement with actual results of parts of Madhya Pradesh and Andhra Pradesh. Compared to 2013, the model is ahead with better matches.

Rainfall over Assam, Meghalaya, West Bengal, Jammu and Kashmir, Madhya Pradesh and parts of Andhra Pradesh are reported as extremely wet under the cumulative SPI values from IMD for the year 2015(Attri et al., 2015). Akin to the factual IMD report, ANN based output as strikingly similar results for the year 2015. And in respect of dry conditions, a reasonably good match is obtained for parts of Kerala, interior Karnataka, parts of Tamil Nadu, Telengana, Maharashtra and Gujarat regions. Our model has picked up a few grids in Uttar Pradesh, Haryana, Delhi and Punjab while missing out on parts of Bihar and Odisha. It is suggested that ANN based rainfall forecasting has attained maturity in specifying quantum of rainfall based on cluster approach for different parts of India with a lead time of one month.

BIBLIOGRAPHY

BIBLIOGRAPHY

Agboola A. H., Iyare O. and Falaki S.O., (2012): Iyare 6 An artificial neural network model for rainfall forecasting in South-Western Nigeria. Canadian Journal on Computing in Mathematics, Natural Sciences, Engineering and Medicine, 3,188-196.

Alory G., Susan W. and Gary M., (2007): Observed temperature trends in the Indian Ocean over 1960-1999 and associated mechanisms. Geophysical Research Letters, 34, 1-6.

Annamalai H., Liu P. and Xie S-P.,(2005):South west Indian Ocean SST variability: Its local effect and remote influence on Asian monsoons. Journal of Climate, 18, 4150-4167.

Annual Rainfall Report., (2013): Indian Meteorological Department, 1-91.

Aoki S., (1997): Trends and Inter annual variability of surface layer temperature in the Indian sector of the Southern ocean observed by Japanese Antarctic Research Expeditions. Journal of Oceanography, 53, 623-631.

Aralikatti S.S.,(2005): Effects of Arabian Sea Parameters on Indian monsoon. Indian Institute of Tropical Meteorology, 339-346.

Ashok K., Pai D.S., Singh J.V., Ranjeet. and Sikka D.R.,(2012): Statistical Models for Long –Range forecasting of Southwest monsoon rainfall over India using step wise regression and Neural Network. Atmospheric and Climate Sciences, 2, 322-336.

Attri S.D. and Ajit T., (2010): Met Monograph No 11, Environment Meteorology-01.

Bibliography

Attri S.D., Laskar S.I., Singh U.P., Bhatnagar M.K., (2015): Annual rainfall report. Indian Meteorological Department, 1-111.

Attri S.D., Singh U.P., Dinesh Khanna., (2014): Annual rainfall report. Indian Meteorological Department, 1-108.

Bhat G.S., (2006): The Indian drought of 2002-a sub-seasonal phenomenon. Quarterly Journal of the Royal Meteorological Society, 132, 2583-2602.

Bijoy T., Gnanaseelan C., Anant P. and Salvekar P.S., (2008): North Indian Ocean warming and sea level rise in an OGCM. Journal of Earth Systems Science, 2, 169-178.

Bose N. K. and Liang P., (1998): Neural network fundamentals with graphs, algorithms and applications. Tata McGraw –Hill, New Delhi.

Bothmer V. and Daglis I.A., (2006): Space weather: Physics and effects. Springer Praxis Books, Environmental Sciences.

Box G.E.P., Jenkins G.M. and Reinsel G.C., (1976): Time Series Analysis Forecasting and Control. 3rd Edition, Pearson Education, 1-223.

Bryan C.W., (1979): A statistical study of the relationships between ocean surface temperatures and Indian monsoon, Journal of the Atmospheric Sciences, 36, 2279-2291.

Bryson A. E. and Ho Y.C., (1969): Applied optimal control: Optimization, estimation and control. Blaisdell Publishing Company, Waltham, 481.

Chang J.H., (1967): The Indian Summer Monsoon. Geographical Review, 57(3), 373-396.

Chaudhari D., Rana D.P. and Mehta R. G., (2013): Data mining with meteorological data. International Journal of Advanced Computer Research, 3, 25-29.

Chauhan P., Nagur C.R.C., Mohan M., Nayak S.R., Navalgund R.R.,(2001):Surface chlorophyll-a distribution in Arabian Sea and Bay of Bengal using IRS-P4 Ocean color Monitor satellite data. Scientific Correspondence, Current Science, 80, 127-129.

Chowdary J.S.,Gnanaseelan C.,Vaid B.H. and Salvekar P.S.,(2006):Changing trends in the Tropical Indian Ocean during La Nina years. Geophysical Research Letters, 33, 1-5.

Clark C.O., Cole J. E. and Webster P. J., (2000): Indian ocean SST and Indian summer rainfall: predictive relationships and their decadal variability. Journal of Climate, 13, 2503-2519.

Daniel P.S. and James J.M., (2002): Interactions and global climate change: Some lessons from Earth history. 605 - 619.

De U.S., Dube R.K. and Prakash Rao G.S., (2005): Extreme weather events over India in the last 100 years. Indian Journal of Geophysics, 9,173-187.

Dinesh Kumar P.K.,Paul Y.S., Muraleedharan K.R., Murthy V.S.N., Preenu P.N., (2016): Comparison of long term variability of sea surface temperature in the Arabian Sea and Bay of Bengal. Regional Studies in Marine science, 3, 67-75.

Dostal P. and Pokorny P., (2008): Cluster analysis and Neural Networks. 17th Annual Conference Proceedings, Prague, Czech Republic, Department

of Informatics, Brno University of Technology and Institute of Mathematics, Brno University of Technology.

Dubey S.C., (2014): Solar variability and global climate change. *Indian Journal of Geo-Marine Sciences*, 43(5), 871-875.

Dugam S.S., (2012): Long –term change in pre-monsoon thermal index over Central Indian region and south west monsoon variability. *International Journal of Applied Engineering and Technology*, 2(1), 6-11.

Elsner J.B. and Tsonis A.A., (1992): Nonlinear prediction, chaos and noise. *Bulletin of the American Meteorological Society*, 73, 49-60.

Fausett L., (2006): *Fundamentals of Neural Networks-Architectures, Algorithms, and Applications*. Pearson Education.

Folorunsho O. and Adesesan B.A., (2012): Application of Data mining techniques in weather prediction and climate change studies. *International Journal of Information Engineering and Electronic Business*, 4, 51-59.

Francis P. A. and Sulochana G., (2013): A note on new indices for the equatorial Indian Ocean oscillation. *Journal of Earth System Science*, 122, 1005-1011.

Gadgil S.,Srinivasan J.,Nanjundiah R.S., Kumar K.K., Munot A. A. and Rupa Kumar K.,(2002): On forecasting the Indian summer monsoon: the intriguing season of 2002. *Current Science*, 83, 394–403.

Gadgil S.,Srinivasan J.,Nanjundiah R.S.,Kumar K. K.,Munot A. A. and Rupa Kumar K., (2005): On forecasting the Indian summer monsoon - the intriguing season of 2002. *Current Science*, 83(4), 394–403.

Ganguly A.R. and Steinhaeuser K., (2008): Data mining for climate change and impacts. Data mining workshops, ICDMW'08, IEEE International Conference, Pisa, 385-394.

Ganguly A.R., Kodra E.A., Agrawal A., Banerjee A., Boriah S., Sn.Chatterjee, So. Chatterjee, Choudhary A., Das D., Faghmous J., Ganguli P., Ghosh S., Hayhoe K., Hays C., Hendrix W., Fu Q., Kawale J., Kumar D., Kumar V., Liao W., Liess S., Mawalagendra R., Mithal V., Oglesby R., Salvi K., Snyder P.K., Steinhaeuser K., D.Wang D. and Wuebbles D., (2014) : Toward enhanced understanding and projections of climate extremes using physics –guided data mining techniques. *Nonlinear processes Geophysics*, 21, 777-795.

Ghosh S., Vishal L. and Anant G., (2009): Trend analysis of Indian summer monsoon rainfall at different spatial scales. *Atmospheric Science Letters*, 10, 285-290.

Goswami B.N., Venugopal V., Sengupta D., Madhusoodanan M.S. and Xavier P.K., (2006): Increasing trend of extreme rain events over India in a warming environment. *Science*, 314, 1442-1445.

Goswami P. and Srividya., (1996): A novel neural network design for long range prediction of rainfall pattern. *Current Science*, 70, 447-457.

Goutami C., Surajit C. and Rajni J., (2010): Multivariate forecast of winter monsoon rainfall in India using SST anomaly as a predictor: Neuro computing and statistical approaches. *Comptes Rendus Geo Science*, 342, 755-765.

Bibliography

Gowariker V., Thapliyal V., Kulshrestha S. M., Mandal G. S., Roy S. N. and Sikka D. R., (1991): A power regression model for long range forecast of southwest monsoon rainfall over India. *Mausam*, 42, 125-130.

Gowariker V., Thapliyal V., Sarkar R.P., Mandal G.S. and Sikka D. R., (1989): Parametric and power regression models: New approach to long range forecasting of monsoon rainfall in India. *Mausam*, 40, 115-122.

Graham N.E., (1994): Decadal scale variability in the 1970's and 1980's: Observations and model results. *Climate Dynamics*, 10, 60-70.

Guhathakurta P. and Rajeevan M., (2008): Trends in the rainfall pattern over India. *International Journal of Climatology*, 28, 1453-1469.

Guhathakurta P., Rajeevan M. and Thapliyal V., (1999): Long range forecasting Indian summer monsoon rainfall by a hybrid principal component neural network model. *Meteorological Atmospheric Physics*, 71, 225-266.

Halkidi M. and Michalis V., (2001): Clustering Validity Assessment: Finding the optimal partitioning of a data set. *Proceedings of the IEEE International Conference on Data Mining*, San Jose, California, 187-194.

Han J., Kamber M. and Pei J., (2012): *Data mining concepts and techniques*. 3rd edition, Morgan Kaufmann Publishers, 567-571.

Haroon M.A. and Afsal M., (2012): Spatial and temporal variability of Sea Surface Temperature of the Arabian Sea over the past 142 years. *Pakistan Journal of Meteorology*, 9, 99-105.

Harrison D.E. and Carson M., (2007): Is the World Ocean Warming? Upper –Ocean temperature trends: 1950-2000. *Journal of Physical Oceanography*, 37, 174-187.

Hartmann B. and Gerd Wendler., (2005): The significance of the 1976 Pacific climate shift in the climatology of Alaska. *Journal of Climate*, 18, 4824-4839.

Hastenrath S.,(1988): Prediction of Indian Monsoon Rainfall: Further Exploration. *Journal of Climate*, 1(3), 298–305.

Haykin S. and Simon., (1999): *Neural Networks: A Comprehensive Foundation*, second edition. Prentice-Hall, Upper Saddle River, NJ.

Heitzman J. and Worden R.L.,(1996): *India: A Country Study*. Library of Congress (Area Handbook Series), ISBN 0844408336.

http://apdrc.soest.hawaii.edu/datadoc/hadley_en4.phm,p.

<http://bhuvan3.nrsc.gov.in/applications/bhuvanstore.php>.

<http://www.imdpune.gov.in>

http://www.ucsusa.org/global_warming/science_and_impacts/science/effect-of-sun-on-climate.

Huffman G.J., Adler R.F., Arkin A., Chang A., Ferraro R., Gruber A., Janowiak J., McNab A., Rudolf B.and Schneider U.,(1997):The Global Precipitation Climatology Project(GPCP) combined precipitation dataset. *Bulletin of the American Meteorological Society*, 78, 5 – 20.

Bibliography

Ihara C., Yochanan K. and Mark A. C., (2008): Warming trend of the Indian Ocean SST and Indian Ocean Dipole from 1880 to 2004. *Journal of Climate*, 21, 2035-2046.

IPCC Climate Change 2001: The Scientific Basis, Contribution of Working Group I to the Third Assessment Report of the Intergovernmental Panel on Climate Change.

IPCC 4th assessment report - Climate Change 2007: Working Group I: The Physical Science Basis.

IPCC Fifth assessment Report- Climate Change 2013.

Inter Governmental Panel on Climate change (IPCC), (2014): Climate change 2014 : Impacts, Adaptation, and Vulnerability. Contribution of working group II to the Fifth Assessment Report.

Iyengar R. N. and Raghu Kanth S.T.G., (2005): Intrinsic mode functions and a strategy for forecasting Indian monsoon rainfall. *Meteorological Atmospheric Physics*, 90, 17-36.

Joseph P.V. and Pillai P.V., (1984): Air sea interaction on a seasonal scale over north Indian Ocean, part I: inter annual variability of sea surface temperature and Indian summer monsoon rainfall. *Mausam*, 35, 323 – 330.

Kenyon K.E., (2014): Northwest Indian Ocean's spring cooling. *Natural Science*, 6, 760-766.

Kitoh A., (1993): Decade –scale changes in the atmosphere –ocean system in the winter Northern Hemisphere. *Umi to Sora (Sea and Sky)*, 68, 29-40 (in Japanese).

Kohail S. N. and El-Halees A. M., (2011): Implementation of data mining techniques for meteorological data analysis (A case study for Gaza Strip). *International Journal of Information and Communication Technology Research*, 96-100.

Kovács F., Legány C. and Babos A., (2005): Cluster validity measurement Techniques. *Proc.6th International Symposium of Hungarian Research on Computational Intelligence (CINTI)*, Budapest, Hungary.

Kripalani R.H., Kulkarni A. and Sabade S.S., (2003): Indian Monsoon Variability in a Global Warming Scenario. *Natural Hazards*, 29, 189-206.

Krishna Kumar K., Soman M.K. and Rupa Kumar K., (2010): Seasonal forecasting of Indian summer monsoon rainfall: A review. *Indian Institute of Tropical Meteorology*.

Krishna Kumar K., Soman M. K. and Rupa Kumar K., (1995): Seasonal forecasting of Indian summer monsoon rainfall: A review. *Weather*, 50, 449-467.

Krishnan R., Ramesh K.V.M., Samala B.K., Meyers G., Slingo J.M. and Fennessy M. J., (2006): Indian Ocean-monsoon coupled interactions and impending monsoon droughts. *Geophysical Research Letters*, 33, 1-4.

Lebedev S.A., (2007): Inter annual trends in the Southern Ocean sea surface temperature and sea level from remote sensing data. *Russian Journal of Earth Sciences*, 9, 1-6.

Levittus S., Antonov J.L., Wang T.L., Delworth K.W., Dixon. and Broccoli A.J., (2001): Anthropogenic warming of Earth's climate system. *Science*, 292, 267-270.

Bibliography

Levitus S.,Antonov J.and Boyer T.,(2005): Warming of the world ocean, 1955-2003. *Geophysical Research Letters*, 32, 1-4.

Maharana P.and Dimri A.P., (2014): Study of seasonal climatology and inter annual variability over India and its sub regions using a regional climate model (RegCM3). *Journal of Earth System Science*, 123, 1147-1169.

Mark Denny.,(2011): *How the Ocean works, An introduction to Oceanography*. Overseas Press (India) Private Limited.

Mckee T.B.,Doesken N.J. and Kleist J.,(1993):The relationship of drought frequency and duration to time scales, eighth Conference on Applied climatology, Anaheim, CA.

Meghali A., Kalyankar and Alaspurkar S.J., (2013): Data mining technique to analyze the meteorological data. *International Journal of Advanced Research in Computer Science and Software Engineering*, 3,114-118.

Mooley D.A. and Parthasarathy B., (1984): Fluctuations in All-India summer monsoon rainfall during 1871-1978. *Climatic Change*, 6, 287-301.

Mujumdar P.P.and Nagesh Kumar D., (2012): Floods in a changing climate Hydrologic modeling. *International Hydrology series*, Cambridge University press, 2, 3.

Muller B. and Reinhardt J., (1991): *Neural Networks: An Introduction*. Springer Verlag, Berlin.

Nagendra S.M.S. and Khare M.,(2006): Artificial neural network approach for modeling nitrogen dioxide dispersion from vehicular exhaust emissions. *Ecological Modeling*, 190, 99-115.

Nagesh Kumar., Janga Reddy M. and Maity R., (2007): Regional rainfall forecasting using large scale climate tele-connections and artificial intelligence techniques. *Journal of Intelligent Systems*, 16, 307-321.

Naidu C.V., Srinivasa Rao B.R.and Bhaskar Rao D.V., (1999): Climatic trends and periodicities of annual rainfall over India. *Meteorological Application*, 6, 395-404.

Nair A., Ajith Joseph K. and Nair K.S., (2014): Spatio- temporal analysis of rainfall trends over a maritime state (Kerala) of India during the last 100 years. *Atmospheric Environment*, 88, 123-132.

Navone H.D. and Ceccatto H. A., (1994): Predicting Indian summer monsoon rainfall: A neural network approach. *Climate Dynamics*, 10, 305-312.

Nilesh K.,Waghlikar K.C.,Sinha R., Sen P.N. and Pradeep Kumar.,(2014): Trends in seasonal temperatures over the Indian region. *Journal of Earth System Science*, 123, 673-687.

Nocke T.,Schumann H. and Bohm U.,(2004):Methods for the visualization of clustered climate data. *Computational Statistics*, 19(1), 75-94.

Oza M. and Kishtawal C.M., (2014): Spatial analysis of Indian summer monsoon rainfall. *Journal of Geomatics*, 8, 40-47.

Pai M.L., Saji P.K., Pramod K.V. and Balchand A.N., (2015): Trend Analysis of Sea Surface Temperature of Indian Ocean during the Period 1960-2012. *International Journal of oceans and oceanography*, 9, 229-242.

Parthasarathy B., (1988): Inter annual and long term variability of Indian summer monsoon rainfall. *Proceedings of Indian Academy of Sciences, Earth Planet Science*, 93, 371-385.

Prasanna V., (2014): Impact of monsoon rainfall on the total food grain yield over India. *Journal of Earth System Science*, 123, 1129-1145.

Pregibon D., (1997): Data Mining. *Statistical Computing and Graphics*, 7, 8.

Rajeevan M., (2001): Prediction of Indian summer monsoon: status, problems and prospects. *Current Science*, 81, 1451-1458.

Rajeevan M., Jyoti Bhate. and Jaswal A.K.,(2008): Analysis of variability and trends of extreme rainfall events over India using 104 years of gridded daily rainfall data . *Geophysical Research letters*, 35, 1-6.

Rajeevan M., Pai D. S., Anil Kumar R. and Lal B., (2007): New statistical models for long range forecasting of southwest monsoon rainfall over India. *Climate Dynamics*, 28, 813-828.

Rajeevan M., Pai D.S.and Anil Kumar R., (2006): New statistical models for long range forecasting of south west monsoon rainfall over India, National Climate Centre, Pune.

Rajeevan M., Sulochana G.and Jyoti B., (2008): Active and break spells of Indian summer monsoon. National Climate Center (NCC) Research Report, 7, 1-45.

Rajeevan M.,Sulochana G. and Jyoti B.,(2010): Active and break spells of Indian summer monsoon. *Journal of Earth System Science*, 119, 229-247.

Ramesh Kumar M. R., Sankar S., Fenning K., Pai D. S., Schulz J. and Grassel H., (2005): Air sea interaction over the Indian Ocean during the contrasting years 2002 and 2003. *Geophysical Research Letters*, 32, 1-4.

Ramesh Kumar M.R. and Schlüssel P., (1998): Air sea interaction over the Indian Ocean during the two contrasting monsoon years 1987 and 1988 studied with satellite data. *Theoretical and Applied Climatology*, 60, 219-231.

Rao A.D., Mahapatra D.K.,Babu S.V. and Smita Pandey.,(2012): Spatial temporal variation and mechanism associated with mini-cold pool off the southern tip of India during summer and winter monsoon season . *Water Quality Research Journal of Canada*, IWA Publishing, 334-352.

Rao K.G. and Goswamy B.N., (1988): Inter annual variations of sea surface temperature over the Arabian Sea and the Indian monsoon: a new perspective. *Monthly Weather Review*, 116, 558 – 568.

Rao S.A., Ashish R.D.,Subhodh K.S.,Somnath M.,Hemanth K.S.,Chaudhari.,Samir Pokhrel. and Sobhan K. Sabu.,(2012): Why is Indian ocean warming consistently?. *Climate Change*, 110, 709-719.

Rao S.A., (2013): Indian Ocean warming and its impact on Indian monsoon variability. Indo European Research facilities for studies on Marine Ecosystem and climate in India workshop II on monsoon and ocean variability, *Climate Change & Sea Level Variations*, Nansen Environmental Research Centre, Kochi.

Roxy M.K., Ritika K., Terray P. and Masson S., (2014): The curious Case of Indian Ocean Warming. *American Meteorological Society*, 27, 8501-8509.

Rumelhart D.E., Hinton G. E. and Williams R.J., (1986): Learning representations by back- propagating errors. *Nature Publishing Group*, 323, 533-536.

Rupa Kumar K., Pant G. B., Parthasarathy B. and Sontakke N.A., (1992): Spatial and sub-seasonal patterns of the long-term trends of Indian summer monsoon rainfall. *International Journal of Climatology*, 12, 257-268.

Sahai A.K., Soman M.K. and Satyan V., (2000): All India summer monsoon rainfall prediction using an artificial neural network. *Climate Dynamics*, 16, 291-302.

Sahai A.K., Grimm A.M., Satyan V. and Pant G. B., (2003): Long lead prediction of Indian summer monsoon rainfall from global SST evolution. *Climate Dynamics*, 20, 855-863.

Sarah N. K. and Alaa M. El-Halees., (2011): Implementation of Data mining techniques for Meteorological data analysis. *The Islamic University of Gaza, International Journal of Information and Communication Technology Research*, 1, 96-100.

Shanmuganathan S., Philip Sallis. and Ajit Narayanan., (2010): Data Mining Techniques for Modelling Seasonal Climate Effects on Grapevine yield and Wine quality. 2010 Second International Conference on

Computational Intelligence, Communication Systems and Networks, Liverpool, 84-89.

Sharad K.J., Pushpendra K.A. and Vijay P.S.,(2012): Hydrology and water resources of India, Water, Science and Technology Library. Springer International edition, 57.

Shukla J., Mooley D.A., (1987): Empirical prediction of the summer monsoon rainfall over India. Monsoon Weather Review, 115, 695-703.

Singh O.P. and Sarker M.A.,(2003): Recent sea surface temperature variability in the coastal regions of north Indian Ocean. Indian Journal of Marine Science, 32, 7-13.

Singh O.P., (1999): Recent trends in summer temperature over the North Indian Ocean. Indian Journal of Marine Sciences, 29, 7-11.

Singh P. and Bhogeshwar.,(2013): Indian summer monsoon rainfall prediction using artificial neural network. Stochastic Environmental Research and Risk Assessment, 27, 1585-1599.

Sivanandam S.N. and Paulraj M.,(2003): Introduction to Artificial Neural Networks. Vikas Publishing House Pvt. Ltd.

Srivastava H. N., Dewan B. N., Dikshit S. K., Prakash Rao G. S., Singh S. S. and Rao K. R., (1992): Decadal trends in climate over India. Mausam, 43, 7-20.

Subash N. and Sikka A.K.,(2014): Trend analysis of rainfall and temperature and its relationship over India. Theoretical and Applied Climatology, 117, 449–462.

Sudipta S. and Menas K., (2004): Inter annual variability of vegetation over the Indian subcontinent and its relation to the different meteorological parameters. *Remote Sensing of Environment*, 90, 268-280.

Suryajit C., (2007): Feed forward Artificial Neural Network model to predict the average summer monsoon rainfall in India. *Acta Geophysica*, 55, 369-382.

Svozil D., Vladimir KvasniEka, Jie Pospichal.,(1997): Introduction to multi-layer feed –forward neural networks . *Chemometrics and Intelligent Laboratory Systems*, 39, 43-62.

Thapliyal V., (1982): Stochastic dynamic model for long range prediction of monsoon rainfall in Peninsular India. *Mausam*, 33, 399-404.

Thapliyal V., Kulshreshtha S., (1992): Recent models for long-range forecasting of southwest monsoon rainfall over India. *J Arid Environ* , 43, 239–248.

Trenberth K.E., (1990): Recent observed inter decadal climate changes in the northern hemisphere. *Bulletin of the American Meteorological Society*, 71, 988-993.

Tripathi K.C.,Shailendra R.,Pandey A.C. and Das I. M. L., (2008): Southern Indian Ocean SST indices as early predictors of Indian summer monsoon. *Indian Journal of Marine Sciences*, 37, 70-76.

Varikoden H. and Preethi B., (2013): Wet and dry years of Indian summer monsoon and its relation with Indo-Pacific sea surface temperatures. *International Journal of climatology*, 33, 1761-1771.

Venkateswan., Raskar S.D., Tambe S. S., Kulkarni B. D. and Kesavamurthy R. N., (1997): Prediction of all India summer monsoon rainfall using error-back-propagation neural networks. *Meteorological Atmospheric Physics*, 62, 225-240.

Vinayachandran P. N. and Shetye S. R., (1991): The warm pool in the Indian Ocean, *Proc. Indian Acad. Sci., (Earth & Planetary Sci.)*, 100, 165-175.

Vinayachandran P.N., (2009): Impact of Physical Processes on Chlorophyll Distribution in the Bay of Bengal. *Indian Ocean Biogeochemical Processes and Ecological Variability*, Geophysical Monograph Series 185, Copyright 2009 by the American Geophysical Union, 10.1029/2008GM000705.

Vivekanandan E., (2010): Impact of climate change in the Indian Marine Fisheries and the potential adaptation options. In: *Coastal Fishery Resources of India- Conservation and sustainable utilization*, Society of Fisheries Technologists, 169-185.

Walker G.T., (1910): Correlation in seasonal variations of weather II. *Memoirs of the India Meteorological Department*, 21 (part 2), 22-45.

Wang C., Xie S-P. and Carton J.A., (2004): A global survey of Ocean-Atmosphere interaction and climate variability. *Geo physics monograph*, 147, 1-19.

Wang, B., (1995): Inter decadal changes in El Nino onset in the last four decades. *Journal of Climate*, 8, 267-285.

Bibliography

Woodruff S. D., Steven J. W., Sandra J. L., Zaihua Ji., Eric F. J., David I. B., Philip B., Elizabeth C.K., Richard W.R., Shawn R.S. and Clive W., (2011): ICOADS release 2.5: extensions and enhancements to the surface marine meteorological archive. *International Journal of Climatology*, 31, 951-967.

Worley S.J., Woodruff S. D., Reynolds R. W., Lubker S.J. and Lott N., (2005): ICOADS Release 2.1 data and products. *International Journal of Climatology*, 25, 823-842.

Yen Yi Loo., Lawal Billa. and Ajit Singh., (2015): Effect of climate change on seasonal monsoon in Asia and its impact on the variability of monsoon rainfall in South East Asia. *Geo Science Frontiers*, 6,817-823.

Zahoor Jan., Abrar M., Shariq Bashir. and Anwar M.M., (2008): Seasonal to Inter-annual climate prediction using Data mining KNN technique. *IMTIC, CCIS*, 20, 40-51.

Zhou T.,Yu R., Li.H. and Wang B., (2008): Ocean forcing to changes in Global Monsoon Precipitation over the Recent Half- century. *American Meteorological Society*, 21, 3833-3852.

Zurada. and Jacek M.,(1992): *Introduction to Artificial Neural System*.West Publishing Company. St. Paul, MN.

The following are the list of publications that form part of Doctoral work.

1. Maya L. Pai, P. K. Saji, K. V Pramod, A. N Balchand., (2015):Trend Analysis of Sea Surface Temperature of Indian Ocean during the Period 1960-2012, International Journal of Oceans and Oceanography, Vol. 9(2) , 229-242.
2. Maya L. Pai, K. V Pramod, A .N Balchand, M. R Ramesh Kumar., (2015):Can the Drought/Flood Monsoon Conditions over the Indian subcontinent be forecasted using Artificial Neural Networks? Indian Journal of Geo-Marine Science (accepted).
3. Maya L. Pai, Kalavampara V. Pramod, Alungal N. Balchand., (2014): Long Range Forecast on South West Monsoon Rainfall using Artificial Neural Networks based on Clustering Approach, International Journal of Information Technology and Computer Science (IJITCS), Vol. 6(7), 1-8.

Trend Analysis of Sea Surface Temperature of Indian Ocean during the Period 1960-2012

Maya L. Pai¹, P. K. Sajj², K. V. Pramod³, A. N. Balchand^{2*}

¹ Department of Mathematics, Amrita Vishwa Vidyapeetham, Cochin 682024.

² Department of Physical Oceanography, CUSAT, Cochin 682016.

³ Department of Computer Applications, CUSAT, Cochin 682022.

Corresponding author: *balchand57@gmail.com

Abstract

Oceans are currently undergoing a warming phase in response to global climate change. Rate of warming is however not uniform within a particular ocean and also between the oceans. Utilizing ICOADS Sea Surface Temperature (SST) data of 53 years (1960-2012), we studied the warming trend(s) in Indian Ocean (IO) on monthly, seasonal and annual scale applying statistical regression tools. Higher warming rate [0.30°C/decade] has been identified in the equatorial IO. Over the tropical Indian Ocean, rate of warming had varied from 0.05 to 0.30°C/decade. We also find that ICOADS data has limitations in producing the basin wide estimate of long term warming trend due to the limited data coverage.

Keywords: Globalwarming, SST, Indian Ocean, Trend analysis

Introduction

The two key environmental issues among climate researchers in the last two decades are global warming and climate change. Both are related in such a way that the reason for ongoing climate changes is the impact of global warming. There is a steady increase in the greenhouse gases since the industrial revolution and 70% increase was noticed between 1970 and 2004 [1]. Many studies have confirmed that Indian Ocean (IO) is warming consistently and with a higher rate compared to other oceans [2-6]. It is observed that the changes in net air-sea heat flux induced by green house gases are responsible for this warming [2-5, 7].

Can the Drought/Flood Monsoon Conditions over the Indian subcontinent be forecasted using Artificial Neural Networks?

Maya L. Pai¹, K. V. Pramod², A. N. Balchand^{3*}, M. R. Ramesh Kumar⁴

¹Department of Mathematics, Amrita Vishwa Vidyapeetham, Cochin
682024

²Department of Computer Applications, Cochin University of Science and
Technology, Cochin 682022

^{3*}Department of Physical Oceanography, Cochin University of Science
and Technology, Cochin 682016

⁴Physical Oceanography Division, NIO Goa 403004

*[Email: balchand@rediffmail.com]

The Indian summer monsoon rainfall during the months June, July, August and September (JJAS) has been classified into seven climatic zones, according to standard precipitation index. Prediction of rainfall within the six hydrological zones of India was attempted with the oceanic predictors, which highly influence the terrestrial precipitation, such as Sea Surface Temperature (SST), Sea Level Pressure (SLP), Humidity and zonal and meridional components of Surface Wind (u and v) to quantify the rainfall amounts by clustering based artificial neural networks for the distinguishable dry and wet years. In the present analysis, we have used data for the period 1960 – 2012, which incidentally had several extreme events (of drought and flood conditions) over the Indian subcontinent. Next, the results indicate that the predicted values are well comparable with the actual measured values proving the usefulness of this approach. In addition, this approach has improved upon the past and recent attempts to

I.J. Information Technology and Computer Science, 2014, 07, 1-8 Published
Online June 2014 in MECS (<http://www.mecs-press.org/>) DOI: 10.5815/ijitcs.2014.07.01

Copyright © 2014 MECS *I.J. Information Technology and Computer Science*, 2014, 07,
1-8

Long Range Forecast on South West Monsoon Rainfall using Artificial Neural Networks based on Clustering Approach

Maya L. Pai

Department of Mathematics, Amrita Vishwa Vidyapeetham, Cochin, 682024, India
Email: mayalpai@gmail.com

Kalavampara V. Pramod

Department of Computer Applications, CUSAT, Cochin, 682022, India
Email: pramodkv4@gmail.com

Alungal N. Balchand

Department of Physical Oceanography, CUSAT, Cochin, 682016, India
Email: balchand@rediffmail.com

Abstract— The purpose of this study is to forecast Southwest Indian Monsoon rainfall based on sea surface temperature, sea level pressure, humidity and zonal (u) and meridional (v) winds. With the aforementioned parameters given as input to an Artificial Neural Network (ANN), the rainfall within 10x10 grids of southwest Indian regions is predicted by means of one of the most efficient clustering methods, namely the Kohonen Self-Organizing Maps (SOM). The ANN is trained with input parameters spanning for 36 years (1960-1995) and tested and validated for a period of 9 years (1996-2004). It is further used to predict the rainfall for 6 years (2005-2010). The results show reasonably good accuracy for the summer monsoon periods June, July, August and September (JJAS) of the validation years.

Index Terms— South West Monsoon, Clustering, Artificial Neural Networks, Self-Organizing Map.

